Universidad CEU San Pablo
CEINDO - CEU Escuela Internacional de Doctorado

PROGRAMA en CIENCIA Y TECNOLOGÍA DE LA SALUD

Pleiotrophin: a novel modulator of the metabolic activity of the liver

TESIS DOCTORAL

Presentada por:

BEGOÑA ZAPATERÍA GÓMEZ

Dirigida por:

MARÍA DEL PILAR RAMOS ÁLVAREZ

JULIO SEVILLANO FERNÁNDEZ

MADRID

2021

AGRADECIMIENTOS

Después de 4 años de trabajo, unos cuantos ratones, muchos experimentos, noches sin dormir y una pandemia mundial…¡¡TESIS ACABADA!!

Sin embargo, esta experiencia llena de subidas y bajadas no habría sido lo mismo sin la gente que la ha compartido conmigo.

En primer lugar, quiero agradecer a Pilar y a Julio la confianza que han tenido en mí desde el primer día. Gracias por todas vuestras correcciones, consejos, ánimos y por enseñarme tanto a lo largo de todo este tiempo.

A todo el grupo GESTOBES. María Gracia, María Limones, María Haro, Jimena, Gloria, Miriam, Aurora, Gonzalo, y a las nuevas incorporaciones Javi y Lucía, os escribiría un agradecimiento a cada uno, pero necesitaría otra tesis, así que voy a resumir y espero haberos mostrado mi gratitud durante estos 4 años. Gracias por vuestra disponibilidad y apoyo, no me llevo solo compañeros de trabajo, sino amigos. A Alejandro, por tu buen humor y por estar siempre dispuesto a ayudar desde Madrid o desde Graz.

A mis compañeras doctorandas, Alba, Agata, Cristina y Eva. Esto es una carrera de resistencia y se hace menos dura cuando cuentas con gente a tu alrededor como vosotras. Gracias por las risas, los bailes, las conversaciones filosóficas y porque los agobios compartidos se llevan mejor.

A Elena y Yanira. Hemos hecho este camino juntas y seamos sinceras no ha sido fácil, pero es una suerte haberos tenido a vosotras cerca. Además, ¡qué bien sientan unas cervezas juntas para desahogarnos! Gracias y a por la siguiente etapa.

A los compañeros de otros laboratorios. Gonzalo, Esther, Rosalía, Martín, Maribel, Nuria, Carolina y Rubén porque también estáis presentes en los buenos momentos que he vivido estos años. Y a Alicia, por siempre dedicarme palabras de ánimo y por sus conversaciones cuando estaba sola en el laboratorio.

A otros grupos de investigación que han contribuido en este proyecto por toda su ayuda. Al grupo Lipobeta, en especial a Gema, Adriana y Patricia, por su buen hacer, sus aportaciones y sugerencias para mejorar esta investigación, y su amabilidad. Al grupo de Ángela Valverde y sobre todo a Patricia por su paciencia, por aguantar mis innumerables preguntas y correos electrónicos. Sin vosotras no hubiese conseguido aislar hepatocitos. Y a la gente del IMMA, Paloma, Virginia y Javier, por su ayuda con el microscopio y la rapidez en el procesado de muestras. Gracias a todos.

También quiero agradecer a personas cuyo trabajo a veces pasa desapercibido y sin las cuales esta tesis no sería lo que es. A toda la gente del animalario, Jesús, Marta e Inma, por vuestra disponibilidad, paciencia y amabilidad. A Sergio por sus conversaciones, consejos, profesionalidad y por ser salvavidas cuando los pedidos de suero o antibióticos no llegaban.

A toda la gente del Karolinska Institutet. En especial a Ismael y Noah, por toda su ayuda antes de mi llegada a Estocolmo, durante mi estancia y después, que también ha sido mucha. Gracias por confiar en mi desde el minuto cero, y por darme la oportunidad de trabajar con vosotros. To all the friends I made there, Francesca, Patricia, Dimitri, Montse, Philip, Rafael, Ale, Essam for welcoming me so well and making me feel accompanied despite being so far from home and in the middle of a pandemic. I will never forget those four months I spent with you. Thank you.

A mis amigos de toda la vida, Sergio, Marta, Alejandro, Miguel, Teresa, Andrés y Kieran. Técnicamente, ninguno habéis hecho un doctorado, pero este es un poquito vuestro. Gracias por haberme apoyado siempre, por estar presentes en cualquier momento, y animarme cuando lo necesitaba. Sin vosotros todo sería mucho más aburrido. Sois una parte muy importante de mí. Gracias.

Felipe, como los demás siempre has estado presente, pero estos dos últimos años te has convertido en un pilar fundamental. Gracias. Te subiste al barco quizá en el “peor” momento, al final de la tesis, pero no me has dejado sola nunca, ni siquiera a 3000 km de distancia. Gracias por apoyarme y animarme, por escuchar mis divagaciones, quejas y aguantar mis cambios de humor. Pero por encima de todo, gracias por las risas, por tu compañía, por nuestras escapadas y por todo el cariño que me das cada día. Prometo compensarte las ausencias y planes por hacer.

Por último, necesito agradecer a mi familia. Las palabras se me quedan cortas para expresar mi gratitud por todo lo que habéis hecho por mí, no solo en estos años de tesis, sino siempre. Alberto, el artista de la casa, gracias por tus dibujos, si esta tesis es bonita es gracias a ti. Gracias por haber escuchado no una, ni dos, ni tres veces (he perdido la cuenta) mis presentaciones, pero ya sabes, para eso está la familia (y todavía queda la defensa, prepárate!). A mis padres, por su incondicional apoyo siempre. Cualquier cosa que os pueda decir es poca. Gracias por creer en mí más que nadie, por escucharme, entenderme y animarme, por los consejos, el empuje, las bromas y la paciencia, han sido muchos nervios pagados con vosotros. No podría haber llegado hasta aquí sin vosotros. Gracias por estar siempre conmigo, os quiero.

TABLE OF CONTENTS

ABBREVIATIONS

A

ABCA1: ATP-binding cassette transporter 1
Acadl: Acyl-CoA dehydrogenase long chain
Acadvl: Acyl-CoA dehydrogenase very long chain
Acat2: Acetyl-CoA acetyltransferase-2
Acc: Acetyl-CoA carboxylase
Acly: ATP citrate lyase
Acox1: Acyl-CoA oxidase 1
ACSL: Long-chain acyl-coenzyme A synthase
Adamts: ADAM metallopeptidase with thrombospondin
ADP: Adenosine diphosphate
AGPAT: 1-acylglycerol-3-phosphate acyltransferase
Akgdh: Alpha ketoglutarate dehydrogenase
AKT: Protein kinase B (PKB)
ALK: Anaplastic lymphoma kinase
AMP: Adenosine monophosphate
AMPK: AMP-activated protein kinase
ANOVA: Analysis of Variance
ApoB100: Apolipoprotein B 100
ApoC2: Apolipoprotein C2
Aqp9: Aquaporin 9
Arg: Arginase
ATGL: Adipose triglyceride lipase
ATP: Adenosine triphosphate
AUC: Area under the curve

B

BAT: Brown adipose tissue
BCA: Bicinchoninic acid assay
Bip: Heat shock protein family A (Hsp70) member 5
BSA: Bovine Serum Albumin

C

cAMP: Cyclic adenosine monophosphate
Cd-11b: Cluster of differentiation 11b
Cd-11c: Cluster of differentiation 11c
Cd68: Cluster of differentiation 68
cDNA: Complementary DNA
CE: Cholesteryl esters
Cebpα: CCAAT/enhancer binding protein, α
CETP: Cholesteryl ester transfer protein
Chop: C/EBP homologous protein
ChREBP: Carbohydrate-responsive element-binding protein
CNS: Central nervous system
Col4a1: Collagen type IV alpha 1 chain
Col6a2: Collagen type VI alpha 2 chain
Cox-2: Cyclooxygenase-2
Cps1: Carbamoyl-phosphate synthase 1
Cpt1α: Carnitine palmitoyltransferase 1 α
CREB: cAMP responsive element binding protein
Cs: Citrate synthase
Ctnnb: β-catenin
CYP: Cytochrome P450
CVD: Cardiovascular disease

D

DAG: Diacylglycerol
Dgat: Diacylglycerol O-acyltransferase
DHAP: Dihydroxyacetone phosphate
DHEA: Dehydroepiandrosterone
DIO2: Deiodinase 2
DMEM: Dulbecco's Modified Eagle Medium
DNA: Deoxyribonucleic acid
DNL: *De novo* lipogenesis

E

Edem: ER degradation enhancing alpha-mannosidase like protein 1
EDTA: Ethylenediaminetetraacetic acid
EGTA: Ethylene glycol tetraacetic acid
ER: Endoplasmic reticulum
ERAD: ER-associated degradation
ETC: Electron transport chain

F

FABP: Fatty acid binding protein
Fas: Fatty acid synthase
FATP: Fatty acid transporter
Fbp1: Fructose-1,6 bisphosphatase
FBS: Fetal bovine serum
Fgf21: Fibroblast growth factor 21
FOXO1: Forkhead box protein O1
FSH: Follicle-stimulating hormone

G

G6pc: Glucose-6-phosphatase, catalytic

G6pd: Glucose-6-phosphate dehydrogenase

GAG: Glycosaminoglycans

Gck: Glucokinase

GDM: Gestational diabetes mellitus

GH: Growth hormone

GIP: Glucose-induced insulinotropic peptide

Glud1: Glutamate dehydrogenase 1

Glut2: Glucose transporter 2

GP: Glycogen phosphorylase

Gpat: Glycerol-3-phosphate acyltransferase

GPD1: Glycerol-3-phosphate dehydrogenase 1

GS: Glycogen synthase

Gsk-3b: Glycogen synthase kinase 3 β

GTT: Glucose tolerance test

H

Hadha: Hydroxyacyl-CoA dehydrogenase, α

HBSS: Hank's Balanced Salt Solution

HDL: High-density lipoprotein

HEPES: 4-(2-hydroxyethyl)-1-piperazineethanesulfonic acid

HFD: High-fat diet

Hk-III: Hexokinase III

HMG-CoA: 3-hydroxy-3-methylglutaryl Coenzyme A

Hmgcr: 3-hydroxy-3-methylglutaryl-CoA reductase

Hmgcs: 3-hydroxy-3-methylglutaryl-CoA synthase

HNF4α: Hepatocyte nuclear factor 4 α

HOMA-IR: homeostatic model assessment- insulin resistance

Hprt: Hypoxanthine guanine phosphoribosyl transferase

HSCs: Hepatic stellate cells

HSP90: Heat shock protein 90

I

Idh3g: isocitrate dehydrogenase 3 γ

IDL: Intermediate density lipoprotein

IGF-1: Insulin-like growth factor 1

Il-1β: Interleukin 1 β

Il-6: Interleukin 6

IMGU: Insulin-mediated glucose uptake

iNos: Inducible nitric oxide synthase

J

JNK: c-Jun N-terminal kinase

K

KCs: Kupffer cells

Kd: dissociation constant

L

LCAT: Lecithin-cholesterol acyltransferase

Ldh: Lactate dehydrogenase

LDL: Low-density lipoprotein

Ldlr: Low-density lipoprotein receptor

LH: Luteinizing hormone

Lipc: Hepatic lipase

LPA: Lysophosphatidic acid

Lpin2: Lipin 2

Lpl: Lipoprotein lipase

LPS: Lipopolysaccharide

LRP1: LDLR-related protein

LSECs: Liver sinusoidal endothelial cells

LXR: Liver X receptor

M

M1: Proinflammatory macrophage

M2: Antiinflammatory macrophage

MAPK: Mitogen-activated protein kinases

Mdh: Malate dehydrogenase

Mfn: Mitofusin

Mk: midkine

mRNA: Messenger RNA

mTOR: Mechanistic target of rapamycin

N

NADH: Nicotinamide adenine dinucleotide

NADPH: Nicotinamide adenine dinucleotide phosphate

NAFLD: Non-alcoholic fatty liver disease

Nampt: Nicotinamide phosphoribosyltransferase

NASH: Non-alcoholic steatohepatitis

NEFA: Non-esterified fatty acids

NF-κB: nuclear factor kappa-light-chain-enhancer of activated B cells

NIMGU: Non-insulin-mediated glucose uptake

Nur77: mice isoform of NR4A1 factor

O

OCR: Oxygen consumption rate
Opa1: mitochondrial dynamin-like GTPase
ORF: Open reading frame
OXPHOS: Oxidative phosphorylation

P

PBS: Phosphate buffered saline
Pc: Pyruvate carboxylase
PCR: Polymerase chain reaction
PDGF: Platelet-derived growth factor
Pdha1: Pyruvate dehydrogenase E1 α 1
Pdi: Protein disulfide isomerase
PEP: Phosphoenolpyruvate
Pepck: Phosphoenolpyruvate carboxykinase
PFK: Phosphofructokinase
Pgc1α: PPAR gamma coactivator 1 α
PI3K: Phosphatidylinositol 3-kinase
Pk: Pyruvate kinase
Plin2: Perilipin 2
Ppar: Peroxisome proliferator activated receptor
PTN: Pleiotrophin
Ptn$^{+/+}$: Wild-type genotype for pleiotrophin
Ptn$^{-/-}$: Knock-out genotype for pleiotrophin
PTPRZ1: Protein tyrosine phosphatase receptor Z1
PTT: Pyruvate tolerance test
PVDF: Polyvinylidene fluoride

Q

QUICKI: Quantitative Insulin Sensitivity Check Index

R

RNA: Ribonucleic acid
ROS: Reactive oxygen species
Rpl13: Ribosomal protein L13
Rptpg: Receptor protein tyrosine phosphatase gamma
Rxrα: Retinoid X receptor α

S

SAT: Subcutaneous adipose tissue
Scd1: Stearoyl-CoA desaturase 1
SDC: Syndecan
SDS: Sodium dodecyl sulfate
SEM: Standard error of the mean
Soat: Sterol O-acyltransferase
SR-B1: Scavenger receptor B1
Src: SRC proto-oncogene, non-receptor tyrosine kinase
Srebp-1c: Sterol regulatory element-binding transcription factor 1

T

T_3: Triiodothyronine
T2D: Type 2 diabetes
TAG: Triacylglycerides
TBP: TATA-binding protein
TBST: Tris-buffered saline with Tween
TCA: Tricarboxylic acid cycle
Tkt: Transketolase
TLC: Thin layer chromatography
Tlr4: Toll-like receptor 4
Tnfα: Tumour necrosis factor α
TSR-1: Thrombospondin type-1 repeat

U

UDP: Uridine diphosphate

V

VAT: Visceral adipose tissue
VLCFA: Very-long-chain fatty acid
VLDL: Very low-density lipoprotein

W

WAT: White adipose tissue
WB: Western-blot
WNT: Wingless-type MMTV integration site family

FIGURES LIST

ABSTRACT

Ageing and pregnancy are two conditions that imply a series of challenges for the organism, which tries to adapt through physiological changes that affect its metabolism. Both situations are accompanied by metainflammation (low-grade systemic inflammation produced in response to an excess of nutrients or energy) and insulin resistance. As the main metabolic organ, the liver plays an essential role in the response of the organism towards these changes. Pleiotrophin is a heparin-binding growth factor that has already been demonstrated to regulate lipid turnover, energetic homeostasis, insulin sensitivity, and adipose tissue plasticity. Furthermore, pleiotrophin is highly implicated in inflammatory processes in several tissues, where its expression has been shown to be significantly increased.

Against this background, we hypothesise that pleiotrophin could modulate the maintenance of glucose and lipid homeostasis in the liver. Thus, we set out to study the involvement of pleiotrophin in the hepatic metabolic adaptations in two physiological situations associated with low-grade inflammation (metainflammation) and insulin resistance, such as the last third of pregnancy and ageing.

To do so, we used two experimental models consisting of female knock out mice with the deletion of the *Ptn* gene ($Ptn^{-/-}$) and their respective controls ($Ptn^{+/+}$). For the ageing model, we used 3-, 6-, 12-, and 15-months old mice, whereas for the gestation model, we used 18 days pregnant mice. We analysed the biochemical profile of all mice and characterised the mRNA and protein expression of the enzymes, transporters, and transcription factors involved in the key metabolic pathways in the liver.

Our data show that pleiotrophin deletion is associated with a lower body and liver weight and a reduced hepatic lipid accumulation in both models. In fact, the expression of the main proteins involved in lipogenesis, TAG synthesis, and β-oxidation and the transcription factors that regulate them is diminished in *Ptn* deficient mice. On the other hand, *Ptn* deletion triggers the development of glucose intolerance, and in the ageing model, it is associated with marked hyperinsulinaemia in the old mice. Our results highlight the important modulatory role of glycerol kinase in maintaining glucose homeostasis in the pregnancy model.

Moreover, our data reveal that pleiotrophin modulates mitochondrial function and biogenesis in the liver. The absence of *Ptn* increases the process of mitochondrial fusion in young mice, while the exogenous addition of recombinant pleiotrophin favours the mitochondrial respiration to the detriment of the glycolytic pathway.

Based on our results, we can conclude that pleiotrophin is essential in maintaining hepatic homeostasis, thereby contributing to the whole-body homeostatic regulation. Moreover, pleiotrophin deletion may protect against the development of hepatic steatosis, as it avoids the ectopic accumulation of fat in the liver.

RESUMEN

El envejecimiento y la gestación son dos situaciones que suponen una serie de desafíos para el organismo, el cual trata de adaptarse mediante un conjunto de cambios fisiológicos que afectan a su metabolismo. Ambas situaciones se acompañan de metainflamación (inflamación sistémica de bajo grado producida en respuesta a un exceso de nutrientes o energía) y resistencia a la insulina. El hígado como principal órgano metabólico desempeña un papel fundamental en la respuesta del organismo a dichos cambios. La pleiotrofina es un factor de crecimiento que se ha demostrado que interviene en la regulación del recambio lipídico, la homeostasis energética, la sensibilidad a la insulina y en la plasticidad del tejido adiposo. Además, la pleiotrofina está muy implicada en los procesos inflamatorios de diversos tejidos, en los que se ha visto que su expresión aumenta considerablemente.

Con estos antecedentes, nuestra hipótesis es que la pleiotrofina podría modular el mantenimiento de la homeostasis glucídica y lipídica en el hígado. Así, nos propusimos estudiar la implicación de la pleiotrofina en las adaptaciones metabólicas del hígado en dos situaciones fisiológicas asociadas a inflamación de bajo nivel (metainflamación) y resistencia a la insulina, que son el último tercio de la gestación y el envejecimiento.

Para ello, se emplearon dos modelos experimentales en ratones hembra a los que se había delecionado el gen de la pleiotrofina (*Ptn*$^{-/-}$) y sus respectivos controles (*Ptn*$^{+/+}$). Para el modelo de envejecimiento se emplearon ratones de 3, 6, 12 y 15 meses de edad, mientras que para el modelo de gestantes se emplearon ratones en el día 18 de gestación. En todos los animales se llevó a cabo un análisis del perfil bioquímico, y también se caracterizó la expresión génica y proteica de las enzimas, transportadores y factores de transcripción implicados en las principales rutas metabólicas del hígado.

Nuestros datos muestran que la deleción de pleiotrofina se asocia a un menor peso corporal y hepático, así como a una menor acumulación de lípidos en el hígado en ambos modelos. De hecho, la expresión de las principales proteínas implicadas en la lipogénesis, síntesis de triacilglicéridos, y β-oxidación, y de los factores de transcripción que los regulan se encuentra disminuida en los animales deficientes de *Ptn*. Por otro lado, la deleción de *Ptn* causa intolerancia a la glucosa, y en el modelo de envejecimiento se asocia a una marcada hiperinsulinemia en ratones de edad avanzada. Asimismo, nuestros resultados destacan el importante papel modulador de la glicerol quinasa en el mantenimiento de la homeostasis glucídica durante la gestación.

Además, nuestros datos muestran que la pleiotrofina modula la biogénesis y función de las mitocondrias hepáticas. La ausencia de *Ptn* incrementa el proceso de fusión mitocondrial

en los ratones jóvenes, mientras que la adición exógena de pleiotrofina recombinante favorece la respiración mitocondrial en detrimento de la ruta glucolítica.

Ante estos resultados, podemos concluir que la pleiotrofina es esencial en el mantenimiento de la homeostasis hepática y por tanto contribuye en la regulación homeostática de todo el organismo. Además, la deleción de pleiotrofina parece proteger ante el desarrollo de esteatosis hepática, ya que evita la acumulación ectópica de grasa en el hígado.

GENERAL INTRODUCTION

1. THE LIVER

The liver is the main metabolic organ. It maintains the organism's homeostasis by controlling the whole-body energy metabolism and playing essential crosstalk with extrahepatic tissues like muscle and adipose tissue.

Anatomically, the human liver is formed by four lobes (right, left, caudate, and quadrate). Mice and rats each have 4 liver lobes: median (or middle), left, right, and caudate. Mice and humans have a gall bladder, but not the rat. Blood reaches the liver either through the hepatic artery that supplies oxygenated blood or the hepatic portal vein, which transports blood from the gastrointestinal tract (rich in nutrients), gallbladder, pancreas, and spleen. The liver is covered by the Glisson's capsule, a membrane formed by fibrous connective tissue that sheaths the hepatic artery, portal vein, and bile ducts within the liver.

The liver is composed of different cell types separated into two groups, parenchymal and non-parenchymal cells. The parenchymal cells are the hepatocytes, which constitute the major cell population in the liver, between 60-80% of all cells (1), and perform the bulk of hepatic metabolic functions such as carbohydrate and lipid metabolism and detoxification. The non-parenchymal cells constitute 20-40% of the total number of liver cells. Within these non-parenchymal cells, liver endothelial sinusoidal cells (LSECs) comprise approximately 50% of the cells and mediate the exchange of substrates between blood and hepatocytes, regulate immunotolerance, and preserve the sinusoidal microenvironment.

Kupffer cells (KCs) are the resident macrophages in the liver and constitute 20% of the non-hepatocyte cell population. They are located within the sinusoids and play a vital role in the innate immune response along with other cells like natural killer cells, natural killer T lymphocytes and dendritic cells (2). KCs are placed close to parenchymal and non-parenchymal cells, which confers them the ability to regulate hepatic function (3). Their primary function is phagocytising pathogens and macromolecules that enter the liver from the portal and arterial circulation, which are too large for LSECs. Therefore, activation of Kupffer cells is crucial for the liver response to infections as well as to physical and toxic injuries.

Finally, hepatic stellate cells or HSCs represent less than 1% of the non-hepatocyte cells. The activation of HSCs prompts collagen production and favours hepatic fibrosis and cirrhosis.

The liver plays a critical role in metabolism, distribution of nutrients and detoxification of xenobiotics and harmful metabolites and maintains lipid, glucose, and energy metabolism of the organism. Briefly, in the postprandial state, the liver synthesizes fatty acids and

cholesterol, stores glucose as glycogen and esterifies fatty acids as triacylglycerides and packages them into lipoproteins that are subsequently released into the bloodstream. On the other hand, in fasting periods, the liver maintains blood glucose levels via gluconeogenesis and glycogenolysis and synthesizes ketone bodies that can be used as essential metabolic fuels by extrahepatic tissues like the brain and muscle during starvation and exercise.

1.1. Liver carbohydrate metabolism

The liver has a central role in carbohydrate metabolism both in the fed and fasting states. On feeding, circulating glucose enters hepatocytes through GLUT2 and is phosphorylated to glucose-6-phosphate by glucokinase (GCK). The phosphorylation renders in a lower intracellular concentration of glucose, which favours the glucose uptake by hepatocytes. In the liver, glucose-6-phosphate can be used for glycolysis, the pentose phosphate pathway, and the excess of glucose can be converted into glycogen (Figure 1) or lipids. Moreover, glucose uptake suppresses the expression of genes involved in endogenous glucose production (4).

Glucokinase is the main hexokinase present in the liver. Whereas hexokinase is stimulated by glucose and inhibited by glucose-6-phosphate, glucokinase is not regulated by glucose-6-phosphate concentrations but is highly dependent on insulin (activation) and glucagon (inhibition) signalling (5). This mechanism is impaired in diabetic patients.

1.1.1. Glycolysis

The liver consumes approximately 20-30% of glucose for energy metabolism through the glycolytic pathway (6). In glycolysis, a molecule of glucose is degraded in a series of enzyme catalysed reactions to yield two molecules of pyruvate, two molecules of ATP and two molecules of NADH as described below:

$$Glucose + 2P_i + 2ADP + 2NAD^+ \rightarrow 2\ Pyruvate + 2ATP + 2NADH + 2H^+ + 2H_2O$$

In a fed state, glucose-6-phosphate is transformed into fructose-6-phosphate, and then phosphofructokinase 1 (PFK1) phosphorylates fructose-6-phosphate into fructose-1,6-bisphosphate (Figure 1). PFK1 is regulated allosterically; it is activated by fructose-2,6-bisphosphate and AMP and inhibited by ATP and citrate. Moreover, in the fed state, the increment in the insulin levels also promotes glycolysis in the liver by dephosphorylating and activating PFK2 activity of the bifunctional enzyme, which increases the concentration of fructose-2,6-bisphosphate. On the contrary, during the fasting state, in which the glucose and insulin levels are low, the bifunctional enzyme is phosphorylated by protein kinase A, the fructose 2,6 bisphosphatase activity is increased, and the PFK2 activity is inhibited what decreases fructose-2,6-bisphosphate concentration and inhibits glycolysis (6).

Subsequently, fructose-1,6-bisphosphate is cleaved into dihydroxyacetone phosphate and glyceraldehyde 3-phosphate. Dihydroxyacetone phosphate is converted into glyceraldehyde 3-phosphate that proceeds further into glycolysis and, after several reversible reactions, is converted into phosphoenolpyruvate. In the last reaction of glycolysis, phosphoenolpyruvate is transformed into pyruvate by pyruvate kinase (PK) (Figure 1). This last enzyme has both short and long-term regulation. In the short term, PK is activated by fructose-1,6-bisphosphate and inhibited by ATP, acetyl-CoA, alanine, and long-chain fatty acids. On the other hand, PK activity is also modulated by reversible dephosphorylation or phosphorylation in the liver in the presence of insulin and glucagon, respectively (7).

In anaerobic conditions, pyruvate is reduced to lactate by lactate dehydrogenase (LDH). On the other hand, in aerobic conditions, pyruvate enters the mitochondria, is converted into acetyl-CoA by the pyruvate dehydrogenase complex (PDHA1) and acetyl-CoA is completely oxidized to generate ATP in the tricarboxylic acid cycle and oxidative phosphorylation (Figure 1) or used to synthesize fatty acids through lipogenesis (7).

1.1.2. Glycogen metabolism

Alternatively, glucose-6-phosphate can isomerize to glucose-1-phosphate and be activated to UDP-glucose, the immediate precursor of glycogen synthesis. The glucosyl (Glc) moiety of UDP-glucose is added to the nonreducing end of glycogen molecules by glycogen synthase (GS). The branching of glycogen is accomplished by the branching enzyme that transfers a fragment of α (1→4) glucan units into the same or a neighbouring chain by α (l→6) linkage. In the fasted state, glycogen phosphorylase (GP) cleaves with inorganic phosphate the terminal α (1→4) bonds of glycogen releasing molecules of glucose 1-phosphate, whereas the debranching enzyme cleaves the α (l→6) linkages releasing glucose (8).

Glycogen metabolism is highly regulated, and several molecules have key roles in that regulation. Firstly, glucose-6-phosphate is an allosteric activator of glycogen synthase and an allosteric inhibitor of glycogen phosphorylase. Posttranslational modifications are also important modulators of the activity of both enzymes. GS activity is inhibited when it is phosphorylated by glycogen synthase kinase 3 (GSK-3), which on the other hand, phosphorylates GP, increasing its activity and favouring glycogen catabolism (Figure 1). In addition, hormones play a critical role in glycogen regulation. In the fed state, insulin stimulates glycogenesis and GS by phosphorylating and inactivating GSK-3 via Akt activation. Insulin also suppresses glycogenolysis as it enhances the acetylation of GP, which promotes its dephosphorylation and inhibits its activity. Additionally, insulin stimulates

the expression of GCK, which, as mentioned before, phosphorylates glucose, generates glucose-6-phosphate and increases glucose uptake by hepatocytes (4).

Oppositely, in short-termed fasting, glycogenolysis is promoted by decreased insulin/glucagon ratio. Glucagon signalling increases cAMP levels, which activates protein kinase A, which in turn activates glycogen phosphorylase to break down glycogen to glucose-1-phosphate. Glucose-1-phosphate isomerizes to glucose-6-phosphate that is dephosphorylated by glucose-6-phosphatase (G6PC) to glucose. The liver releases this glucose into the bloodstream to provide a substrate for extrahepatic tissues for energy production. Glucagon, unlike insulin, avoids the acetylation of glycogen phosphorylase, preventing its inactivation (4).

1.1.3. Pentose phosphate pathway

The pentose phosphate pathway aims to generate NADPH and synthesize pentoses monophosphate. NAPDH is required to synthesize fatty acids and sterols, and it is required to maintain the antioxidant machinery of the cells. On the other hand, pentoses monophosphates can be employed for nucleotide synthesis that, in turn, are used for the production of nucleic acids (9).

The pentose phosphate pathway is carried out in the cytoplasm of cells from tissues with high proliferative activity or high rate of lipid synthesis like the liver, kidneys, adipose tissue and mammary glands. Pentose phosphate pathway reactions are divided into two phases: an oxidative and a non-oxidative phase. During the oxidative phase, glucose-6-phosphate is transformed into ribulose-5-phosphate (Figure 1) by a series of irreversible reactions whose goal is to generate reducing power (NADPH). Afterwards, ribulose-5-phosphate can be either transformed into ribose-5-phosphate or xylulose-5-phosphate. The non-oxidative phase aims to synthesize fructose-6-phosphate and glyceraldehyde-phosphate. It begins with the reaction of xylulose-5-phosphate with ribose-5-phosphate, and all reactions are reversible (10).

The regulation of the pentose phosphate pathway is mediated by the metabolic needs of the cells. When the cell equally needs NADPH and pentoses monophosphate, it activates the oxidative phase, whereas if the need for pentoses is greater, the cell will promote glycolysis to obtain fructose-6-phosphate and glyceraldehyde and perform the inverse reactions of the non-oxidative phase to synthesize pentose phosphate. In the situation where the requirement for NADPH is higher, the cell activates the oxidative pathway, xylulose and ribose continue through the non-oxidative phase to obtain fructose-6-phosphate and glyceraldehyde that will produce glucose-6-phosphate via gluconeogenesis, and the cycle will start again. Lastly, if the cell needs not only NADPH but also ATP, it activates both the

oxidative and non-oxidative phases. Glyceraldehyde and fructose-6-phosphate then undergo glycolysis and are used for the obtention of ATP (9).

1.1.4. Gluconeogenesis

Hepatocytes synthesize glucose during prolonged fasting periods using pyruvate, lactate, glycerol, and amino acids as substrates.

Lactate dehydrogenase (LDH) can oxidize lactate to generate pyruvate. Pyruvate enters the mitochondria, where it is transformed into oxaloacetate by pyruvate carboxylase (PC). Oxaloacetate is reduced to malate by the mitochondrial isoform of malate dehydrogenase and exported to the cytoplasm. Once in the cytosol, the cytoplasmic isoform of malate dehydrogenase re-oxidizes malate to oxaloacetate. Oxaloacetate is then converted into phosphoenolpyruvate (PEP) by phosphoenolpyruvate carboxykinase (PEPCK). After several reactions, PEP is transformed into fructose-1,6-bisphosphate, which is subsequently dephosphorylated to render fructose-6-phosphate by fructose 1,6-bisphosphatase (FBP1). Fructose-6-phosphate is converted to glucose-6-phosphate that ultimately is dephosphorylated by glucose-6-phosphatase (G6PC) to generate glucose (Figure 1) (4). PC, PEPCK and G6PC are the rate-determining steps of gluconeogenesis. Hepatic deficiency of these enzymes is associated with metabolic disorders such as the accumulation of TCA cycle intermediates, hepatic steatosis, hyperlipidaemia, lactic acidosis, uricemia and hepatomegaly (4).

During fasting, the mobilization of adipose triacylglycerides provides free fatty acids and glycerol. The molecules of glycerol that are released during lipolysis can also be used as gluconeogenic substrates. Glycerol enters the hepatocyte via aquaporin 9 (AQP9) and is then phosphorylated by glycerol kinase. Following phosphorylation of glycerol, glycerol-3-phosphate is oxidized to dihydroxyacetone phosphate (DHAP) by cytosolic glycerol-3-phosphate dehydrogenase 1 (GPD1) (4).

In addition, during fasting, muscle proteins can be broken down into amino acids. All amino acids, except leucine and lysine, can be degraded to TCA cycle intermediates and converted to oxaloacetate and subsequently into pyruvate that can be used for gluconeogenesis.

Gluconeogenesis is a tightly regulated process with multiple mechanisms that include the regulation of the availability of substrates, posttranslational modifications (acetylation and phosphorylation), allosteric regulation, regulation of gene expression by transcription factors (CREB, FOXO1, C/EBPα/β), the metabolic state, the circadian clock, and the levels of hormones (11). Gluconeogenesis and glycolysis are coordinated, which allows that in the

hepatocyte one of these pathways is relatively inactive while the other is highly active. Accordingly, the inhibitors of glycolysis are activators of gluconeogenesis.

Gluconeogenesis is activated in fasting conditions by glucagon and inhibited in the fed state by insulin. Acetyl-CoA is required for PC activity, as PC is catalytically inactive in the absence of acetyl-CoA. On the other hand, an increment of the concentrations of ADP and a decrease in the cellular energy levels inhibits both PC and PEPCK. PEPCK enzyme levels are increased in the fasting state in response to glucagon, thyroid hormone (T_3) and glucocorticoids.

The activity of FBP1 is controlled by fructose-2,6-bisphosphate levels and by the ATP/ADP ratio. If the ATP/ADP ratio is high, fructose-1,6-bisphosphatase activity is increased. Fructose-2,6-bisphosphate is an allosteric inhibitor of FBP1 activity and an activator of PFK1 in glycolysis. Glucagon and catecholamines stimulate cAMP production by adenylate kinase, which leads to the activation of cAMP-dependent protein kinase (PKA). PKA phosphorylates the bifunctional enzyme. When the bifunctional enzyme is phosphorylated, it is active as a fructose-2,6-bisphosphatase that transform fructose-2,6-bisphosphate into fructose-6-phosphate. The reduction in fructose-2,6-bisphosphate concentration increases FBP1 activity and decreases PFK1 activity (4,12).

Gluconeogenesis is also regulated by changes in the mRNA expression of gluconeogenic genes. cAMP signalling activates CREB phosphorylation. Once phosphorylated, CREB interacts with the cAMP response elements, recruits coactivator molecules, and activates the expression of the target genes. Another molecule involved in the regulation of the expression of gluconeogenic genes is PGC-1α (peroxisome proliferator-activated receptor-γ coactivator-1α), which expression is also regulated by cAMP. PGC-1α interacts with the glucocorticoid receptor, hepatic nuclear factor 4α (HNF4α) and the forkhead transcription factor (FOXO1) inducing gluconeogenesis. Insulin is known to suppress gluconeogenesis through the phosphorylation of FOXO1 and its subsequent exclusion from the nucleus. C/EBPα/β exerts its functions on PEPCK by activating or enhancing its gene expression. Moreover, C/EBPα promotes amino acid catabolism what increases the production of gluconeogenic substrates. On the other hand, C/EBPβ inactivation by AMPK decreases hepatic glucose production and blood glucose in mice (11).

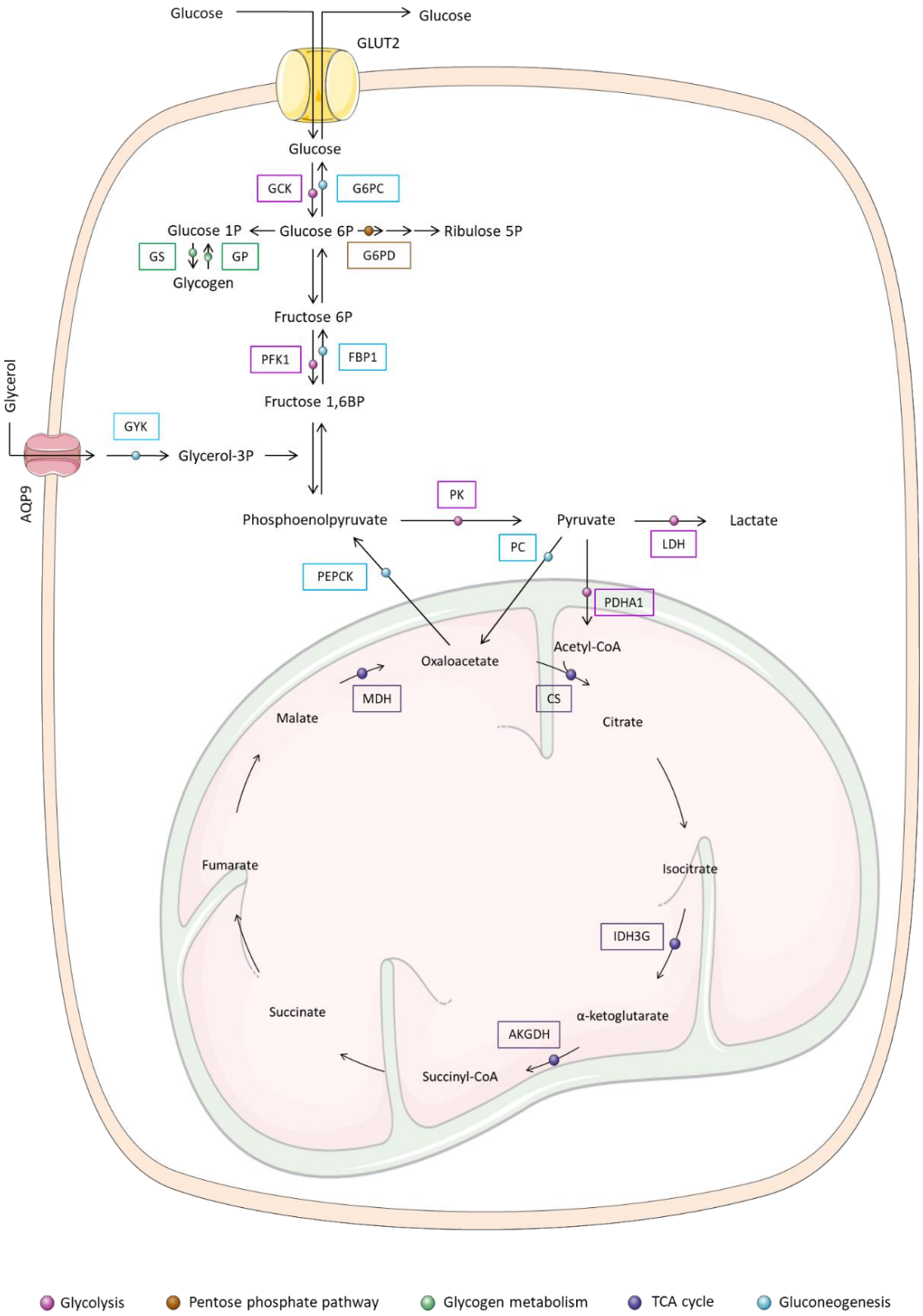

Figure 1. Carbohydrate metabolism in the liver.

1.2. Liver lipid metabolism

The liver has a constant influx of lipids as it uptakes the dietary fats and the free fatty acids (FFA) originated by lipolysis in the adipose tissue. Once fatty acids are in the hepatocytes, they can be directed to esterification or oxidation depending on the physiological and nutritional state of the organism. Furthermore, the liver can synthesize fatty acids by *de novo* lipogenesis and cholesterol from acetyl-CoA subunits. In a healthy organism, there is a balance between hepatic lipid synthesis, fatty acid uptake, and fatty acid disposal from the liver.

1.2.1. De novo fatty acid synthesis

The liver can use carbohydrates and proteins as substrates for fatty acid synthesis through a process known as *de novo* lipogenesis. Once the synthesis is complete, fatty acids can be esterified, incorporated into VLDL particles, and delivered to extrahepatic tissues through the bloodstream.

As explained in detail before, pyruvate obtained from glycolysis can be transformed into acetyl-CoA by pyruvate dehydrogenase. In the mitochondria, acetyl-CoA condenses with oxaloacetate to form citrate in a reaction catalysed by citrate synthase (CS) (Figure 1). For *de novo* lipogenesis, citrate is then exported to the cytosol and converted to cytosolic acetyl-CoA and oxaloacetate by ATP citrate lyase (ACLY). In the cytoplasm, the carboxylation of acetyl-CoA by acetyl-CoA carboxylase (ACC) forms malonyl-CoA. Malonyl-CoA and NADPH are the substrates for palmitate synthesis by fatty acid synthase (FAS). Once palmitate is synthesized, it can be elongated to generate long-chain fatty acids and/or desaturated by stearoyl-CoA desaturases (SCD) (Figure 2) to generate unsaturated fatty acids (6).

Lipogenesis is regulated by reversible covalent modification, allosteric regulation and transcriptional regulation of ACC and FAS. Insulin promotes fatty acid synthesis through the regulation of the rate-limiting enzyme ACC. ACC activity is modulated by phosphorylation and dephosphorylation. During a fasting period, AMPK is activated and phosphorylates ACC inhibiting its activity, whereas, after a meal, insulin levels increase and stimulate ACC dephosphorylation, increasing ACC activity. Moreover, ACC is also activated by citrate and inhibited by malonyl-CoA (6).

The transcriptional regulation of *Acc* and *Fas* is carried out primarily by sterol regulatory element-binding protein 1c (SREBP-1C) and carbohydrate-responsive element-binding protein (ChREBP). Both require nuclear translocation to activate the transcription of their target genes, including *Acc* and *Fas*. Additionally, both SREBP and ChREBP are stimulated

by liver X receptor (LXR), which in turn is activated by cholesterol intermediates and insulin (13).

1.2.2. Fatty acid uptake

After a meal, dietary triacylglycerides (TAG) and cholesterol esters are assembled and secreted into the circulation as chylomicrons. Chylomicron-derived TAGs are hydrolysed by lipoprotein lipase (LPL), releasing non-esterified fatty acids (NEFA) and glycerol that are taken up by the peripheral tissues (in particular adipose tissue). LPL activity is modulated by coactivators such as ApoA4, ApoA5, and ApoC2 and suppressors like ApoC3. Chylomicron remnants are mostly removed in the liver via the LDL receptor (LDLR) or LDLR-related protein (LRP1). In the liver, chylomicrons remnants are hydrolysed by lysosomes releasing fatty acids. Hepatic LDLR and LRP1 expression are key to control this process and modulate dyslipidaemia. In NAFLD and obesity, the expression of LDLR and LRP1 might be downregulated, which results in a longer stay of remnants in the bloodstream and contributes to the increased plasma concentration of TAGs (13).

On the other hand, the principal hepatic supply of NEFA is precisely the intracellular hydrolysis of TAG in adipose tissue or lipolysis. TAG hydrolysis in the adipose tissue is highly controlled by insulin, which inhibits the activities of adipose triglyceride lipase (ATGL) and hormone-sensitive lipase. Thereby, serum levels of NEFA are increased in a fasting state and decreased after a meal (13).

Non-esterified fatty acids enter the hepatocytes through the transporters CD36, FATP2, FATP4 and FATP5. FATP5 is exclusively expressed in the liver, and FATP4 is mainly localised in peroxisomes mediating the transport of long-chain fatty acids (4).

1.2.3. Triacylglyceride synthesis

Hepatocytes can synthesize TAG via the glycerol-3-phosphate pathway. In this pathway, glycerol is phosphorylated by glycerol kinase and acylated by glycerol-3-phosphate acyltransferase (GPAT) in the endoplasmic reticulum (ER) to form lysophosphatidic acid (LPA). LPA is then acylated by the family of 1-acylglycerol-3-phosphate acyltransferases (AGPAT) to produce phosphatidate (14). Next, lipin 2 (LPIN2) hydrolyses and removes the phosphate group from phosphatidate, yielding a diacylglycerol (DAG). The final step is the esterification of DAG to TAG by diacylglycerol O-acyltransferases (DGAT) (Figure 2).

In the fed state, when insulin levels are high, and glycolysis is highly active in the liver, hepatocytes can use the DHAP derived from glycolysis for triglyceride synthesis. Thus, DHAP is reduced to glycerol-3-phosphate by cytosolic glycerol-3-phosphate dehydrogenase, and TAG synthesis continues as explained above.

The TAG synthesis pathway is activated in the fed state and inhibited in a fasted state. In the liver, GPAT is regulated at the transcriptional level. Insulin and a high-carbohydrate and fat-free diet upregulate *Gpat1* mRNA through the expression of SREBP-1C, whereas glucagon has an opposite effect by elevating cAMP levels (14). Therefore, hepatic TAG synthesis is modulated hormonally and nutritionally via SREBP-1C mediation (15). Additionally, GPAT activity is regulated via dephosphorylation and phosphorylation by casein kinase II and AMPK (16,17).

1.2.4. β-oxidation

β-oxidation is the main hepatic oxidative pathway for energy production. It occurs predominantly in mitochondria but can also occur in peroxisomes. Liver fatty acid β-oxidation is active in the fasted state and inactive in the fed state (18).

Mitochondrial β-oxidation is involved in the oxidation of short- (<C8), medium- (C8–C12), and long- (C14–C20) chain fatty acids and allows the production of ATP via oxidative phosphorylation. Prior to β-oxidation, long-chain fatty acids must be first converted to acyl-CoAs by long-chain acyl-CoA synthetase (ACSL). The entrance of fatty acyl-CoA into the mitochondria is mediated by a carnitine-dependent transport system via CTP1, the rate-determining step for β-oxidation. Once in the mitochondria, long-chain acyl-CoA molecules are broken down to acetyl-CoA molecules in a cycling process involving dehydrogenation, hydration, and acylation reactions (19).

VLCFAs (>C20) are β-oxidized in peroxisomes, and although long-chain fatty acids are predominantly β-oxidized in mitochondria, peroxisomes also participate in the oxidation of these substrates (19). The peroxisomal β-oxidation is very similar to the mitochondrial, but oxidation of the end-products of peroxisomal fatty acid oxidation, notably acetyl-CoA, can only occur in mitochondria. Therefore, long-chain fatty acids are shortened in peroxisomes and further oxidized in the mitochondria (Figure 2).

CPT1 is the rate-limiting step in β-oxidization, and it is inhibited by malonyl-CoA. Consequently, when lipogenesis is active, β-oxidation is inhibited. Another primary modulator of fatty acid oxidation is the peroxisome proliferator activated receptor α (PPARα), which action is stimulated by fatty acids and glucagon and downregulated by insulin (13).

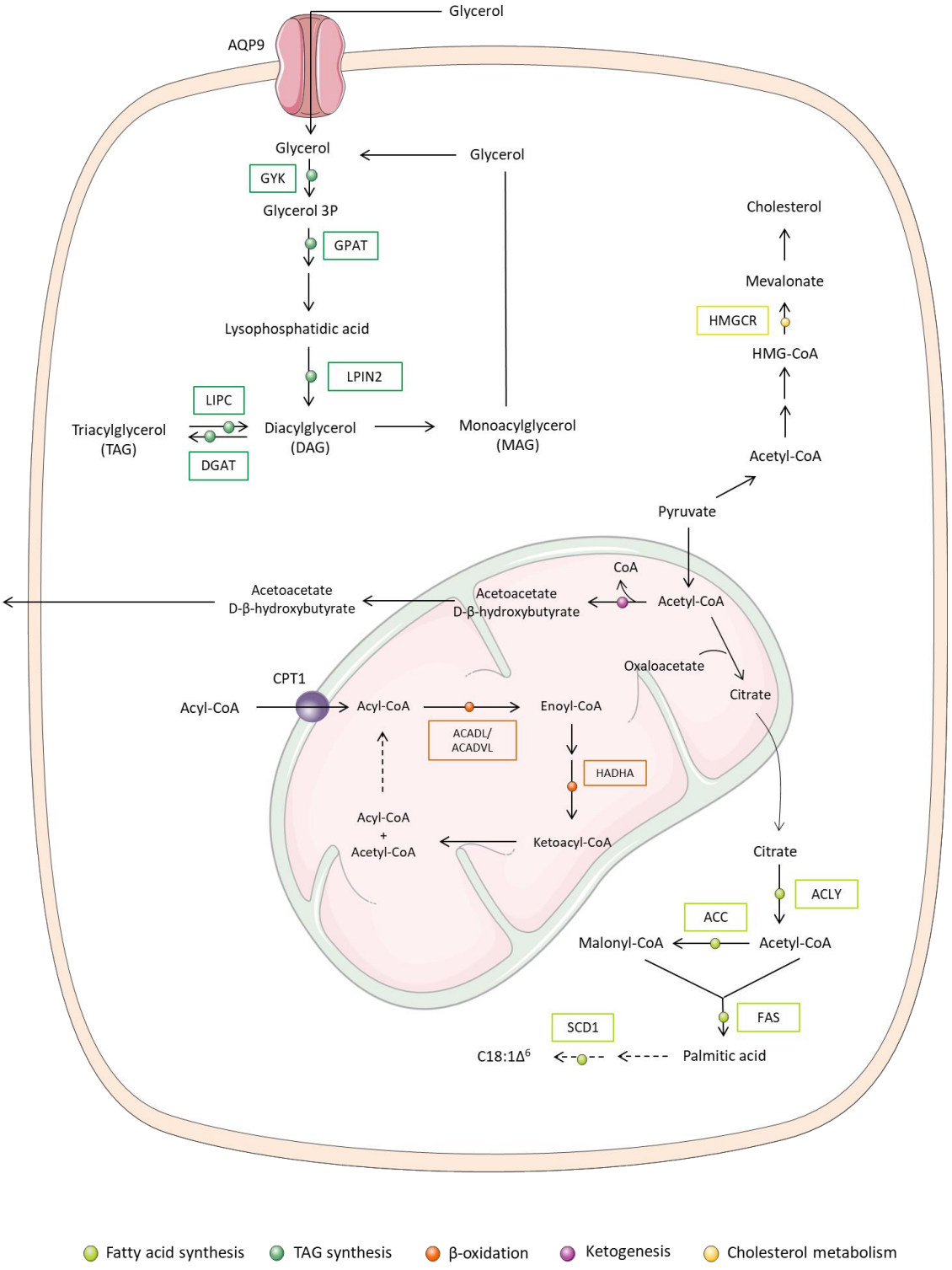

Figure 2. Pathways of lipid metabolism in the liver.

1.2.5. Ketone body synthesis

The mitochondrial acetyl-CoA molecules produced in β-oxidation can either enter the TCA cycle and be completely oxidized or be used for ketogenesis, depending on the availability of oxaloacetate. When there is enough oxaloacetate, acetyl-CoA enters the TCA cycle and produces 12 ATP. However, in a fasting situation, oxaloacetate is used for gluconeogenesis and acetyl-CoA is derived to ketone bodies synthesis (acetone, acetoacetate and D-β-hydroxybutyrate). Two acetyl-CoA molecules are condensed to form acetoacetyl-CoA by thiolase. Acetoacetyl-CoA is transformed by HMG-CoA synthase into HMG-CoA and is converted to acetoacetate by HMG-CoA lyase. Acetoacetate can be further transformed into either beta-hydroxybutyrate by beta-hydroxybutyrate dehydrogenase or into acetone by decarboxylation (20). After hepatic synthesis, ketone bodies are delivered to other tissues, mainly the brain and muscle, for energy production during long-term starvation (Figure 2).

Regulation of ketogenesis is mediated by the availability of substrate. Ketogenesis is upregulated by glucagon, cortisol, thyroid hormones, and catecholamines, as these hormones favour the breakdown of free fatty acids, increasing the substrate availability, and it is inhibited by insulin (21,22).

1.2.6. Cholesterol metabolism in the liver

Cholesterol is the precursor of steroid hormones, vitamin D and bile acids. There are two main sources of cholesterol: the diet and the *de novo* hepatic synthesis of cholesterol. *De novo* cholesterol synthesis begins with the condensation of 2 molecules of acetyl-CoA to form acetoacetyl-CoA. Then, HMG-CoA synthase adds a third molecule of acetyl-CoA forming 3-hydroxy-3-methylglutaryl-CoA (HMG-CoA). HMG-CoA reductase reduces HMG-CoA to mevalonate, and a series of subsequent reactions convert mevalonate to 3-isopentenyl pyrophosphate, farnesyl pyrophosphate, squalene, lanosterol, 7-dehydrocholesterol and cholesterol (Figure 2). The rate-limiting enzyme of this metabolic pathway is HMG-CoA reductase (HMGCR) (23).

De novo cholesterol synthesis is modulated by the intracellular levels of cholesterol and oxysterols (24). Regulation of the cholesterol synthesis rests mainly on the HMGCR, which has a short-term regulation that involves reversible phosphorylation/dephosphorylation, as well as a change in the orientation of its active centre. In addition, HMGCR also has a long-term regulation exerted by SREBP, which inhibits the transcription of the *Hmgcr* gene (23).

The liver can export cholesterol to peripheral tissues by assembling and secreting VLDL particles that contain TAG (50-80%), cholesterol and cholesteryl esters (5-15%), and

phospholipids (10-20%). VLDL deliver TAG to adipose tissue for storage and to other organs for energy production.

The apolipoproteins are an essential component of this mechanism by which the tissues can uptake cholesterol. Once in the bloodstream, VLDL particles with Apo B-100 gradually take up other apolipoproteins such as ApoC-II, ApoC-III, ApoA-V, and ApoE. On the surface of blood capillaries, LPL is activated by ApoC-II, hydrolyses TAG from VLDL and release fatty acids and glycerol. Due to the action of LPL and the loss of TAG, the VLDL become IDL. The new particles continue to exchange TAG through the action of LPL, but the gain of ApoE, allows hepatic lipase also to hydrolyse TAG. After unloading TAG, IDL finally become LDL which are taken up by the liver via LDL receptor. LDL exhibit ApoB-100 on their surface and provides the liver cholesteryl esters that can be used for the formation of new VLDL, to synthesize vitamin D and steroid hormones or the synthesis of bile acids (6).

Moreover, the liver can also receive cholesterol from peripheral tissues through reverse cholesterol transport. This mechanism consists of the removal of excess cholesterol from the cells. HDL particles contain ApoA-I, which allows their interaction with the ATP-binding cassette A1 (ABCA1), through which they uptake cholesterol. These initial HDL particles are known as pre-β-HDL. Next, lecithin-cholesterol acyltransferase (LCAT) esterifies the cholesterol to obtain cholesteryl esters (CE), thereby promoting the formation of mature HDL. Cholesteryl ester transfer protein (CETP) then facilitates the exchange of ApoE, ApoC-II, and CE between HDL and TAG-rich apolipoproteins such as VLDL and chylomicrons. Mature HDL loaded with CE bind the scavenger receptor B1 (SR-B1) located in the membrane of hepatocytes and transfer the CE to the liver for elimination (25).

1.3. Hepatic drug metabolism and detoxification

One of the most characteristic functions of the liver is to metabolize and detoxify drugs and xenobiotics to allow their elimination. When a xenobiotic is absorbed through the gastrointestinal tract, it enters the portal circulation and is delivered to the liver. Xenobiotic and drug metabolism is usually divided into three phases (6).

Phase I reactions are broadly grouped into three categories: oxidation, reduction, and hydrolysis. These reactions add or expose polar functional groups such as $-NH_2$ or -OH in the drugs. Phase I involves several enzymes, including the polymorphic cytochrome P450 (CYP) enzymes, which metabolize a great variety of drugs through complex reactions. P450 enzymes are haemoproteins that contain a Fe^{3+} group that oxidize drugs and substrates by using O_2, forming hydroxylated products. The major P450 enzyme for drug metabolism is CYP3A4, which is capable of metabolizing approximately 70% of human drugs (immunosuppressants, macrolide antibiotics, benzodiazepines, statins, antidepressants,

opioids, and anticancer drugs). Moreover, some pro-drugs need to be metabolized by P450 enzymes to achieve their active form. On the other hand, other drugs are metabolized by P450 enzymes to become inactive. Secondly, CYP monooxygenases can also metabolize xenobiotics and turn them into non-toxic compounds. Thereby, xenobiotic-metabolizing enzymes have a dual role in mediating both the activation and detoxification of drugs. Depending on the prevailing process, the xenobiotic is completely and safely eliminated, or on the contrary, it can lead to toxicity in the organism (26).

In phase II of liver drug metabolism, the xenobiotic metabolites are conjugated by reactions like sulfation, methylation, and glucuronidation. The purpose of these reactions is to increase the solubility of the generated metabolites to favour their secretion (6).

In phase III, the oxidized metabolites are taken up through transporters located in the membrane of hepatocytes and are transferred into bile for their elimination of the organism (6).

2. PLEIOTROPHIN

Pleiotrophin (PTN) is an 18 kDa extracellular matrix-associated protein (27) whose discovery was reported around 1900 by several independent research groups (28-31). It is known by different names, heparin-binding neurotrophic factor (HBNF), heparin-binding growth-associated molecule (HB-GAM), heparin affin regulatory peptide (HARP), heparin-binding brain mitogen (HBBM), heparin-binding growth factor 8 (HBGF-8), and neurite growth-promoting factor 1 (NGPF1), among others (32-34). Pleiotrophin was firstly purified from the bovine uterus (35) and the neonatal rat brain (36). It is considered a heparin-binding growth factor, and along with midkine (MK), it comprises a new family of growth factors. PTN and MK share a 50% homology in their amino acid sequences.

2.1. Pleiotrophin structure

PTN is highly conserved within species, in humans, bovine and rodents (mice and rats). Although it is a heparin-binding growth factor, it has marked structural differences with other heparin-binding factors such as FGF, HGF or PDGF (37).

2.1.1. Structure of the Ptn gene

Ptn gene is located in chromosome seven, band 7q33 in the human genome and chromosome 6 in the mouse genome and is 116 kb long (data obtained from NCBI). The open reading frame (ORF) of the coding region is 507 bases long. A variety of studies have reported a different number of exons in the *Ptn* gene; however, the latest tissue RNA

sequencing analysis determined that it has up to seven exons and nine splicing variants (38).

2.1.2. Structure of the PTN protein

The protein sequence identity is over 90% among mammals, even in the unstructured regions (34). PTN comprises 168 amino acid residues, 32 are the secretory signal peptide, and 136 comprehend the mature protein (39). PTN consists of two β-sheet domains (N- and C-terminals) of about forty residues that allow its binding to heparin. Each domain consists of three antiparallel β-sheet structures and a thrombospondin type-1 repeat (TSR-1) motif. Both domains are to some extent independent and able to move regarding each other. Thus, the linker region between them is flexible. Finally, PTN also contains two clusters rich in basic amino acids (24% lysine residues and cysteine) at the N- and C-terminal domains (Figure 3) and five intrachain disulphide bonds responsible for the stabilisation of the domains (40). Reduction of the disulphide bonds renders in a marked decrease of heparin binding, which suggests that PTN native structure is vital for the binding. Moreover, no posttranslational modifications of PTN have been identified (34).

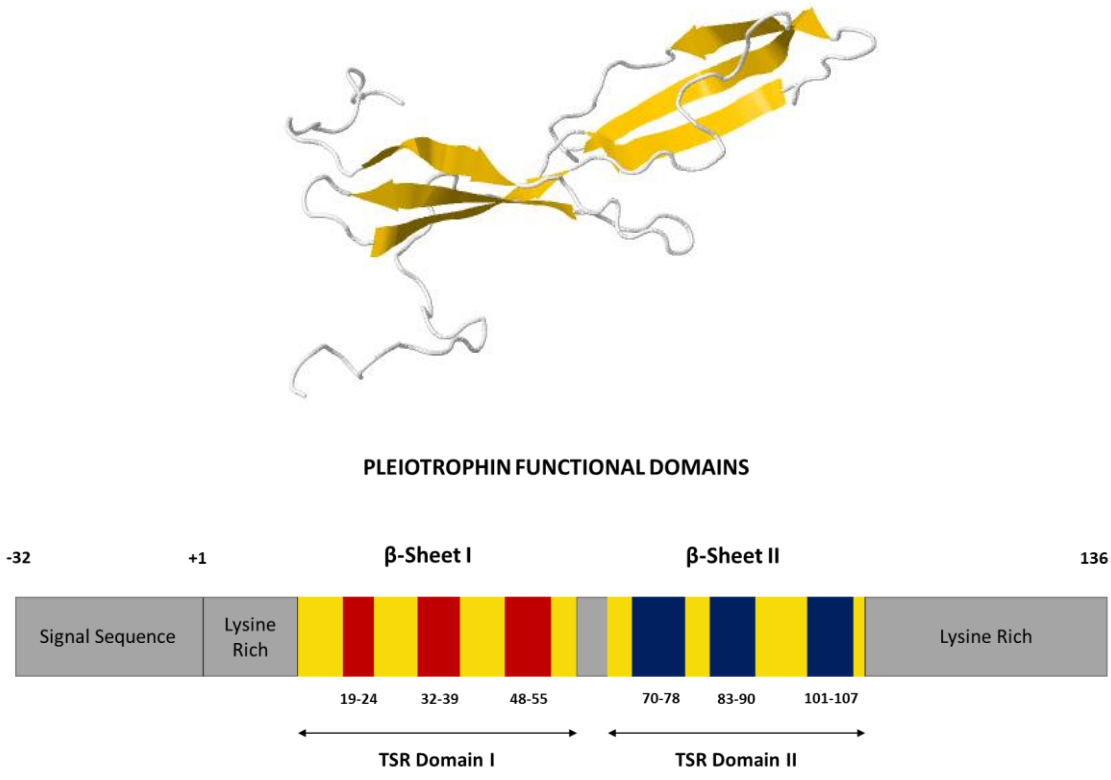

Figure 3. 3D structure of pleiotrophin. *In yellow are the three antiparallel β-sheet structures of each domain. Image taken from Protein Data Bank (Ryan, E.O., Shen, D., Wang, X) and Deuel, T.F. et al. (41).*

2.2. Receptors of pleiotrophin

Several molecules have been proposed to be PTN receptors over the last decades, including PTPRZ1, anaplastic leukaemia kinase (ALK), different isoforms of syndecans, nucleolin, integrins, Notch, and multimolecular complexes (34,42). In the current thesis, only those in which seems to be a consensus are explained (Figure 4).

2.2.1. RPTP β/ζ

Receptor-type tyrosine phosphatase (RPTP) β/ζ or PTPRZ is a chondroitin sulphate proteoglycan located in the transmembrane with an intracellular domain with a tyrosine phosphatase activity. The ectodomain of the receptor is composed of a carbonic anhydrase domain, a fibronectin type III domain and at least five glycosaminoglycans (GAG) chains (34). There are three isoforms of RPTP β/ζ: PTPRZ-A, the full-length form, PTPRZ-B with a truncated ectodomain, and PTPRZ-S, a soluble form consisting only in the ectodomain.

PTN has been shown to bind to the chondroitin sulphate portion of RPTP β/ζ, but the receptor has two binding sites with different affinities for PTN. Pleiotrophin binds to the site with the highest affinity with a Kd = 0.25 nM, whereas to the low-affinity site, the binding constant Kd is 3.0 nM (43). It is noteworthy to mention that the Kd of RPTP β/ζ to MK is 0.56 nM (44), which indicates that PTN is more likely to bind RPTP β/ζ efficiently. RPTP β/ζ is considered the primary receptor involved in the processes of migration of neurons and osteoblast and the survival of embryonic neurons (44).

The binding of PTN to RPTP β/ζ results in the dimerization or oligomerisation of the receptor and the inhibition of its phosphatase catalytic activity. This inactivation of the phosphatase domain is responsible for the increment of the amount of tyrosine phosphate in the cytoplasm and increased phosphorylation of proteins such as β-catenin, ALK, Src, PI_3K and ERK1/2, among others (34,44).

2.2.2. Syndecans

Syndecans (SDC) are a family of heparin sulphate proteoglycans that interact with many extracellular matrix components and cytokines (45). SDCs are formed by a single transmembrane helix, an ectodomain, and a small cytoplasmic domain. The syndecan family comprises four members: syndecan-1, mainly expressed in the epithelial cells; syndecan-2, expressed in mesenchymal stem derived cells; syndecan-3, the main one in the brain and cartilage; and syndecan-4 that is expressed in several types of tissues (34). Syndecan-3 was the first molecule discovered as a PTN receptor and is considered the receptor in the neurite outgrowth of embryonic neurons induced by PTN. The binding of PTN to SDC-3 is believed to occur through the heparan sulphate chains; specifically, the requirements for PTN binding

are the presence of N-sulphated glucosamine and 2-sulphated uronic acid. Moreover, the binding constant (Kd) of PTN to SDC-3 is 0.6 nM (44). The binding of PTN to this receptor might induce oligomerisation of the receptor, as in the case of PTPRZ.

Several studies have shown that interaction between SDC-3 and PTN plays a vital role in cancer like prostate or pancreatic carcinomas (34).

2.2.3. Anaplastic leukaemia kinase (ALK)

ALK is a tyrosine kinase transmembrane receptor that belongs to the insulin receptor superfamily. When it was discovered, it was reported as an orphan tyrosine kinase receptor that was regulated during development and with a restricted distribution among tissues (46). ALK contains an extracellular domain, a transmembrane domain, and an intracellular domain. It is in the extracellular domain where it has its characteristic features, with a low-density lipoprotein receptor class A domain (LDL domain) which is surrounded by two MAM (meprin/A5-protein/PTPmu) domains (47).

There is some controversy about whether or not ALK is a PTN receptor, with studies that support the idea (44,48) and others that state that ALK is not a direct receptor of PTN (49-52). Nevertheless, different researchers were able to determine the affinity of PTN to ALK, stating that PTN binds ALK with a Kd of approximately 0.02-0.03 nM (46,53).

2.2.4. Integrins

Integrins are glycoproteins that form heterodimeric cell surface receptors that play an essential role in cell adhesion and migration, morphogenesis, inflammation, cancer, and stem cell renewal (34,42). Integrins consist of an α subunit and a β subunit. The main integrins involved in the binding of PTN are integrin αvβ3 and αMβ2 (or Mac-1). Interestingly, it has been shown that in addition to binding PTN (42,54), integrin αvβ3 can also form a complex with RPTP β/ζ and nucleolin (34).

2.2.5. Others

Depending on the different studies, some other molecules have been described as PTN receptors. Nucleolin, a shuttle protein that connects the nucleus and cytoplasm, was reported to bind both PTN and MK but with a very low affinity (34,44). As mentioned above, it can also form a complex together with RPTP β/ζ and αvβ3. Finally, neuroglycan C is a chondroitin-sulphated proteoglycan that promotes neurite outgrowth, and both PTN and MK bind to its cluster box domain (42).

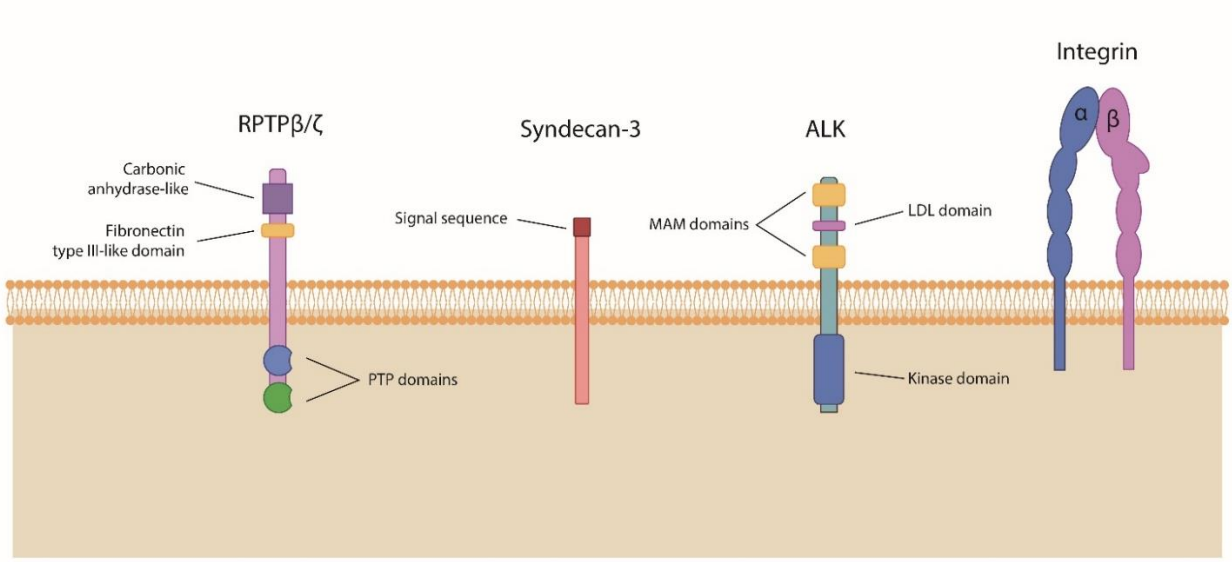

Figure 4. Structure of the receptors of PTN and their principal domains. *From left to right, RPTPβ/ζ (or PTPRZ), syndecan 3, ALK, and integrin.*

2.3. Mechanism of action

PTN can exert its functions through two main signalling pathways: the cell-skeletal remodelling associated and the proliferation, survival and anti-apoptosis associated pathways. The first group includes the PTN/ RPTP β/ζ, Src/FAK and integrin/paxillin pathways and the second one, the MAPK and PI_3K/AKT pathways (42). However, these pathways are not entirely independent and can interfere with each other through crosstalks. In fact, it has been reported that FAK can activate the MAPK and PI_3K/AKT pathways (55).

The signalling pathways also differ on the receptor with which PTN interacts (Figure 5). The binding of PTN to RPTP β/ζ inactivates the tyrosine phosphatase activity that is intrinsic to the receptor. This inhibition renders in a PTN-induced conformational change of RPTP β/ζ, which avoids the access of the substrates to the active site of the receptor (56). As previous studies have demonstrated, PTN favours the dimerization of RPTP β/ζ what blocks the catalytic site and inhibits its phosphotyrosine phosphatase activity directly (41).

PTN/ RPTP β/ζ signalling pathway regulates phosphorylation of downstream targets such as β-catenin, β-adducin, Fyn, G protein-coupled receptor kinase-interactor 1/Cool-associated tyrosine-phosphorylated 1 (GIT1/Cat-1) and GTPase activating protein (GAP) for Rho GTPase (RhoGap). They all play a crucial role in epithelial-mesenchymal transition, cell-cell adhesion, and cell motility and migration (57). Besides, the interaction between PTN and RPTP β/ζ is essential in some cancers, as PTN disrupts the association of β-catenin with E-cadherin necessary for the binding of E-cadherin to the actin cytoskeleton. This directly decreases the stability of the cell adhesions, making them more fragile, and therefore promoting cell metastasis (41).

On the other hand, when blocking syndecan-3, the neurite outgrowth induced by PTN is inhibited. Attached to the cytoplasmic domain of SDC-3 is Src, a non-receptor protein tyrosine kinase (44). It has been postulated that the binding of PTN to SDC-3 may modify Src activity and alter its interaction with cortactin (58). Despite its role in the actin cytoskeleton, several studies have shown that Src might activate Ras, MEK and ERK pathways through its interaction with other factors, and it is also capable of interacting with PI_3K (59).

In the case of ALK, there is controversy about its signalling cascade, with studies that support a direct activation by PTN and others that indicate that the role of PTN is to regulate ALK phosphorylation through its ability to inhibit the phosphatase activity of RPTP β/ζ (56).

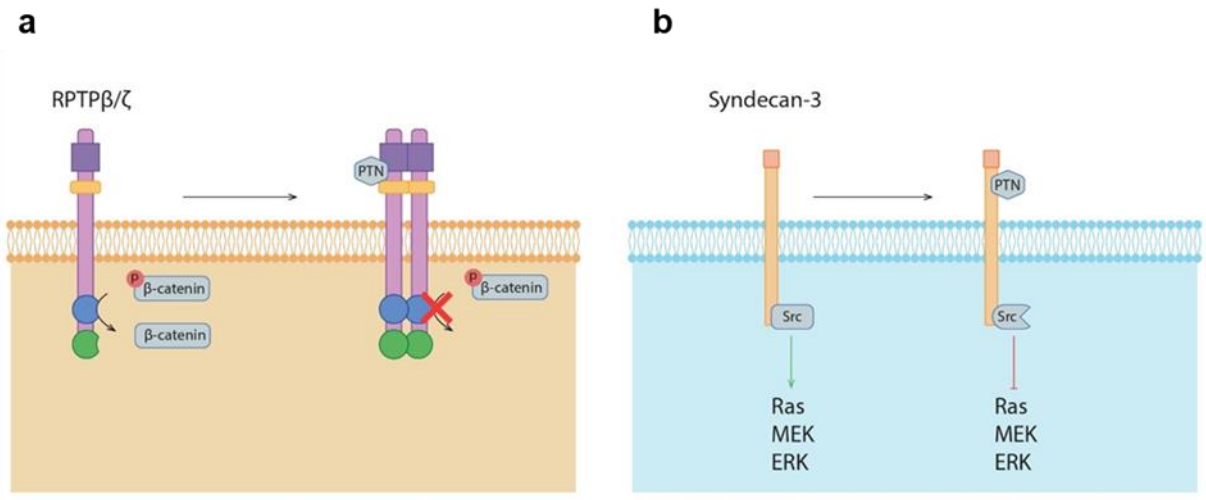

Figure 5. Schematic representation of the main mechanisms of action of PTN. *a) The mechanism of action of PTN on RPTPβ/ζ and b) the mechanism of action of PTN on SDC-3.*

2.4. Biological activities of PTN

PTN and MK are shown to have common activities, and the fact that knock-out animals either for PTN or MK do not present any deleterious defects supports the idea that both cytokines might compensate for each other. However, it has been found that when MK is depleted, PTN expression is enhanced, but not *vice versa* (60), which in turn indicates that the functions of both cytokines might not coincide completely. The differences in the intracellular binding sites between PTN and MK could explain the similar, but not total overlapping, functions of both cytokines.

The biological activities of pleiotrophin include important physiological events (Figure 6), as:

2.4.1. Cell growth and survival

Pleiotrophin is a mitogen that promotes the proliferation of cells from the epithelium, endothelium, and fibroblasts (42). Moreover, PTN stimulates neurite outgrowth in neurons of the central nervous system (CNS), and some researchers suggest that through the peptide Y-P30, it can mediate the stabilisation of axon growth and maturation of the dendritic spine (61,62). Regarding neuron development, neural stem cells (NSC), a subtype of cells that produce newborn neurons, have been shown to secrete PTN to promote the maturation of these new neurons (63).

2.4.2. Development and cell differentiation

During embryo development, the expression levels of PTN are particularly high in the nervous system. Moreover, PTN also participates in the morphogenesis of other organs such as facial processes, limb buds, sense organs (eye and olfactory system) (64), cardiovascular, respiratory, and digestive systems (65). It is important to mention that *Ptn* reaches its maximum expression level around birth (66).

Respecting cell differentiation, PTN can initiate or accelerate the differentiation of oligodendrocytes via an autocrine mechanism (41,67). In fact, *Ptn* deficient mice show a delay in the myelination process (68). Furthermore, pleiotrophin induce the differentiation of neurons by inducing the differentiation of stem cells into dopaminergic neuron-like cells (69).

In peripheric tissues, PTN is likewise involved in adipocyte differentiation and adipose tissue plasticity. Pleiotrophin has been shown to inhibit the maturation of preadipocytes through the PI_3K/AKT/GSK3β/β-catenin pathway. Silencing of *Ptn* in 3T3-L1 cells leads to an increase of PPARγ expression and cellular differentiation (70). In a study from our research group, *Ptn* knocked-out mice exhibit less body fat, enhanced lipolysis, and improved thermogenesis (71). Moreover, we have also demonstrated that *Ptn* deletion favours the browning of white adipose tissue and protects against the development of hepatic steatosis in a model of diet-induced obesity (72).

Finally, pleiotrophin expression decreases in the mammary gland during lobular-alveolar differentiation (73) and ductal development (74), suggesting that PTN can suppress the differentiation of the epithelium.

2.4.3. Angiogenesis

Angiogenesis is defined as a physiological process by which new blood vessels are formed. PTN induces angiogenesis in several model systems *in vivo* (34,41) and *in vitro* (75,76). After an ischemic injury, *Ptn* is only upregulated in the areas with great

neovascularisation. In particular, the cell types expressing *Ptn* are vascular endothelial cells, activated macrophages, and activated astrocytes. On the other hand, the absence of pleiotrophin upregulation in other cells points out the specificity of PTN in regulating the process of formation of new blood vessels (41).

2.4.4. Oncogenesis

Pleiotrophin is considered a protooncogene as it also participates in oncogenesis due to its capacity to promote both cell proliferation and migration as well as angiogenesis.

Ptn expression levels have been shown to increase in a variety of cancerous cell lines such as multiple myeloma, breast cancer and prostate cancer (75-77). In fact, different studies have reported the role of PTN in different types of cancers such as glioblastoma, breast, lung, ovarian and pancreatic cancer, where PTN enhances the angiogenic activity. Moreover, a role for PTN in melanomas, gastrointestinal tumours, testicular and gynaecological tumours, and prostate cancer has also been suggested (38).

In many cancer types, *Ptn* overexpression is associated with metastasis and poor prognosis, although it is necessary to analyse each type of cancer individually since, as with other biomarkers, pleiotrophin could have a dual role.

It is believed that the role of PTN as a protooncogene is due to its interaction with RPTP β/ζ receptor (38), but in some tumours, the primary receptors are syndecan-3 (pancreatic and prostate cancer) (78,79) or ALK (glioblastoma cancer) (80).

2.4.5. Stem cell renewal

Hematopoietic stem cells (HSCs) are undifferentiated or immature cells located in the bone marrow with self-renewal capacity and pluripotency. The self-renewal of these cells is regulated by both intrinsic mechanisms and extrinsic or environmental mechanisms mediated via cell-cell interactions, cytokines, and growth factors (81,82).

In the last decade, several studies have demonstrated that pleiotrophin acts *in vitro* and *in vivo*, promoting the expansion and regeneration of HSCs, respectively. Indeed, it has been shown that after induced myelosuppression, PTN is critical for hematopoietic survival and regeneration (82). Moreover, the mechanisms by which PTN functions in HSCs is by activating PI_3K signalling contributing to bone marrow stem cell expansion (81) and activating the RAS/MEK/ERK pathway in an RPTP β/ζ -dependent manner, which prompts to HSCs regeneration (83).

2.4.6. Tissue repair and inflammation

Pleiotrophin expression levels have been reported to increase following a tissue injury in diverse organs such as the brain (84), peripheral nerves (85), bone marrow (81), bone (86), and liver (87).

PTN is also involved in inflammation, taking part in the chemotaxis of macrophages and neutrophils (42). Indeed, pleiotrophin has a role in diseases characterised by chronic inflammation like rheumatoid arthritis (88). It has been proposed that PTN likely contributes to the inflammatory process due to its role as a mitogen and as an angiogenesis stimulating factor (88). In the liver, after partial hepatectomy, PTN is involved in inflammation and tissue repair by enhancing the recruitment and infiltration of leukocytes (87). Additionally, PTN has been suggested to modulate inflammatory processes through its binding to the integrin Mac-1, a receptor present on the surface of leukocytes (89). Finally, a correlation between fibrosis and pleiotrophin levels has been reported as both PTN levels and *Ptn* mRNA are increased in peritoneal fibrosis (4- and 42-fold, respectively) (90).

On the other hand, pleiotrophin plays a vital role in response to inflammation and tissue damage in the central nervous system. In a series of publications, the research group led by Dr Gonzalo Herradón has demonstrated that PTN is involved in microglial and astrocytic responses promoting neuroinflammation (91,92).

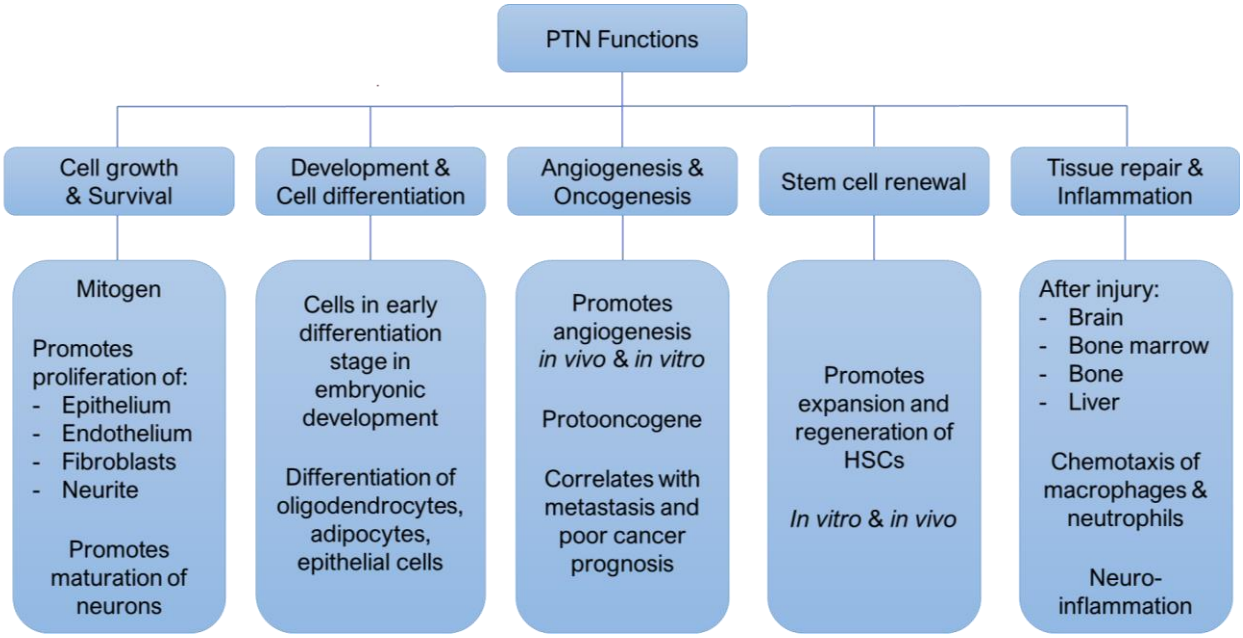

Figure 6. Summary diagram of the main known functions of pleiotrophin. *Image modified from Xu, C. et al. (42).*

2.4.7. Pleiotrophin in the liver

Regarding the role of PTN in the liver, there is not much knowledge yet. Most of the research has been focused on the function of pleiotrophin in hepatocellular carcinoma and liver regeneration after an injury. PTN is considered a mitogen for hepatocytes as it enhances the growth of these cells and their DNA synthesis (93). However, hepatocytes are not the producers of PTN but rather the hepatic stellate cells that subsequently secrete it. Furthermore, the main source of PTN in a healthy liver is the stromal cells (54). It is noteworthy that PTN is a mitogenic factor exclusively for hepatocytes, not for HSC (94).

The expression of the different PTN receptors in the liver has been analysed. None of the hepatic cells expresses ALK, whereas RPTP β/ζ and syndecan expression seem to be induced depending on the cellular conditions, such as injury or treatments that promote increased PTN levels. Additionally, it has been shown that syndecan expression is much higher than that of RPTP β/ζ (93).

As previously mentioned, PTN is expressed mainly during embryonic development and, in the case of the liver, it decreases gradually parallel to the liver bud development progress, suggesting a role of PTN in the early epithelial-mesenchymal interaction (93).

On the other hand, PTN is also necessary for liver regeneration after partial hepatectomy, d-galactosamine (GalN) treatment, and acetylaminofluorene treatment followed by partial hepatectomy. In fact, PTN deficient mice show impaired liver regeneration, enhanced cholestatic liver injury and fibrosis (54,93).

PTN is expressed in a temporary and cell-type dependent-manner, indicating that cells expressing PTN are different between the embryos' organogenesis processes and the adult liver regeneration process. In the foetus, pleiotrophin is expressed in mesenchymal cells and in adults, in HSCs for tissue repair (93).

To sum up, all the available data suggest that pleiotrophin is a growth factor for hepatocytes during developmental and pathological processes in the liver.

2.5. Regulation of pleiotrophin expression

Pleiotrophin is expressed in a developmentally, and in some cases spatially, dependent manner. Even though its expression is restricted in adulthood, during embryogenesis in mice, *Ptn* was reported to have high expression in the brain, digestive and respiratory apparatus, sense organs, limbs, and cartilage and vascular systems (44,54).

The expression of the *Ptn* gene is firmly regulated and is susceptible to a wide range of stimuli. Firstly, it has been shown that *Ptn* expression is upregulated in cells stimulated with

growth factors such as fibroblast growth factor 2 (FGF-2), epidermal growth factor (EGF), and platelet-derived growth factor (PDGF). Some studies have even postulated that pleiotrophin might act as a downstream effector of PDGF (41).

Another very well-known stimulus for increasing *Ptn* expression is the presence of an injury. Levels increase following an incisional wound in the dermis and after ischemic injury in the brain, specifically in endothelial cells, macrophages, and activated astrocytes. Particularly, IFNβ and IFNγ upregulate PTN expression through STAT1 in astrocytes and macrophages, respectively (38). These findings point out a key role for pleiotrophin in differentiation responses in cells with outstanding proliferation characteristics that are usually involved in processes of healing wounds.

PTN expression has been reported to be altered after stimuli of hydrogen peroxide, endothelial nitric oxide synthase (eNOS), cAMP, AP-1, HOXA5, peroxisome proliferator-activated receptor γ (PPARγ) and SOX2 (38).

On the other hand, *Ptn* expression is also conditioned to hormonal regulation. In the uterus, the highest *Ptn* levels are detected in diestrous and the lowest in oestrous, coinciding with the moment when oestradiol serum levels begin to increase (95). Furthermore, *Ptn* expression is upregulated by progesterone (96) and testosterone (97) but attenuated when treated with androgens inhibitors (98).

Finally, recent studies are showing that *Ptn* can also be regulated by micro-interfering RNA (miR). Some of the miRs capable of downregulating the expression of *Ptn* are miR-143, miR-182, miR-384, and miR-137 (99-102).

AIMS AND OBJECTIVES

Ageing and pregnancy are two conditions that lead to the physiological development of insulin resistance. In both situations, insulin resistance is associated with critical changes in carbohydrate and lipid metabolism. Furthermore, both ageing and pregnancy have been shown to have an inflammatory component that contributes to the insulin-resistant state.

Pleiotrophin is a cytokine that is overexpressed in central pathologies with persistent inflammation and has been suggested to potentially share its signalling cascade with insulin. Previous research from our group has demonstrated the novel role of PTN in regulating lipid turnover, thermogenesis, and insulin sensitivity. These preliminary data seem to support our idea that PTN could be one key player in the modulation of carbohydrate and lipid metabolism.

In this scenario, the central hypothesis of this study is that pleiotrophin could be involved in the regulation of the metabolism of the liver in physiological situations associated with insulin resistance, low-grade inflammation, and oxidative stress such as ageing and late pregnancy.

To confirm this hypothesis, we proposed two specific objectives that will be resumed in two chapters that are:

1. The characterization of the role of PTN in the liver in ageing by,
    1.1. Evaluating whether the deletion of *Ptn* is associated with alterations in hepatic metabolism and its possible role in the modulation of the metabolic changes that take place during ageing.
    1.2. Determining if PTN modulates inflammation and endoplasmic reticulum stress in the liver during ageing.
2. The characterization of the role of PTN in liver metabolism during late pregnancy.

GENERAL MATERIALS AND METHODS

1. ANIMAL MODELS AND EXPERIMENTAL GROUPS

PTN genetically deficient female mice (*Ptn*$^{-/-}$) were obtained from The Scripps Research Institute (T. F. Deuel laboratory, La Jolla, USA). Briefly, animals were generated using a targeted clone microinjected into C57BL/6J blastocytes that produce a null allele of *Ptn* and subsequently a chimeric animal. Homozygous mice were obtained by intercrosses between these animals (103). Animals were maintained under regulations established by the Animal Facility from San Pablo CEU University and the European Union Laboratory Animal Care Rules (86/609/ECC directive). The Animal Research Committee of San Pablo CEU University approved all experimental protocols (PROEX 137/14 and PROEX 137/18). As possible, the smallest number of animals was used, and the maximum number of samples were extracted for all the experimental procedures.

Animals were sacrificed after a 6 hour fast, under carbon dioxide anaesthesia by decapitation. Blood was collected in Eppendorf tubes containing 1mg/10µL EDTA. Tissues were rapidly dissected and snap-frozen in liquid nitrogen.

2. *IN VIVO* EXPERIMENTAL TECHNIQUES

2.1. Glucose Tolerance Test

For the glucose tolerance test (GTT), after the obtention of a basal blood sample from 6 hours fasted animals, mice were injected intraperitoneally with a dose of 2g of glucose/kg of body weight. Glucose determination was performed in blood at different times (5, 10, 15, 20, 30, 45, and 60 minutes after glucose administration) in all animals using test strips attached to a blood glucose monitoring system (Accutrend GC®, Roche). Areas under the curve (AUCs) for glucose were calculated for each experimental group.

2.2. Pyruvate Tolerance Test

For the pyruvate tolerance test (PTT), after the obtention of a basal blood sample 18 months old mice fasted for 15 hours were injected intraperitoneally with a dose of 2g of pyruvate/kg of body weight. Glucose was analysed in blood at different times (15, 30, 45, 60, 90, and 120 minutes after pyruvate administration) using test strips attached to a blood glucose monitoring system (Accutrend GC®, Roche). Areas under the curve (AUCs) for glucose were calculated for each experimental group.

2.3. Glycerol Tolerance Test

For the glycerol tolerance test, after the obtention of a basal blood sample 18 months old mice fasted for 15 hours were injected intraperitoneally with a dose of 2g of glycerol/kg of

body weight. Glucose determination was performed in blood at different times (15, 30, 45, 60, 90, and 120 minutes after glycerol administration) in all animals using test strips attached to a blood glucose monitoring system (Accutrend GC®, Roche). Areas under the curve (AUCs) for glucose were calculated for each experimental group.

3. EX VIVO EXPERIMENTAL TECHNIQUES

3.1. Plasma biochemical parameters determination

3.1.1. Glucose analysis

Glucose determination was performed by a colourimetric enzymatic assay using the glucose oxidase-peroxidase method (Spinreact, Spain) based on the following reactions:

$$\beta\text{-D-Glucose} + O_2 + H_2O \xrightarrow{GOD} \text{Gluconid acid} + H_2O_2$$

$$H_2O_2 + \text{Phenol} + \text{4-AP} \xrightarrow{POD} \text{Quinone} + H_2O$$

To accomplish the assay, 5µL of plasma sample and 250µL of reactive were used. After a 10 minutes incubation at 37ºC, absorbance was measured at 505 nm using the SPECTROstar Nano plate reader (BMG LABTECH).

3.1.2. Insulin analysis

Insulin was measured using the immunoassay Mercodia Mouse Insulin ELISA (Mercodia, Sweden), based on the incubation of 10 µL of the plasma sample with specific monoclonal antibodies directed against separate antigenic determinants on the insulin molecule. During the 2h incubation, insulin in the sample reacts with anti-insulin antibodies bound to microplate wells and peroxidase-conjugated anti-insulin antibodies. A simple washing step removes unbound enzyme labelled antibody. The bound conjugate is detected by reaction with 200 µL of 3,3',5,5'-tetramethylbenzidine (TMB). The reaction is stopped by adding 50 µL of acid to give a colourimetric endpoint that is read spectrophotometrically at 450nm with the SPECTROstar Nano plate reader (BMG LABTECH). The kit has an assay range of 0.2-6.5 µg/L and a detection limit lower than or equal to 0.2 µg/L.

3.1.3. Cholesterol analysis

Total cholesterol was determined using the colourimetric enzymatic CHOD-POD commercial kit (Spinreact, Spain) following the instructions of the assay.

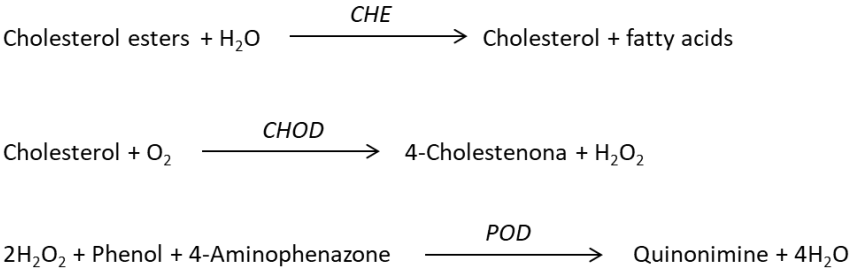

For the assay, 5 µL of plasma or the supernatant after VLDL and LDL precipitation (see below) were mixed with 200 µL of working reagent and incubated for 5 min at 37ºC. The absorbance was measured at 505nm in the SPECTROstar Nano microplate reader (BMG LABTECH).

3.1.4. Triacylglycerols analysis

Quantification of triacylglycerols in plasma was carried out with triacylglycerides GPO-POD kit (Spinreact, Spain), that is based on the following reactions:

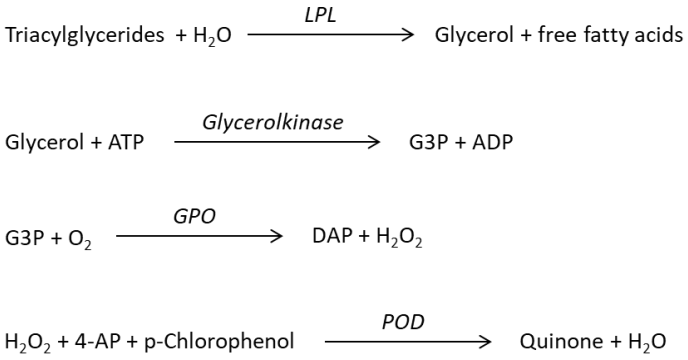

For the assay accomplishment, 5 µL of plasma were mixed with 200 µL of working reagent. After 5 min incubation at 37ºC, absorbance was read at 505nm in the SPECTROstar Nano microplate reader (BMG LABTECH).

3.1.5. HDL and VLDL/LDL analysis

HDL cholesterol (HDLc) was measured using the HDLc-P commercial kit (Spinreact, Spain). This kit contains phosphotungstate and magnesium ions that precipitate the very low density (VLDL) and low density (LDL) lipoproteins from the plasma sample, whereas the high density (HDL) lipoproteins remain in the supernatant. Cholesterol-HDL determination is then performed in the supernatant using the colourimetric enzymatic CHOD-POD commercial kit (Spinreact, Spain), as previously described.

For the precipitation assay, 25 µL of the plasma sample were incubated with 2.5 µL of precipitating reagent for 10 min at room temperature and then centrifuged at 12000 rpm for

10 min. The supernatant was collected into a new tube, and 5 µL of the supernatant were used for cholesterol determination as indicated in 3.13. After 5 min incubation at 37ºC, the absorbance was measured at 505nm in the SPECTROstar Nano microplate reader (BMG LABTECH). To calculate the LDL cholesterol (LDLc), the Friedewald formula was used as shown below:

$$LDLc = Total\ cholesterol - HDLc - \left({}^{Triacylglycerides}/_{5}\right)$$

3.1.6. Ketone bodies analysis

Ketone bodies concentration in the plasma of *Ptn*$^{+/+}$ and *Ptn*$^{-/-}$ mice was determined using a commercial kit (Megazyme, Ireland), based on the measurement of D-3-hydroxybutyrate. The assay involves two enzymatic reactions, the first one catalysed by 3-hydroxybutyrate dehydrogenase and the second one by diaphorase:

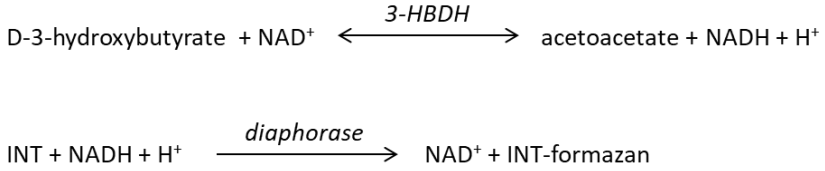

To perform the assay, 10 µL of plasma sample were mixed with 50 µL of buffer, 20 µL of NAD^+/Iodonitrotetrazolium (INT) and 2 µL of diaphorase. The mixture was incubated for 2 minutes. After measuring the absorbance at 492 nm (A_1), 2 µL of 3-hydroxybutyrate dehydrogenase (3-HBDH) were added to start the reaction, and the mix was incubated for 6 additional minutes. Absorbance was measured again at 492 nm (A_2) in the SPECTROstar Nano microplate reader (BMG LABTECH). All the incubations were performed at 25ºC. INT is an electron acceptor that, on reduction processes, forms formazan, a red dye that can be used in colourimetric assays.

The calculations to determine the total concentration of ketone bodies are:

$$D-3-\text{hydroxybutyrate}\ (g/L) = \frac{\Delta A_{sample}}{\Delta A_{standard}} * \ g/L\ standard$$

3.2. Lipid extraction and separation

3.2.1. Lipid extraction

Lipids were extracted from 100 mg of liver tissue as described (72). Extraction was carried out by the incubation of the tissue with a mixture of chloroform:methanol in a 2:1 (v/v) proportion for 24 hours with agitation. Subsequently, the organic solvent was removed and

stored. On the residual tissue, two more extractions equal to the previous one were performed for 2 hours. All aliquots of organic solvent were put together, and the final volume of the extract was made up to 6.5 ml with chloroform:methanol 2:1 (v/v).

To purify the extract, the extract was washed 3 times. The first wash was performed with 2.5 ml of distilled water and the other two washes with 2% NaCl. In the first two washes, after the removal of the aqueous phase, the volume of the lipid extract was made up to 6.5 ml with methanol. After the final wash, the volume of the lipid extract was made up to 6.5 ml with 2:1 chloroform:methanol.

Two aliquots of 2 ml of each sample were dried, and the total lipid content was determined by gravimetry. Lipid content was expressed as mg of lipids/ g of tissue. A standard of cholesterol formate with a final concentration of 0.2 mg/ml was used.

3.2.2. Lipid fractions separation by thin layer chromatography (TLC)

Lipid fractions separation was carried out following the protocol described by Ruiz (104). The TLC technique requires two phases: a stationary phase and a mobile phase. The stationary phase used here consisted of a plate of silica gel 60 F_{254} (Merck, Germany), and the mobile phase was a solvent mixture. Lipids migrate depending on their polarity, which makes them traceable when compared with different patterns. The pattern used for the identification of lipid fractions contained: phosphatidylcholine, free cholesterol, cholesterol oleate, oleic acid, and triolein. In addition, the standard of cholesterol formate was also included in the pattern.

For the TLC, dry lipids were resuspended in 300 µL of toluene. Next, 4.5 µL of pattern and samples (in duplicates) were placed in the silica plate. Following that, the plate was immersed consecutively in three mixtures of different solvents:

- Mixture 1: Chloroform: methanol: formic acid, 25:50:25
- Mixture 2: n-Heptane: diisopropylether: acetic acid, 70:30:2
- Mixture 3: Heptane

The lipid fractions were visualized by placing the plate in 10% $CuSO_4$ (v/v) and 8% phosphoric acid (v/v) for 5 seconds. Finally, the plate was incubated at 200ºC for 4 minutes, which improves the sharpness of the bands. Lipid fractions were quantified using ImageJ software (NIH, USA). With the data obtained from the patterns, samples were interpolated to calculate the exact concentration of each lipid fraction.

3.3. Histology

Livers from 18 days-pregnant, 6 and 15 months-old *Ptn*$^{+/+}$ and *Ptn*$^{-/-}$ mice were paraffin-embedded in tissue blocks, and several sections were mounted on slides. Sections were stained with hematoxylin-eosin. Sections were scanned and visualized with Aperio ImageScope software (Leica Biosystems, Spain).

This work has been done in collaboration with the Institute of Applied Molecular Medicine (IMMA) at San Pablo CEU University and the *Mechanism of lipotoxicity in animal models* (LIPOBETA) research group at Universidad Rey Juan Carlos.

3.4. Gene expression analysis

3.4.1. RNA extraction

Total RNA was extracted from 30 mg of liver tissue using NZY Total RNA Isolation kit (Nzytech, Portugal), following the manufacturer's instructions. RNA quantity and quality were determined using the spectrophotometer NanoVue Plus (GE-Healthcare, England). RNA was stored at -80ºC until required.

The 260/280 ratio expresses the purity of the RNA extracted, as 260 nm is the absorbance peak of nucleic acids and 280 nm is the absorbance peak of proteins. The value of the ratio must be ranged between 1.8 and 2 to be accepted as pure RNA. Abnormal 260/280 ratios could indicate contamination with phenol derived from the extraction protocol.

3.4.2. cDNA synthesis

Reverse transcription (RT) from RNA to cDNA was performed using the First-strand cDNA Synthesis kit (Nzytech, Portugal). The protocol for the first-strand cDNA synthesis is as follows:

10 µL of NZYRT 2x Master Mix (containing the primers, dNTPs, $MgCl_2$, and an optimized RT buffer) + 2 µL of NZYRT Enzyme Mix (Reverse Transcriptase) + RNA of each sample (2 µg) + H_2O (up to 20 µL of total volume).

The RT-PCR was carried out in the Eppendorf Mastercycler gradient using the following program: 10 min at 25ºC, 30 min at 50ºC, and 5 min at 85ºC.

Next, samples were chilled on ice, 1 µL of RNase H was added to each sample and incubated for 20 min at 37ºC. RNase H specifically degrades the RNA template in cDNA-RNA hybrids after the first-strand cDNA synthesis. cDNA was stored at -20ºC until required.

3.4.3. Quantitative Real-Time PCR

The study of gene expression was carried out by real-time PCR using the thermal cycler CFX96™ Real-Time System (Bio-Rad Laboratories, USA). 3 µL of cDNA (15ng) and 12 µL of the reaction mix were used. The mix contains 7.5 µL of QUANTIMIX EASY KIT (Biotools, Spain), 2.5 µL of dH_2O and 1/1 µL of forward and reverse primers (1µM). Biotools kit includes DNA polymerase, dNTPs, $MgCl_2$, and the reaction buffer, including the fluorophore (SybrGreen). The dynamic range for each primer pair was assessed with a standard curve using a pooled sample and the appropriate dilution factors. Amplification efficiency for all primer pairs was determined from the standard curve slope and ranged between 90% and 110%. The real-time program was run following the manufacturer's indications (see Figure 7). The amount of fluorescence emitted is proportional to the amount of amplification product obtained in the PCR.

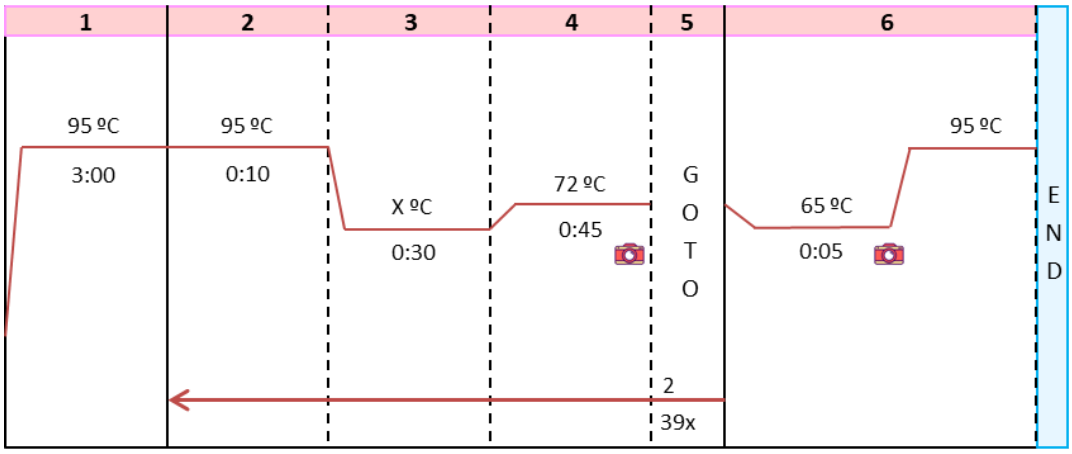

Figure 7. RT-qPCR protocol for gene expression analysis. *The first step consists of an initial denaturation of the cDNA (1). Following is the amplification process with 3 phases: denaturation, annealing, and elongation (2, 3, 4) repeated 40 times. Finally, the program performs the melting curve analysis (6). X represents the annealing temperature, and it varies depending on the primers used.*

Primer sets used for gene expression analysis are shown in **Appendix 1**. The relative expression of each gene was normalized against *Hprt* and *Rpl13* used as reference standards.

The $2^{-\Delta\Delta CT}$ or Livak method was used for relative gene expression analysis. Target and reference genes efficiencies were determined, and all were similar and near 100%, confirming that this method is suitable for the analysis. The Livak method consists of three steps:

- First, normalize the C_T of the target gene to the C_T of the reference gene for both test and calibrator samples:

$$\Delta C_{T(test)} = C_{T\,(target)} - C_{T\,(reference)}$$

$$\Delta C_{T\,(calibrator)} = C_{T\,(target)} - C_{T\,(reference)}$$

- Second, normalize the ΔC_T of the test sample to the ΔC_T of the calibrator:

$$\Delta\Delta C_T = \Delta C_{T\,(test)} - \Delta C_{T\,(calibrator)}$$

- Third, calculate the expression ratio:

$$2^{-\Delta\Delta C_T} = Normalized\ expression\ ratio$$

3.5. Protein expression analysis

3.5.1. Total protein isolation

For protein extraction, 30 mg of liver tissue was homogenized in a buffer containing 30mM HEPES, 5mM EDTA, 0.5% sodium deoxycholate, 1% Triton X-100, 8mM Na_3VO_4, 1mM NaF and 2mM of protease inhibitor mixture (Roche Diagnostics, Spain). Tissue disintegration was carried out using the TissueLyser LT (Qiagen, USA) programmed at 45 Hz for 4 min. Cellular debris was discarded by centrifugation at 14000 rpm at 4ºC for 30 min. The supernatant was collected, and an aliquot was taken for later determination of protein concentration.

3.5.2. *Nuclear extracts and cytoplasmic protein isolation*

For the extraction of cytoplasmic and nuclear protein fractions, 100 mg of liver tissue was homogenized using a Potter-Elvehjem PTFE pestle (Sigma-Aldrich, USA), with cold PBS 1X. Samples were maintained on the ice during the whole course of the extraction process. After homogenization, the homogenate was centrifuged at 10000g for 15 min at 4ºC. The supernatant was discarded. The pellet was resuspended by pipetting in 75 µL of a cold buffer A (10mM HEPES, 0.2mM EDTA, 10mM KCl, 0.1% β-mercaptoethanol, 1mM Na_3VO_4, 5mM NaF, 0.1mM protease inhibitor mixture (Roche), 0.6% IGEPAL CA-360). The mix was incubated for 30 min on ice and then centrifuged at 10000g for 5 min at 4ºC. The supernatant contains the cytoplasmic protein fraction. Next, the pellet was once again resuspended in 50µL of a cold buffer B (20mM HEPES, 2mM EDTA, 420mM NaCl, 0.1% β-mercaptoethanol, 1mM Na_3VO_4, 5mM NaF, 0.1mM protease inhibitor mixture (Roche Diagnostics, Spain)) and incubated 30 min on ice. Afterwards, the mixture was centrifuged at 12000g for 10 min at 4ºC. The supernatant is the nuclear protein extract.

An aliquot of each fraction was collected to determine the protein concentration. The remaining supernatant was stored at -80ºC until required.

3.5.3. Protein quantification by BCA

Protein quantification was performed by the bicinchoninic acid (BCA) method using the commercial Pierce BCA Protein Assay Kit (Thermo-Scientific, USA). The assay combines the reduction of Cu^{2+} by proteins in an alkaline medium (biuret reaction) with the colourimetric detection of the cuprous cation by BCA. The coloured reaction product obtained with this method results from the chelation of two molecules of BCA with one cuprous ion. The purple complex formed exhibits a maximum absorbance at 562 nm.

For this assay, 25 µL of sample or BSA protein standard and 200 µL of working reagent were used. The BCA working reagent was prepared by mixing 50 parts of BCA Reagent A with 1 part of BCA Reagent B. Reaction mix was incubated at 37ºC for 30 minutes, and absorbance was measured at 562 nm using the SPECTROstar Nano microplate reader (BMG LABTECH).

3.5.4. Protein quantification by Bradford

Protein concentration of both cytoplasmic and nuclear fractions was measured using a Bradford assay (PanReact AppliChem, Spain) due to the interference of the components of the nuclear extraction buffers with the BCA method. The Bradford method is based on the absorbance of an acid solution of Coomassie Brilliant Blue G-250. When the dye binds to proteins, the absorbance shifts from 465 nm to 595 nm. Hydrophobic and ionic interactions in the reaction stabilize the dye in its anionic form, causing a colour change from brown to blue. The assay range is 5-25 µg/ml.

For this method, 200 µL of Bradford reagent were added to 20 µL of sample or standard (albumin solution). The absorbance was read at 595 nm in the SPECTROstar Nano microplate reader (BMG LABTECH).

3.5.5. Electrophoresis and immunodetection

All protein samples were mixed with 3X Laemmli buffer and adjusted to a final concentration of 1.5 mg/mL total protein, 2% SDS, 10% glycerol, 5% β-mercaptoethanol, 62.5 mM Tris-HCl, and <0.01% bromophenol blue. Samples were boiled at 96ºC for 5 minutes and centrifuged at 15000 rpm for 20 minutes.

30 µg of protein were loaded onto SDS-polyacrylamide gels (7.5-12% depending on the molecular weight of the target protein). Electrophoresis was run at 25 mA for 60 min using a

running buffer containing 0.25M Tris-HCl, 1.92M glycine and 1% SDS. A molecular weight marker (NZYColour Protein Marker II, Nzytech, Portugal) was also included in each run.

Proteins were transferred to PVDF membranes (Amersham-GE Healthcare, United Kingdom) at 250 mA for 45 min in an ice-cold buffer. Transfer buffer contains 0.25M Tris-HCl, 0.192M glycine, 0.2% SDS and 20% methanol. Once the transference was completed, membranes were blocked with 10% skimmed powder milk in TBST (10mM Tris-HCl, 0.15M NaCl, and 0.05% Tween, pH 8) for 30 minutes at room temperature to avoid antibodies non-specific bindings.

After blocking, membranes were washed and probed overnight at 4ºC with specific primary antibodies prepared in a 5% BSA solution with TBST and 0.05% NaN_3. See **Appendix 2** for primary antibodies characteristics and dilutions. After the incubation, membranes were washed with TBST buffer to remove traces of primary antibody and incubated for 30 minutes with a peroxidase-labelled secondary antibody (Sigma-Aldrich, USA) in 10% skimmed milk and TBST solution as indicated in **Appendix 2**. Finally, secondary antibody was discarded, and membranes were washed 3 times for 10 minutes with TBST buffer.

Proteins were visualized by chemiluminescence using ECL (GE-Healthcare, England) or Affinity® ECL Western Blotting Substrate (Affinity Biosciences, USA) commercial kits and the ChemiDoc™XRS+ system (Bio-Rad Laboratories, USA). The bands were quantified using ImageJ software (NIH, USA).

3.6. Primary mouse hepatocytes isolation

Primary mouse hepatocytes were isolated from non-fasted C57BL/6J animals. Mice were killed by neck dislocation, and the abdominal area was exposed from the bladder to the liver. The inferior vena cava was cannulated, and the liver was perfused with 20-25 ml of HBSS to wash out the blood and circulating cells from the liver as well as to eliminate calcium via EGTA until the liver turned yellow-white. See **Table 1** for the composition of all solutions used.

When the liver was completely clean, it was perfused with 10 ml of a collagenase solution. As digestion progressed, the liver began to soften. The liver was dissected out with forceps, the gall bladder was removed, and the liver was transferred into a petri dish containing warm plating media. The liver sack was opened with fine tip forceps along the liver surface, and the cells were gently released by shaking the tissue. The cell suspension was homogenized using a 10 mL pipette, and the crude homogenate preparation was filtered through a 70 µm cell strainer (Corning®, Sigma-Aldrich) into a 50 mL falcon tube.

Cells were centrifuged at 50g for 5 min, the supernatant was discarded, and the pellet was resuspended in 10 mL of fresh plating media. The cell suspension was mixed with a Percoll solution (Sigma-Aldrich, USA) to isolate the hepatocytes from the crude homogenate and centrifuged at 110g for 10 min. The pellet obtained containing the hepatocytes was resuspended and washed in 20 mL of fresh plating media by centrifuging it at 50g for 5 min twice. After the last wash, cells were resuspended in an appropriate volume of plating media.

Table 1. *Solutions used for primary hepatocytes isolation from a mouse model.*

Solution	Composition
HBSS solution	HBSS, no calcium, no magnesium (Gibco, Thermo-Scientific) 1M HEPES (Gibco, Thermo-Scientific) EGTA (Sigma-Aldrich)
Collagenase solution	William's E Medium (Gibco, Thermo-Scientific) Collagenase from *Clostridium histolyticum* (IV) (Sigma-Aldrich) 1M HEPES (Gibco, Thermo-Scientific)
Plating media	DMEM High glucose (Gibco, Thermo-Scientific) 10% fetal bovine serum (Gibco, Thermo-Scientific) 0.001mM dexamethasone (Sigma-Aldrich) 1% Penicillin-Streptomycin (Gibco, Thermo-Scientific)

3.7. Cell culture of primary cells

To calculate the cell viability, an aliquot of cell suspension was mixed with Trypan Blue 0.4%, and cells were counted in a Neubauer counting chamber. Empty plates were coated with a solution of collagen (diluted 1/10 with PBS 1X) (Sigma-Aldrich, USA). After incubating the plates with the collagen solution for 10-20 min, the wells were washed with PBS and let dry for 30 min-1h. Cells were seeded in collagen-coated 12-well plates at a density of 150,000 cells/well with plating media and maintained in this medium for 24h to let the cells attach to the plate. Then the medium was changed according to the different experiments.

3.8. Seahorse studies in primary hepatocytes

Prior to the start of the XF assay, 10,000 cells/well were seeded into an XF cell culture microplate and let to attach for 24h in plating media. On the day of the assay, the medium was changed to low-glucose media (DMEM glucose-free (Gibco, Thermo-Scientific, USA), supplemented with 5.5 mM glucose (Sigma-Aldrich, USA)), and some of the wells were supplemented with 0.1 µg/mL of recombinant mouse PTN (R&D Systems, USA). For the

specific design of the experiment, see Figure 8. Cells were incubated in this medium for 3 hours.

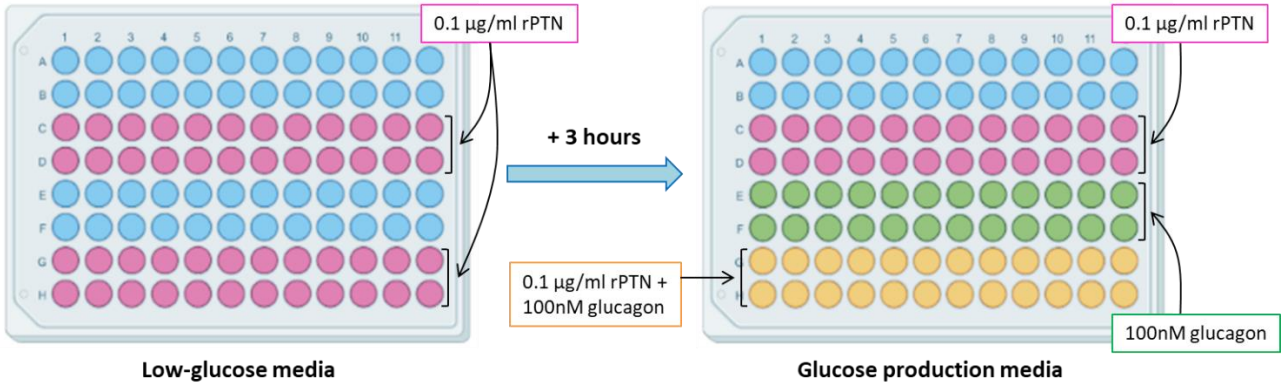

Figure 8. Primary hepatocytes Seahorse experimental design. *On the left side, cells were starved in a low-glucose media for 3 hours, and half of them were pre-treated with 0.1 µg/ml rPTN. On the right side, after starvation, cells were placed in glucose production media and were incubated with the glucose production media in the presence or absence of 0.1 µg/ml rPTN and or 100nm µg/ml rPTN and or 100nm glucagon. Image created with BioRender.com*

After the incubation, cells were washed with PBS, and glucose production media was added (DMEM glucose-free medium supplemented with 20 mM lactate (Sigma-Aldrich, USA), 2 mM pyruvate (Sigma-Aldrich, USA), 2 mM glutamine (Gibco, Thermo-Scientific, USA)). Cells were treated with or without 0.1 µg/mL of recombinant PTN in the presence or absence of 100 nM glucagon (Sigma-Aldrich, USA).

For the measurement of the oxygen consumption rate (OCR) of live cells, the assay cartridge was placed into the XF analyzer to allow automatic calibration of the sensors. After the calibration, the 96-well cell culture plate was inserted into the instrument. To determine mitochondrial OCR and the potential effects of PTN and glucagon, final concentrations of 5 µM oligomycin, 0.5 FCCP (Carbonyl cyanide-4-(trifluoromethoxy)phenylhydrazone), 2.5 µM FCCP (Carbonyl cyanide-4-(trifluoromethoxy)phenylhydrazone), and 4 µM rotenone/antimycin A were injected individually into the media in each well.

4. STATISTICAL ANALYSIS

Results are expressed as mean ± SEM. A Grubbs' test was run to detect outliers. Statistical comparisons between two groups were made using the unpaired Student's t-test; when variances were not equal, the analysis was made by the Mann-Whitney test.

On the other hand, comparisons between three or more groups were made using one or two-way ANOVA followed by Bonferroni's post hoc test. To check if data is normally

distributed, a Shapiro-Wilks test was performed. When data were not normally distributed, the statistical tool of choice was the Kruskal-Wallis test. All analyses were done using GraphPad Prism v8 (San Diego, CA, USA).

CHAPTER I. AGEING

1. INTRODUCTION: AGEING

In 2019, the United Nations established the European population aged 65 or over in 140,410 thousand and estimated that by 2050 this value would reach almost 200 million. Specifically in Spain, in 2019, the population aged 65 or over was around 9 million, while in 2050, it is estimated to be around 16 million. Moreover, the world's population aged 80 years or older is expected to triple between 2019 and 2050, reaching a 102.6% increase in Europe and North America (105).

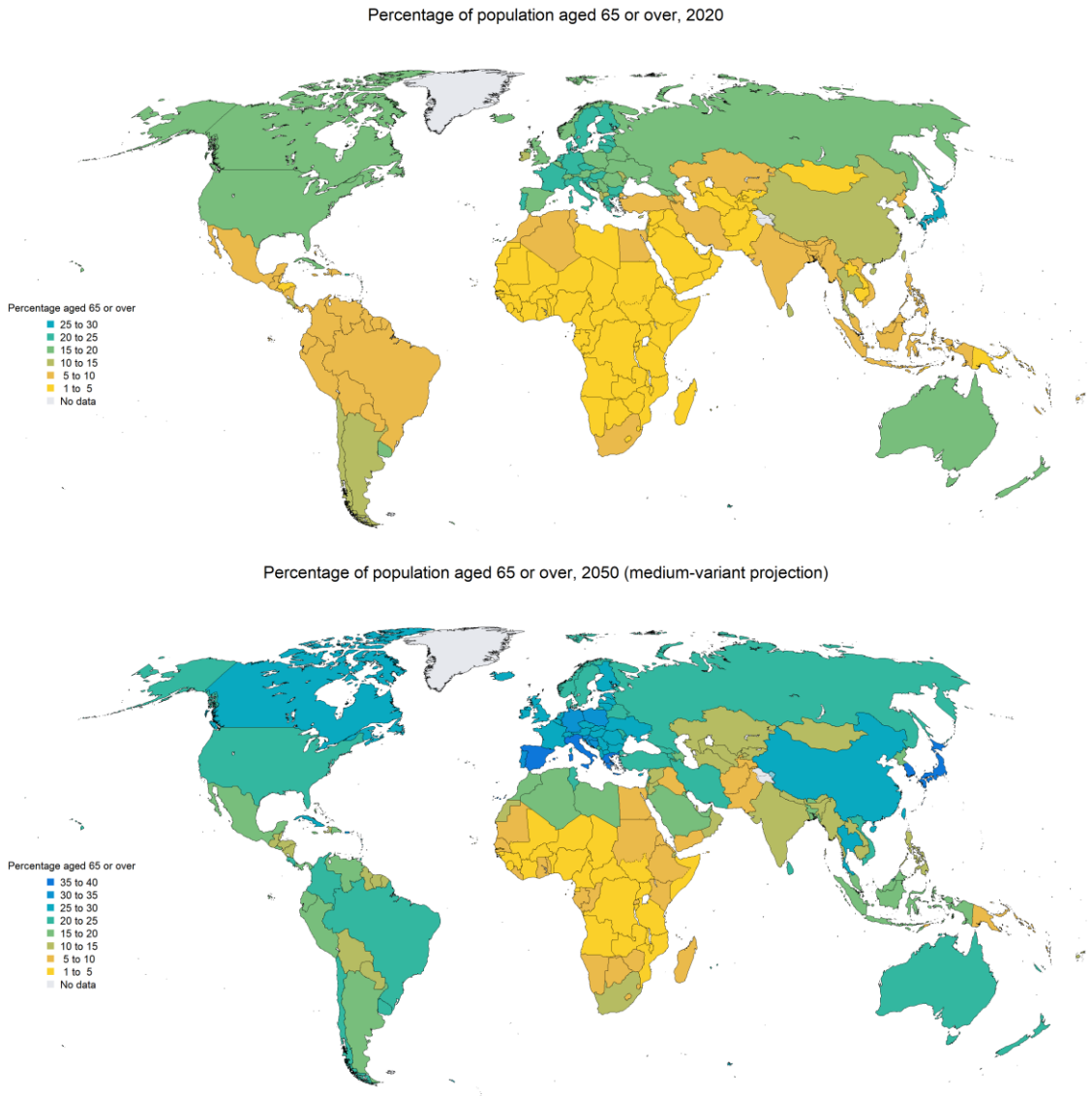

Figure 9. Representation of the evolution of world population aged 65 years or over in 2020 and the projections for 2050. *Source: United Nations, Department of Economic and Social Affairs (DESA), Population Division. World Population Prospects 2019. https://population.un.org/wpp/*

Ageing entails both physical and mental ailments such as inflammatory, neurodegenerative, metabolic, and cardiovascular diseases (106). In fact, the ageing of the population is currently putting financial pressure on old-age support systems, and as

projections point out, this will be even greater in the upcoming years. Therefore, it is essential to improve the elderly's quality of life and prevent age-related pathologies.

Focusing on the cardiovascular and metabolic perspective, the most predominant pathologies in aged people are obesity and type 2 diabetes (T2D), with approximately 66% and 14% incidence respectively in the population over 65 years, being the third pathology more prevalent atherosclerosis (106). In humans and rodents, ageing is associated with a decrease in insulin sensitivity (107), a characteristic symptom of obese and T2D patients.

1.1. The physiological process of ageing

Ageing is a physiological and multifactorial process associated with the progressive degeneration of organ systems and tissues and with the inability to activate and/or modulate adaptive homeostasis. The *"hallmarks of ageing"* are the biochemical changes that occur during biological ageing and include: genome instability, telomere attrition, epigenetic alterations, loss of proteostasis, deregulated nutrient sensing, mitochondrial dysfunction, cellular senescence, stem cell exhaustion and altered intercellular communication (108-110). Although these events should be considered as a set of mechanisms that help to understand the process of ageing (109), there is an overlap between the hallmarks and the pathogenesis of some chronic diseases (110).

Ageing has different consequences on the different tissues. It increases lipid accumulation in adipose tissue but also increases fat deposition in other organs like the muscle, the liver, and the bone marrow (111). During ageing, the fat distribution also varies, shifting from subcutaneous adipose tissue (SAT) to visceral adipose tissue (VAT) (112). Ectopic fat deposition and fat depot redistribution, especially in overweight and obese patients, have been associated with increased age-related cardiometabolic disease. The accumulation of ectopic fat has a lipotoxic effect in the tissues (113,114) and is associated with a higher risk of developing metabolic disorders including hypertension, atherosclerosis, hyperlipidaemia, insulin resistance and diabetes.

Besides, adipocytes are also affected by ageing, as their carbohydrate and lipid metabolism is altered, as well as the secretion of adipokines. Serum levels of leptin are known to steady increase with age, but studies with rodents have demonstrated that old animals have a lower response to this cytokine due to reduced leptin sensitivity. In fact, leptin resistance is associated with the age-related increase of adiposity and leads to impaired regulation of the energy balance by leptin (115,116). On the other hand, adiponectin is a cytokine that favours insulin sensitivity, reducing the risk of developing diabetes. In fact, a negative correlation has been detected between insulin levels, the HOMA-IR index, and adiponectin plasma levels (117). During ageing, circulating levels of

adiponectin decrease, which has been associated with higher mortality. Furthermore, several studies have shown that both long-lived rodents and centenarian humans have significantly higher adiponectin levels (117-119).

Skeletal muscle maintains the skeleton, permits locomotion, and plays a pivotal role in whole-body metabolic homeostasis. During ageing, there is a loss in muscle mass, which leads to an age-related functional impairment of the extremities (upper and lower), and various degrees of inability to perform the daily activity and decreasing the quality of life of the elderly (120). In fact, sarcopenia, the atrophy of the skeletal muscle and the decline in its strength, is also considered a hallmark of ageing in the muscle (121). Even though the molecular mechanisms underlying loss of muscle mass with age are still unclear, numerous studies highlight the multifactorial nature of sarcopenia and point out the factors involved in its development: hormone imbalances (122), chronic inflammation (123,124), neurodegeneration (125), ectopic fat deposition (126), impaired satellite cell functionality (127), increased oxidative stress (128,129) and the decline in mitochondrial function (121). Aside from muscle mass loss, skeletal muscle is considered the primary organ for glucose disposal and one of the biggest stores of amino acids. In the muscle, insulin stimulates glucose uptake and contributes to the modulation of blood glucose levels. Ageing is associated with impaired muscle metabolism, including mitochondrial dysfunction and insulin resistance (130), and it is linked to reduced (131) or retarded (132) muscle regeneration and enhanced fibrosis after injury (133).

During ageing, the central nervous system experiences anatomical and morphological changes. Neurodegeneration and dementia are also common features related to age. One of the main changes observed in aged brains is 11% of brain weight loss (134). This decrease might be associated with the loss of neurons, glial cells or myelin. Brain ageing encompasses various processes such as impaired protein homeostasis that usually turns to the development of inclusion bodies, DNA damage and epigenetic changes, dysregulation of the lysosomal function and immune dysregulation (135). However, aged brains have also been reported to accumulate proteins, carbohydrates, and lipids (136), indicating that metabolic pathways may be altered. Nevertheless, the most common impairment seems to be defective proteostasis. Several studies have reported increased accumulation of specific altered proteins in aged brains, including TAU and β-amyloid peptide (hallmarks of Alzheimer disease), α-synuclein and Lewis bodies (hallmarks of Parkinson disease and dementia), and the TAR DNA binding protein 43 (TDP43) (involved in frontotemporal dementia and motor neuron disease, FTD-MND) (134,135,137).

The endocrine system regulation has also been shown to suffer a wide range of changes during ageing. However, these alterations are highly variable amongst individuals. The

thyrotropic axis and, thus, the concentration of thyroid hormones is one of the endocrine axes modulated by the ageing process. Data from different studies (138,139) suggest that the activity of the thyroid hormone axis declines with age, which is reflected in increasing concentrations of the thyroid-stimulating hormone and a decrease in free triiodothyronine (T_3).

Somatotropin or growth hormone (GH) is the main component of the somatotropic axis and stimulates IGF-1 secretion. Ageing is accompanied by a progressive decrease in growth hormone secretion and, therefore, lower IGF-1 concentrations. Studies in mice have shown that downregulated activity of the GH/IGF-1/insulin pathway could be beneficial for extended longevity (140). However, these findings have not been corroborated in humans.

Furthermore, ageing affects endocrine factors involved in the regulation of appetite and food intake. Appetite and food intake decrease with normal ageing, predisposing to the development of under-nutrition. The hormonal changes involved in the anorexia of ageing include increased activity of cholecystokinin, leptin and various cytokines and reduced activity of ghrelin and testosterone (141).

Age also affects the adrenal axis headed by glucocorticoids and dehydroepiandrosterone (DHEA). Ageing is related to impaired concentration and irregular secretion patterns of cortisol. However, it is not well established whether these changes are due to age *per se* or reflects other effects such as the presence of low-grade inflammation that ultimately is associated with ageing. On the other hand, secretion of DHEA and of its sulphate (DHEAS) steadily decreases over time. In fact, higher concentrations of DHEA and DHEAS are linked to improved muscle strength and bone density and immunoregulatory and anti-inflammatory actions (138).

Changes in sex hormones are also common with ageing and are usually referred to as menopause in females (oestrogen) and andropause in males (testosterone).

Women in the menopause phase present lower concentrations of serum oestradiol and increased follicle-stimulating hormone (FSH) and luteinizing hormone (LH) compared to younger women. Consequences of these alterations in serum levels include a higher risk of cardiovascular disease, accelerated loss of skeletal mass, vasomotor instability or hot flushing, and atrophy of oestrogen responsive tissue (ovaries and vagina). During menopause and ageing, oestrogen withdrawal is also associated with the loss of bone, enhanced bone sensitivity to the parathyroid hormone, and decreased intestinal calcium absorption dependent on oestrogen. In addition to oestrogen fall, menopausal women experience a reduction in testosterone levels, which can relate to decreased libido (139).

Andropause is defined as a progressive age-dependent decline in testosterone levels in healthy men. Diminished production rates cause a reduction in testosterone concentration, and however, LH and FSH plasmatic levels increase with age. On the other hand, older men experience lesser testosterone response to LH and a loss in the circadian rhythm-stimulated testosterone secretion. Similarly to women, impairment in testosterone concentrations is associated with bone and muscle mass loss, increased fat mass, fatigue, anaemia, poor libido, erectile deficiency, insulin resistance, and increased cardiovascular risk (139).

Respiratory function (142), bones (143,144), and cartilage (145), among other systems, also experience the effects of ageing. However, in this thesis, we will focus on the effects of ageing on liver metabolism and homeostasis.

1.2. Effect of ageing in the liver morphology and function

The liver plays a vital role in maintaining the body homeostasis and regulation of energy metabolism. Specific changes associated with age have been reported to affect liver morphology, physiology, and oxidative capacity. In addition, ageing compromises liver capacity for xenobiotic and endobiotic clearance (110) and can affect drug metabolism and drug pharmacokinetics (146).

1.2.1. Hepatocytes

One of the best described age-related changes in the liver is the loss of organ volume accompanied by a reduction in hepatic blood flow (147,148). In aged livers, the number of hepatocytes is decreased, but there is an increase in hepatocytes size, polyploidy and binuclear index (149,150) and a reduction in mitochondria number, leading to impaired oxidative respiration (106,110,112,146). Genomic instability in hepatocytes is due to reduced rates of DNA synthesis and repair and epigenetic alterations, which is considered the first step in the hepatic development of the “ageing phenotype” (151). Epigenetic alterations include DNA methylation, non-coding RNAs, histone marks, transcription factors and nucleosome positioning (110). DNA hypermethylation in hepatocytes is associated with changes in the expression of genes involved in inflammation, key proteins of metabolic networks and the Wnt signalling pathway (152).

The senescence of hepatocytes also correlates with telomere shortening. In this context, ageing upregulates diverse cellular senescence markers such as heterochromatin protein 1β (HP1β), p21, p16, γ-H2AX and enhanced senescence-associated-β-galactosidase activity (153). In addition to telomere attrition, mitogens, other proliferation signals, and the previously mentioned genomic damage contribute to senescence of these cells and affect liver metabolism (154). Senescent hepatocytes accumulate lipid droplets to a greater extent

than young cells, show an increase in production of ROS, and have a decreased mitochondrial oxidising capacity (155).

Ageing is also associated with alterations in mitochondrial activity in hepatocytes, including decreased mitochondrial biogenesis and mitophagy, reduced expression of mitochondrial enzymes such as mitochondrial nitric oxide synthase (mtNOS), manganese superoxide dismutase (MnSOD), reduced expression of complexes I and IV of the respiratory chain and the dissociation of ATP synthase complex subunits (156), and increased accumulation of reactive oxygen species (ROS). Altogether, these alterations can increase DNA damage, impair the respiratory chain complexes activities, and elevate oxidative stress (110).

Proteostasis encompasses the processes of protein synthesis, folding, trafficking and degradation. Loss of proteostasis is also a hallmark of ageing that in the liver is associated with epigenetic factors (157). The mechanism by which cells maintain proteostasis is autophagy. Autophagy is a catabolic process that degrades damaged organelles and cytoplasmic material through the formation of lysosomes. There are three co-existing types of autophagy: macroautophagy (usually referred to simply as autophagy), microautophagy and chaperone-mediated autophagy. In macroautophagy, intracellular components are sequestered in a double-membrane vesicle called autophagosome. The autophagosome fuses with lysosomes, and its content is degraded by lysosomal hydrolases. In microautophagy, cytosolic material is internalised by endosomes as single-membrane vesicles to be degraded. Lastly, in chaperone-mediated autophagy, cytosolic proteins are recognised and directed to lysosomes by a chaperone. Chaperones facilitate the unfolding of targeted proteins so they can cross the lysosomal lipid layer through a translocation complex and be degraded (158).

Macroautophagy is a crucial target of hepatic ageing that maintains the homeostasis and energy balance of the liver by proteolysis and hydrolysis of lipid depots and glycogen (159,160). Autophagy is tightly controlled, being stimulated during fasting and by the circadian liver clock, and restrained by high levels of fatty acids, insulin, and ATP (161). Microautophagy and chaperone-mediated autophagy also have an essential role in hepatic ageing. In fact, the dysregulation of microautophagy increases lipid oxidation and misfolding and aggregation of proteins. Moreover, decreased mitophagy, the process by which damaged mitochondria are autophagocytosed, triggers the production of inflammatory cytokines, which contributes to the senescence phenotype (162). On the other hand, chaperone-mediated autophagy is usually responsible for the degradation of hepatic enzymes involved in glycolysis and lipogenesis, helping the organism to adapt to nutritional changes. It has been shown that this type of autophagy declines with age and renders cells

more susceptible to oxidative stress (163). Impaired autophagy, and consequently a defective removal of damaged or inadequate folded proteins, leads to the formation of protein aggregates such as lipofuscins, which are commonly found in aged hepatocytes and give the elderly liver a characteristic brown colour (162).

The liver can regenerate after either surgical removal or chemical injury. However, ageing reduces liver regenerative capacity after partial hepatectomy (164,165) due to a lesser, or even absent, activation of genes such as those specific of the S-phase of the cellular cycle, DNA polymerase, cMyc, Cdc2 or Foxo-1β (166). Furthermore, age-associated oxidative stress blocks the activation of progenitor liver cells (167) and altogether may delay repair and proliferation cascades of hepatocytes. Moreover, a study in rodents shows that oxidative stress can induce the upregulation of pro-apoptotic genes, enhancing hepatocytes sensitivity towards oxidative injury (168).

1.2.2. Endothelial cells

With ageing, LSECs experience significant changes in their structure and function. The most significant changes are the reduction in the number and size of fenestrations (169,170), thickening of the endothelium, enhanced deposition of basal lamina and collagen, and impaired expression of genes like von Willebrand factor and CD31. Regarding their involvement in the clearance of macromolecules in the blood, LSECs experience a drop in their endocytic activity (171).

Similar to hepatocytes, LSECs are involved in the hepatic blood flow decrease, inflammatory processes (CD68 positive endothelial cells increase with age along with higher expression of IL-6), cellular senescence (upregulation of p16, a tumour suppressor implicated in cell cycle regulation by arresting cell cycle in the G1 phase), and express fewer markers of the regulation of hepatocyte regeneration (172).

1.2.3. Kupffer cells

Ageing has also a crucial role in inflammatory processes, increasing M1 macrophages polarization and stimulating the inflammatory response (173). Franceschi postulated the inflamm-aging theory, which states that ageing occurs when there is an unbalance between the stimulation and response of the immune system that prompt a rise in the levels of inflammatory markers (cytokines, chemokines and ROS) and a reduction of antioxidant enzymes (174). This theory proposes that the susceptibility to age-associated diseases is a consequence of the maintained inflammatory stimuli over time. A physiological change that favours the inflammatory state is the redistribution of fat store depots mentioned previously. The visceral adipose tissue or VAT is known to secrete the pro-inflammatory cytokines

TNFα, IL-6, IL-8 and MCP-1, promoting the hepatic activation of the nuclear factor-kappa B (NF-κB) and the c-jun N-terminal kinase (JNK) signalling pathways, among others (110,112).

Alterations in the functional activity of KCs have been described in a wide range of diseases (175-178). Although not much is still known about the effects of ageing in KCs, it has been reported that ageing reduces autophagy and phagocytosis and increases the production of cytokines that facilitates the inflamm-aging phenotype in macrophages (110). Ageing is associated with an increased number of Kupffer cells, with a redistribution to lymphoid collections (179), and with lower phagocytic activity (180) that triggers pathogen invasion and systemic inflammation (3).

1.2.4. Stellate cells

Although there is still some uncertainty on how age affects HSCs, it is believed that there is a dissociation between lipid droplet metabolism and HSC activation in the liver at advanced ages (110). Moreover, upregulation of PDGFR-β was also observed in activated HSCs, which may indicate enhanced expression of PDGF, a key mitogen for HSCs proliferation (172,181). In fact, livers from senescent rodents contain an increased number and size of lipid droplets in HSCs and increased expression of markers involved in stellate cell activation and collagen deposition. Accordingly, a high prevalence of fibrosis (40%) and cirrhosis (14%) in the liver of old individuals have been found (182).

1.3. Changes in liver metabolism during ageing

As explained before, the liver is a crucial organ in metabolism, distribution of nutrients and detoxification of xenobiotics and harmful metabolites. Hepatic glucose and lipid metabolism are regulated by multiple factors, including nutrients and hormones that maintain the liver metabolic homeostasis. Alterations in liver metabolism, impaired mitochondrial function, chronic liver diseases, NAFLD, alcoholic fatty liver disease, non-alcoholic steatohepatitis, obesity, insulin resistance, and diabetes are associated with ageing (6).

1.3.1. Carbohydrate metabolism

Although there is still controversy, different studies suggest that age may play an important role in the dysfunction of glucose metabolism. Age is associated with physiological changes in glucose homeostasis. Thus, the alterations in body composition, such as fat redistribution from subcutaneous to visceral fat depots, negatively correlate with total body and hepatic insulin sensitivity and impair hepatic glucose output in the elderly (183).

Several studies have demonstrated a deterioration in glucose metabolism and the development of insulin resistance with ageing. The liver provides around 90-95% of the

circulating glucose in the postprandial state (184), is the glucose supplier for the brain and other tissues (6), and has a central role in maintaining euglycaemia. An exacerbated glucose production in both aged humans and rodents supports the progression from euglycemia to hyperglycaemia and type 2 diabetes with age (185). From a more molecular perspective, a recent study has demonstrated that old rats show increased levels of the gluconeogenic enzymes PEPCK, glucose 6 phosphatase and pyruvate carboxylase, and consequently higher glucose production (185). These results are supported by other authors that correlate this increment of the enzyme levels with age and obesity (186-190). Furthermore, some transcription factors such as PGC-1α, HNF-4α and C/EBP-β are proposed to modulate hepatic gluconeogenesis in an age-dependent manner (185).

Moreover, ageing also alters glucose uptake, which further ameliorates insulin resistance (191). Glucose can be taken up via two differentiated mechanisms: insulin-mediated glucose uptake and non-insulin-mediated glucose uptake. Non-insulin-mediated glucose uptake occurs in the brain and splanchnic organs, which include the liver (184). A reduction in the number of glucose transport and metabolic units occurs with ageing. The insulin resistance of ageing is in part due to a reduction in the capacity of the glucose uptake system, as glucose disposal decrease by 30-35% in the elderly in the presence of similar levels of hyperinsulinemia (192,193).

Ageing has also been associated with ER stress, insulin resistance and with impaired insulin signalling (185). In addition, mitochondrial dysfunction, inflammation, and cellular senescence can also contribute to insulin resistance. If maintained over time, insulin resistance can lead to type 2 diabetes as β-cells fail to keep up with the increased need of the body for insulin to control plasmatic glucose levels (184).

Insulin secretion by β-cells has also been described to be affected by ageing. Insulin is secreted by two pulsations: rapid low amplitude pulses and ultradian pulses. Rapid low amplitude pulses inhibit hepatic glucose production and prevent the insulin receptor's downregulation, and the ultradian pulses stimulate peripheral glucose disposal. It has been reported that these pulses are altered in patients with glucose intolerance, obesity and type 2 diabetes. Moreover, in healthy lean individuals, ageing has been related to disturbances in insulin secretion by modifications in the pulses. Specifically, age is associated with decreased amplitude and mass of rapid pulses and a reduced frequency of the ultradian pulses (184).

Moreover, adipokines secreted by visceral adipose tissue can also modulate the activity of the signalling pathways in the liver. In fact, the insulin signalling pathway can be impaired by the TNFα secreted by visceral adipose tissue (112).

On the other hand, it has been reported that two pathways also involved in modulating the life span are insulin/IGF1 signalling (194) and mTOR (195). The downregulation of both seems to delay the ageing process.

1.3.2. Lipid metabolism

The liver plays a critical role in regulating systemic lipid metabolism as it is the main producer of plasma lipoproteins and bile. Dysregulation of lipid metabolism triggers the development of diseases such as obesity, hepatic steatosis, and insulin resistance. Hepatic pathologies due to impaired metabolism include alterations associated with enhanced lipid uptake and accumulation, increased lipid synthesis, decreased β-oxidation, and increased circulating lipids. Moreover, glucose and lipid metabolism are closely related, so it is not surprising that lipid metabolism is affected by the changes in carbohydrate metabolism described above (196).

Changes in the metabolism of the liver are also related to the ageing process, when a shift in lipid metabolism towards lipogenesis occurs, correlating with the increased incidence of hepatic steatosis and NAFLD among the elderly population. It is well established that ageing and insulin resistance increase lipid accumulation in the liver and elevate free fatty acid levels in circulation (197).

Here we will disclosure the alterations caused during ageing in the main checkpoints of lipid metabolism. Firstly, once fatty acids are taken up by the hepatocytes, they bind to fatty acid-binding protein 1 (FABP-1) to be directed to the cell compartment where they are needed. It has been reported in rodents that there is a reduction of FABP-1 levels with age (198) as well as in genetic lipid disorders and NAFLD (199). FABP-1 can interact with the transcription factor PPAR-α and alter its expression levels which could impair β-oxidation. Defective oxidation of fatty acids, in turn, enhances lipotoxicity and contributes to the pathogenesis and progression of NAFLD. On the other hand, in humans, FABP-1 is associated with obesity, insulin resistance, hypertriglyceridemia and low HDL-cholesterol (200).

Secondly, there is no evidence that ageing per se affects the *de novo* lipogenesis (DNL) process; instead, age-associated changes in DNL are thought to be mainly through alterations in the growth hormone-insulin-like growth factor I (GH/IGF-I) axis and insulin resistance. DNL is responsible for 5-10% of the hepatic triacylglyceride content under normal conditions, but it represents more than 25% in patients with NAFLD. DNL is regulated via transcriptional regulation of SREBP1c and ChREBP and protein modification of ACC (201). SREBP1c is activated by insulin, resulting in the upregulation of ACC (202). Moreover,

targeting ACC with antisense oligonucleotide reduces hepatic glucose production and thus, improve insulin sensitivity (203).

On the other hand, ageing affects the GH/IGF-1 axis promoting a steady reduction of the signalling cascade. Regarding liver metabolism, hepatic lipid content is significantly increased when the GH pathway is decreased. Studies in animals with specific GH receptor deficiency in the liver revealed a 2-fold increase in DNL. Similar results were obtained in humans. Altogether, these findings suggest that during ageing and as an effect of the decline in several signalling pathways, there is an increase in the liver's DNL and fatty acid content, which exacerbates hepatic steatosis via upregulation of PPAR-γ that stimulates the expression of genes involved in lipid uptake (204). Age-related insulin resistance is commonly associated with higher levels of ApoB, an increase in VLDL secretion, and hypertriglyceridemia (205). Lastly, ageing has also been shown to decrease fatty acid oxidation in both mice and humans (106,206).

2. EXPERIMENTAL DESIGN. Study of metabolic adaptations associated with ageing in a Ptn deficient mouse model

Female *Ptn*$^{+/+}$ and *Ptn*$^{-/-}$ mice were housed in controlled conditions, at 22-24ºC with 12h light/dark cycles and free access to chow diet (Panlab, Barcelona, Spain) and water. Mice were fed ad libitum and randomly separated considering their genotype (*Ptn*$^{+/+}$ or *Ptn*$^{-/-}$) and sacrificed at different time points, as shown in Figure 10.

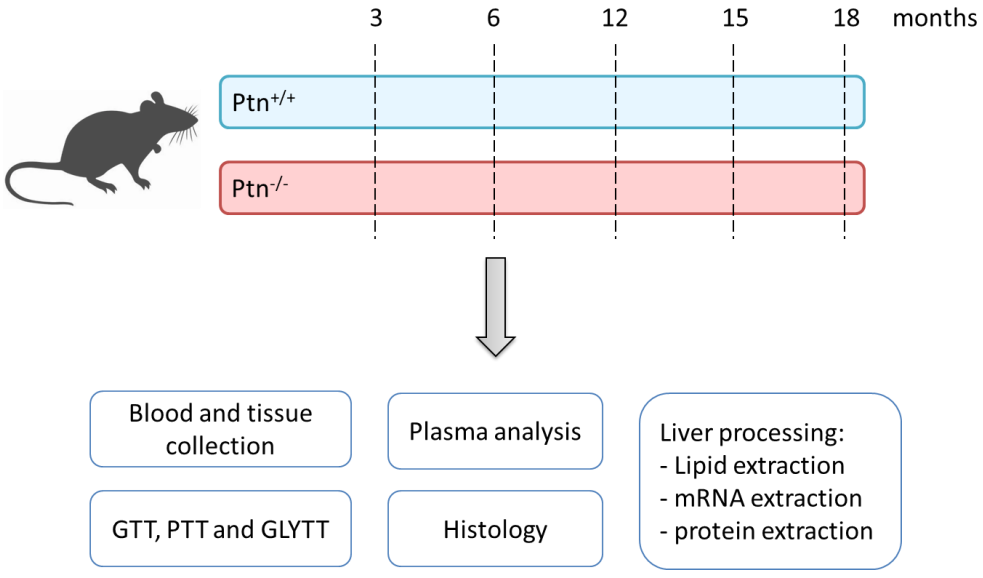

Figure 10. Experimental design of the ageing mice model to determine the role of PTN in the metabolism of the liver.

Moreover, pyruvate and glycerol tolerance tests were assessed in 18 months old *Ptn*$^{+/+}$ and *Ptn*$^{-/-}$ mice.

Animals were sacrificed after a 6 hour fast, under carbon dioxide anaesthesia by decapitation. Blood was collected in Eppendorf tubes containing 1mg/10µL EDTA and centrifuged at 3000 rpm for 20 minutes at 4ºC to obtain the plasma. Tissues were rapidly dissected and snap-frozen in liquid nitrogen. Tissues and plasma were preserved at -80ºC till its later analysis.

3. RESULTS

3.1. Effects of pleiotrophin deletion on liver metabolism in an ageing model

In this first chapter, we will summarise the results obtained after the analysis of the effects of pleiotrophin deletion and ageing on the glucose/insulin homeostasis and liver metabolism of 3, 6, 12, and 15 months old *Ptn*$^{+/+}$ and *Ptn*$^{-/-}$ mice.

3.1.1. Altered circulating lipid profile, impaired glucose tolerance, and insulin resistance are age-related phenomena in Ptn$^{-/-}$ mice

According to previous results from our group, *Ptn*$^{-/-}$ mice are smaller than *Ptn*$^{+/+}$ mice. Moreover, pleiotrophin deletion triggers a switch in fat distribution from a high degree of adiposity in young mice to a slimness in older mice (71).

As altered adiposity has been related to deteriorated lipid and glucose homeostasis, we analysed the circulating biochemical profile. *Ptn*$^{-/-}$ mice showed lower plasma triacylglycerol levels from 6 to 15 months of age than *Ptn*$^{+/+}$ controls (Figure 11a), and circulating plasma NEFA were also significantly lower in 15-month-old *Ptn*$^{-/-}$ mice (Figure 11b) (71).

Although fasting plasma glucose was similar in both groups (Figure 11c), we found significant differences in insulinemia. In *Ptn*$^{-/-}$ mice, insulin departs from lower levels in young mice to hyperinsulinemia in 15-month-old animals (Figure 11d).

On the other hand, GTTs did not reveal differences in the AUC for glucose in young mice (3 and 6-month-old). However, at 9, 12 and 15 months, the AUC for glucose was significantly higher in *Ptn*$^{-/-}$ than in *Ptn*$^{+/+}$ mice, indicating an impaired glucose tolerance in the knock-out animals with age (Figure 11e). Additionally, 15-month-old *Ptn*$^{-/-}$ mice exhibited significantly lower QUICKI and higher HOMA-IR values than their age-matched controls (Figure 11f and 11g), suggesting decreased insulin sensitivity in later life (71).

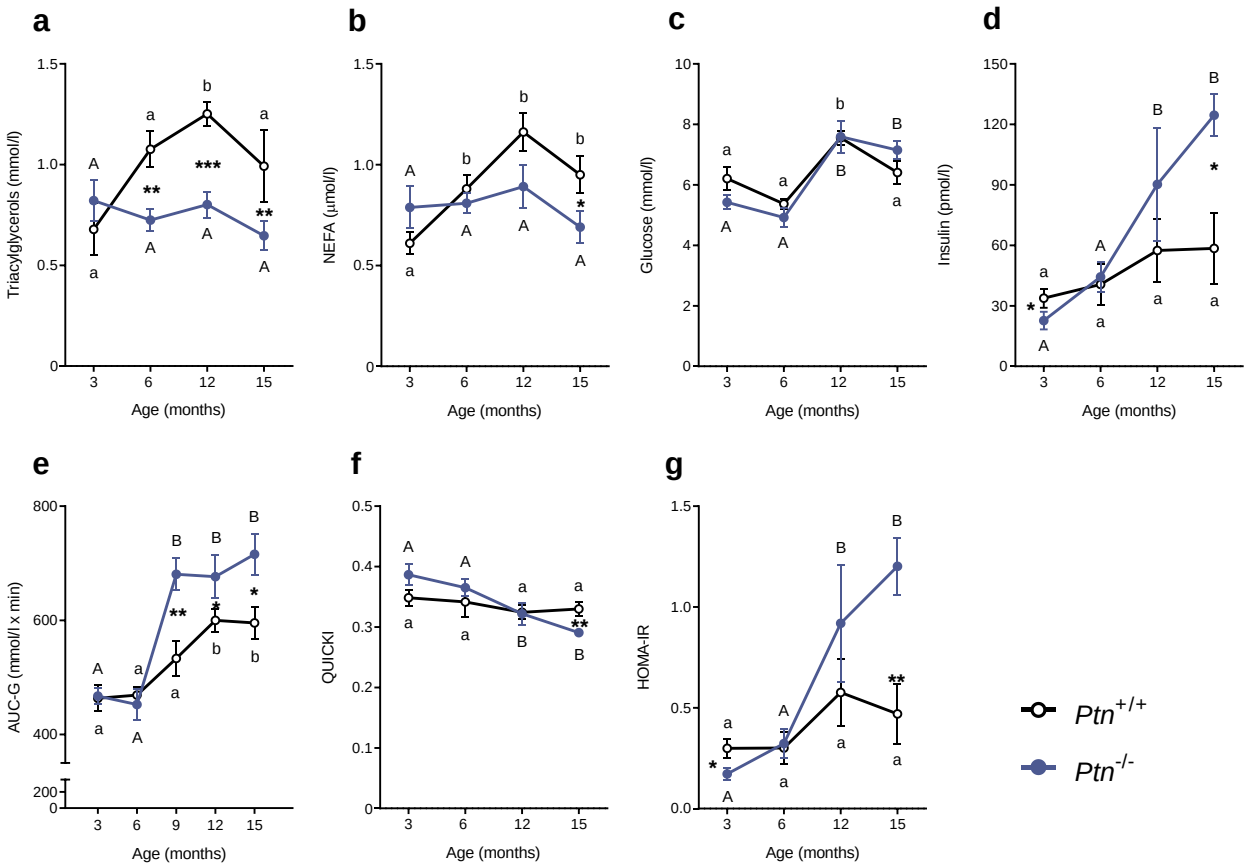

Figure 11. Changes in plasma lipid profile, impaired glucose tolerance and insulin resistance are associated with ageing in Ptn$^{-/-}$ mice. *a) Triacylglycerides; b) NEFA; c) Glucose; d) Insulin; e) AUC for glucose (AUC-G); f) QUICKI; and g) HOMA-IR in 3, 6, 12, and 15-months-old Ptn$^{+/+}$ (black lines) and Ptn$^{-/-}$ (blue lines) female mice. Data are presented as mean ± SEM of n=8 mice/group. Different letters indicate statistically significant differences in the effect of ageing within the same genotype. Lowercase letters indicate statistically significant differences for Ptn$^{+/+}$ and capital letters for Ptn$^{-/-}$; *p<0.05, **p<0.01, ***p<0.001 for differences between Ptn$^{+/+}$ and Ptn$^{-/-}$ mice of the same age.*

We have also performed a pyruvate tolerance test and a glycerol tolerance test in 18-months-old mice to assess whether *Ptn* deletion affects gluconeogenesis. We found that after 15 hours of fasting, basal glycemia was markedly decreased in 18-months-old *Ptn*$^{-/-}$ animals when compared to *Ptn*$^{+/+}$ mice in both tests.

In the PTT, the peak of maximum glucose production was reached 15 minutes after the pyruvate injection in both genotypes of mice (Figure 12a). After that, the hepatic glucose production steadily decreases in *Ptn*$^{-/-}$ mice, whereas the reduction is quicker in the control animals. No differences between genotypes were found in the AUC for glucose production (Figure 12b). However, when we calculated the net hepatic glucose production (increment in glucose levels from the basal values), we found that from 15 minutes onwards, *Ptn*$^{-/-}$ animals have higher glucose levels (Figure 12c) and the AUC of glucose in the PTT was higher in *Ptn*$^{-/-}$ animals than in *Ptn*$^{+/+}$ mice (Figure 12d).

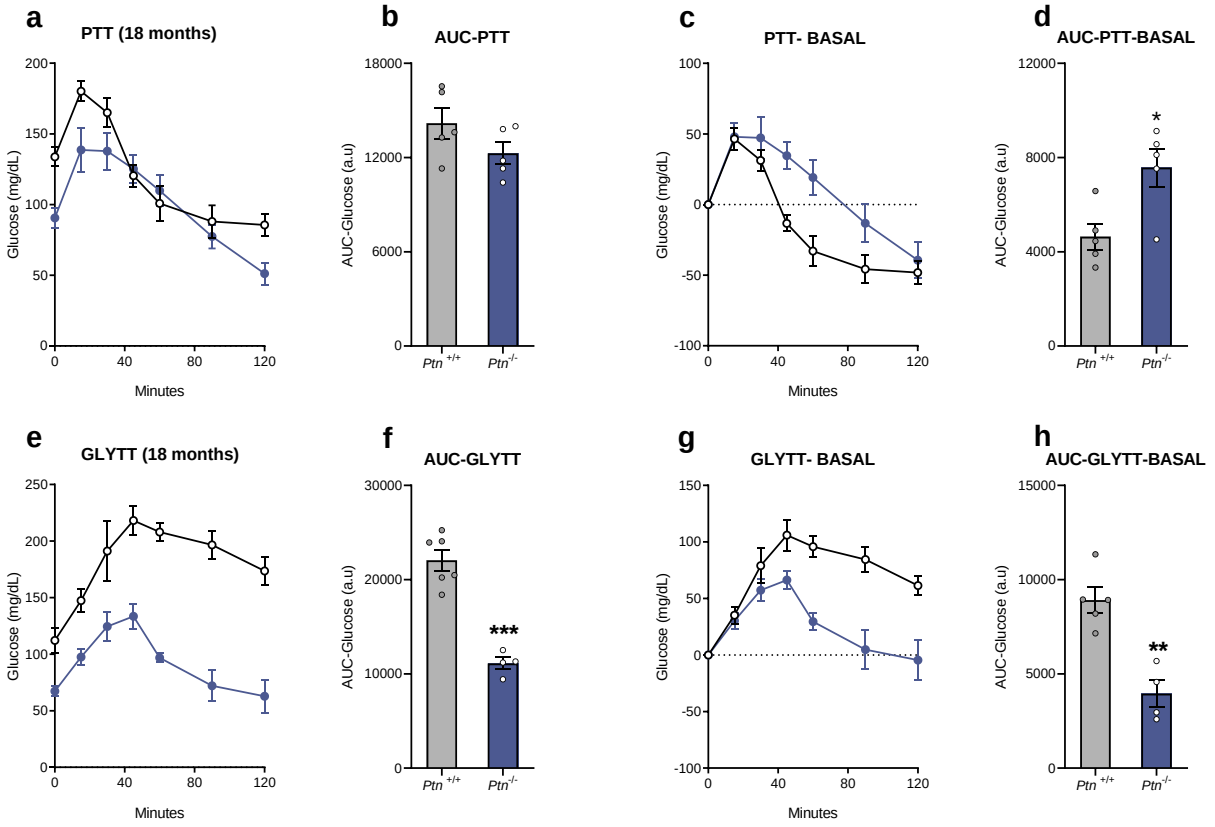

Figure 12. Glycerol and pyruvate tolerance tests in 18 months old Ptn$^{-/-}$ mice. *a) Pyruvate tolerance test; b) AUC-PTT for glycemia; c) Pyruvate tolerance test (basal: net change in glycemia versus basal); d) AUC-PTT for net glycemia; e) Glycerol tolerance test; f) AUC-GLYTT for glucose; g) Glycerol tolerance test (basal: net change in glycemia versus basal); and h) AUC-GLYTT for net glycemia in 18-months-old Ptn$^{+/+}$ (black lines) and Ptn$^{-/-}$ (blue lines) female mice. Data are presented as mean ± SEM of n=4 mice/group. Different letters indicate statistically significant differences in the effect of ageing within the same genotype. Lowercase letters indicate statistically significant differences for Ptn$^{+/+}$ and capital letters for Ptn$^{-/-}$; *p<0.05, **p<0.01, ***p<0.001 for differences between Ptn$^{+/+}$ and Ptn$^{-/-}$ mice.*

On the other hand, we found that in the GLYTT of the *Ptn*$^{+/+}$ and *Ptn*$^{-/-}$ mice, the peak in the hepatic glucose production was reached 45 minutes after the injection of glycerol (Figure 12e). Moreover, after 120 min, *Ptn*$^{-/-}$ mice recovered the initial plasma glucose levels, whereas *Ptn*$^{+/+}$ mice did not (Figure 12e). The AUC for glucose in the GLYTT was significantly lower in *Ptn*-deficient mice compared to the *Ptn*$^{+/+}$ mice (Figure 12f). Similarly, when basal values are equalized, the net blood glucose values and the AUC were significantly reduced in *Ptn*$^{-/-}$ animals (Figure 12g-h).

The analysis of total cholesterol, c-HDL and c-LDL levels in the plasma of 3- and 15-months old animals showed that young *Ptn*$^{-/-}$ mice exhibited higher cholesterol, c-LDL and c-HDL levels than the control animals, but although ageing induced an increase in triacylglycerides, c-LDL and c-HDL in the 15-months old *Ptn*$^{+/+}$, no differences were found

between 3- and 15-months-old *Ptn*$^{-/-}$ animals (Figure 13c-d). Moreover, triacylglycerides, c-HDL and c-LDL levels were significantly lower in old *Ptn*$^{-/-}$ mice than in the control group (Figure 13). The analysis of ketone bodies revealed that plasma levels of D-3-hydroxybutyrate increased with age in *Ptn*$^{+/+}$ mice, whereas no changes were observed with age in *Ptn*$^{-/-}$ mice (Figure 13e).

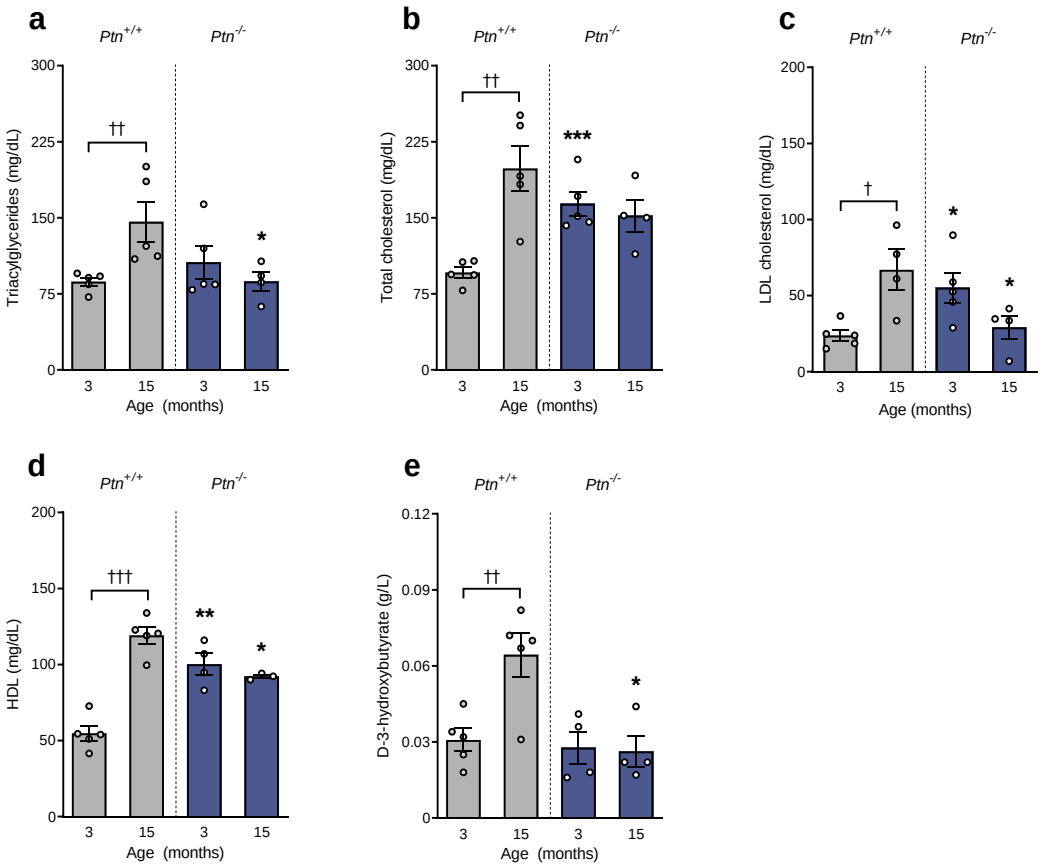

Figure 13. Circulating lipid fractions in the mice plasma. *a) Triacylglycerides; b) Total cholesterol; c) LDL cholesterol; d) HDL cholesterol; and e) D-3-hydroxybutyrate in 3 and 15-months-old Ptn$^{+/+}$ and Ptn$^{-/-}$ female mice. Data are presented as mean ± SEM for n=5 mice/group. †p<0.05, ††p<0.01, †††p<0.001 for differences in the effect of ageing 3 months vs 15 months within the same genotype *p<0.05, **p<0.01, ***p<0.001 for differences between Ptn$^{+/+}$ and Ptn$^{-/-}$ miceof the same age.*

3.1.2. Ptn$^{-/-}$ mice have a decreased hepatic lipid content

We next analysed if the changes that we have observed in the plasma lipid profile could be associated with changes in the liver lipid content. First, the weight of the liver of *Ptn*$^{-/-}$ mice was significantly lower when compared with age-matched controls (Figure 14a). As shown in Figure 14b, although no changes were observed in young mice, the liver lipid content was also significantly lower in 6 to 15 months *Ptn*$^{-/-}$ mice. The increased accumulation of lipids with age in 15 months old *Ptn*$^{+/+}$ mice was also observed in the

haematoxylin-eosin staining of liver sections. Although at 6 months of age, we did not find any difference in the presence of lipid droplets between genotypes, the liver sections of 15 months old mice showed an accumulation of lipid droplets in *Ptn*$^{+/+}$ mice, whereas no accumulation was evident in the *Ptn*$^{-/-}$ mice (Figure 14c).

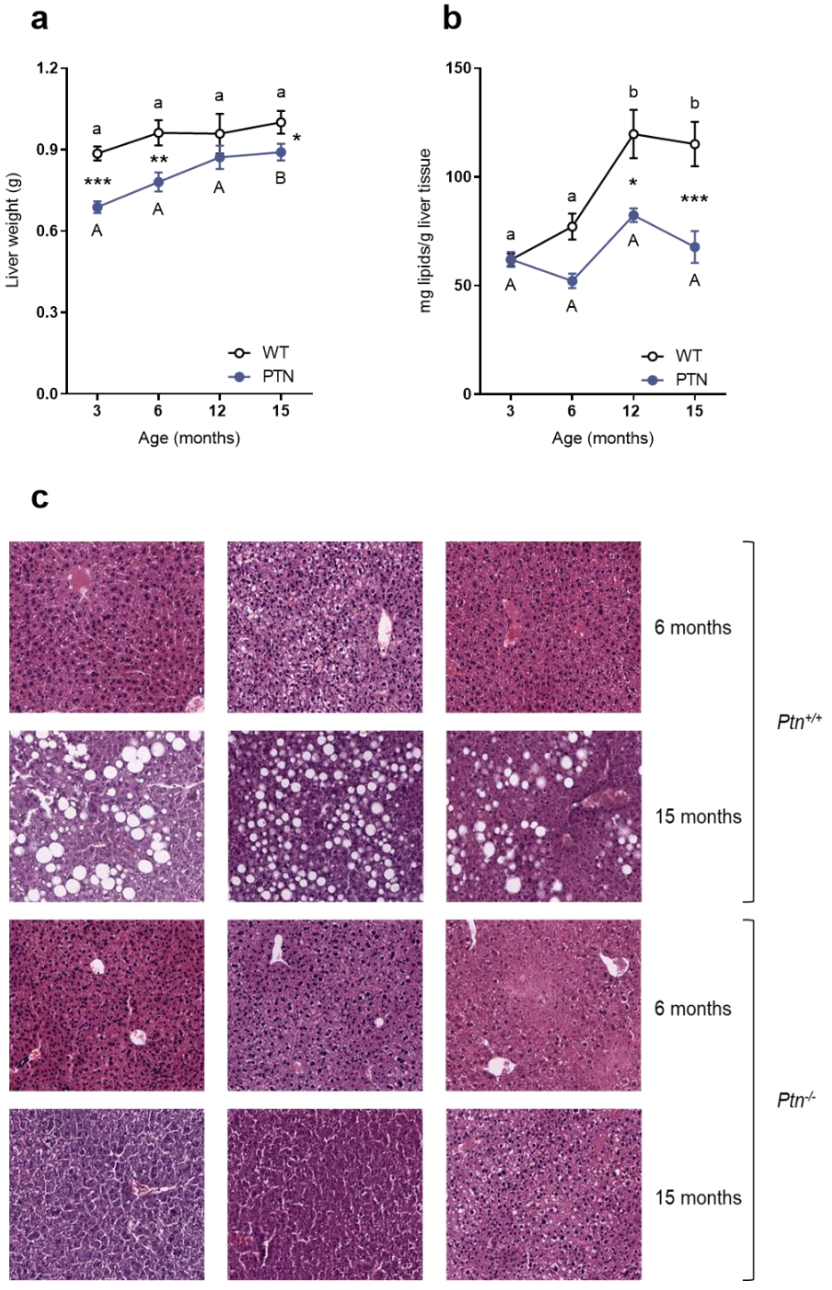

Figure 14. Evolution in liver weight and hepatic lipid content. *a) Liver weight; b) Hepatic lipid content in 3, 6, 12, and 15-months-old Ptn*$^{+/+}$ *(black lines) and Ptn*$^{-/-}$ *(blue lines) female mice, and c) hematoxylin-eosin staining of formalin-fixed paraffin-embedded liver in 6 and Ptn*$^{+/+}$*, 15 month-old Ptn*$^{+/+}$ *and Ptn*$^{-/-}$ *female mice. Data are presented as mean ± SEM. Different letters indicate statistically significant differences in the effect of ageing within the same genotype. Lowercase letters indicate statistically significant differences for Ptn*$^{+/+}$ *and capital letters for Ptn*$^{-/-}$*; *p<0.05, **p<0.01, ***p<0.001 for differences between Ptn*$^{+/+}$ *and Ptn*$^{-/-}$ *mice of the same age.*

3.1.3. Effect of Ptn deletion on fatty acid synthesis in the liver

The marked reduction in total hepatic lipid content of *Ptn*$^{-/-}$ mice prompted us to analyse the mRNA of the critical enzymes involved in fatty acids synthesis. As shown in Figure 15b, no differences were found in the mRNA of acetyl-CoA carboxylase (*Acc),* neither by the effect of age or genotype.

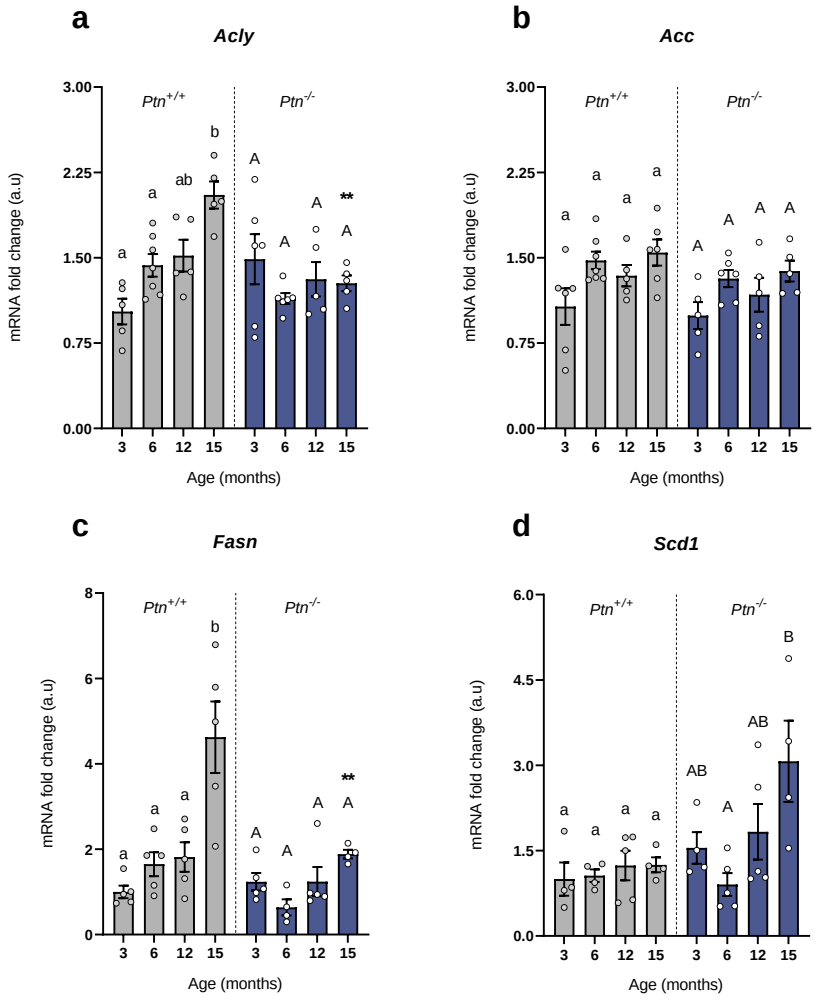

Figure 15. Hepatic mRNA of enzymes involved in fatty acid synthesis in Ptn$^{+/+}$ and Ptn$^{-/-}$ mice. *a) ATP citrate lyase (Acly) mRNA; b) Acetyl-CoA carboxylase (Acc) mRNA; c) Fatty acid synthase (Fas) mRNA; and d) Stearoyl-CoA desaturase 1 (Scd1) mRNA. Data are presented as mean ± SEM for n=5-6 mice/group. Different letters indicate statistically significant differences in the effect of ageing within the same genotype. Lowercase letters indicate statistically significant differences for Ptn$^{+/+}$ and capital letters for Ptn$^{-/-}$; *p<0.05, **p<0.01, ***p<0.001 for differences between Ptn$^{+/+}$ and Ptn$^{-/-}$ mice of the same age.*

However, the mRNA of ATP citrate lyase (*Acly*) and fatty acid synthase (*Fas*) increased with age in *Ptn*$^{+/+}$ mice but were not modified with age in *Ptn*$^{-/-}$ animals (Figure 15a and c). In fact, 15 months old *Ptn*$^{-/-}$ mice showed significantly lower expression of *Acly* and *Fas* than

their age-matched controls. The ANOVA analysis revealed an interaction in the effect of age and genotype in *Acly* and *Fas* (F(3,36)=7.172; p-value=0.0007 and F(3,30)=4.962; p-value=0.0065, respectively). On the other hand, although *Scd1* mRNA was constant with age in the $Ptn^{+/+}$ mice, ageing induced a significant increase in *Scd1* levels in $Ptn^{-/-}$ mice (Figure 15d). However, no interaction between both factors was observed in the ANOVA analysis for *Scd1*.

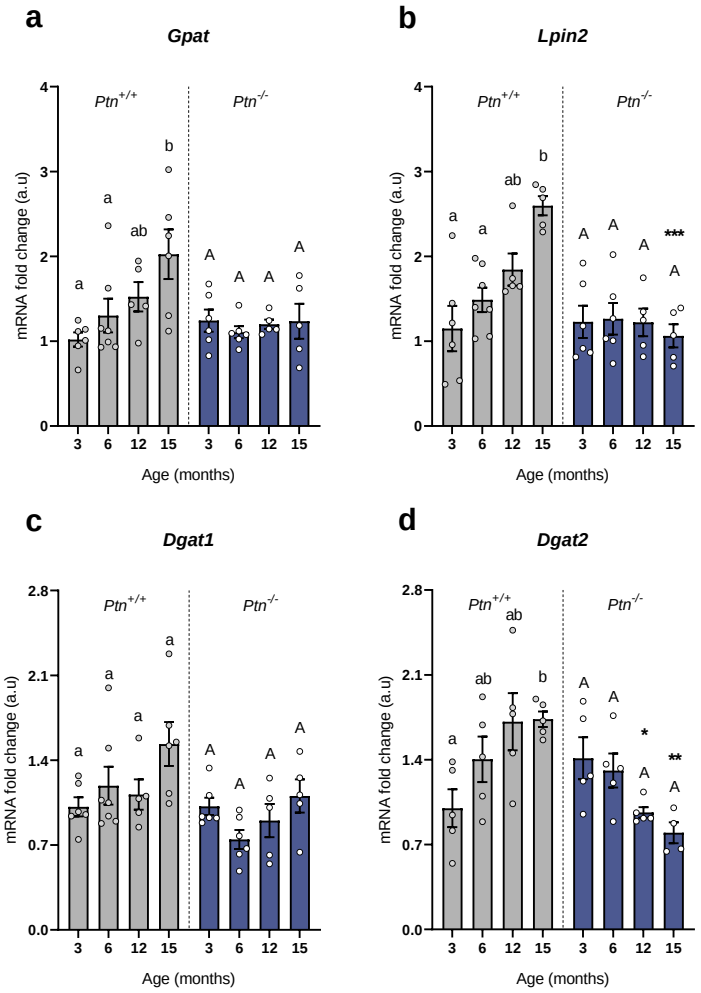

Figure 16. Liver mRNA of enzymes involved in triacylglycerides synthesis in $Ptn^{+/+}$ and $Ptn^{-/-}$ mice. *a) Glycerol-3-phosphate acyltransferase (Gpat) mRNA; b) Lipin 2 (Lpin2) mRNA; c) Diacylglycerol O-acyltransferase 1 (Dgat1) mRNA; and d) Diacylglycerol O-acyltransferase 2 (Dgat2) mRNA. Data are presented as mean ± SEM for n=5-6 mice/group. Different letters indicate statistically significant differences in the effect of ageing within the same genotype. Lowercase letters indicate statistically significant differences for $Ptn^{+/+}$ and capital letters for $Ptn^{-/-}$; *p<0.05, **p<0.01, ***p<0.001 for differences between $Ptn^{+/+}$ and $Ptn^{-/-}$ mice of the same age.*

3.1.4. Deletion of Ptn blocks the effect of ageing on the key enzymes of triacylglyceride synthesis

In view of the changes described above, we determined the expression of the enzymes involved in hepatic TAG synthesis (Figure 16). We observed that the mRNA of glycerol-3P-acyltransferase (*Gpat*), lipin 2 (*Lpin2*), and diacylglycerol O-acyltransferase 2 (*Dgat2*) increased with age in the $Ptn^{+/+}$ mice (Figure 16a,b,d). Similarly, mRNA of diacylglycerol O-acyltransferase 1 (*Dgat1*) also increased with age in these animals, although the differences were not statistically significant (Figure 16c).

The deletion of *Ptn* completely blocked the age-related increment in the mRNA of the enzymes involved in triacylglycerol synthesis (Figure 16a-d). Thus, *Lpin2* and *Dgat2* mRNA were significantly lower at 15 months in the $Ptn^{-/-}$ mice when compared with their age-matched controls. In fact, the ANOVA analysis showed a combined effect of age and genotype ($F(3,37)=6.967$; p-value=0.0008 for *Lpin2*; $F(3,31)=8.168$; p-value=0.0004 for *Dgat2*). These results are in accordance with the decreased content of liver triacylglycerides and the decreased plasma levels observed both in triacylglycerides and NEFA in the 15 months old $Ptn^{-/-}$ mice (71).

3.1.5. Deletion of Ptn is associated with a downregulation of the apolipoproteins mRNA but does not alter the mRNA of hydroxymethylglutaryl-CoA reductase

As we have found changes in cholesterol distribution in the different fractions of lipoproteins, we analysed the expression of proteins involved in cholesterol and lipoprotein metabolism. In $Ptn^{+/+}$ mice, mRNA levels of hydroxymethylglutaryl-CoA reductase (*Hmgcr*), the key enzyme involved in the regulation of cholesterol synthesis, tend to increase with age, whereas in $Ptn^{-/-}$ mice are stable along time (Figure 17a). The expression of LDL receptor (*Ldlr*) increases progressively from 3 months to 15 months of age, whereas in $Ptn^{-/-}$ mice, the higher levels of *Ldlr* are observed at 3 months of age and are not affected or even decrease with age. In fact, *Ldlr* mRNA is significantly reduced in 15 months $Ptn^{-/-}$ mice compared to the age-matched $Ptn^{+/+}$ mice (Figure 17b). The ANOVA analysis also showed a strong interaction between age and genotype in *Hmgcr* and *Ldlr* ($F(3,34)=4.031$; p-value=0.0148 and $F(3,26)=8.065$; p-value=0.0006).

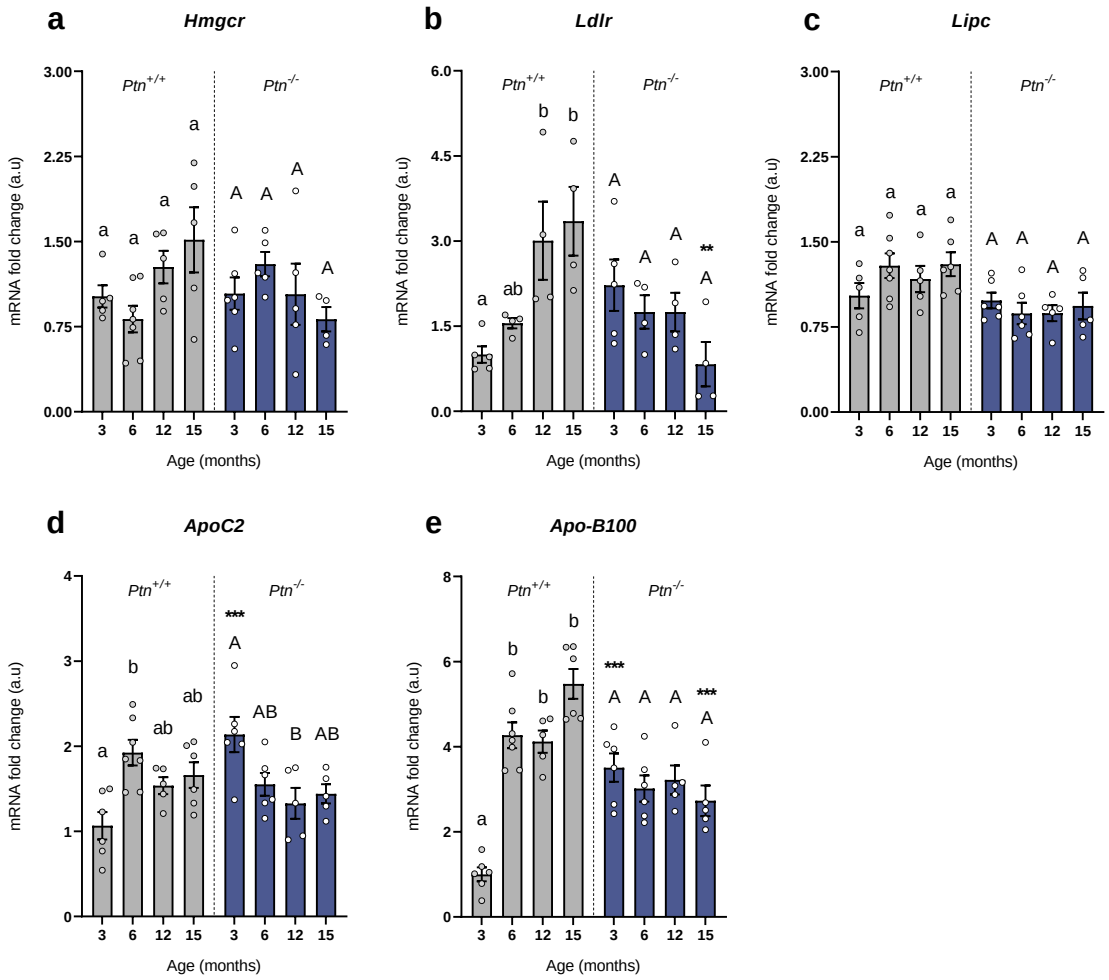

Figure 17. Effects of Ptn deletion in the mRNA of proteins involved in cholesterol and lipoprotein metabolism. *a) Hydroxymethylglutaryl-CoA reductase (Hmgcr) mRNA; b) Ldl receptor (Ldlr) mRNA; c) Hepatic lipase (Lipc) mRNA; d) Apo C-II (ApoC2) mRNA; and e) Apo B-100 (ApoB100) mRNA. Data are presented as mean ± SEM for n=5-6 mice/group. Different letters indicate statistically significant differences in the effect of ageing within the same genotype. Lowercase letters indicate statistically significant differences for $Ptn^{+/+}$ and capital letters for $Ptn^{-/-}$; *p<0.05, **p<0.01, ***p<0.001 for differences between $Ptn^{+/+}$ and $Ptn^{-/-}$ mice of the same age.*

Additionally, we analysed the mRNA of different proteins involved in the metabolism of lipoproteins. As shown in Figure 17c, the expression of hepatic lipase (*Lipc*), an enzyme that participates in the metabolism of IDL and large LDL, and in the conversion of HDL2 to HDL3, was not modified either by the effect of age or genotype. The mRNA of *ApoC-II*, the activator of lipoprotein lipase (LPL) that is required for efficient lipolysis of TG-rich lipoproteins in the circulation, increased from 3 to 6 months in the $Ptn^{+/+}$ mice. On the other hand, 3 months old $Ptn^{-/-}$ animals had the highest mRNA levels of *Apo C-II* that decreased progressively from young to old animals (Figure 17d). The *ApoB100* mRNA levels were 3-fold higher in 3 months old $Ptn^{-/-}$ mice than in the age-matched $Ptn^{+/+}$ animals and were not modified by age

in *Ptn*$^{-/-}$ mice. *ApoB100* expression has a 5-fold increment from 3 to 15 months in the *Ptn*$^{+/+}$ mice and was significantly higher in 15 months old *Ptn*$^{-/-}$ mice than in the age-matched *Ptn*$^{+/+}$ mice (Figure 17e). The ANOVA analysis of *Apo C-II* and *ApoB100* mRNA revealed that the changes due to the effect of age are highly associated with the presence/absence of *Ptn* (ANOVA F(3,38)=9.656; p-value<0.0001 for *Apo C-II*, and F(3,38)=26.20; p-value<0.0001 for *ApoB100*).

3.1.6. Effect of Ptn deletion and ageing on hepatic mRNA expression of glycerol and fatty acid transporters

As shown in Figure 18a, ageing did not modify the expression of glycerol transporter aquaporin 9 (*Aqp9*), but the mRNA levels were lower in *Ptn*$^{-/-}$ mice. Regarding the expression of the fatty acid transporter members 4 and 5 (*Fatp4 and Fatp5*), the expression of *Fatp5* increased with age in *Ptn*$^{+/+}$ mice (Figure 18c), whereas *Fatp4* mRNA decreased with age from 3-12 months of age to next increase at 15 months of age, (Figure 18b). On the other hand, fatty acid transporters *Fatp4* and *Fatp5* mRNA levels did not vary with age in *Ptn*$^{-/-}$ mice.

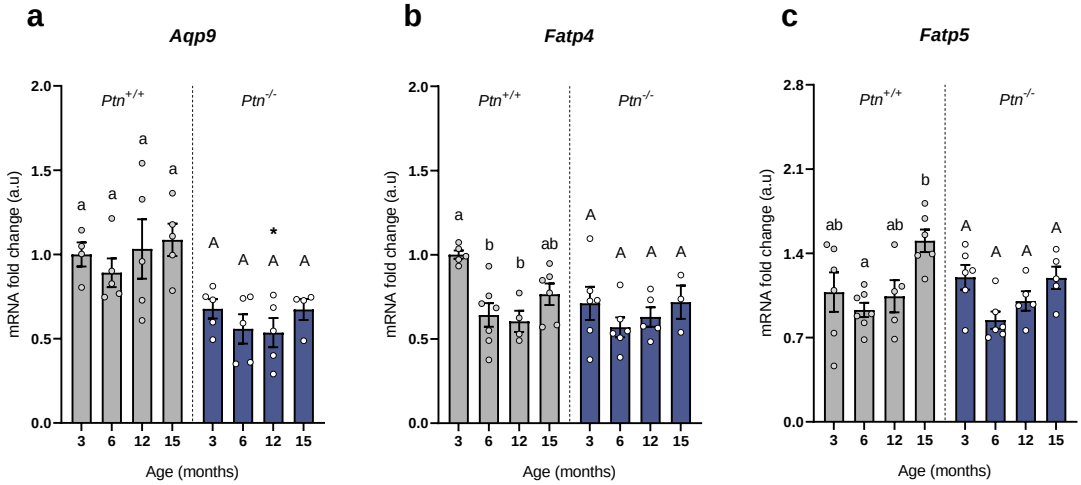

Figure 18. Ptn deletion alters the mRNA levels of glycerol and fatty acids transporters. *a) Aquaporin 9 (Aqp9) mRNA; b) Fatty acid transporter member 4 (Fatp4) mRNA; and c) Fatty acid transporter member 5 (Fatp5) mRNA. Data are presented as mean ± SEM for n=5-6 mice/group. Different letters indicate statistically significant differences in the effect of ageing within the same genotype. Lowercase letters indicate statistically significant differences for Ptn*$^{+/+}$ *and capital letters for Ptn*$^{-/-}$*; *p<0.05, **p<0.01, ***p<0.001 for differences between Ptn*$^{+/+}$ *and Ptn*$^{-/-}$ *mice of the same age.*

3.1.7. Effect of Ptn deletion and ageing on hepatic mRNA expression of key enzymes of β-oxidation

We next evaluated the effects of *Ptn* deletion on hepatic fatty acid oxidation. We first analysed the mRNA of carnitine palmitoyltransferase 1α (*Cpt1α)*, which regulates the entrance of the acyl-CoAs in the mitochondria before their oxidation.

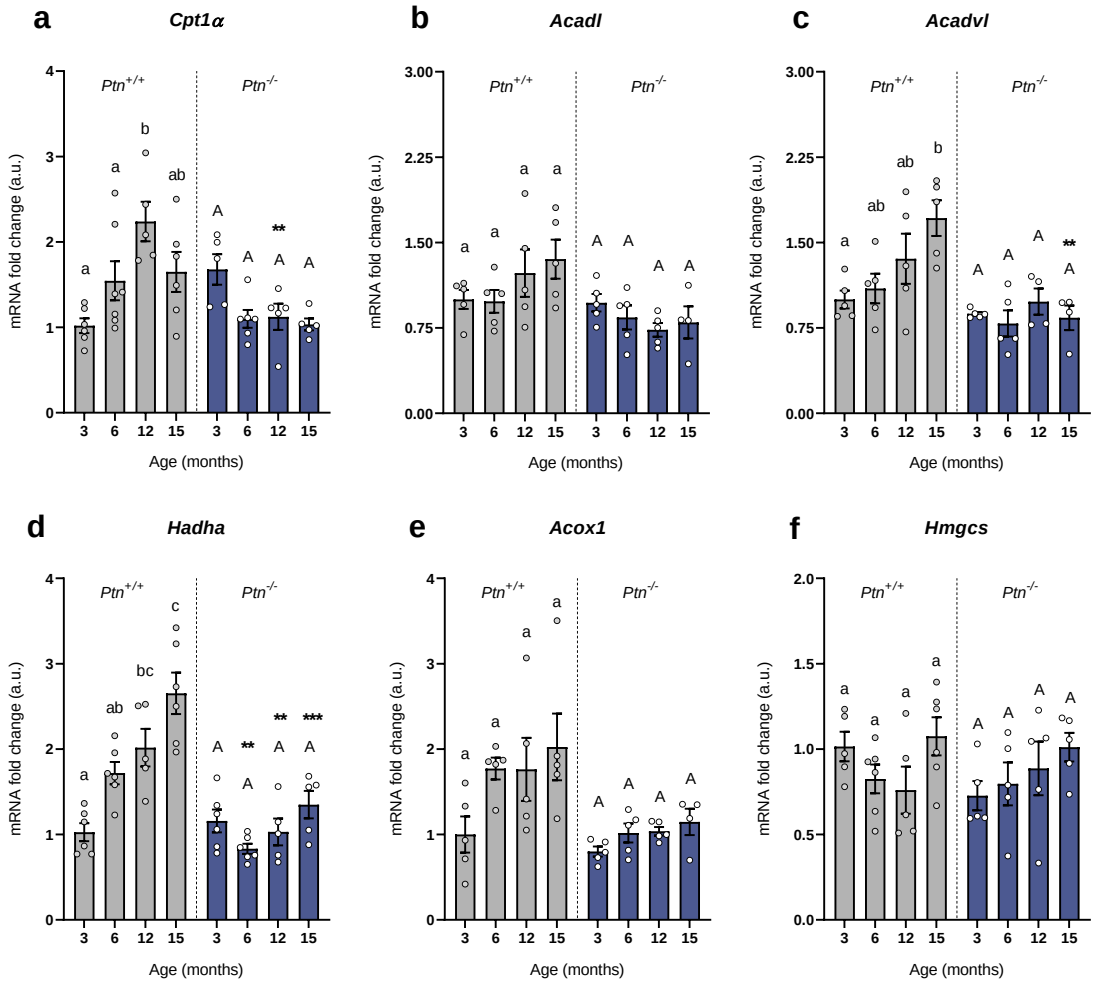

Figure 19. Ptn deletion downregulates the mRNA of critical enzymes of β-oxidation in old mice. *a) Carnitine palmitoyltransferase 1α (Cpt1α) mRNA; b) Acyl-CoA dehydrogenase, long-chain (Acadl) mRNA; c) Acyl-CoA dehydrogenase, very long-chain (Acadvl) mRNA; d) Hydroxyacyl-CoA dehydrogenase α (Hadha) mRNA; e) Acyl-CoA oxidase 1 (Acox1) mRNA and f) Hydroxymethylglutaryl-CoA synthase (Hmgcs) mRNA. Data are presented as mean ± SEM for n=5-6 mice/group. Different letters indicate statistically significant differences in the effect of ageing within the same genotype. Lowercase letters indicate statistically significant differences for $Ptn^{+/+}$ and capital letters for $Ptn^{-/-}$; *p<0.05, **p<0.01, ***p<0.001 for differences between $Ptn^{+/+}$ and $Ptn^{-/-}$ mice of the same age.*

The mRNA expression of *Cpt1α* increased with age in $Ptn^{+/+}$ and was not modified or even decreased from 3 to 15 months in $Ptn^{-/-}$ mice (Figure 19a). The ANOVA analysis showed that the differential expression of *Cpt1α* with age is affected by the genotype ($F(3,37)=8.222$; p-value=0.0003). On the other hand, the analysis of the β-oxidation enzymes (*Acadl*, *Acadvl* and *Hadha*) revealed an increment in their mRNA with age in $Ptn^{+/+}$ mice, and that this effect was blunted after *Ptn* deletion (Figure 19b-d). The statistical analysis with the ANOVA test showed an interaction of age and genotype in *Hadha* ($F(3,37)=7.922$; p-value=0.0003). We did not find significant differences either with ageing or *Ptn* deletion in mRNA expression of *Acox1*, an enzyme involved in the peroxisomal oxidation of fatty acids (Figure 19e).

We also determined the effect of pleiotrophin deletion and ageing on ketogenesis and measured the mRNA of *hydroxymethylglutaryl-CoA synthase*. As shown in Figure 19f, neither genotype nor age had any effect on the mRNA levels of *Hmgcs*.

3.1.8. Effects of Ptn deletion and ageing in mRNA expression of the enzymes of the tricarboxylic acid cycle (TCA)

One of the destinies of the molecules of acetyl-CoA produced by β-oxidation is the complete oxidization to CO_2 in the tricarboxylic acid cycle (TCA). The analysis of the mRNA of the enzymes of the TCA revealed that the mRNA levels of citrate synthase (*Cs*), isocitrate dehydrogenase (*Idh3g*) and α-ketoglutarate dehydrogenase (*Akgdh*) (Figures 20a-c) did not change with age either in $Ptn^{+/+}$ or in $Ptn^{-/-}$ mice. However, *Akgdh* mRNA levels were higher in 3 and 15 months old $Ptn^{-/-}$ mice compared to $Ptn^{+/+}$ animals (Figure 20c), but no interaction age-genotype was found when we performed the ANOVA test. In the $Ptn^{+/+}$ mice, the mRNA of the mitochondrial and cytoplasmic isoenzymes of malate dehydrogenase (*Mdh1* and *Mdh2)* progressively increased with age. However, the levels of *Mdh1* were not modified with age in $Ptn^{-/-}$ mice, being significantly lower at 15 months than in their age-matched $Ptn^{+/+}$ controls (Figure 20d), and *Mdh2* mRNA was significantly higher in the 3 months old $Ptn^{-/-}$ mice than in the 3 months old $Ptn^{+/+}$ animals, but it decreased with age (Figure 20e). In both cases, there is a strong link between age and genotype effects as shown by the ANOVA analysis ($F(3,36)=5.512$; p-value=0.0032 for *Mdh1*, and $F(3,37)=10.36$; p-value<0.0001 for *Mdh2*).

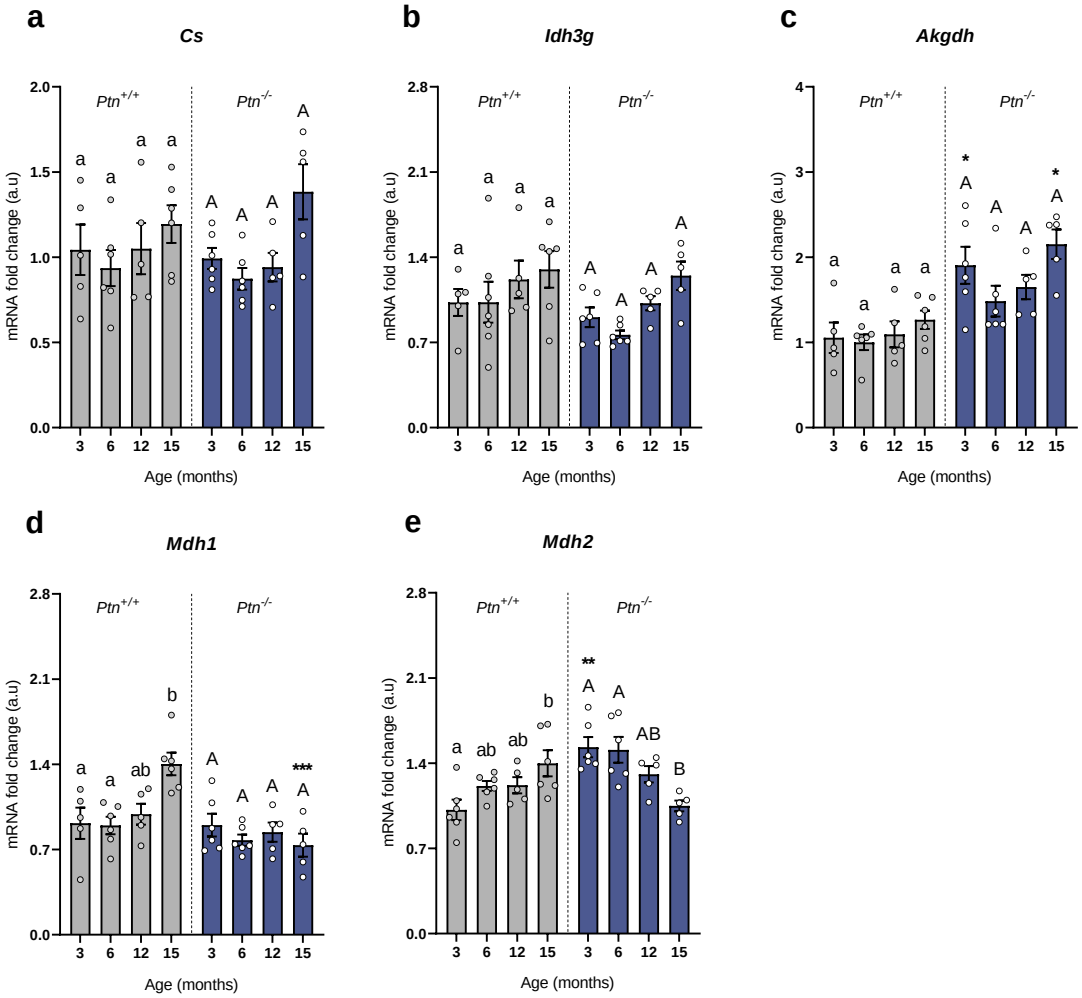

Figure 20. Effects of Ptn deletion in mRNA levels of the enzymes of the tricarboxylic acid cycle. *a) Citrate synthase (Cs) mRNA; b) Isocitrate dehydrogenase-3 gamma (Idh3g) mRNA; c) Alpha-ketoglutarate dehydrogenase (Akgdh) mRNA; d) Malate dehydrogenase, isoform 1 (Mdh1) mRNA; and e) Malate dehydrogenase, isoform 2 (Mdh2) mRNA. Data are presented as mean ± SEM for n=5-6 mice/group. Different letters indicate statistically significant differences in the effect of ageing within the same genotype. Lowercase letters indicate statistically significant differences for $Ptn^{+/+}$ and capital letters for $Ptn^{-/-}$; *p<0.05, **p<0.01, ***p<0.001 for differences between $Ptn^{+/+}$ and $Ptn^{-/-}$ mice of the same age.*

3.1.9. Effects of Ptn deletion and ageing on the key enzymes of the glycolytic pathway

The glucose intolerance and hyperinsulinemia observed in the knock-out mice prompt us to investigate whether pleiotrophin deletion may alter the expression of enzymes involved in the glycolytic pathway. We first analysed the mRNA of the main hepatic glucose transporter in the liver, but no changes were found in *Glut2* mRNA levels in either genotype. However,

15 months-old *Ptn*$^{-/-}$ mice showed a slightly higher mRNA of *Glut2* compared to younger *Ptn*$^{-/-}$ animals and to 15 months-old *Ptn*$^{+/+}$ mice (Figure 21a).

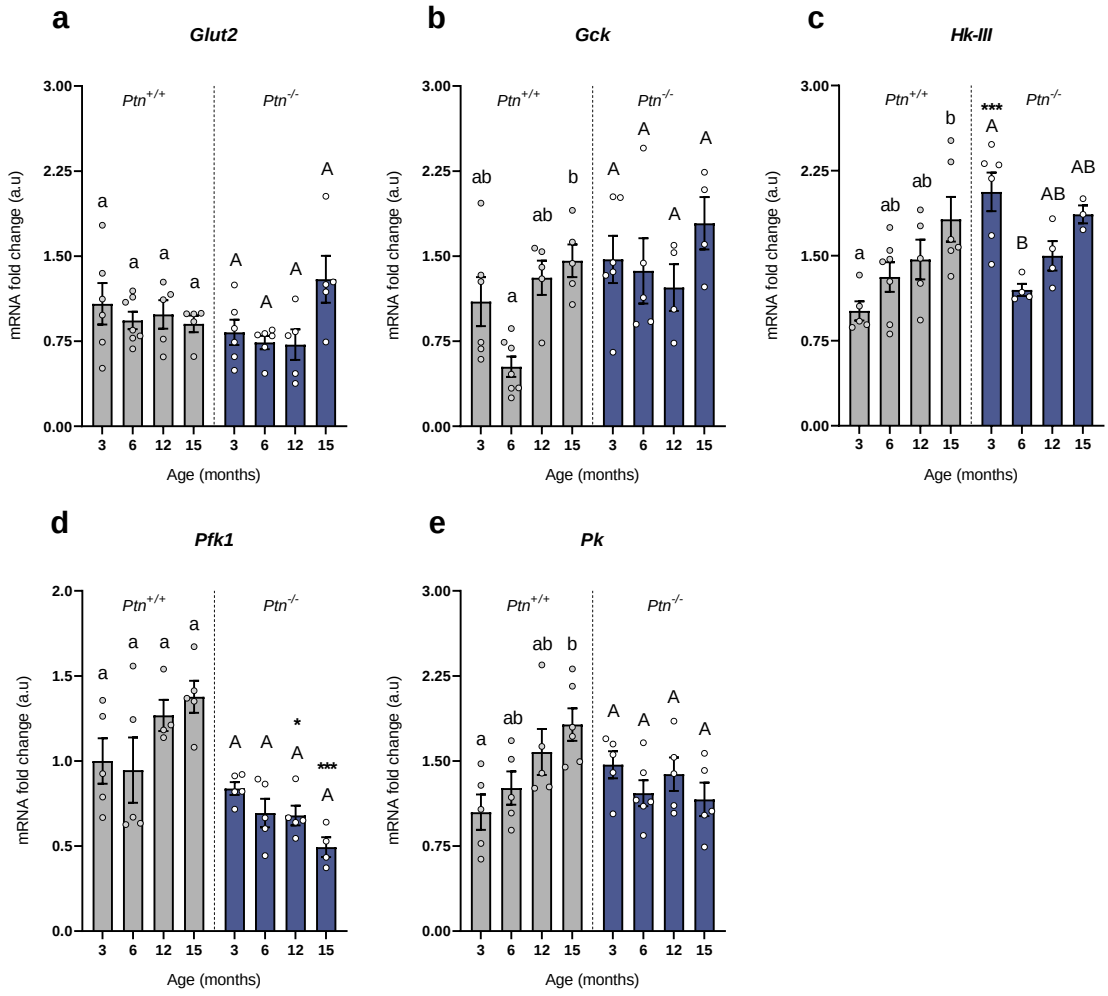

Figure 21. Effect of Ptn deletion in the mRNA of key enzymes of glycolysis. *a) Glut2 mRNA; b) Glucokinase (Gck) mRNA; c) Hexokinase-III (Hk-III) mRNA; d) Phosphofructokinase I (Pfk1) mRNA; and e) Pyruvate kinase (Pk) mRNA. Data are presented as mean ± SEM for n=5-6 mice/group. Different letters indicate statistically significant differences in the effect of ageing within the same genotype. Lowercase letters indicate statistically significant differences for Ptn$^{+/+}$ and capital letters for Ptn$^{-/-}$; *p<0.05, **p<0.01, ***p<0.001 for differences between Ptn$^{+/+}$ and Ptn$^{-/-}$ mice of the same age.*

We next analysed the mRNA expression of the main liver hexokinases. Glucokinase, or hexokinase-IV, is the major isoform in the liver. *Gck* mRNA levels were found to decrease in 6 months *Ptn*$^{+/+}$ mice, but no significant differences were found between 3, 12 and 15-months-old *Ptn*$^{+/+}$ mice. In *Ptn*$^{-/-}$ animals, *Gck* remained stable along time (Figure 21b). On the other hand, *hexokinase-III* significantly increased with age in *Ptn*$^{+/+}$ animals (Figure 21c). Although the mRNA of *hexokinase* was higher in 3-months-old *Ptn*$^{-/-}$ mice than in their age-matched controls, these differences disappeared from 6 months on ($F(3,32)=6.387$; p-value=0.0016). No significant differences were found in *phosphofructokinase* (*Pfk1*) due to

age either in *Ptn*$^{+/+}$ and *Ptn*$^{-/-}$ mice, despite the mRNA levels tend to increase in the *Ptn*$^{+/+}$ mice and to decrease in the *Ptn*$^{-/-}$ mice. According to these trends, 12 and 15 months *Ptn*$^{-/-}$ animals showed a significantly lower expression of *Pfk1* than their age-matched *Ptn*$^{+/+}$ controls (Figure 21d), indicating that age-related changes of *Pfk1* are linked to genotype (F(3,30)=4.631; p-value=0.0089). Finally, pyruvate kinase (*Pk*) mRNA increased with age in *Ptn*$^{+/+}$ mice, but it remained unchanged in *Ptn*$^{-/-}$ animals (F(3,34)=4.497; p-value=0.0092) (Figure 21e).

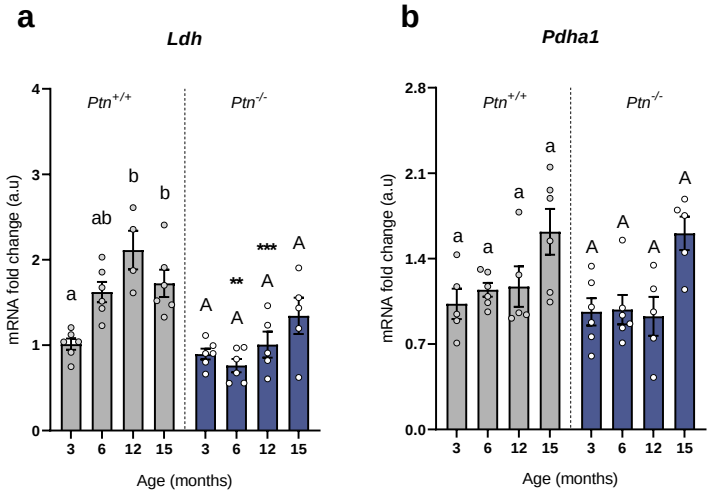

Figure 22. Effect of Ptn deletion in the mRNA expression of lactate dehydrogenase and pyruvate dehydrogenase. *a) Lactate dehydrogenase (Ldh) mRNA; and b) Pyruvate dehydrogenase (Pdha1) mRNA. Data are presented as mean ± SEM for n=5-6 mice/group. Different letters indicate statistically significant differences in the effect of ageing within the same genotype. Lowercase letters indicate statistically significant differences for Ptn*$^{+/+}$ *and capital letters for Ptn*$^{-/-}$*; *p<0.05, **p<0.01, ***p<0.001 for differences between Ptn*$^{+/+}$ *and Ptn*$^{-/-}$ *mice of the same age.*

As shown in Figure 22, we also analysed the mRNA of the enzymes involved in the transformation of pyruvate into lactate (lactate dehydrogenase) and into acetyl-CoA (pyruvate dehydrogenase). *Ldh* mRNA increased with age in *Ptn*$^{+/+}$ mice, but this age-related increment of gene expression was not found in *Ptn*$^{-/-}$ animals, who showed significantly lower levels at 6 and 12 months of age compared to the age-matched *Ptn*$^{+/+}$ mice (Figure 22a). The ANOVA analysis revealed a strong association in the effect of age and genotype (F(3,36)=5.352; p-value=0.0038). On the other hand, pyruvate dehydrogenase *(Pdha1)* mRNA levels were affected neither by age nor genotype (Figure 22b).

3.1.10. Effects of Ptn deletion and ageing in the pentose phosphate pathway

As glucose can also be diverted to the pentose phosphate pathway for the obtention of ribose 5P and NADPH, we analysed the mRNA of glucose-6-phosphate dehydrogenase (*G6pd*), the enzyme that catalyses the first reaction of the pathway, and the mRNA of transketolase (*Tkt*), an enzyme that is involved in the non-oxidative phase of the pathway and that can modulate the carbon flux between the non-oxidative phase of the pentose phosphate pathway and glycolysis or gluconeogenesis.

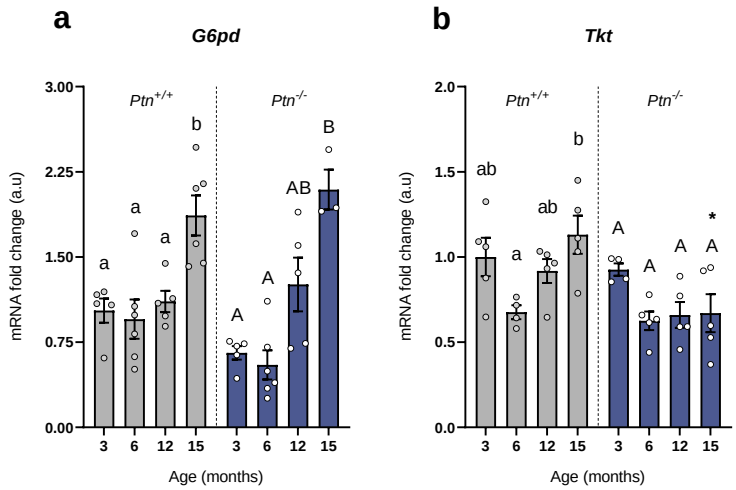

Figure 23. mRNA of pentose phosphate pathway key enzymes in liver of Ptn$^{+/+}$ and Ptn$^{-/-}$ mice. *a) Glucose-6-phosphate dehydrogenase (G6pd) mRNA; and b) Transketolase (Tkt) mRNA. Data are presented as mean ± SEM for n=5-6 mice/group. Different letters indicate statistically significant differences in the effect of ageing within the same genotype. Lowercase letters indicate statistically significant differences for Ptn$^{+/+}$ and capital letters for Ptn$^{-/-}$; *p<0.05, **p<0.01, ***p<0.001 for differences between Ptn$^{+/+}$ and Ptn$^{-/-}$ mice of the same age.*

G6pd mRNA levels are upregulated in a similar way with age in both *Ptn*$^{+/+}$ and *Ptn*$^{-/-}$ animals (Figure 23a). *Tkt* transcripts levels also increased from young to old *Ptn*$^{+/+}$ animals, whereas age did not affect *Tkt* expression in *Ptn*$^{-/-}$ mice. Consequently, *Tkt* mRNA was found to be significantly lower in 15 months-old *Ptn*$^{-/-}$ animals than in the same-aged *Ptn*$^{+/+}$ mice (Figure 23b). However, no interaction between the two factors was found in the ANOVA analysis.

3.1.11. Effects of Ptn deletion and ageing on gluconeogenic gene expression

We next analysed whether *Ptn* deletion could affect the mRNA of enzymes involved in the *de novo* synthesis of glucose. The age-related changes in pyruvate carboxylase (*Pc*) mRNA have an opposite trend in the two genotypes, reporting the strong interaction between age and genotype ($F(3,34)=16.37$; p-value<0.0001). In fact, *Pc* expression increased with age in

Ptn$^{+/+}$ animals but progressively decreased in *Ptn*$^{-/-}$ mice. Despite the higher *Pc* mRNA levels in young *Ptn*$^{-/-}$ mice, in 15-months *Ptn*$^{-/-}$ animals, *Pc* was significantly lower than in *Ptn*$^{+/+}$ mice (Figure 24a).

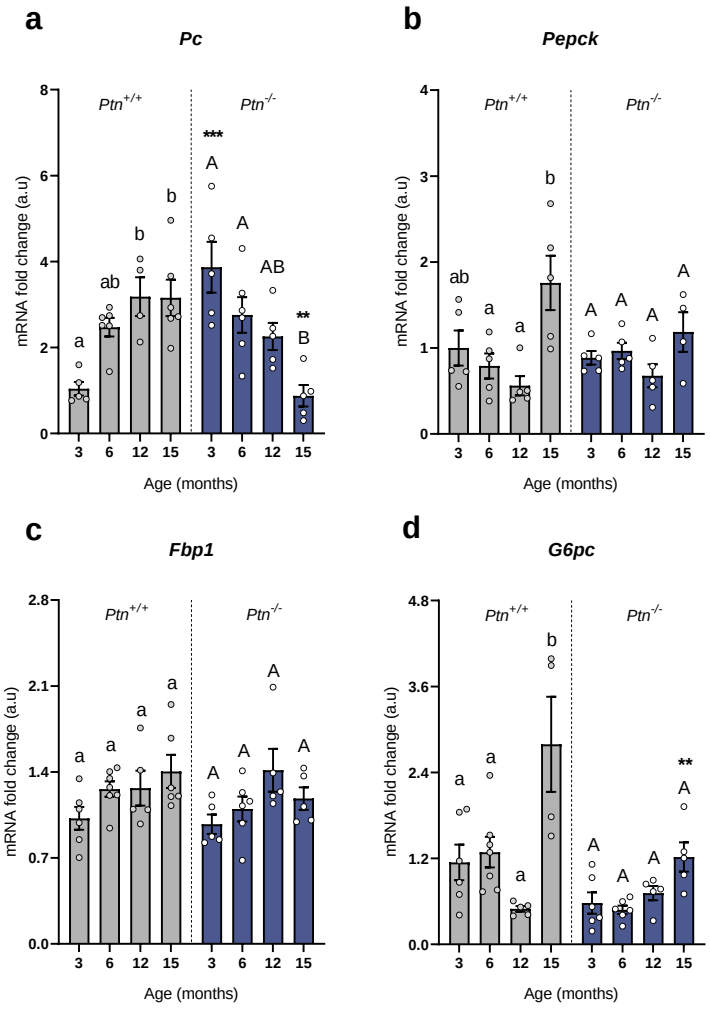

Figure 24. Pleiotrophin deletion impairs the mRNA levels of key enzymes involved in gluconeogenesis. *a) Pyruvate carboxylase (Pc) mRNA; b) Phosphoenolpyruvate carboxykinase (Pepck) mRNA; c) Fructose 1,6 bisphosphatase (Fbp1) mRNA; and d) Glucose 6-phosphatase catalytic subunit (G6pc) mRNA. Data are presented as mean ± SEM for n=5-6 mice/group. Different letters indicate statistically significant differences in the effect of ageing within the same genotype. Lowercase letters indicate statistically significant differences for Ptn*$^{+/+}$ *and capital letters for Ptn*$^{-/-}$*; *p<0.05, **p<0.01, ***p<0.001 for differences between Ptn*$^{+/+}$ *and Ptn*$^{-/-}$ *mice of the same age.*

Secondly, phosphoenolpyruvate carboxykinase (*Pepck*) increased in old *Ptn*$^{+/+}$ mice but did not change in *Ptn*$^{-/-}$ animals (Figure 24b). Despite the absence of significant differences, fructose-1,6-biphosphatase (*Fbp1*) mRNA tends to increase with age (Figure 24c). Finally, glucose-6-phosphatase (*G6pc*) mRNA increased in the 15 months old mice, but this increment was not significant in *Ptn*$^{-/-}$ animals. Therefore, 15 months old *Ptn*$^{-/-}$ mice had

significantly lower *G6pc* expression than their age-matched *Ptn*$^{+/+}$ controls (Figure 24d), pointing out an interplay between age and genotype (F(3,36)=4.269; p-value=0.0112).

3.1.12. Effects of Ptn deletion and ageing on the mRNA of the key enzymes of the metabolism of nitrogenous compounds

To analyse the role of pleiotrophin on the metabolism of nitrogenous compounds, we measured the mRNA of glutamate dehydrogenase 1 (*Glud1*) and carbamoyl-phosphate synthase 1 (*Cps1*). *Glud1* catalyses the deamination of glutamate to α-ketoglutarate and ammonia, and carbamoyl-phosphate synthase 1 is the enzyme responsible for the first reaction of the urea cycle, which involves the synthesis of carbamoyl phosphate from ammonia and bicarbonate. In our ageing mice model, we did not find differences caused by ageing or pleiotrophin deletion itself in *Glud1* mRNA (Figure 25a). However, the ANOVA analysis showed an interaction between both factors (F(3,37)=3.312; p-value=0.0304).

We also observed an age-related upregulation of *Cps1* in the *Ptn*$^{+/+}$ mice (Figure 25b). On the other hand, although 3 months old *Ptn*$^{-/-}$ animals showed a significantly higher expression of *Cps1* than 3 months old *Ptn*$^{+/+}$ mice, *Ptn* deletion was associated with a progressive decrease in the mRNA levels of *Cps1* with age. These different trends were confirmed in the ANOVA analysis that revealed an interaction in the influence of age and genotype on *Cps1* mRNA expression (F(3,38)=11.39; p-value<0.0001).

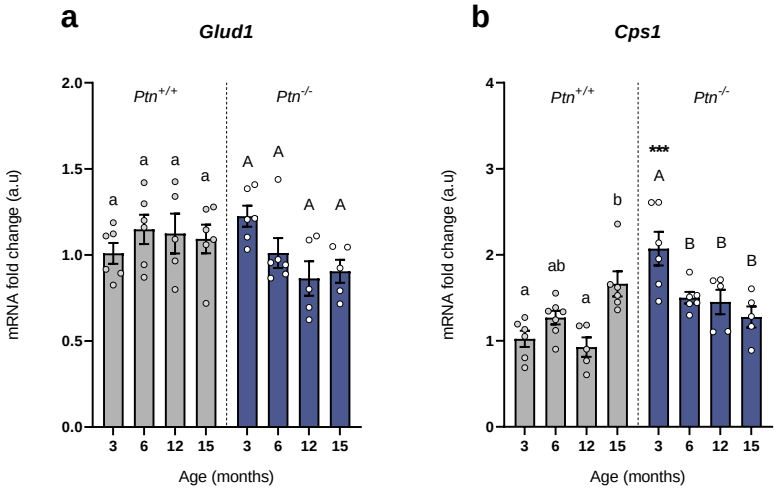

Figure 25. Effect of Ptn deletion and ageing in the metabolism of the nitrogenous compounds. *a) Glutamate dehydrogenase I (Glud1) mRNA; and b) Carbamoyl phosphate synthetase I (Cps1) mRNA. Data are presented as mean ± SEM for n=5-6 mice/group. Different letters indicate statistically significant differences in the effect of ageing within the same genotype. Lowercase letters indicate statistically significant differences for Ptn$^{+/+}$ and capital letters for Ptn$^{-/-}$; *p<0.05, **p<0.01, ***p<0.001 for differences between Ptn$^{+/+}$ and Ptn$^{-/-}$ mice of the same age.*

3.1.13. Ptn deletion and ageing alters the hepatic mRNA of transcription factors of critical genes in lipid and glucose metabolism

To decipher the molecular mechanisms that may be involved in the changes in lipid metabolism observed after *Ptn* deletion, we measured the mRNA of several transcription factors that have been shown to regulate the expression of the key enzymes involved in lipid metabolism.

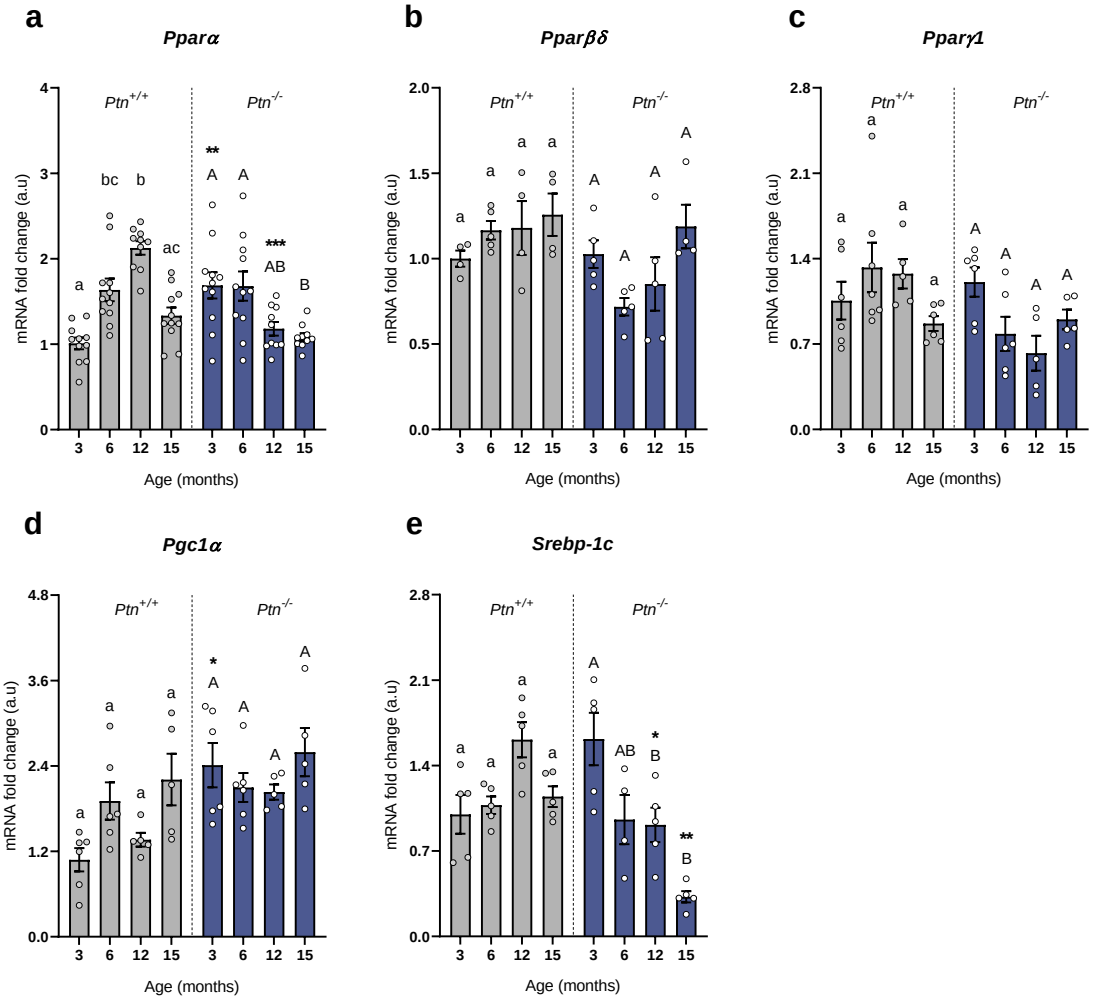

Figure 26. Effect of Ptn deletion in the mRNA of several transcription factors key in lipid metabolism. *a) Ppar-α mRNA; b) Ppar-βδ mRNA; c) Ppar-γ1 mRNA; d) PPAR gamma, coactivator 1 alpha (Pgc1α) mRNA; and e) sterol regulatory element-binding transcription factor 1 (Srebp-1c) mRNA. Data are presented as mean ± SEM for n=5-6 mice/group. Different letters indicate statistically significant differences in the effect of ageing within the same genotype. Lowercase letters indicate statistically significant differences for Ptn$^{+/+}$ and capital letters for Ptn$^{-/-}$; *p<0.05, **p<0.01, ***p<0.001 for differences between Ptn$^{+/+}$ and Ptn$^{-/-}$ mice of the same age.*

First, we analysed the mRNA levels of the different PPAR isoforms. *Pparα* mRNA increased from 3 to 12 months in $Ptn^{+/+}$ animals and then decreased from 12 to 15 months (Figure 26a). In $Ptn^{-/-}$ mice, *Pparα* mRNA levels were higher in the 3 months old $Ptn^{-/-}$ mice than in their respective controls and progressively decreased with age. The ANOVA test confirmed that variations in *Pparα* mRNA were due to an interaction between age and genotype ($F(3,77)=17.26$; p-value<0.0001).

No differences were found either in *Pparβδ* or *Pparγ1* mRNA levels (Figure 26b-c), but the ANOVA test revealed an interaction of age and genotype in *Pparγ1* ($F(3,38)=3.991$; p-value=0.0145).

The analysis of the mRNA of *Pgc1α* revealed that whereas the levels of *Pgc1α* in $Ptn^{+/+}$ animals tend to increase with age, no changes were observed in $Ptn^{-/-}$ mice. Noteworthy, the mRNA levels of *Pgc1α* were 2-fold higher in 3 months old $Ptn^{-/-}$ animals than in the age-matched $Ptn^{+/+}$ mice (Figure 26d). Nevertheless, no statistically significant differences were obtained in the ANOVA test.

Although no differences were found in the *Srebp-1c* mRNA of $Ptn^{+/+}$ mice, 3 months old $Ptn^{-/-}$ animals showed significantly higher levels of *Srebp-1c* than $Ptn^{+/+}$ mice, and the mRNA of *Srebp-1c* decreased with age in $Ptn^{-/-}$ mice (Figure 26e). The ANOVA analysis reported that age-related variations in mRNA levels of *Srebp-1c* are related to the genotype ($F(3,31)=11.07$; p-value<0.0001).

In order to investigate the molecular mechanisms involved in the changes in the expression of gluconeogenic genes related to ageing and pleiotrophin deletion, we analysed the mRNA and protein content of NUR77. NUR77 is a transcription factor that has been implicated in the regulation of liver metabolism. As glycerol kinase is a corepressor of NUR77 in the liver, we have also analysed the mRNA and protein levels of this enzyme.

As shown in Figure 27, no differences were found in the mRNA and protein levels of either glycerol kinase or NUR77 in the liver of $Ptn^{+/+}$ mice. However, mRNA and protein levels of glycerol kinase were increased in $Ptn^{-/-}$ mice compared with $Ptn^{+/+}$ animals, reaching maximum significance at 15 months. The ANOVA analysis did not show an interaction between age and genotype in the upregulation of glycerol kinase mRNA and protein levels. On the other hand, *Nur77* mRNA gradually increased with age in $Ptn^{-/-}$ mice (Figure 27c). Finally, the protein amount of NUR77 exhibited high variability and no differences were found between $Ptn^{+/+}$ and $Ptn^{-/-}$ mice (Figure 27d). However, the ANOVA analysis showed an effect of ageing in the protein expression ($F(3,25)=5.508$, p-value=0.0048).

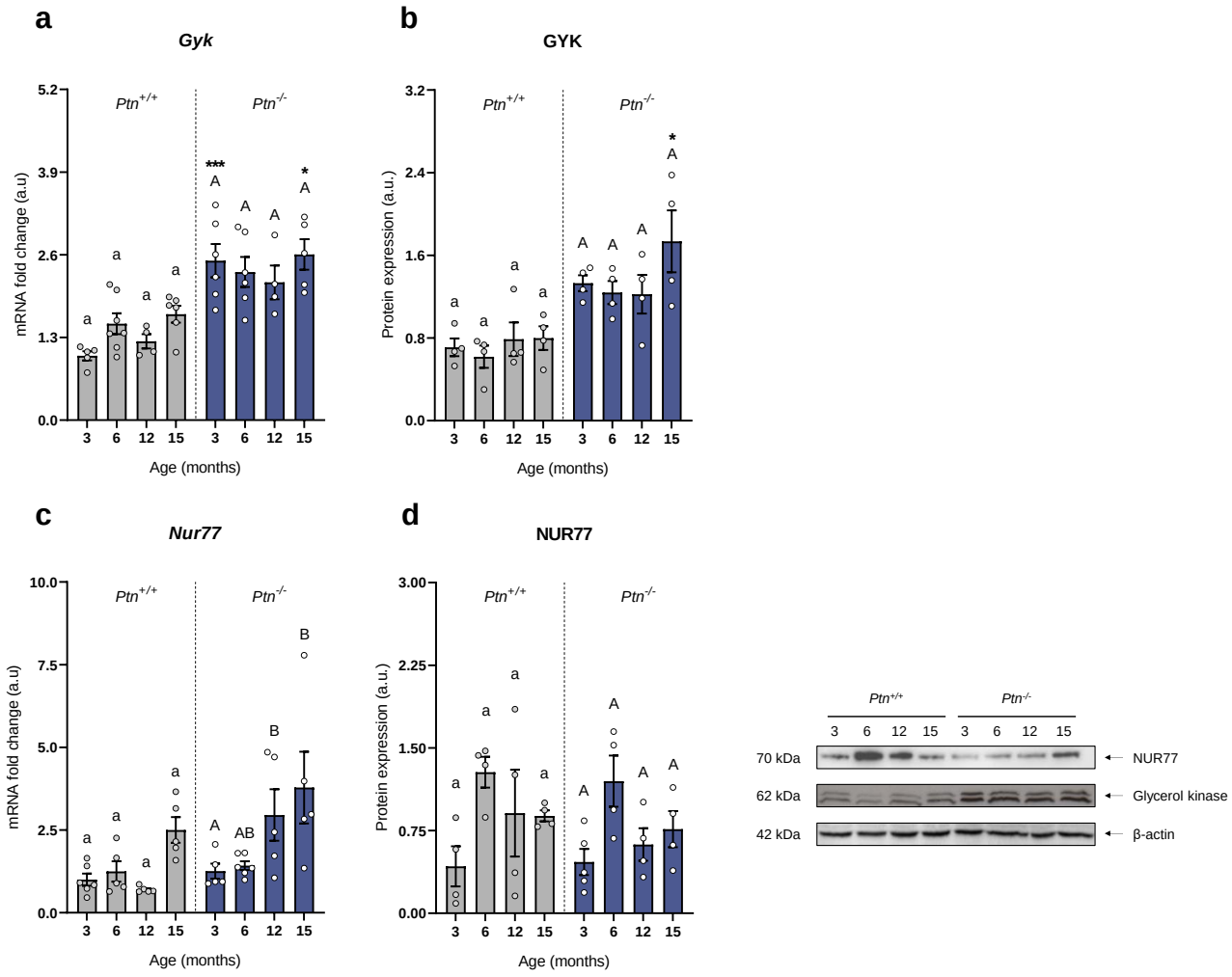

Figure 27. Transcription factors that mediate glucose metabolism regulation. *a) Glycerol kinase (Gyk) mRNA; b) Glycerol kinase protein; c) Nur77 mRNA; and d) NUR77 protein. Data are presented as mean ± SEM for n=4-5 mice/group. Different letters indicate statistically significant differences in the effect of ageing within the same genotype. Lowercase letters indicate statistically significant differences for $Ptn^{+/+}$ and capital letters for $Ptn^{-/-}$; *p<0.05, **p<0.01, ***p<0.001 for differences between $Ptn^{+/+}$ and $Ptn^{-/-}$ mice of the same age.*

3.2. Role of pleiotrophin in mitochondria biogenesis and endoplasmic reticulum function in an ageing model

3.2.1. Deletion of pleiotrophin enhances the expression of markers of mitochondrial biogenesis in young mice

As explained in the introduction of this chapter, ageing is associated with endoplasmic reticulum stress and impaired mitochondrial function. In this next section, we have analysed the effect of pleiotrophin deletion and ageing on hepatic mitochondria biogenesis and endoplasmic reticulum stress.

First of all, we have analysed three different markers of mitochondria biogenesis: mitofusin 1 (*Mfn1*) and mitofusin 2 (*Mfn2*) (localised in the outer mitochondrial membrane), and mitochondrial dynamin-like GTPase Opa1 (in the inner mitochondrial membrane). All these proteins participate in mitochondrial fusion, which consists of the physical merging of both the outer and inner membranes of two different mitochondria. This process of mitochondria fusion is essential for the maintenance of mitochondrial function as it enables to repair mitochondrial genome defects.

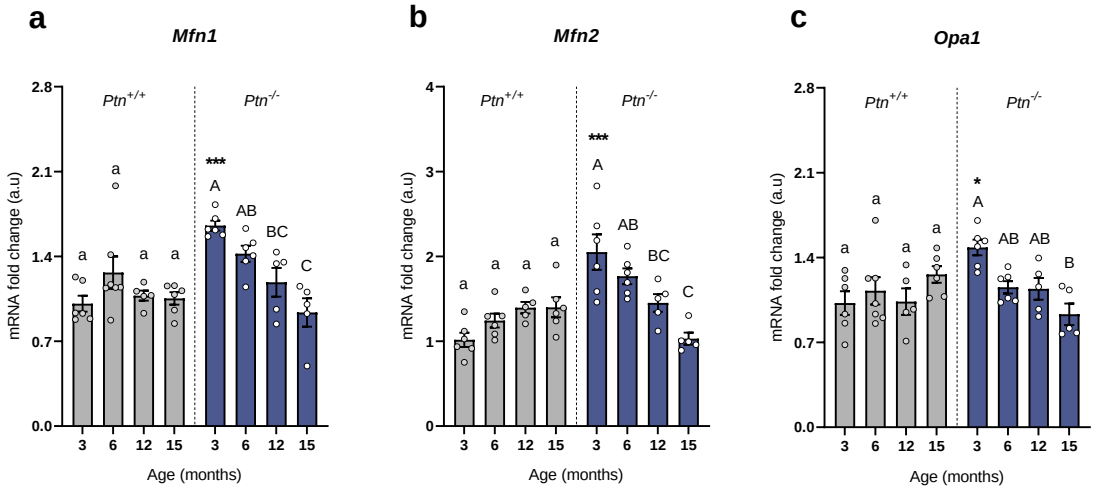

Figure 28. Deletion of Ptn increases mitochondria biogenesis in young mice. *a) Mitofusin 1 (Mfn1) mRNA; b) Mitofusin 2 (Mfn2) mRNA; and c) Opa 1 mitochondrial dynamin-like GTPase (Opa1) mRNA. Data are presented as mean ± SEM for n=5-6 mice/group. Different letters indicate statistically significant differences in the effect of ageing within the same genotype. Lowercase letters indicate statistically significant differences for $Ptn^{+/+}$ and capital letters for $Ptn^{-/-}$; *p<0.05, **p<0.01, ***p<0.001 for differences between $Ptn^{+/+}$ and $Ptn^{-/-}$ mice of the same age.*

In $Ptn^{+/+}$ animals, the expression of the markers (*Mfn1*, *Mfn2*, and *Opa1*) did not change with age. On the other hand, 3 months old $Ptn^{-/-}$ mice showed a 1.5-2 fold increment of the mRNA of *Mfn1*, *Mfn2*, and *Opa1* than 3 months old $Ptn^{+/+}$ controls. However, the expression of these markers diminishes progressively with age in $Ptn^{-/-}$ mice to expression levels like those of 3-month-old $Ptn^{+/+}$ mice (Figure 28a-c). The ANOVA analysis reported that the differential expression observed with age is affected by the genotype in all cases ($F(3,38)=6.519$; p-value=0.0011 for *Mfn1*, $F(3,37)=13.71$; p-value<0.0001 for *Mfn2*, and $F(3,38)=6.605$; p-value=0.0011 for *Opa1*).

3.2.2. The addition of exogenous PTN alters the mitochondrial respiration of primary hepatocytes

We next investigated whether PTN could affect mitochondrial metabolism. To do so, we carried on a small-scale study at the Karolinska Institutet, Sweden, during a 4-month international stay under the supervision of Dr Noah Moruzzi.

In this study, we isolated primary hepatocytes from wild-type C57BL/6J mice and incubated them with recombinant PTN, as explained in the *Materials and methods* section, and measured cellular respiration using extracellular flux analysis (Seahorse). With the Seahorse XF Analyzer, it is possible to perform the measurements of oxygen consumption rate (OCR) and extracellular acidification rate (ECAR) simultaneously and in real time. Thus, it allows getting an accurate insight into the cellular metabolic function in cultured cells. Respiration (oxygen consumption) and glycolysis (proton production) cause measurable changes to the concentrations of dissolved oxygen and free protons in the medium, altering the pH. Solid-state sensor probes measure these concentrations and then calculate the OCR and ECAR. In addition, the analyser has an integrated drug delivery system that allows the addition of different compounds in each well at user-defined intervals to analyse the effect of these compounds on the OCR and ECAR. We added oligomycin (an inhibitor of the complex V of ATP synthase), Carbonyl cyanide-4-(trifluoromethoxy)phenylhydrazone (FCCP) (uncoupler protonophore that disrupts the mitochondrial membrane potential and potentiates the respiration), and rotenone/antimycin A (inhibitors of complex I and III, which blocks mitochondrial respiration).

The measurement of oxygen consumption rate or mitochondrial respiration (OCR), in combination with different inhibitors and uncoupler, is used to estimate the mitochondria oxidative phosphorylation (OXPHOS). Thus, we measured the basal or steady-state OCR, coupling efficiency, which estimates the amount of ATP-linked to oxygen consumption, and maximal OCR. Basal OCR is the sum of all O_2 consuming processes in the cell. A higher basal OCR could be the consequence of an increase in ATP turnover, proton leak or non-mitochondrial respiration (i.e., other cellular oxidases). Contrarily, amongst several potential causes, lower respiration would indicate lower ATP demand, a lack of substrate availability, or electron transport chain (ETC) impairment. The maximal OCR represents the maximal respiratory rate the cell can sustain when an uncoupler is provided. When diminished, the most common causes are a lower mitochondrial mass, mitochondrial impairments, or a decrease in substrate availability.

As shown in Figure 29a, when primary hepatocytes were treated with recombinant PTN for 3 hours, they exhibited increased basal and ATP-linked OCR, but no differences were

found in maximal OCR compared with the control condition, suggesting that the addition of exogenous PTN to hepatocytes cause an enhanced oxygen consumption and ATP demand. As expected, due to the activation of cellular signalling and glucose synthesis, when cells were treated with glucagon to determine if PTN alters gluconeogenesis, we observed that the three OCRs were higher than the control.

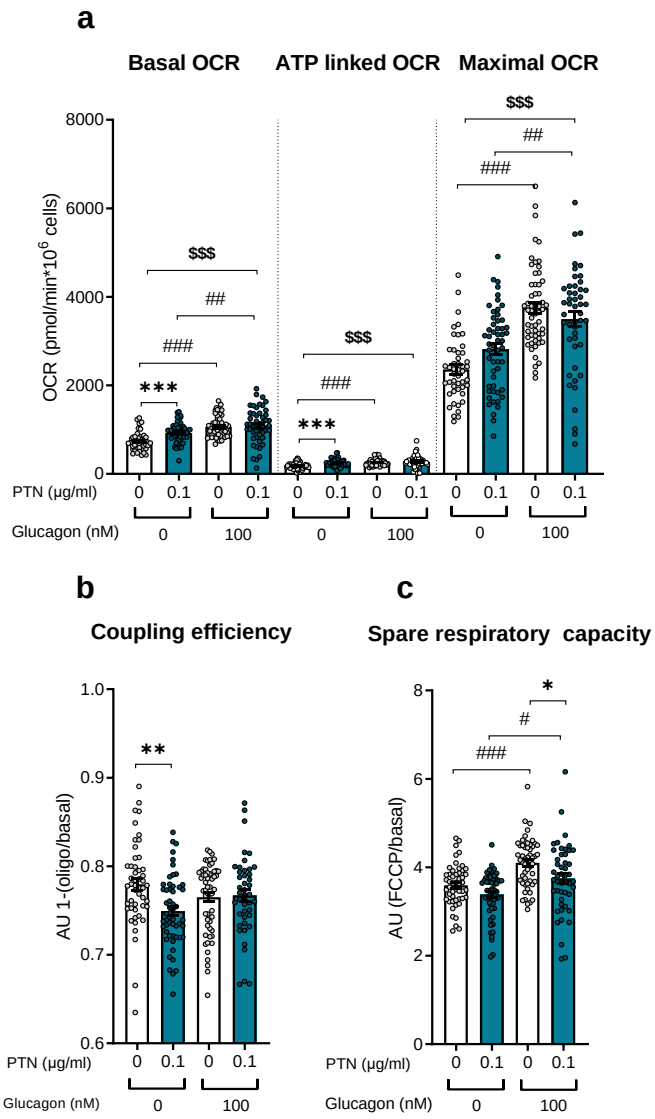

Figure 29. Cellular respiration of primary hepatocytes and basal effect of pleiotrophin or pleiotrophin plus glucagon. *a) Oxygen consumption rate (OCR): basal OCR, ATP linked OCR and maximal OCR; b) Coupling efficiency; and c) Spare respiratory capacity. Data are presented as mean ± SEM. *p<0.05, **p<0.01, ***p<0.001 for differences due to effect of pleiotrophin. $^{\#}$p<0.05, $^{\#\#}$p<0.01, $^{\#\#\#}$p<0.001 for differences due to the effect of glucagon $^{\$}$p<0.05, $^{\$\$}$p<0.01, $^{\$\$\$}$p<0.001 for differences due to the combined effects of pleiotrophin + glucagon.*

Furthermore, cells treated with glucagon plus PTN also increased over the control, but no differences were detected in comparison to the glucagon-treated cells. When looking at the cells treated with PTN and glucagon + PTN, the only one that did not show differences was the ATP-linked OCR. These results indicate that PTN itself is enough to alter basal OCR and ATP-linked OCR but not maximal OCR in the absence of glucagon. In fact, when treated jointly with PTN and glucagon, the effect of PTN on metabolism is lost.

Next, we analysed the apparent coupling efficiency, i.e., the proportion of oxygen consumption used to make ATP. It is calculated as 1-(Oligomycin OCR/basal OCR). We observed that cells treated with PTN alone reduced their coupling efficiency (Figure 29b), indicating that 0.1μM PTN might increase proton leak across the inner mitochondrial membrane or activating mechanisms that dissipates proton (i.e. ion exchanger). No differences were found between the controls and glucagon and glucagon + PTN treated cells.

Finally, mitochondrial spare capacity is defined as the ratio between maximal and basal respiration. In line with the OCR data shown in Figure 29a, PTN itself did not alter the spare respiratory capacity of the hepatocytes, but glucagon did. However, when treated with glucagon and PTN, respiratory capacity was slightly decreased compared to cells treated only with glucagon (Figure 29c). This can be due to a slight increase in basal respiration that we were not able to pick up after normalization or may suggest that in a condition of gluconeogenic stimulation, PTN might blunt the effect of glucagon.

3.2.3. Effects of pleiotrophin deletion on the expression of endoplasmic reticulum stress markers during ageing

Endoplasmic reticulum (ER) stress occurs when the capacity of the ER to fold proteins becomes saturated. ER stress is associated with a range of diseases, including ischemia/reperfusion injury, neurodegeneration, diabetes, non-alcoholic steatohepatitis, hyperinsulinemia, and inflammation (207). We next analysed if ageing and/or pleiotrophin deletion may modify the development and response to ER stress.

We first analysed mRNA levels of *Bip*, also known as HSPA5 or heat shock protein family A (HSP70) member 5. This gene encodes a chaperone involved in protein folding and assembling in the ER and is essential for regulating ER homeostasis. In $Ptn^{+/+}$ mice, *Bip* mRNA is constant in the early stages of life but significantly increased at 15 months. However, in $Ptn^{-/-}$ animals, the levels did not vary with age and were significantly lower in the eldest animals than in the age-matched $Ptn^{+/+}$ control mice (Figure 30a).

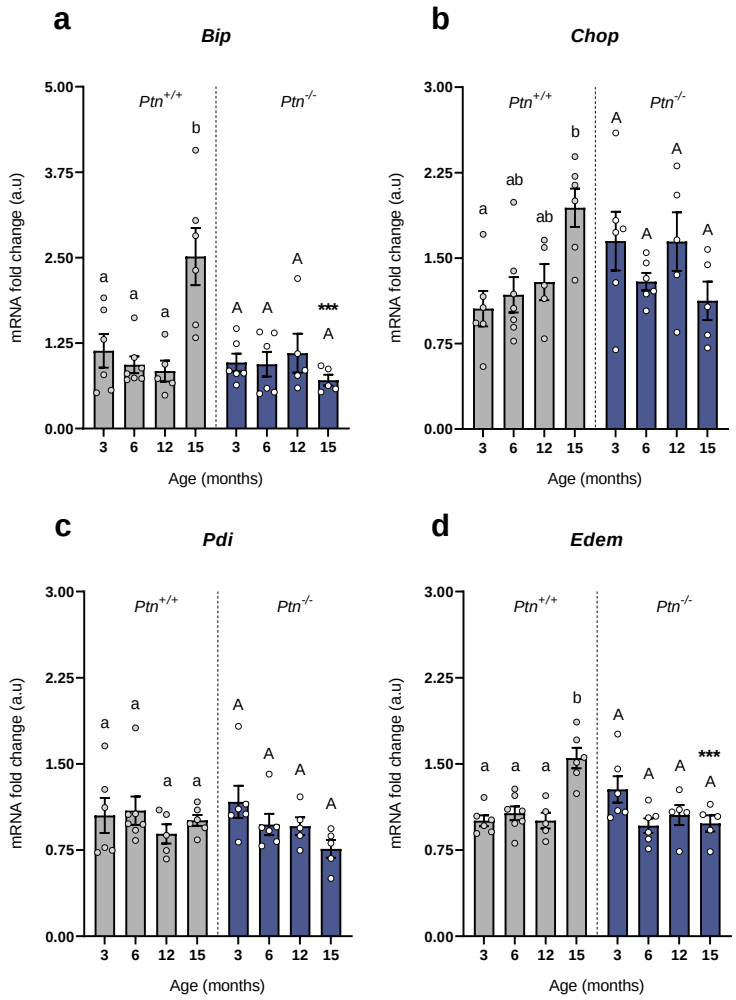

Figure 30. Effects of pleiotrophin deletion on the mRNA of endoplasmic reticulum stress markers during ageing. *a) Heat shock protein family A (HSP70) member 5 (Bip) mRNA; b) C/EBP homologous protein (Chop) mRNA; c) ER degradation enhancing alpha-mannosidase like protein 1 (Edem) mRNA; and d) Protein disulphide isomerase (Pdi) mRNA. Data are presented as mean ± SEM for n=5-6 mice/group. Different letters indicate statistically significant differences in the effect of ageing within the same genotype. Lowercase letters indicate statistically significant differences for* $Ptn^{+/+}$ *and capital letters for* $Ptn^{-/-}$*; *p<0.05, **p<0.01, ***p<0.001 for differences between* $Ptn^{+/+}$ *and* $Ptn^{-/-}$ *mice of the same age.*

Next, we determined *Chop* (C/EBP homologous protein) and *Pdi* (protein disulphide isomerase), a pair of enzymes that are activated by ER stress. Figures 30b and 30c showed that in $Ptn^{+/+}$ mice, *Chop* mRNA progressively increased with age, whereas *Pdi* remained unchanged. On the other hand, in $Ptn^{-/-}$ mice, the mRNA of these enzymes was not affected by the ageing process.

Ultimately, we measured the mRNA of ER degradation enhancing alpha-mannosidase like protein 1 (*Edem*), a protein closely related to the ER-associated degradation of misfolded or unassembled proteins. Similarly to *Bip*, *Edem* mRNA is upregulated in 15

months old *Ptn*$^{+/+}$ animals, while there was no variation of mRNA levels in the *Ptn*$^{-/-}$ mice. Accordingly, the eldest *Ptn*$^{-/-}$ mice have significantly lower mRNA levels than the same-aged *Ptn*$^{+/+}$ animals (Figure 30d). The 2 way-ANOVA analysis displayed that in all genes (except *Pdi*), there was an interaction of both factors indicating that the effect of ageing is dependent on the genotype: F(3,38)=8.006; p-value=0.0003 for *Bpi*, F(3,38)=5.627; p-value=0.0027 for *Chop*, and F(3,38)=10.28; p-value<0.0001 for *Edem*.

3.3. Effects of pleiotrophin deletion on the hepatic inflammation in an ageing model

Ageing is usually associated with increased inflammation and a defective inflammatory response of the organism. Moreover, several pathologies with high and growing incidence, such as obesity and diabetes, have been suggested to exhibit a substantial inflammatory component. In this section of the chapter, we have investigated the possible implication of pleiotrophin and ageing in hepatic inflammation.

3.3.1. Deletion of pleiotrophin triggers macrophage recruitment in old mice

We first analysed two markers of the presence of macrophages in the liver. As can be observed in Figures 31a and 31b, in a physiological condition of ageing, no changes were found in the mRNA of *Cd68* and *F4/80* in the *Ptn*$^{+/+}$ mice. Nevertheless, when *Ptn* is deleted, there was an approximately 2-fold increase at 15 months of age in both genes (Figure 31a and 31b), suggesting an elevated presence of macrophages in the liver of *Ptn*$^{-/-}$ old mice. The multivariance analysis showed a strong association between genotype and ageing for *Cd68* and *F4/80* (F(3,36)=19.68; p-value<0.0001 and F(3,36)=13.83; p-value<0.0001 respectively).

To further clarify whether the increased mRNA of macrophage markers is due to an increment in the number of Kupffer cells or due to the presence of bone marrow-derived macrophages, we also analysed *Cd-11b* and *Cd-11c* as markers of bone marrow-derived macrophages. Noteworthy, although *Cd-11b* is expressed in Kupffer cells, its expression is much higher in the bone marrow macrophages. It is important to note that Cd-11b is also known as Mac-1 or $\alpha_M\beta2$ and has been identified as a PTN receptor.

In our model, the mRNA of *Cd-11b* and *Cd-11c* was not modified with ageing in *Ptn*$^{+/+}$ mice, but an increment in the mRNA levels of these macrophage markers was observed in old *Ptn*$^{-/-}$ animals (Figure 31c and 31d). The variance analysis revealed that only *Cd-11c* displayed an interaction of genotype and age (F(3,37)=4.202; p-value=0.0118). Notably, the increase of *Cd-11b* in *Ptn*$^{-/-}$ animals at 15 months is more than 2.5 times the levels of 15-months-old *Ptn*$^{+/+}$ mice and 10 times the levels of 3-months-old *Ptn*$^{+/+}$ mice (Figure 31c).

Thus, *Ptn* deletion and ageing seems to favour the infiltration of bone marrow-derived macrophages in the liver.

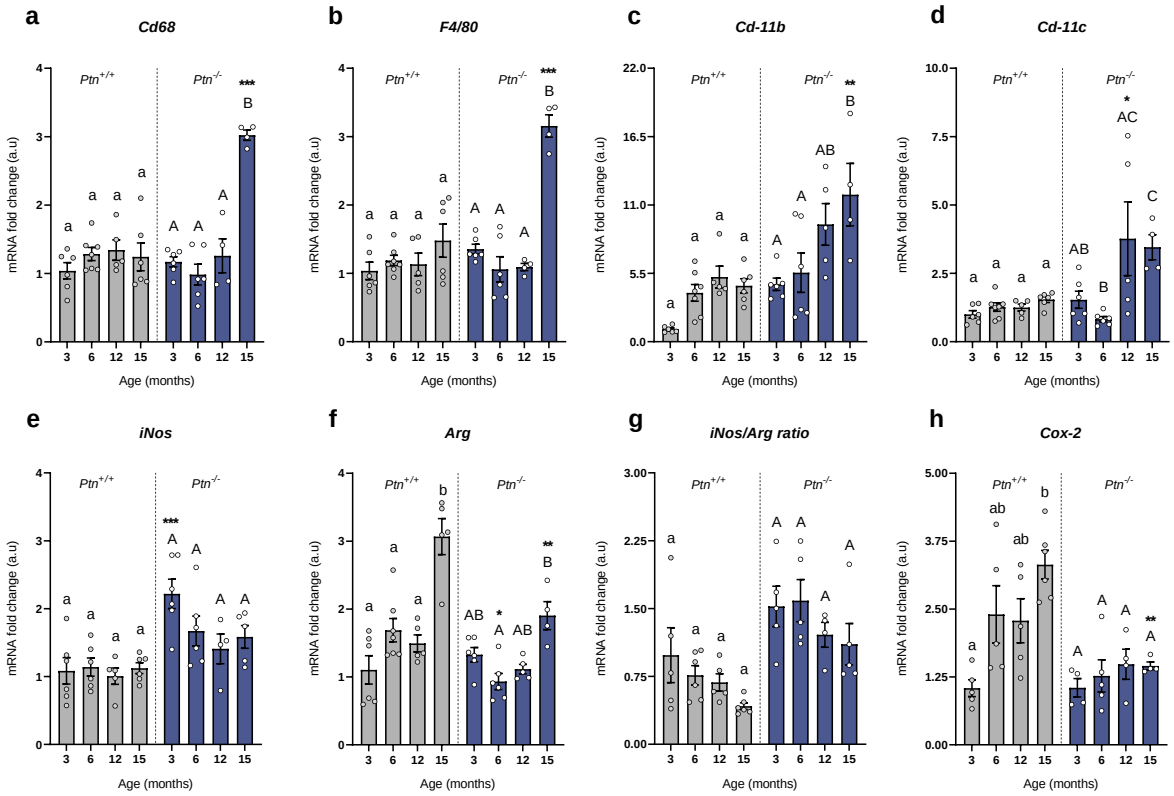

Figure 31. Effects of pleiotrophin deletion and ageing on the mRNA of macrophage markers. *a) Cd68 mRNA; and b) F4/80 mRNA c) Cd-11b mRNA; d) Cd-11c mRNA; e) Inducible nitric oxide synthase (iNos) mRNA; f) Arginase (Arg) mRNA; g) iNos/Arginase mRNA ratio; and h) cyclooxygenase-2 (Cox-2) mRNA. Data are presented as mean ± SEM for n=5-6 mice/group. Different letters indicate statistically significant differences in the effect of ageing within the same genotype. Lowercase letters indicate statistically significant differences for $Ptn^{+/+}$ and capital letters for $Ptn^{-/-}$; *p<0.05, **p<0.01, ***p<0.001 for differences between $Ptn^{+/+}$ and $Ptn^{-/-}$ mice of the same age.*

Furthermore, we also analysed two opposite markers of macrophage polarisation, the inducible nitric oxide synthase (*iNos*) and arginase (*Arg*). *iNos is* expressed by M1 or pro-inflammatory macrophages, whereas *Arg* is expressed by M2 or anti-inflammatory macrophages. The mRNA of *iNos* was not affected by age in either $Ptn^{+/+}$ or $Ptn^{-/-}$ mice. However, $Ptn^{-/-}$ animals had higher mRNA levels of *iNos* at 3 months of age than the same aged $Ptn^{+/+}$ mice (Figure 31e). *Arg* mRNA was upregulated in both 15-months-old $Ptn^{+/+}$ mice and $Ptn^{-/-}$ animals, although the increment of *Arg* is lower in $Ptn^{-/-}$ mice (Figure 31f). The ANOVA test showed the interplay between age and *Ptn* deletion in the variation of *Arg* mRNA levels (F (3, 36) = 5,940; p-value=0.0021).

To further characterize macrophage polarization, we calculated the *iNos*/*Arg* ratio. As shown in Figure 31g, *Ptn* deletion was associated with a higher *iNos*/*Arg* ratio, which suggests the presence of a larger population of pro-inflammatory M1 macrophages in the liver of $Ptn^{-/-}$ mice compared to $Ptn^{+/+}$ animals.

An alternative pathway involved in the activation of macrophages involves C3a and C5a from the complement system that ultimately stimulates the production of prostaglandins by COX-2. Finally, although there was no difference in the effect of genotype in the mRNA of cyclooxygenase-2 (*Cox-2*) in 3 months old mice, *Cox-2* levels gradually increased with age in $Ptn^{+/+}$ mice, whereas no variation was observed in $Ptn^{-/-}$ animals. Accordingly, at 15 months of age, mRNA levels are significantly lower in $Ptn^{-/-}$ mice than in the same-aged $Ptn^{+/+}$ animals (Figure 31h). However, no significant differences were found in the 2-way ANOVA analysis for *Cox-2*.

3.3.2. The inflammatory response is enhanced in old mice lacking pleiotrophin

As pleiotrophin deletion is associated with an age-related increment in the expression of liver macrophages markers and pleiotrophin has been shown to regulate inflammatory processes, we next measured the mRNA of *Tlr4*, *Ptprg*, and different inflammatory cytokines.

TLR4 signalling cascade is involved in the activation of macrophages. In fact, LPS-induced TLR4 activation leads to the production and secretion of TNFα, IL-1β and IL-6, among other cytokines, as well as the production of nitric oxide by iNOS.

In our study, $Ptn^{+/+}$ mice showed stable mRNA levels of *Tlr4* (Figure 32a), *Tnfα* (Figure 32b), and *Il-6* (Figure 32d). However, in $Ptn^{-/-}$ animals *Tlr4* and *Tnfα* mRNA levels increased with age, being significantly higher in the 15 months old $Ptn^{-/-}$ mice than in the age-matched $Ptn^{+/+}$ animals (Figure 32a and 32b), whereas no changes were observed in *Il-6* (Figure 32d). The effect of ageing in *Tlr4* mRNA was highly dependent on the genotype, as shown by the ANOVA analysis ($F(3,31)=6.867$; p-value=0.0011). In addition, the mRNA analysis of *Il-1β* revealed an increment with ageing in both genotypes (Figure 32c).

Moreover, we analysed the mRNA levels of *Ptprg,* a member of the protein tyrosine phosphatase receptors, that has been associated with the inflammatory signalling in the liver (208). *Ptprg* in $Ptn^{+/+}$ mice showed its lowest mRNA expression at 3 months and then significantly increased at 6, 12 and 15 months. Age did not affect the mRNA in $Ptn^{-/-}$ animals, but *Ptprg* levels were significantly higher at 3 months and lower at 6 and 15 months compared to their respective age-matched $Ptn^{+/+}$ controls (Figure 32e). The ANOVA analysis revealed an interaction of age and genotype ($F(3,37)=28.43$; p-value<0.0001 for *Ptprg*).

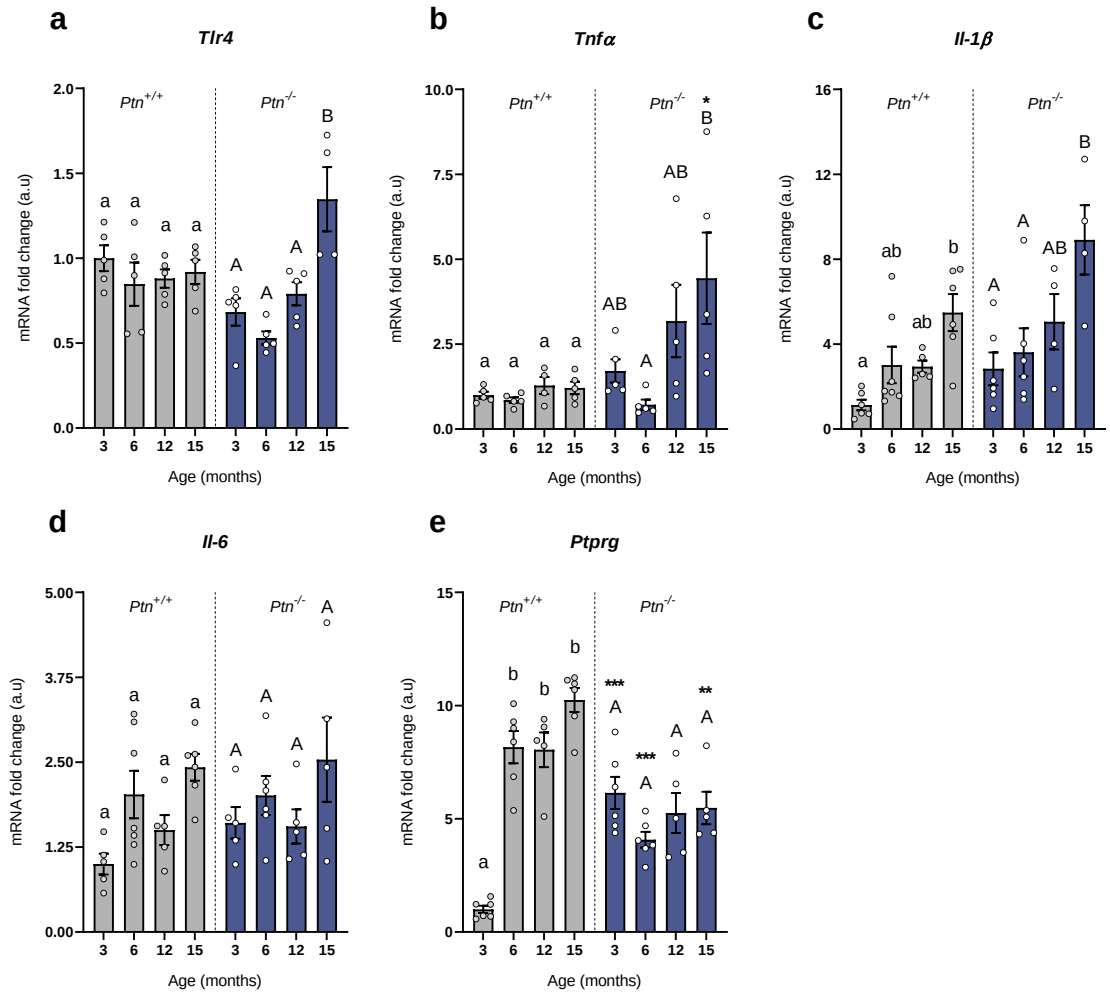

Figure 32. Deletion of Ptn alters the mRNA of several inflammatory markers. *a) Toll-like receptor 4 (Tlr4) mRNA; b) Tumour necrosis factor, alpha (Tnfα) mRNA; c) Interleukine-1 beta (Il-1ß) mRNA; d) Interleukine-6 (Il-6) mRNA; and e) Protein tyrosine phosphatase receptor gamma (Ptprg) mRNA. Data are presented as mean ± SEM for n=5-6 mice/group. Different letters indicate statistically significant differences in the effect of ageing within the same genotype. Lowercase letters indicate statistically significant differences for* $Ptn^{+/+}$ *and capital letters for* $Ptn^{-/-}$*; *p<0.05, **p<0.01, ***p<0.001 for differences between* $Ptn^{+/+}$ *and* $Ptn^{-/-}$ *mice of the same age.*

3.4. Collagen as a marker of liver fibrosis

Ageing is associated with a dysfunction in hepatic macrophages and HSCs and has been suggested to be a risk factor for the progression of liver fibrosis. To determine if *Ptn* deletion may favour liver fibrosis, we analysed the mRNA of collagen type IV (*Col4a1*) and type VI (*Col6a2*). Both in $Ptn^{+/+}$ and $Ptn^{-/-}$ mice, Col*4a1* mRNA had its maximum expression at 3 months and then dropped with age (Figure 33a). On the other hand, *Col6a2* levels decreased gradually along with age in $Ptn^{+/+}$ mice but remained constant in $Ptn^{-/-}$ animals (Figure 33b).

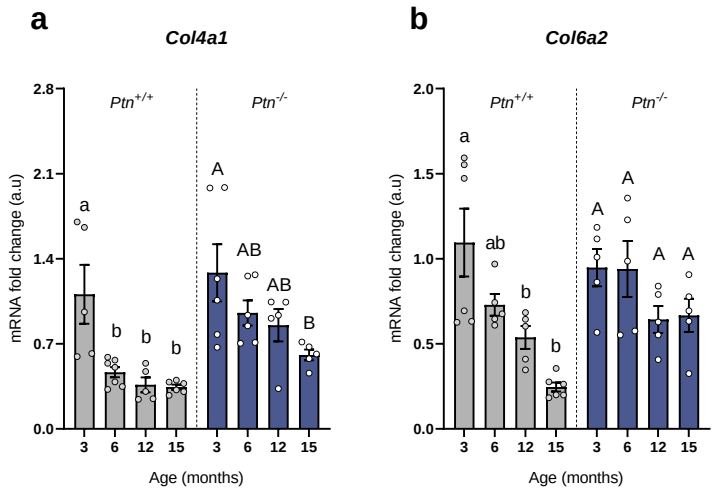

Figure 33. Collagen mRNA decreases parallel to ageing. *a) Collagen, type IV, alpha-1 (Col4a1) mRNA; and b) Collagen, type VI, alpha-2 (Col6a2) mRNA. Data are presented as mean ± SEM for n=5-6 mice/group. Different letters indicate statistically significant differences in the effect of ageing within the same genotype. Lowercase letters for $Ptn^{+/+}$ and capital letters for $Ptn^{-/-}$; *p<0.05, **p<0.01, ***p<0.001 for differences between $Ptn^{+/+}$ and $Ptn^{-/-}$ mice of the same age.*

3.5. Pleiotrophin signalling cascade and the connexion with other pathways

3.5.1. Effects of pleiotrophin deletion in its signalling pathway

As explained in the introduction, PTN is a heparin-binding growth factor that belongs to the same family of midkine (MK). Due to their high homology in their sequences, it is widely believed that PTN and MK have overlapping functions. To analyse if pleiotrophin deletion can be compensated with an upregulation of MK expression, we measured *Ptn* and *Mk* mRNA levels in our mice. Secondly, we also analysed the mRNA expression of the proteins that are known to be PTN receptors.

First, we observed that *Ptn* mRNA remained constant at all ages in $Ptn^{+/+}$ mice, even though there was a slight decrease at 15 months, but it did not reach significance (Figure 34a). We also confirmed that $Ptn^{-/-}$ mice do not express the *Ptn* gene. On the other hand, *Mk* did not vary in $Ptn^{+/+}$ mice, whereas in $Ptn^{-/-}$ animals, the expression was higher at 3 months compared to the same-aged $Ptn^{+/+}$ mice and then decreased steadily with age (Figure 34b). However, no joint effect of age and genotype in *Mk* mRNA levels was observed in the ANOVA test.

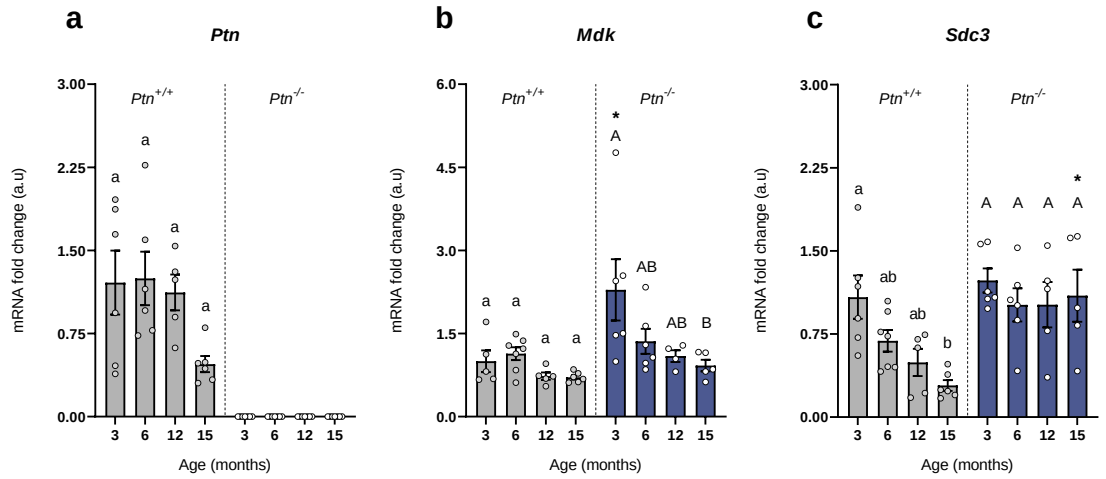

Figure 34. Pleiotrophin deletion increases Mk mRNA in young mice and prevents the effects of ageing in its receptor. *a) Pleiotrophin (Ptn) mRNA; b) Midkine (Mk) mRNA; and c) Syndecan-3 (Sdc3) mRNA. Data are presented as mean ± SEM for n=5-6 mice/group. Different letters indicate statistically significant differences in the effect of ageing within the same genotype. Lowercase letters indicate statistically significant differences for $Ptn^{+/+}$ and capital letters for $Ptn^{-/-}$; *p<0.05, **p<0.01, ***p<0.001 for differences between $Ptn^{+/+}$ and $Ptn^{-/-}$ mice of the same age.*

Regarding the expression of the known receptors of pleiotrophin, we did not observe any expression of *Ptprz* nor *Alk* in the liver. However, we did find expression of syndecan-3 (*Sdc3*). The mRNA levels of *Sdc3* had a 4-fold decrease with age from 3 to 15 months in $Ptn^{+/+}$ mice. We did not observe any changes in the mRNA levels of *Sdc3* in $Ptn^{-/-}$ mice, who showed significantly higher *Sdc3* levels at 15 months of age compared to the same-aged $Ptn^{+/+}$ animals (Figure 34c).

3.5.2. Pleiotrophin and Wnt signalling cascade crosstalk

Finally, we measured the mRNA of the main components of the Wnt/β-catenin pathway, as several studies have reported the crosstalk between PTN and WNT signalling cascades in different tissues (70,209).

Glycogen synthase kinase 3β (GSK-3β) has been proposed as the link connecting both PTN and WNT pathways. In $Ptn^{+/+}$ animals, *Gsk-3β* expression was upregulated with age. In fact, we observed a 3-fold increment in 15 months old $Ptn^{+/+}$ mice compared to the 3 months old $Ptn^{+/+}$ mice. On the other hand, *Gsk-3β* mRNA levels were higher in 3-month-old $Ptn^{-/-}$ mice than in their age-matched $Ptn^{+/+}$ mice and were not modified with age (Figure 35a). The ANOVA analysis showed an interaction between genotype and ageing ($F(3,38)=25.5$; p-value < 0.0001).

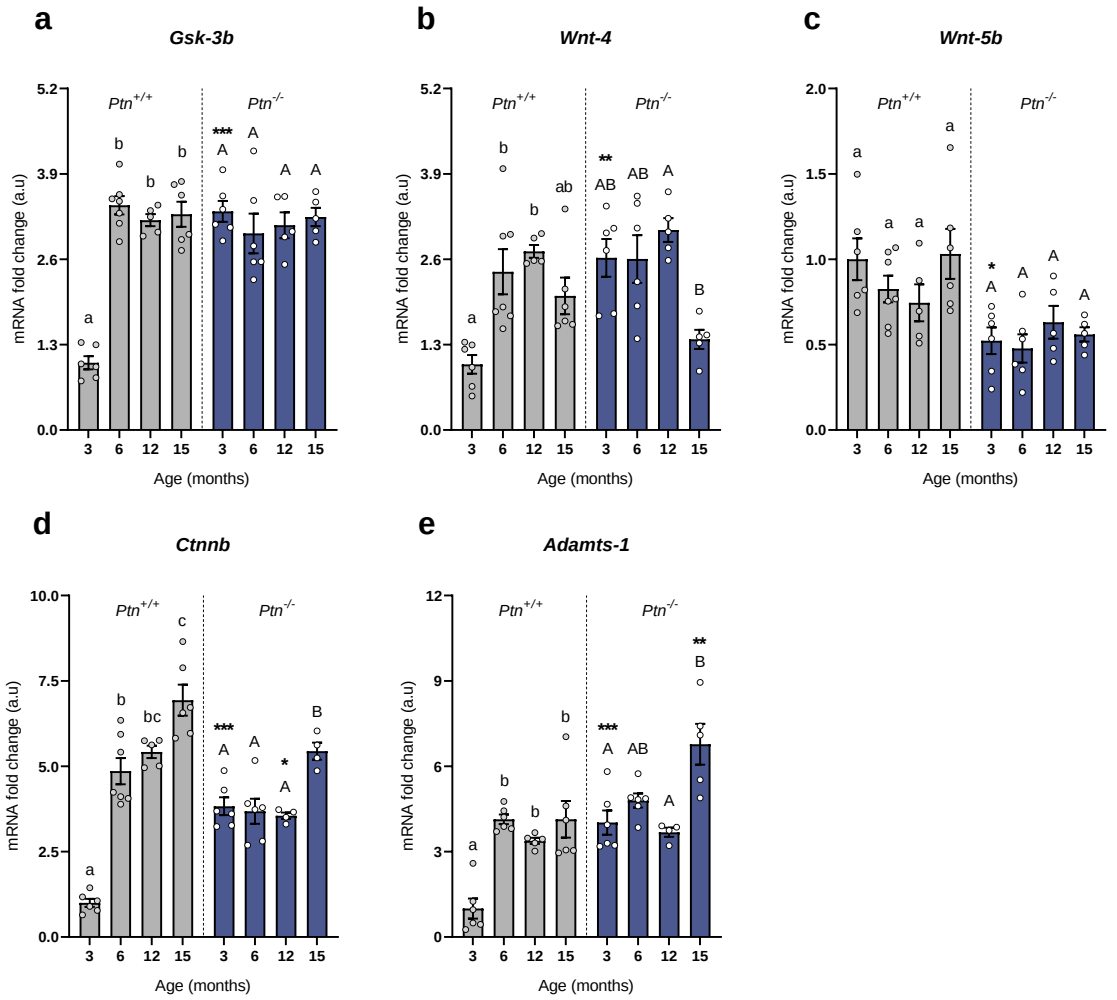

Figure 35. Pleiotrophin influence in Wnt signalling cascade during the ageing process. *a) Glycogen synthase kinase 3 beta (Gsk-3b) mRNA; b) Wnt-4 mRNA; c) Wnt-5b mRNA; d) Beta-catenin (Ctnnb) mRNA; and e) ADAM metallopeptidase with thrombospondin type 1 (Adamts1) mRNA. Data are presented as mean ± SEM for n=5-6 mice/group. Different letters indicate statistically significant differences in the effect of ageing within the same genotype. Lowercase letters indicate statistically significant differences for $Ptn^{+/+}$ and capital letters for $Ptn^{-/-}$; *p<0.05, **p<0.01, ***p<0.001 for differences between $Ptn^{+/+}$ and $Ptn^{-/-}$ mice of the same age.*

Next, we analysed *Wnt-4* and *Wnt-5b* mRNA levels, as these are the isoforms of WNT with higher expression in the mouse liver. *Wnt-4* mRNA augmented from 3 to 6 months in $Ptn^{+/+}$ mice. On the contrary, in $Ptn^{-/-}$ mice, *Wnt-4* expression was significantly higher at 3 months of age compared to 3 months old $Ptn^{+/+}$ animals but was significantly lower in 15 months old $Ptn^{-/-}$ mice (Figure 35b). As shown by the ANOVA test, there was an interaction between the effect of age and genotype (F(3,38)=6.248; p-value=0,0015). Regarding *Wnt-5b*, age did not affect the mRNA levels, but the expression was lower in $Ptn^{-/-}$ animals than in $Ptn^{+/+}$ mice, particularly at 3 months (Figure 35c).

GSK-3β dependent phosphorylation/dephosphorylation regulates the degradation in the proteasome or the translocation of β-catenin (CTNNB) to the nucleus. In our study, mRNA of *Ctnnb* was markedly upregulated from 3 to 6 months and continued increasing with age in $Ptn^{+/+}$ mice. On the other hand, although *Ctnnb* expression was significantly higher in 3-month-old $Ptn^{-/-}$ mice compared to their age-matched $Ptn^{+/+}$ controls, *Ctnnb* mRNA levels were not modified from 3 to 12 months of age and increased from 12 to 15 months of age (Figure 35d). The joint effect of both ageing and genotype was confirmed by the ANOVA test ($F(3, 36) = 23{,}95$; p-value<0.0001).

Finally, ADAMTS1 has been shown to induce *Ptn* expression via the WTN/β-catenin signalling pathway. In $Ptn^{+/+}$ mice, the changes in *Adamts1* mRNA expression were analogous to *Gsk-3β*, as it increased from 6 months onward. On the other hand, 3-month-old $Ptn^{-/-}$ mice had higher *Adamts1* levels than their corresponding $Ptn^{+/+}$ controls, and *Adamts1* expression showed an upregulation in 15 months $Ptn^{-/-}$ mice (Figure 35e). The ANOVA analysis showed an interaction of age and genotype in *Adamts1* ($F(3,36)=5{,}196$; p-value=0.0044).

4. DISCUSSION

According to the United Nations, in 2019, the elderly world population stood at 703 million, but it is expected to reach 1.5 billion in 2050 (105). Ageing causes increased pressures on old-age support systems, making it essential to find mechanisms to improve elderly life quality. One of the age-related alterations that trigger the development of diseases such as obesity, hepatic steatosis, and insulin resistance is the dysregulation of lipid metabolism (210). The liver plays a critical role in regulating systemic lipid metabolism as it is the main producer of plasma lipoproteins and bile (13,211). Thus, impaired lipid metabolism in the liver may lead to an increment in circulating lipids (212), increased lipid synthesis, decreased hepatic β-oxidation (211,213) and/or enhanced lipid uptake and accumulation. Moreover, hepatic lipid accumulation could favour hepatic and systemic alterations, including steatohepatitis, cirrhosis, impairment of systemic glucose metabolism and metabolic syndrome, thereby contributing to age-related diseases (148).

The characterisation of new targets involved in the regulation of liver metabolism is of particular interest for the treatment and prevention of age-related diseases. Pleiotrophin is a cytokine that has been shown to be highly expressed during embryonic development and pathological processes, but traditionally its expression has been stated to be residual in adulthood. In the liver, *Ptn* mRNA levels are increased after liver injury and/or after partial hepatectomy to promote tissue regeneration (93). However, our research has pointed out that PTN also has a role in adult tissues by regulating glucose homeostasis, energy

metabolism and adipose tissue plasticity (71). Moreover, we have recently published that PTN also modulates hepatic metabolism through crosstalk between the liver and the adipose tissue, which protects against the development of high-fat diet-induced steatosis (72). In this first chapter of the thesis, we have provided novel insights into the actions of PTN as a key player in the regulation of hepatic lipid metabolism during the physiologic process of ageing.

Ptn deficient mice have a reduction of the age-related increment in body weight, a decrease in the liver weight and a reduction in hepatic lipid content compared with the wild-type animals. This reduction in the hepatic accumulation of lipids in this pleiotrophin knock-out model could be associated with a reduction in the lipid synthesis, reduced secretion of VLDL, reduced lipid uptake and/or an increased β-oxidation.

First of all, pleiotrophin deletion blunted the age-related increment of cholesterol synthesis, decreased LDL clearance and altered cholesterol distribution in the different lipoproteins. In fact, mRNA levels of hydroxymethylglutaryl-CoA reductase (*Hmgcr*) and *Ldlr* augmented with age in the control animals and were not affected or even decreased with age in the $Ptn^{-/-}$ mice. Accordingly, although young $Ptn^{-/-}$ mice exhibited higher plasma cholesterol, c-HDL and c-LDL levels than the control animals, ageing increased plasma lipid levels in the control group but not in $Ptn^{-/-}$ mice.

Ageing is also associated with a shift in liver lipid metabolism towards lipogenesis, which can contribute to the risk of developing fatty liver or hepatic pathologies in later life (214). Accordingly, we have observed that ageing is associated with an upregulation of the enzymes of fatty acid synthesis (*Acly*, *Fas)* and triacylglycerides synthesis (*Gpat*, *Lpin2*, and *Dgat2)* in the wild-type animals, which may favour the development of steatosis. In fact, hepatic *Gpat* expression positively correlates with the development of hepatic steatosis in mice (13), and *Dgat2* overexpression in mice has also been shown to favour hepatic lipid accumulation (215). On the other hand, in our mouse model, the deletion of *Ptn* blocked the age-related upregulation of the key enzymes of lipogenesis and triacylglycerides synthesis. As a result, *Ptn* deficiency is associated with an altered lipid synthesis that averts the age-related hepatic lipid accumulation, which may protect against the development of age-induced steatosis.

We next explored if *Ptn* deletion may also alter the hepatic secretion of triacylglycerides as very-low-density lipoproteins (VLDL). Plasma levels of triacylglycerides and the mRNA of *Apo B-100 and Apo C-II* (main apolipoproteins involved in VLDL metabolism) are significantly reduced in 15-months-old $Ptn^{-/-}$ animals. No significant differences were observed in the mRNA of hepatic lipase (*Lipc*), an enzyme that facilitates the clearance of

triacylglyceride from VLDL and contributes to the regulation of the plasma levels of triacylglycerides, neither with ageing nor *Ptn* deletion.

Moreover, previous experiments from our group that have analysed the role of pleiotrophin in adipose tissue at different ages revealed that *Ptn* deletion blocks the age-related increment in adiposity due to impaired adipose tissue expandability and a decreased capacity to store lipids (71). We found alterations in adipocyte cell size and turnover, which are essential factors for the development of obesity and metabolic disorders. Thus, 15-month-old $Ptn^{-/-}$ mice showed reduced adipocyte size in periovarian adipose tissue, increased catecholamine-induced lipolysis and a reduction in the antilipolytic response to insulin when compared to the wild-type mice. Interestingly, in 12-month-old mice, β_3-adrenoceptor expression paralleled the catecholamine-activated lipolytic activity of the tissue, being significantly higher in the periovarian adipose tissue of $Ptn^{-/-}$ mice than in wild-type controls. Thus, there is an increment flux into the circulation of fatty acids and glycerol released from the adipose tissue in response to increased adrenergic stimulation of lipolysis in the 15-month-old $Ptn^{-/-}$ mice.

Despite the intense lipolysis in the adipose tissue, the reduced plasma NEFA levels of the $Ptn^{-/-}$ mice suggest an increment in the uptake and/or the oxidation of fatty acids in peripheral tissues, like the liver. Thus, we examined the effect of *Ptn* deletion in the transporters of glycerol and fatty acids in the liver. No differences were found in *Aqp9*, *Fatp4*, and *Fatp5* mRNA levels, suggesting that the hepatic uptake of glycerol and fatty acids is not altered in *Ptn*-deficient mice. We also examined the mRNA of the key enzymes of β-oxidation, the primary pathway for energy production in the liver, that occurs mainly in the mitochondria and peroxisomes (13,211). Entry of fatty acids into the mitochondria occurs via CPT1α, and then a series of reactions, including dehydrogenation, hydration, and acylation, degrade fatty acids to form acetyl-CoA. In our model, we observed that mRNA of CPT1α increases in old $Ptn^{+/+}$ mice, whereas no changes in mRNA of CPT1α were observed in $Ptn^{-/-}$ animals with age. On the contrary, the mRNA of the enzymes involved in the reactions of mitochondrial β-oxidation is reduced in the old $Ptn^{-/-}$ mice. Some studies have suggested that ageing downregulates fatty acid oxidation in the liver and impairs mitochondrial NEFA oxidation, which has been associated with insulin resistance (206,216-218). Secondly, fasting is a known inducer of β-oxidation and ketogenesis (219). In our study, after 6 hours of fasting, the mRNA of the enzymes of β-oxidation was found to be upregulated with age in wild-type animals, and no changes were found in $Ptn^{-/-}$ mice. Besides, although ageing induced an increment in plasma D-3-hydroxybutyrate levels in the wild type animals, plasma ketone bodies did not increase with age in $Ptn^{-/-}$ mice. These data confirm that *Ptn* deletion is associated with a reduced hepatic ectopic lipid accumulation due to reduced lipid

synthesis despite the reduction in the liver β-oxidation and ketogenesis observed in the old *Ptn*$^{-/-}$ mice.

According to previous studies of the respiratory exchange rate, *Ptn*$^{-/-}$ mice consumed a combination of glucose and fatty acids during the dark period and preferentially used lipids as energy substrates during the light period, which suggests that the energy production from fatty acids is augmented in *Ptn*$^{-/-}$ mice (71). To further analyse the destiny products of the lipolysis of the adipose tissue in the organism rather than the liver, we analysed if other peripheral tissues may have increased utilization of fatty acids, what may protect the liver of *Ptn*$^{-/-}$ animals from hepatic steatosis. The main oxidative tissue in which fatty acids are used as energy substrates by β-oxidation is the skeletal muscle (220). However, according to the data obtained from the metabolic cages, *Ptn*$^{-/-}$ mice exhibited reduced physical activity. Besides, the analysis of muscle lipid content and the mRNA of the enzymes of β-oxidation in the muscle revealed that lipid accumulation is reduced in the *Ptn*$^{-/-}$ mice (data not shown), suggesting that fatty acids may be redirected for oxidation in other tissues.

Moreover, energy expenditure due to cold-induced thermogenesis was significantly higher in *Ptn*$^{-/-}$ than *Ptn*$^{+/+}$ mice. Accordingly, we analysed brown adipose tissue function and demonstrated that T_4 conversion to T_3 is enhanced in *Ptn*-deficient mice due to increased activity of DIO2. In parallel, we also found higher UCP-1 protein expression and thermogenesis in *Ptn*$^{-/-}$ animals (71). This increment in thermogenesis is maintained in *Ptn*$^{-/-}$ animals by the increased adipose tissue lipolytic activity and the preferential oxidation of fatty acids as energy substrates, despite the availability of glucose. This increased utilization of fatty acids instead of glucose, even in the fed state, may contribute to the diminished plasma levels of fatty acids and triacylglycerides, as well as to the reduced adiposity of the periovarian and retroperitoneal adipose tissue of *Ptn*$^{-/-}$ mice (71). In addition, recent results obtained by our group showed that at 6 months of age, there is an increment in the mRNA of specific markers for WAT browning in the periovarian adipose tissue of *Ptn*$^{-/-}$ mice fed with a standard diet compared to *Ptn*$^{+/+}$ controls. Furthermore, histologic examinations of this fat depot revealed UCP-1 enriched multilocular adipocytes (72) that further contribute to increasing the energy expenditure due to cold-induced thermogenesis in *Ptn*$^{-/-}$ mice (71).

We next analysed whether the enhanced oxidation of fatty acids for energy production instead of glucose in the *Ptn*$^{-/-}$ mice could be associated with an amelioration of glucose tolerance or impaired carbohydrate metabolism. First, we investigated if pleiotrophin deletion may affect glycemia, insulinemia, glucose tolerance or insulin sensitivity. It is widely known that ageing is associated with an increment in the insulin levels required to maintain euglycemia and with a reduction in glucose intolerance. *Ptn* deletion did not have any impact on glucose levels, but old *Ptn*$^{-/-}$ mice are hyperinsulinemic. However, there is evidence that

impaired glucose tolerance and insulin resistance may develop under normoglycaemia as a consequence of altered lipid metabolism (221,222). Although glucose tolerance and insulin responsiveness were higher in the young 3-month-old *Ptn*$^{-/-}$ mice, both variables were clearly impaired with ageing, suggesting that *Ptn* deletion could favour glucose intolerance later in life. Moreover, the insulin sensitivity index QUICKI and the insulin resistance HOMA-IR revealed that insulin sensitivity is decreased in 15-months old *Ptn*$^{-/-}$ mice.

We cannot reject the possibility that the glucose intolerance observed in *Ptn*$^{-/-}$ mice may be associated with a lower glucose utilization, increased glucose production, or impaired carbohydrate metabolism in these animals. Glycolysis has been proposed as a contributing factor in developing age-associated diseases (223). Several studies have pointed out that enhanced glycolytic activity triggers the ageing onset, whereas lower glycolytic activity delays the ageing process (224,225). In our model, the mRNA of *Glut-2*, the main glucose transporter involved in glucose uptake in the liver, was not modified either by age or genotype. Nevertheless, ageing was associated with an increment in the mRNA of hepatic glycolytic enzymes in the control animals that was not observed in *Ptn*$^{-/-}$ mice. Besides, the mRNA levels of some glycolytic enzymes were lower in the old *Ptn*$^{-/-}$ mice than in their corresponding wild type animals.

Glucose molecules can also be diverted to the pentose phosphate pathway and used for the obtention of reduced coenzymes required for the synthesis of lipids (NADPH) and the obtention ribose 5-phosphate. Although the mRNA of glucose-6-phosphate dehydrogenase, the key enzyme of the oxidative phase of the pentose phosphate pathway, increased with age in both genotypes, the mRNA analysis of transketolase revealed that the interconversion of monosaccharide phosphate (glyceraldehyde-3-phosphate and fructose-6-phosphate) might be reduced in the *Ptn*$^{-/-}$ at 15 months of age.

This decreased glucose utilization in the *Ptn*-deficient mice can be partially explained by their lower respiratory exchange rate and preferential use of fatty acids as an energy source rather than glucose.

After glycolysis, pyruvate molecules can be transformed into acetyl-CoA that can be further oxidized in the TCA cycle to produce ATP. In our model, we did not find differential mRNA levels on citrate synthase or isocitrate dehydrogenase, but α-ketoglutarate dehydrogenase mRNA levels were higher in *Ptn*-deficient mice. Moreover, pleiotrophin deletion blocked the age-related increment in the mRNA levels of both cytosolic and mitochondrial malate dehydrogenases.

As the liver intensifies glucose production with age, and the hepatic insulin resistance has been associated with the age-related increment in gluconeogenesis in both humans (226)

and rats (227), we next explored the mRNA of the gluconeogenic enzymes. Ageing has been associated with enhanced transcription of genes encoding gluconeogenic enzymes such as pyruvate carboxylase, phosphoenolpyruvate carboxykinase and glucose 6-phosphatase (185). However, *Ptn* deletion suppressed the increment in the transcription of lactate dehydrogenase and of gluconeogenic genes (pyruvate carboxylase, phosphoenolpyruvate carboxykinase and glucose 6-phosphatase) observed in the control animals, suggesting a decreased hepatic glucose production in *Ptn*-deficient mice. Pyruvate carboxylase is involved in regulating the first step in gluconeogenesis and is an important marker in glucose homeostasis. In fact, pyruvate carboxylase inhibition decreases fasting and basal plasma glucose levels and reduces hepatic glucose production (187). In our model, 3-months-old *Ptn*-deficient mice have increased mRNA levels of pyruvate carboxylase that decrease with age being significantly lower at 15 months compared with $Ptn^{+/+}$ mice. Furthermore, it is important to note that apart from its role in gluconeogenesis, pyruvate carboxylase catalyses an anaplerotic reaction and provides oxaloacetate required for the TCA cycle (228).

To further investigate the ability of $Ptn^{-/-}$ animals to use gluconeogenic substrates, we performed a glycerol (GLYTT) and a pyruvate (PTT) tolerance test in 18-month-old mice, as it has been demonstrated that old rodents develop pyruvate and glycerol intolerance with age (185,229). Nevertheless, it is important to note that pyruvate can be used by other tissues and may possibly affect glucose concentration by competing with oxidative processes in extrahepatic tissues.

Firstly, we observed that basal glycemia after 15 hours of fasting was markedly decreased in 18-months-old $Ptn^{-/-}$ animals. This reduction in fasting blood glucose levels suggest that hepatic glucose production is not able to account for the peripheral glucose demand in these mice. Secondly, after the intraperitoneal injection of pyruvate, mice reached the peak of glucose production in 15 minutes in both genotypes, and although the reduction in glycemia was quicker in the control animals, no differences between genotypes were found for the AUC. However, although the relative increase in plasma glucose and the AUC for the relative increase in glycemia were significantly higher in *Ptn* knock out mice, the hepatic glucose production from pyruvate may not be able to compensate for the increased peripheral tissue glucose demand during a long fasting period in these animals.

Thirdly, as hepatic gluconeogenesis can be carried out also using glycerol as a substrate bypassing PEPCK (230), we investigated the effect of *Ptn* deletion in the hepatic *de novo* production of glucose from glycerol. The glycerol tolerance test confirmed that the glucose production from glycerol was also significantly decreased in old $Ptn^{-/-}$ mice. Moreover, the AUC for glucose was significantly lower in *Ptn*-deficient mice suggesting that old $Ptn^{-/-}$

animals are not able to use glycerol as a substrate for gluconeogenesis to the same extent as the controls.

As pyruvate and glycerol tolerance test does not give a complete vision of the gluconeogenic status (231), these results were further confirmed with the mRNA analysis of the gluconeogenic genes in these 15 hours fasted, 18-month-old mice. In this regard, 18-months-old *Ptn*$^{-/-}$ mice have lower mRNA levels of phosphoenolpyruvate carboxykinase and glucose 6-phosphatase, aquaporin 9, glycerol kinase and Nur77 (data not shown in this thesis) than the *Ptn*$^{+/+}$ animals. Altogether these results further confirmed that pleiotrophin deletion blunted the age-related increase in gluconeogenesis and that this effect is particularly observed after prolonged fasting.

Cells metabolism is strongly connected with mitochondrial function since they are the main source of cellular ATP. Mitochondrial morphology is essential for the physiology of the cells, and modifications in their shape have been described during development, cell division, ROS production, apoptotic cell death, and neurodegeneration, among other processes (232). Mitochondrial morphology is linked to mitochondrial bioenergetics, which includes processes of mitochondrial fission and fusion. Moreover, these processes also control individual mitochondrion size, mitochondrial branching, and network formation. The fusion process occurs when the outer and inner membrane of two different mitochondrion fuses, enabling the matrix material from both to come together, mix freely and form again a single mitochondrion. Conversely, fission is the opposite process. Both events are modulated by GTPases; fission is regulated by dynamin-related protein 1 (DRP1), and fusion is regulated by mitofusin isoforms 1 and 2 (MFN1 and MFN2), located in the outer mitochondrial membrane, and by optic atrophy 1 (OPA1), anchored in the inner mitochondrial membrane. The absence of these latter proteins results in fragmented mitochondria, decreased mitochondrial respiration, membrane potential and oxidative phosphorylation (OXPHOS) (121,233). Various lines of evidence have shown that mitochondrial dynamics could contribute to mitochondrial respiration, and ageing might also have an important role. Different studies have demonstrated variations in the expression of *Mfn1*, *Mfn2* and *Opa1* in aged tissues. However, results are contradictory as some have found increased levels in the expression of the three genes in normal human fibroblasts (233), senescent human liver cells (234) and epithelial cells (235), whereas others have demonstrated reduced amounts in the aged heart and skeletal muscle of rats (121). In our model, we did not observe age-related changes in the mRNA expression of fusion genes, but this might be due to the time points in which we have analysed these markers. In this regard, Boengler investigated 25 months old and Ljubicic, 36 months old rats, obtaining opposite results (121,236). We also found that young *Ptn*-deficient mice exhibit enhanced

expression of *Mfn1*, *Mfn2*, and *Opa1* that subsequently decreases with age, suggesting that at a young age, *Ptn*$^{-/-}$ animals have increased mitochondrial fusion.

On the other hand, it has been shown that in normal human fibroblasts, ageing is accompanied by a shift in the cellular metabolism from glycolysis to mitochondrial respiration mediated by MFN1 and OPA1. Indeed, there is an age-related decrease in the extracellular acidification rate (ECAR) and an increase in the OCR, corroborating that shift in the metabolism (233). We did not measure ECAR in our primary cells, but we examined the OCR, and when adding recombinant PTN (rPTN) to the cells, we observed an increase in the basal OCR. This may indicate that PTN could favour the transition from the glycolytic pathway to enhanced mitochondrial respiration, a fact supported by the effects of deleting *Ptn* in the gene expression of *Mfn1* and *Opa1*. In addition, our experiments treating primary hepatocytes with glucagon also support our hypothesis. Glucagon is a hormone that inhibits glycolysis and promotes gluconeogenesis, so adding glucagon to cells should increase the OCR of hepatocytes, which is what we have observed.

As extensive research has linked hepatic ER stress and inflammation with age-related insulin resistance in the liver, we also analysed whether *Ptn* deletion modulates these two processes. Firstly, senescent hepatocytes modify their surrounding environment by secreting cytokines such as IL-1β, IL-6, IL-8, TNF-α, and extend the senescent phenotype to adjacent cells (110,237). Toll-like receptor-4 (TLR4) is a major pro-inflammatory pathway involved in liver inflammation and essential in KCs activation (2). Moreover, amelioration of both the inflammatory pathway and macrophage infiltration have been shown to improve insulin sensitivity in the liver (238). There is some evidence of the role of PTN in inflammation, particularly in the chemotaxis of macrophages and neutrophils in vascular restenosis, interstitial nephritis, renal injury and rheumatoid arthritis (42). However, in our model, *Ptn* deletion favours macrophage infiltration in the liver of the old mice, as evidenced by the increased mRNA of *Cd68*, *F4/80*, *Cd-11b*, and *Cd-11c*. Moreover, *Il-6* presents similar or even reduced mRNA levels, the pro-inflammatory cytokines *Il-1β* and *Tnf-α* are upregulated, and *Tlr4* mRNA levels are higher in old knock-out animals, which may lead to higher activation of Kupffer cells (2). To confirm the phenotype of the macrophages, we have calculated the ratio iNos/arginase, and our results revealed that a proinflammatory M1 profile of macrophages predominates in *Ptn*$^{-/-}$ mice when compared with the *Ptn*$^{+/+}$. Accordingly, although ageing is known to increase the polarization of macrophages to the M1 phenotype (173), this process seems to be enhanced by *Ptn* deletion.

Additionally, the endoplasmic reticulum (ER) stress has been reported to be increased in the liver of aged rats and to be involved in the impairment of insulin signalling (185). *Bip* and *Chop* are two of the best studied genes transcriptionally induced by ER stress. Here we

have shown that *Ptn* deletion blocks the age-related physiological increase in the markers of endoplasmic reticulum *Bip*, *Chop*, and *Edem*, which evidences a better response to ER stress in $Ptn^{-/-}$ mice.

In addition to oxidative stress and inflammation, the aged liver has been shown to exhibit increased fibrosis. As the main contributor to liver fibrosis is collagen, we analysed the mRNA levels of type IV and type VI collagen, which are considered biomarkers of hepatic fibrosis (239,240). Surprisingly, we found that mRNA of both types of collagens diminished along with age in the wild-type mice, conversely to what we would have expected. However, several studies carried out in mice, rats and humans report that whereas in old individuals, collagen content is higher, the transcript levels are lower and thus, the age-related accumulation of collagen may be the result of a dysregulated collagen degradation process (241-243). On the other hand, $Ptn^{-/-}$ mice also experience a decrease in the mRNA levels of *Col4a1* and *Col6a2* with age, but the reduction is less marked than in the $Ptn^{+/+}$ animals.

There is evidence of the presence of crosstalk between insulin, pleiotrophin and Wnt/β-catenin pathways (70,244-246). Due to our findings of glucose intolerance and decreased global insulin sensitivity in old *Ptn*-deficient mice, we decided to analyse the mRNA expression of the main components of Wnt signalling in our animal model. In the absence of a Wnt stimulus, β-catenin is phosphorylated in serine and threonine residues by GSK-3β, favouring proteasomal degradation. The binding of Wnt to the receptor Frizzled inhibits the kinase activity of GSK-3β and leads to the dephosphorylation and stabilisation of β-catenin, stimulating transcriptional processes controlled by β-catenin (244).

Insulin also stimulates Akt-mediated phosphorylation of GSK3β and its inactivation and inhibits β-catenin protein degradation. However, a recent study has also demonstrated that insulin can also stimulate de novo lipogenesis under physiological conditions through PI_3K/mTORC1 signalling, leading to the activation of the Wnt signalling pathway (245).

On the other hand, when PTN signalling is active, PTN can activate AKT through PI_3K and induce serine/threonine phosphorylation of GSK-3β**.** Phospho-GSK-3β loses its phosphorylation activity, allowing β-catenin to accumulate in the cytoplasm, promoting its entrance to the nucleus and modulating the transcription of target genes (70). However, it is also known that RPTP β/ζ both binds β-catenin and functionally reduces its levels of tyrosine phosphorylation. As PTN binds to and functionally inactivates the catalytic activity of RPTP β/ζ, PTN has also been shown to increase the tyrosine phosphorylation of β-catenin in PTN-treated cells (246).

Our results show that *Gsk-3b*, *Ctnnb*, and *Adamts1* mRNA levels increase more than 3-fold in the livers of 6, 12, and 15 months old $Ptn^{+/+}$ mice compared to the 3 months old $Ptn^{+/+}$

mice. On the other hand, *Ptn*$^{-/-}$ animals showed increased mRNA levels of *Gsk-3b*, *Ctnnb*, and *Adamts1* at 3 months compared with their age-matched controls, suggesting enhanced signalling through the Wnt pathway at younger ages but not in old *Ptn*$^{-/-}$ mice. Nevertheless, in order to clarify and propose a reliable mechanism of PTN function in the crosstalk with the Wnt cascade, it would be necessary to analyse the signalling pathway by studying the phosphorylation levels of these proteins.

ADAMTS1 is a disintegrin and metalloproteinase with a thrombospondin type 1 motif and is mainly involved in the processing of ECM components, making it a good target for the study of liver fibrosis. In fact, it has been demonstrated that the expression of ADAMTS1 is positively correlated with the progression of hepatic fibrosis to cirrhosis (247). In the liver, ADAMTS1 is localised in hepatic stellate cells, and its upregulation is associated with HSCs activation, which plays an essential role in hepatic fibrosis. Furthermore, ADAMTS1 induces the activation of the major fibrogenic cytokine, the TGF-β (248). Thus, the higher *Adamts1* mRNA levels at 3 and 15 months of age in *Ptn*$^{-/-}$ mice could indicate an increased predisposition to develop liver fibrosis and/or cirrhosis compared to the control animals.

We next explore the expression of the PTN receptors in the liver. No expression of two of the best characterized receptors of PTN (RPTPβ/ζ or ALK) was found in the liver, but we did find changes in the mRNA levels of syndecan-3. In the liver, the predominant syndecan isoform appears to be syndecan-4, but it has not been identified as a PTN receptor. Syndecan-3 is mainly expressed in the brain and cartilage (34), and no research has addressed the possible involvement of SDC-3 in liver metabolism. However, few studies suggest that heparan sulfate proteoglycans participate in lipid metabolism, modulating the clearance of triacylglyceride-rich and cholesterol-rich lipoproteins (249) and regulating the body weight via the hypothalamus (250). Accordingly, SDC-3 has been reported to take part in the regulation of the energy balance. Mice lacking *Sdc-3* are resistant to diet-induced obesity (DIO) due to lower accumulation of adipose mass and better glucose tolerance, but sex-specific differences were found between male and female mice. *Sdc-3* knocked-out male mice present reduced food intake, whereas, in females, the resistance to DIO is caused by increased energy expenditure (251). On the other hand, a study carried out in rat liver cells revealed that liver macrophages, as well as fat-storing cells, express syndecan-3. Fat-storing cells can turn into myofibroblast in a process that has been identified as a pathogenic event in the onset of liver fibrosis (252). Thus, the increased *Sdc-3* levels in old *Ptn*$^{-/-}$ mice in comparison to their age-matched controls could be explained as these animals have greater macrophage infiltration and may also be implicated in the development of fibrosis.

Despite the absence of RPTPβζ expression, we found changes in the mRNA levels of another receptor protein tyrosine phosphatase, the RPTP isoform γ. Even though it is not a PTN receptor, in a recent study, the hepatic expression of *Ptprg* has been linked to inflammation and the development of insulin resistance (208). The expression of *Ptprg* has been involved in the inflammatory signalling, as mice treated with LPS showed an increased expression of *Ptprg*. Moreover, research using a knock-out model has demonstrated that *Ptprg* antagonises insulin action in the hepatocytes. Amelioration of hyperglycaemia and improved glucose tolerance caused by enhanced insulin-stimulated phosphorylation of proteins with relevant roles in hepatic insulin signalling and glucose metabolism was observed after specific deletion of *Ptprg*. On the other hand, *Ptprg* overexpression is enough to cause insulin resistance (208). In our model, *Ptprg* mRNA is higher in *Ptn*$^{-/-}$ mice at 3 months compared to the controls, but it is significantly lower at 15 months, suggesting that RPTPγ is not responsible for the decreased insulin sensitivity in these animals. Moreover, it has been reported that RPTPγ is positively correlated with the severity of NAFLD (208), suggesting that the reduction in *Ptprg* mRNA after *Ptn* deletion could be beneficial to avoid the development of the disease.

Additionally, to further investigate the molecular mechanism involved in the changes observed after pleiotrophin deletion, we determined the mRNA levels of several transcription factors that could contribute to the effects observed in the liver metabolism and function. The main regulator of β-oxidation is PPARα, whose activity is induced by fatty acids and glucagon. Therefore, in a fasting state, PPARα transcriptional activity is stimulated. PPARα acts as a "sensor" regulating lipid metabolism, fatty acid uptake through membranes, fatty acid activation, intracellular fatty acid trafficking, fatty acid oxidation, ketogenesis, triglyceride storage and lipolysis (13,211) by altering the expression of several target genes (253).

In *Ptn*$^{-/-}$ mice, the mRNA expression of PPARα is higher at 3 months and progressively decreases with age, which is associated with a drop in the expression of the genes regulated by PPARα. Among others, PPARα regulates the transcription of genes involved in lipid transport (*Fatp4* and *Aqp9*), fatty acid and triacylglyceride synthesis (*Fas*, *Scd1*, *Lpin2*, and *Dgat1*), fatty acid oxidation (*Cpt1α*, *Acox1,* and *acyl-CoA dehydrogenases*), and lipoprotein metabolism (*Lipc* and *Lpl*). PPARα is responsible for regulating the transcription of several mitochondrial genes such as *Cpt1α*, *Acadl*, *Acadvl*, and *Hadha* (253,254), which suggests that a marked reduction of PPARα could trigger a decrease in β-oxidation and the subsequent hypertriglyceridemia as shown in a study with Sprague-Dawley rats (255). On the other hand, it has been shown that hyperactivity of PPARα increases the severity of steatosis (256). Accordingly, the lower expression of PPARα in *Ptn*$^{-/-}$ mice could also

explain the decrease of lipid synthesis and the protection versus the development of steatosis that has been observed in these animals.

In previous studies of our group, we have reported that *Ptn* deletion downregulates the mRNA of PPARγ isoforms 1 and 2 in the adipose tissue of young mice. Although mRNA levels of PPARγ1 and PPARγ2 decreased with age in control animals, this reduction was lesser in *Ptn*-deficient mice, suggesting a defective PPARγ activation, which could contribute to impaired lipid and glucose homeostasis (71). Although PPARγ develops its principal role in the adipose tissue, regulating differentiation and proliferation, it has been shown that overexpression of PPARγ could induce fat accumulation in the liver (257). In this study, the analysis of the mRNA levels of PPARγ and PPARβδ in the liver did not reveal any differences, either by the effect of the age or the phenotype. PPARβδ function remains unclear, but recent studies have demonstrated a role for this PPAR isoform in regulating the hepatic expression of genes involved in the modulation of glucose homeostasis and its ability to attenuate chemically-induced hepatotoxicity (258,259).

Sterol regulatory element-binding protein 1c (SREBP) is another important transcription factor that activates the transcription of genes that regulates *de novo* lipogenesis (DNL) as *Acc* and *Fas*. It is also worth noting that hepatic DNL is reported to be higher in individuals with NAFLD and associated with hyperinsulinemia (13). Our findings show no variances of Srebp-1c in $Ptn^{+/+}$ mice, whereas $Ptn^{-/-}$ have a higher mRNA expression at 3 months, but at 15 months, it is significantly decreased, suggesting a protective effect against DNL and NAFLD. Apart from its role in activating fatty acid synthesis genes, SREBP-1c was recently suggested to mediate the action of insulin on promoting GCK transcription in the liver. In fact, insulin stimulates the binding of SREBP-1c on the promoter of GCK, resulting in enhanced glucokinase transcription (260). Thus, the downregulated mRNA of *Srebp-1c* in old knock-out animals may associate with no age-related increase of the glycolytic enzyme in these mice.

Finally, we determined the mRNA and protein levels of NUR77 and GYK. NUR77 is an orphan nuclear receptor that has been reported to be capable of modulating carbohydrate and lipid metabolism through the regulation of gluconeogenesis and lipid metabolic genes (261). NUR77 promotes the transcription of genes involved in gluconeogenesis, but it also participates in the dysregulation of genes of the glycolytic pathway in skeletal muscle (262,263). On the other hand, glycerol kinase has recently been identified as a corepressor of NUR77 in the liver (264,265). A study from 2019 has demonstrated that GYK physically interacts with NUR77 in the cell nucleus, suppressing the transcriptional activity of NUR77 and triggering a negative regulation of the transcription of gluconeogenic genes (264). When we analysed both factors in our model, glycerol kinase mRNA and protein expression were

increased in the absence of *Ptn*, but no differences were detected regarding NUR77 mRNA or protein expression.

This is the first study addressing the important role of pleiotrophin in the maintenance of hepatic homeostasis. Deletion of *Ptn* impairs physiological adaptations that take place during ageing, such as accumulation of ectopic fat, alterations in glucose tolerance/ insulin sensitivity, the inflammatory response, and handling of oxidative stress. Moreover, these changes are accompanied by the modification in energy metabolism and thermogenic function of brown fat, as well as in the dynamics of adipose tissue lipid turnover and plasticity. We found that *Ptn* deficiency and ageing trigger altered expression of genes involved in lipid and carbohydrates metabolism, which may be associated with differential mRNA levels and defective activation of several transcription factors like PPARα, SREBP, GYK in the liver, and PPARγ in the adipose tissue. Finally, we have also demonstrated that the absence of *Ptn* favours the infiltration of macrophages and the production of proinflammatory cytokines by the hepatic cells but seems to protect against ER stress. Moreover, our research highlights the important role of pleiotrophin in biogenesis and mitochondrial function, regulating the balance between glycolysis and mitochondrial respiration.

CHAPTER II. PREGNANCY

1. INTRODUCTION. PREGNANCY

Pregnancy is associated with a wide range of metabolic, anatomical, and hormonal changes to warrant the supply of essential nutrients for the mother and the foetus, to ensure foetal development, and to prepare the mother for lactation (266).

Pregnancy could be divided into two phases according to the metabolic point of view. In the first two-thirds of pregnancy, the mother is in an anabolic stage characterised by hyperphagia, increased insulin sensitivity and the store of lipids in the adipose tissue. These fat depots account for up to 28% of maternal weight in both women (267) and rats (268,269). On the contrary, during the last third of gestation, the mother is in a catabolic state (270,271) characterised by hyperinsulinemia, reduced insulin sensitivity, and enhanced placental transference of nutrients. Maternal glucose is intensively transferred to the foetal site, leading to maternal hypoglycaemia, despite the increased rate in maternal gluconeogenesis. In parallel, maternal tissues adapt their metabolism to decrease the use of glucose and to use alternative energetic substrates such as fatty acids and ketone bodies.

1.1. Changes in lipid metabolism during pregnancy

During a normal pregnancy, changes in lipid metabolism are linked to functional and morphological changes in the adipose tissue and to the development of hyperlipemia. Thus, during the first two-thirds of pregnancy, hypertrophy of adipocytes allows an increment in fat storage. Besides, during this stage of pregnancy, there is an increased activity of LPL in the adipose tissue, which, together with the increment in blood insulin concentration, facilitates the accumulation of lipids (272). This anabolic phase of pregnancy is highly regulated by hormones like insulin, oestrogen, progesterone, and cortisol that promote lipogenesis and suppress lipolysis.

During late pregnancy, adipose tissue shows resistance to the action of insulin (273). In fact, in the third trimester of gestation, there is a switch of maternal metabolism to a catabolic state, characterised by a breakdown of the fat depots, as a consequence of the increased lipolytic activity and decreased lipoprotein lipase activity in the adipose tissue. All these changes are associated with the decrease in insulin sensitivity of late gestation that has been observed both in humans and rodents (274,275). Accordingly, lipolysis of triacylglycerides is enhanced and therefore, free fatty acids and glycerol are released to blood circulation.

Lipid turnover is increased during late pregnancy (276). The liver uptake the products of lipolysis and transform them into acyl-CoA and glycerol-3-phosphate, whereas the hepatic TAGs are predominantly transferred to VLDL particles and released to the circulation,

leading to hypertriglyceridemia in maternal plasma (271). In addition, other lipoproteins that do generally not transport TAGs like LDLs and HDLs also get enriched in TAG (277).

Alternatively, NEFAs are used for β-oxidation and synthesis of ketone bodies, and glycerol is used for hepatic gluconeogenesis. Glycerol is preferred to amino acids for hepatic *de novo* gluconeogenesis during late pregnancy compared to a non-pregnant state (278). Other circulating lipid levels such as cholesterol and phospholipids are also increased but to a lesser extent. These changes in late gestation are thought to be controlled, at least partially, by plasma oestrogen levels that have been shown to stimulate hepatic VLDL production and to reduce hepatic lipase activity (279). Nevertheless, plasma-free fatty acids and triglycerides levels decrease to normal (non-pregnant) levels after delivery (280).

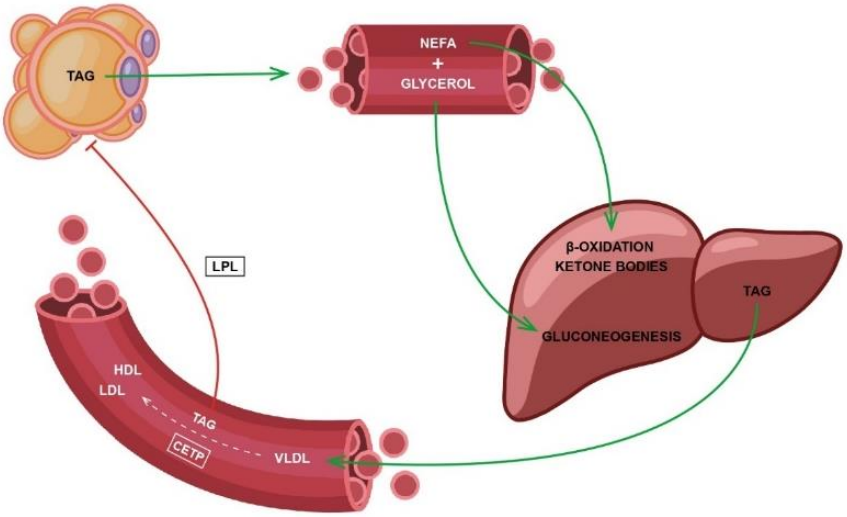

Figure 36. Main lipid metabolism adaptations during late pregnancy. *The catabolic phase is characterised by the insulin resistance condition that regulates the different steps positively (green arrows) or negatively (red arrow). TAG: triacylglycerides, NEFA: non-esterified fatty acids, VLDL: very-low-density lipoproteins, LDL: low-density lipoproteins, HDL: high-density lipoproteins, CETP: cholesterol ester transfer protein, and LPL: lipoprotein lipase. Image adapted from Herrera, E. and Desoye, G. (279).*

1.2. Changes in carbohydrate metabolism during pregnancy

Late pregnancy is characterised mainly by the development of a diabetogenic state of the mother. In late pregnancy, insulin action is physiologically decreased compared to non-pregnant women. Some studies range this decline between 50-70% (281), whereas others range between 33-78% (282). Furthermore, during the last third of gestation, there is a gradual rise in insulin concentrations both in the basal and postprandial states. Moreover, although in late pregnancy insulin secretion is 3 to 3.5-fold greater than in the early stages of pregnancy, there is a decrease in global insulin sensitivity. Thus, pregnant women

experience less hypoglycaemia in response to exogenous insulin than pregravid women, and in late pregnancy, there is an increment in insulin response to exogenous glucose. Although the mechanism underlying this lower insulin sensitivity is uncertain, several researchers suggest that it could be the consequence of alterations in the hormonal milieu (281,282).

As mentioned previously, glucose is the primary energy source for the foetus, so maternal metabolism is adapted to warrant an adequate supply of nutrients to the foetus. Accordingly, there is a 50% reduction in whole-body glucose disposal during gestation, which triggers a progressive reduction in blood glucose levels (283). In the liver, maternal hepatic glucose production is increased by 16-30% to account for the enhanced glucose demand of the foetus and placenta. Hepatic glucose production is generally suppressed by insulin, but gluconeogenesis is increased despite the increasing insulin levels in late pregnancy (281), confirming the reduction in hepatic insulin sensitivity in later pregnancy (280,283).

In the late pregnant mother, there is a preferential use of fatty acids rather than glucose as energetic substrates to obtain energy in the peripheral tissues. This change in maternal metabolism may be caused by rising concentrations of human chorionic somatomammotropin, prolactin, cortisol, and glucagon, which have lipolytic and anti-insulinogenic effects (281).

1.3. Hormonal contributions to the adaptation of the metabolism during pregnancy

The transition from the anabolic to the catabolic phase of gestation is promoted by several hormones that alter the insulin sensitivity in the mother. The insulin secretory response increases from non-pregnant condition to early pregnancy and from early pregnancy to late pregnancy (284). Besides, whole-body insulin sensitivity is not decreased or is even augmented in the early pregnancy (285). On the contrary, in the third trimester, pregnancy metabolism turns to progressive insulin resistance, which may explain the rise in the lipolysis of the adipose tissue and hepatic gluconeogenesis and ketogenesis (286).

The main hormones that seem to be involved in this switch are oestrogen, human placental lactogen, human placental growth hormone, leptin, and adiponectin. Briefly, oestrogen levels increase steadily during pregnancy which is thought to reduce hepatic lipase and promote maternal hyperlipidaemia by diminishing the clearance of circulating lipoproteins rich in TAG. It is also likely that oestrogen stimulates insulin sensitivity due to its effect on adipocytes (266). Human placental lactogen and growth hormone increase throughout gestation, enhancing insulin secretion in pancreatic islets and insulin resistance in late gestation (287-289). During pregnancy, leptin levels increase because of the rise in

fat depots resulting in gestational leptin resistance. Leptin plays a role in the mobilization of maternal fat, which occurs during the second half of pregnancy to prepare the maternal body for the metabolic needs during foetal development (290). Leptin is also produced by the placenta, and this cytokine regulates placental functions in an autocrine or paracrine manner. This cytokine seems to play a crucial role during the first stages of pregnancy as it modulates critical processes such as proliferation, protein synthesis, invasion, and apoptosis in placental cells (291). Adiponectin levels physiologically fall as pregnancy advances, and it has been demonstrated that adiponectin regulates placentation and exhibits protective effects against the symptoms of preeclampsia (292).

1.4. Pathologies derived from the impaired metabolic adaptation: Gestational diabetes

Gestational diabetes (GDM) is a type of diabetes that occurs in pregnant women who have not been diagnosed with diabetes before pregnancy. It is defined as glucose intolerance or hyperglycaemia during gestation and is characterised by the insufficient function of the pancreatic β-cells (293). GDM can happen at any stage of pregnancy, but it usually shows up between the second and third thirds of pregnancy. It normally disappears after delivery, but sometimes it triggers the development of T2D in the mother and increases the risk of the foetus suffering from obesity, glucose intolerance and diabetes in later life (294,295).

GDM is associated with several complications, including foetal hyperglycaemia and foetal hyperinsulinemia, due to increased production and secretion of insulin from the foetal pancreas to counteract the increased foetal glycemia. Due to the elevated insulin levels in the foetus, GDM is associated with foetal macrosomia and increased accumulation of subcutaneous fat. Another complication of GDM is preeclampsia, which usually leads to premature delivery and increases the probability of infants developing respiratory distress syndrome, among other prematurity problems (296). All these alterations could ultimately lead to the premature death of the foetus or infant, pointing out the importance of research focus on avoiding the development of GDM, the early diagnosis, and the establishment of proper treatment.

1.5. Pleiotrophin deletion and maternal metabolism

Previous results from our group analysing the effect of pleiotrophin deletion on the placental function demonstrated that deletion of pleiotrophin has direct consequences in the maternal adipose tissue, plasma biochemical profile, and placental metabolism during pregnancy (297). In that study, *Ptn*$^{-/-}$ mice had lower body weight during pregnancy, and, at

the time of sacrifice, they had lower weight gain than *Ptn*$^{+/+}$ mice. In addition, the estimation of maternal body weight free of conceptus revealed that the reduced body weight of *Ptn*$^{-/-}$ pregnant mice was due to a significant decrease in the weight of maternal structures and the weight of conceptus (foetus-placental structures) and a redistribution of the fat depots (297).

Furthermore, *Ptn* deletion also impaired the plasma biochemical profile and exacerbated glucose intolerance during pregnancy. The circulating levels of NEFA and TAGs were significantly lower in *Ptn*$^{-/-}$ pregnant mice, as well as the LDL and VLDL/IDL fractions. On the other hand, insulinemia was lower, and fasting glycemia was significantly higher in knock-out animals when compared to the *Ptn*$^{+/+}$. The glucose tolerance test (GTT) showed that glucose tolerance was significantly decreased in pregnant *Ptn*$^{-/-}$ mice compared to controls (298).

Even though research has been carried out to understand the role of PTN in liver pathologies, little is known about its involvement in hepatic metabolism during physiological conditions associated with metabolic adaptations, as pregnancy. Thus, this chapter aims to determine the role of pleiotrophin in liver metabolism in 18 days pregnant *Ptn*$^{-/-}$ mice and their corresponding controls (*Ptn*$^{+/+}$).

2. EXPERIMENTAL DESIGN. Study of metabolic adaptations in a Ptn deficient mouse model during gestation

Female *Ptn*$^{+/+}$ and *Ptn*$^{-/-}$ mice were housed in controlled conditions, at 20-22ºC with 12h light/dark cycles and free access to chow diet (Panlab, Barcelona, Spain) and water. 8-week-old female mice were mated, and after verifying the presence of a vaginal plug, that day was considered day 0 of gestation (P0). Mice body weight was monitored daily during the whole course of pregnancy. On day 18 of pregnancy (P18), mice were exposed to carbon dioxide and killed by decapitation (Figure 37).

Another set of 18-days pregnant animals was fasted for 6h and underwent a glucose tolerance test (GTT) as explained below, and finally, they were exposed to carbon dioxide and killed by decapitation.

Blood was collected in Eppendorf tubes containing EDTA 1mg/10µL and centrifuged at 3000 rpm for 20 minutes at 4ºC to obtain the plasma. Tissues were rapidly dissected and snap-frozen in liquid nitrogen. Tissues and plasma were preserved at -80ºC till its later analysis.

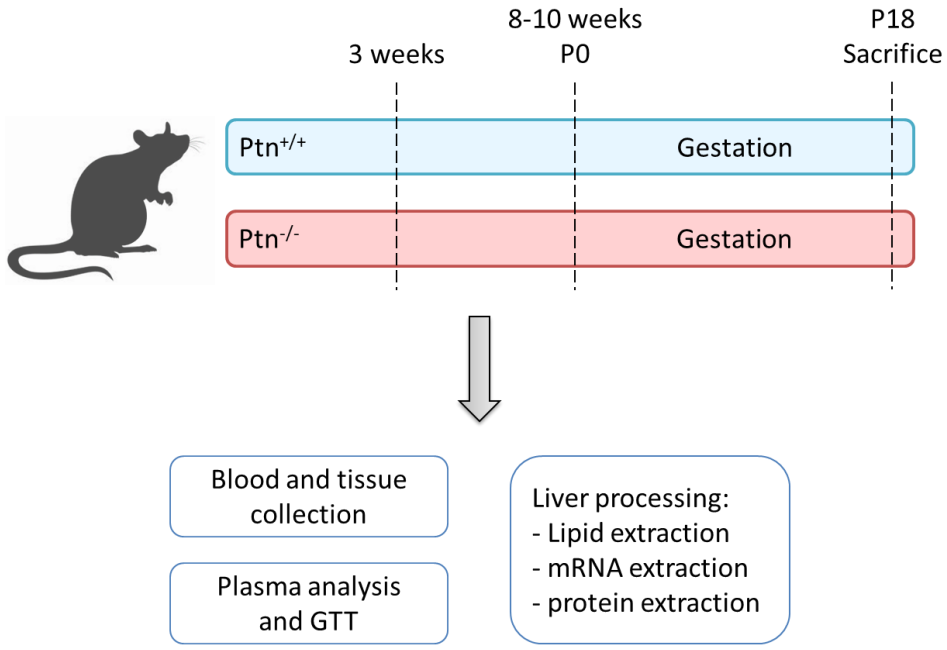

Figure 37. Experimental design of the gestation mice model to evaluate the role of PTN in hepatic metabolism.

3. RESULTS

3.1. *Ptn* deletion upregulates midkine mRNA in the liver of pregnant mice

First of all, we analysed pleiotrophin and midkine mRNA. We corroborated that in *Ptn*$^{-/-}$ mice, the *Ptn* mRNA is completely absent (Figure 38a). On the other hand, the midkine mRNA was significantly upregulated (3-fold) compared with the controls (Figure 38b), suggesting that, as a result of *Ptn* deletion, midkine is overexpressed in a try to compensate for the lack of the former cytokine.

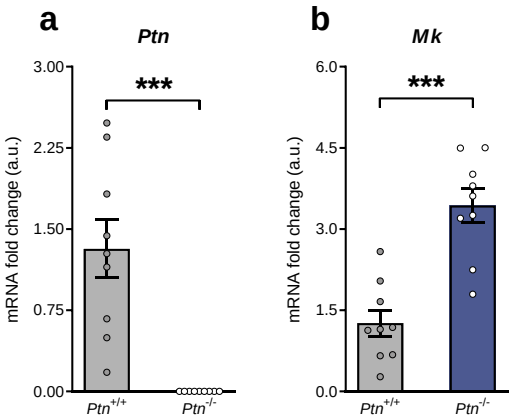

Figure 38. Deletion of pleiotrophin upregulates midkine mRNA in 18-days pregnant Ptn$^{-/-}$ mice. *a) Pleiotrophin (Ptn) mRNA; and b) Midkine (Mk) mRNA. Data are expressed as mean ± SEM (n=10 animals/group) *p<0.05, **p<0.01, ***p<0.001 for differences between Ptn$^{-/-}$ and Ptn$^{+/+}$ mice.*

3.2. *Ptn* deletion causes a lower lipid content

As we have observed before in the previous chapter, pleiotrophin deficiency causes a reduction in liver weight (Figure 39a). This decrease in the liver weight in the pregnant *Ptn*$^{-/-}$ mice was associated with a lower hepatic accumulation of lipids (Figure 39b). Moreover, when we determined the content of the different fractions respecting the total liver weight, a significant decrease was observed in all the lipid fractions in *Ptn*$^{-/-}$ mice compared to control animals (Figure 39c-f).

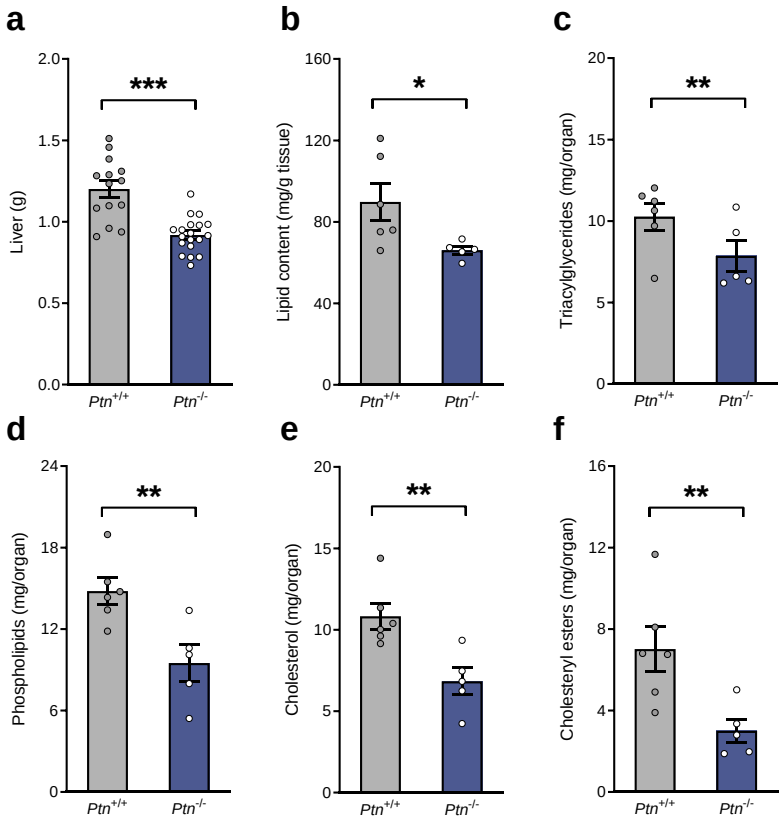

Figure 39. Effect of pleiotrophin deletion on liver weight, total lipid content, and hepatic lipid fractions at day 18 of pregnancy. *a) Liver weight; b) Total lipid content; c) Triacylglycerides; d) Phospholipids; e) Cholesterol; f) Cholesteryl esters. Data are expressed as mean ± SEM (n=5-6 animals/group) *p<0.05, **p<0.01, ***p<0.001 for differences between Ptn$^{-/-}$ and Ptn$^{+/+}$ mice.*

3.3. Deletion of *Ptn* impairs glucose synthesis and catabolism in late pregnancy

Glut2 expression in the liver was lower in pregnant *Ptn*$^{-/-}$ when compared to the control animals (Figure 40a). Moreover, pregnant *Ptn*$^{-/-}$ mice showed lower glucokinase, phosphofructokinase I, and pyruvate kinase expression (Figure 40b-d), suggesting that glucose uptake and its transformation into pyruvate are both reduced.

mRNA expression of the enzymes responsible for the transformation of pyruvate into lactate (lactate dehydrogenase), acetyl-CoA (pyruvate dehydrogenase), and oxaloacetate (pyruvate carboxylase) were decreased in the pregnant *Ptn*$^{-/-}$ mice when compared with the wild-type pregnant mice (Figure 40e-g).

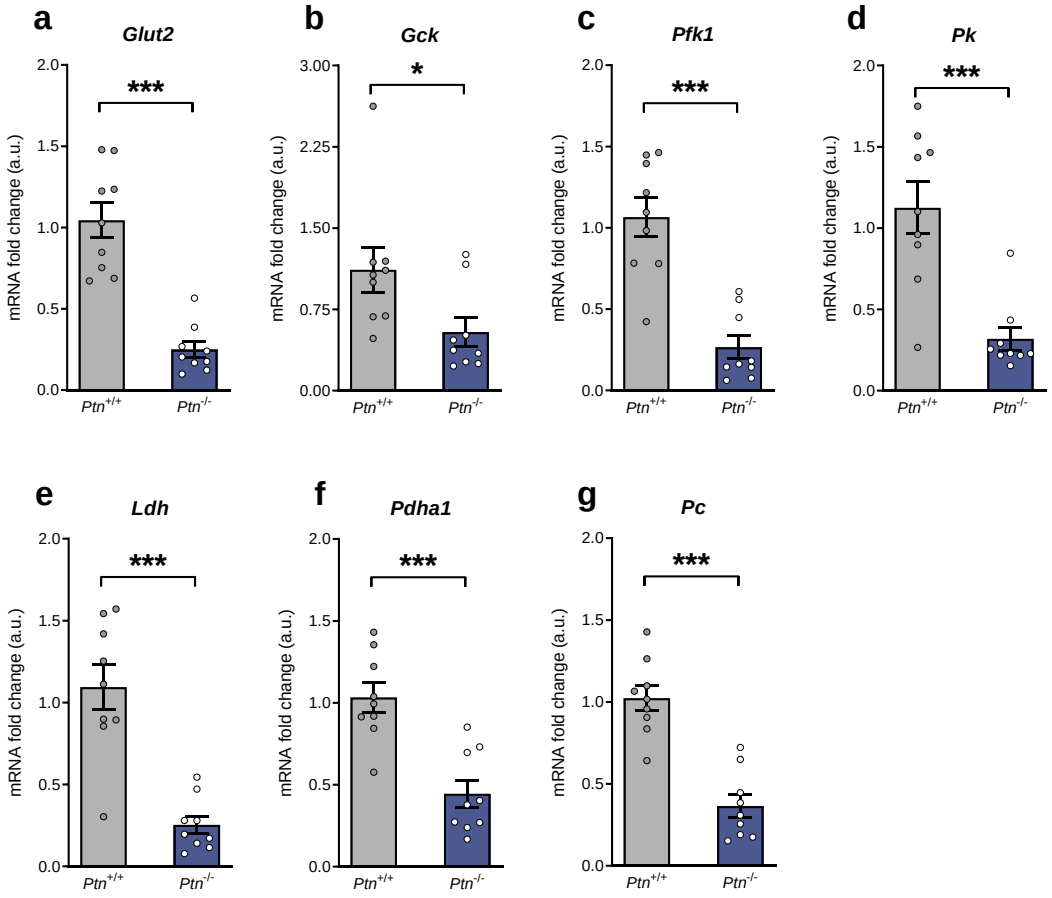

Figure 40. Deletion of pleiotrophin impairs hepatic glucose metabolism in 18 days pregnant mice. *a) Glut2 mRNA; b) Glucokinase (Gck) mRNA; c) Phosphofructokinase I (Pfk1) mRNA; d) Pyruvate kinase (Pk) mRNA; e) Lactate dehydrogenase (Ldh) mRNA; f) Pyruvate dehydrogenase α1 (Pdha1) mRNA; g) Pyruvate carboxylase (Pc) mRNA. Data are expressed as mean ± SEM (n=10 animals/group) *p<0.05, **p<0.01, ***p<0.001 for differences between Ptn$^{-/-}$ and Ptn$^{+/+}$ mice.*

In addition, the analysis of the gluconeogenic enzymes phosphoenolpyruvate carboxykinase, fructose 1,6 bisphosphatase, and glucose 6-phosphatase revealed a two-fold decrease in the mRNA expression (Figure 41a-c) in *Ptn*$^{-/-}$ pregnant mice when compared to the *Ptn*$^{+/+}$ animals.

On the other hand, the expression of glucose 6-phosphate dehydrogenase, the limiting enzyme of the pentose phosphate pathway, was increased in the *Ptn*$^{-/-}$ pregnant mice compared with the control animals (Figure 41d).

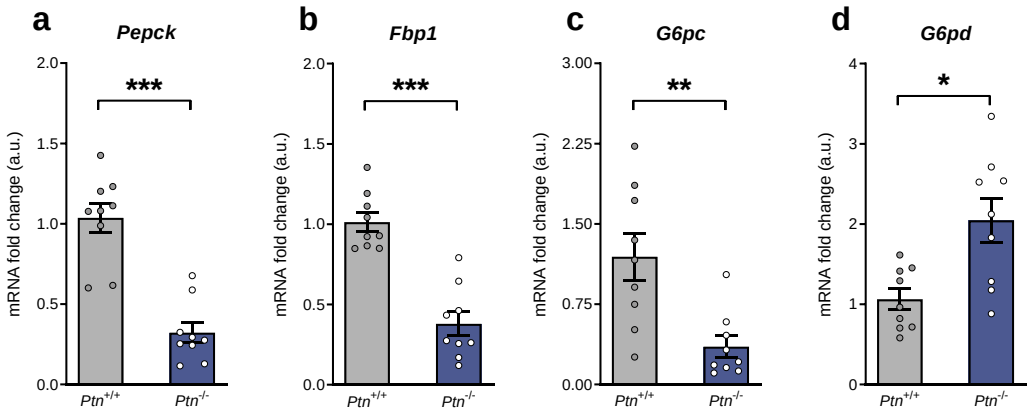

Figure 41. Deletion of pleiotrophin impairs hepatic gluconeogenesis in 18 days pregnant mice. *a) Phosphoenolpyruvate carboxykinase (Pepck) mRNA; b) Fructose 1,6 bisphosphatase (Fbp1) mRNA; c) Glucose 6-phosphatase (G6pc) mRNA; d) Glucose 6-phosphate dehydrogenase (G6pd) mRNA. Data are expressed as mean ± SEM (n=10 animals/group) *p<0.05, **p<0.01, ***p<0.001 for differences between $Ptn^{-/-}$ and $Ptn^{+/+}$ mice.*

3.4. Deletion of *Ptn* is associated with reduced expression of enzymes related to hepatic oxidation of fatty acids

We next analysed the role of *Ptn* deletion in the oxidation of fatty acids. Figures 42a-d showed that the expression of carnitine palmitoyl transferase 1α, long-chain acyl-CoA dehydrogenase, very long-chain acyl-CoA dehydrogenase, and 3-hydroxyacyl-CoA dehydrogenase was significantly decreased in $Ptn^{-/-}$ mice when compared to the wild-type animals. Moreover, the peroxisomal acyl-CoA oxidase 1 mRNA was reduced in the $Ptn^{-/-}$ mice (Figure 42e).

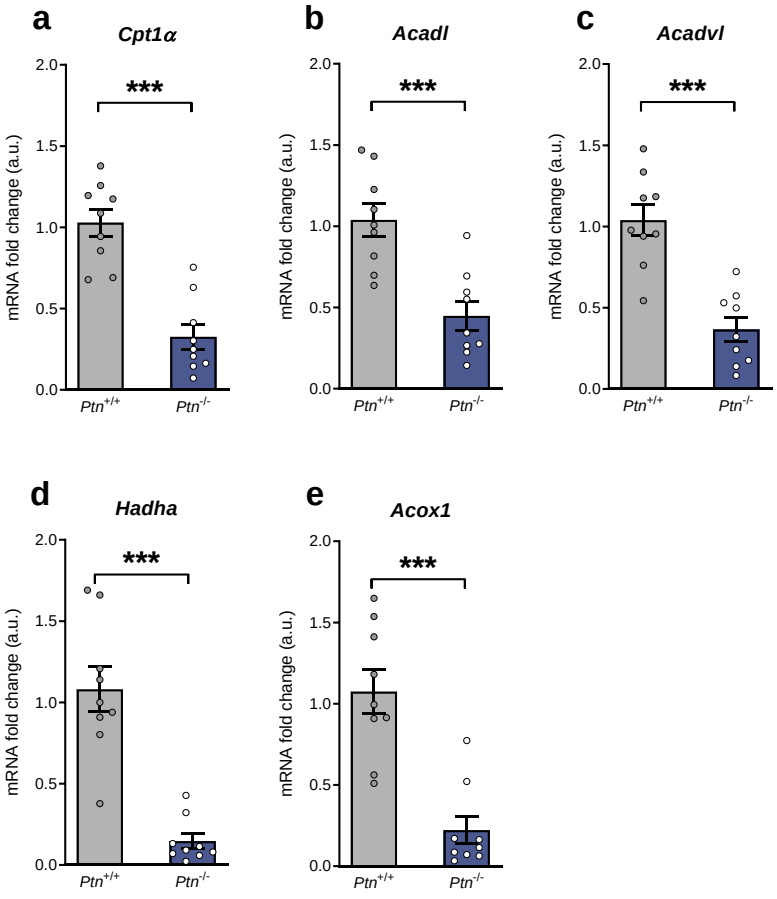

Figure 42. Impaired expression of enzymes involved in fatty acid oxidation in Ptn$^{-/-}$ 18 days pregnant mice. *a) Carnitine palmitoyl transferase 1α (Cpt1 α) mRNA; b) Acyl-CoA dehydrogenase long-chain (Acadl) mRNA; c) Acyl-CoA dehydrogenase very long chain (Acavdl) mRNA; d) 3-Hydroxyacyl-CoA dehydrogenase α (Hadha) mRNA; e) Acyl-CoA oxidase 1 (Acox1) mRNA. Data are expressed as mean ± SEM (n=10 animals/group) *p<0.05, **p<0.01, ***p<0.001 for differences between Ptn$^{-/-}$ and Ptn$^{+/+}$ mice.*

3.5. Hepatic fatty acids, triacylglycerides and cholesterol synthesis are decreased in *Ptn$^{-/-}$* pregnant mice

Given the changes described above, we determined the expression of the enzymes involved in hepatic lipid synthesis. Firstly, *Ptn$^{-/-}$* pregnant animals have a reduced mRNA expression of the enzymes involved in fatty acid synthesis (ATP citrate lyase, acetyl-CoA carboxylase, and fatty acid synthase) (Figure 43a-c) and desaturation (stearoyl-CoA desaturase-1) (Figure 43d). To confirm these results, the protein amount and the phosphorylation of acetyl-CoA carboxylase, the limiting enzyme of lipogenesis, were determined by western blot. We found that not only the mRNA but also the acetyl-CoA carboxylase protein levels were decreased in the liver of *Ptn$^{-/-}$* compared to *Ptn$^{+/+}$* pregnant mice (Figure 43b, 43e). Furthermore, the ratio phospho-acetyl-CoA carboxylase/acetyl-CoA

carboxylase (the inactive state of the enzyme) was significantly higher in these animals (Figure 43f), confirming that deletion of *Ptn* is associated with a significant increase in the inactive form of acetyl-CoA carboxylase.

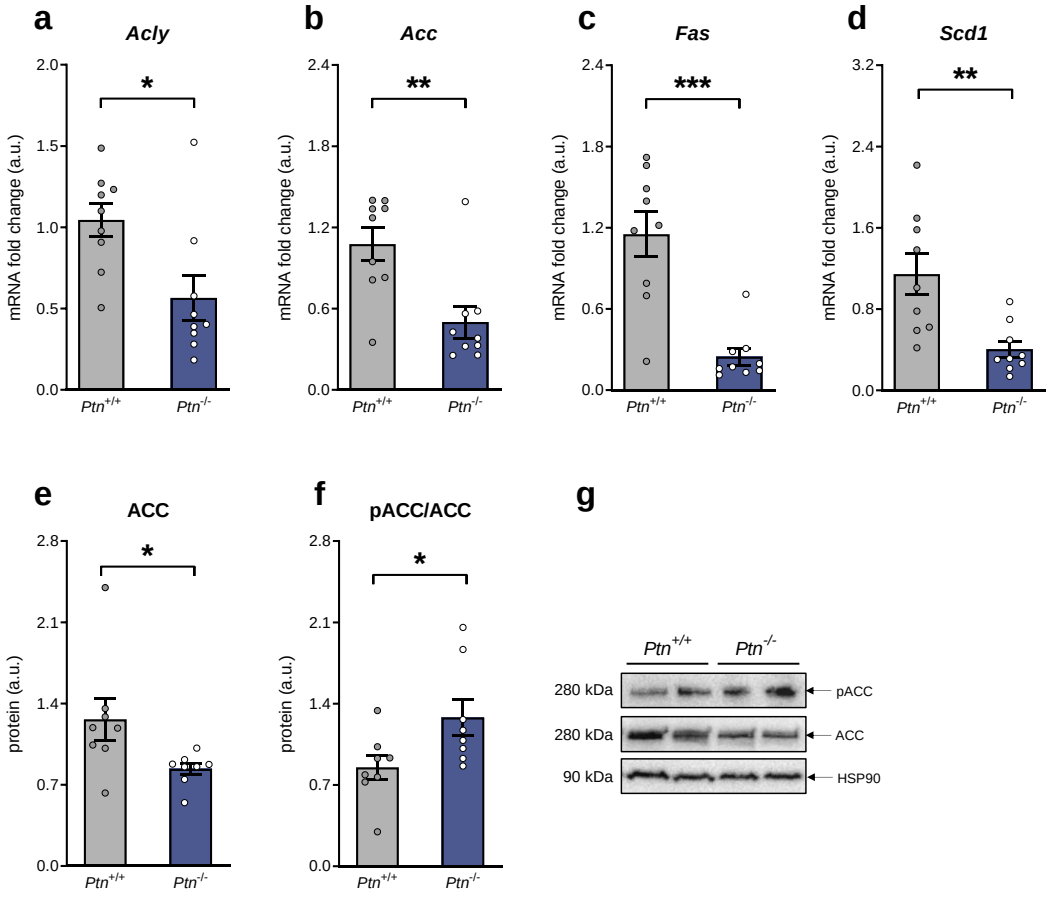

Figure 43. At late pregnancy deletion of pleiotrophin is associated with changes in key enzymes involved in fatty acids synthesis. *a) ATP citrate lyase (Acly) mRNA; b) Acetyl-CoA carboxylase (Acc) mRNA; c) Fatty acid synthase (Fas) mRNA; d) Stearoyl-CoA desaturase-1 (Scd1) mRNA; e) Acetyl-CoA carboxylase total protein/HSP90; f) Ratio of phospho-acetyl-CoA carboxylase/ acetyl-CoA carboxylase protein; g) Representative blots of phospho-acetyl-CoA carboxylase, acetyl-CoA carboxylase and HSP90. Data are expressed as mean ± SEM (n=8-9 animals/group) *p<0.05, **p<0.01, ***p<0.001 for differences between $Ptn^{-/-}$ and $Ptn^{+/+}$ mice.*

Moreover, as shown in Figure 44a-d, the hepatic mRNA expression of enzymes involved in triacylglycerol synthesis, lipin-2, glycerol-phosphate acyltransferase, diacylglycerol acyltransferase-1, and diacylglycerol acyltransferase-2 was also reduced in $Ptn^{-/-}$ as compared to $Ptn^{+/+}$ pregnant mice. Finally, the mRNA of the key enzymes of cholesterol synthesis (*Acat2*, *Hmgcs*, *Hmgcr*) (Figure 44e-g) and esterification (*Soat*) (Figure 44h) were also diminished in $Ptn^{-/-}$ pregnant mice when compared to $Ptn^{+/+}$ pregnant animals.

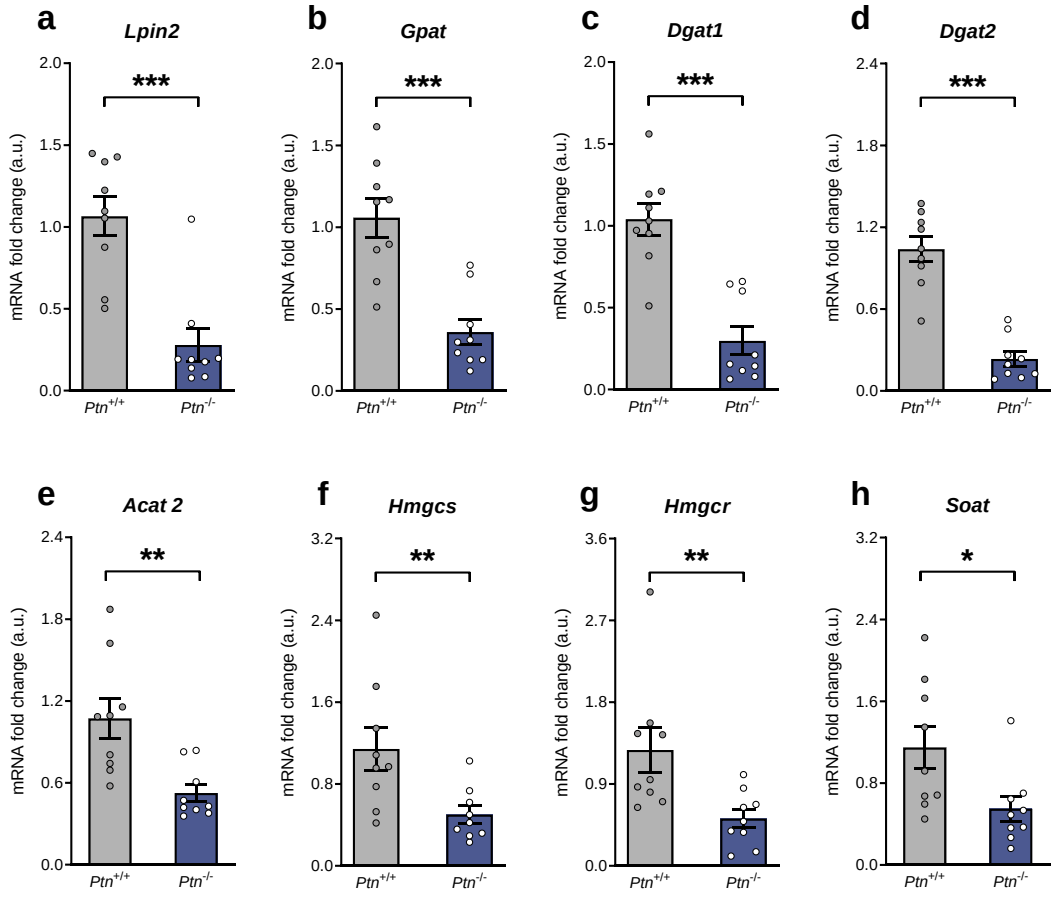

Figure 44. At late pregnancy, deletion of pleiotrophin is associated with changes in key enzymes involved in triacylglycerides and cholesterol synthesis. *a) Lipin 2 (Lpin2) mRNA; b) Glycerol phosphate acyltransferase (Gpat) mRNA; c) Diacyglycerol acyltransferase-1 (Dgat1) mRNA; d) Diacyglycerol acyltransferase-2 (Dgat2) mRNA; e) Acetyl-CoA acetyltransferase-2 (Acat2) mRNA; f) Hydroxymethylglutaryl-CoA synthase (Hmgcs) mRNA; g) Hydroxymethylglutaryl-CoA reductase (Hmgcr) mRNA; h) Sterol O-acyltransferase (Soat) mRNA. Data are expressed as mean ± SEM (n=8-9 animals/group) *p<0.05, **p<0.01, ***p<0.001 for differences between $Ptn^{-/-}$ and $Ptn^{+/+}$ mice.*

3.6. Membrane transporters and lipoprotein related enzymes are altered in the liver of *Ptn*$^{-/-}$ pregnant mice

We did not observe any changes in the expression of lipoprotein lipase mRNA between the two groups (Figure 45a). However, the hepatic triacylglyceride lipase (*Lipc*) expression was diminished in *Ptn*$^{-/-}$ mice (Figure 45b). The expression of the membrane transporters responsible for the hepatic uptake of glycerol and free fatty acids (*Aqp9*, *Fatp4*, and *Fatp5)* were significantly decreased in *Ptn*$^{-/-}$ animals (Figure 45c-e).

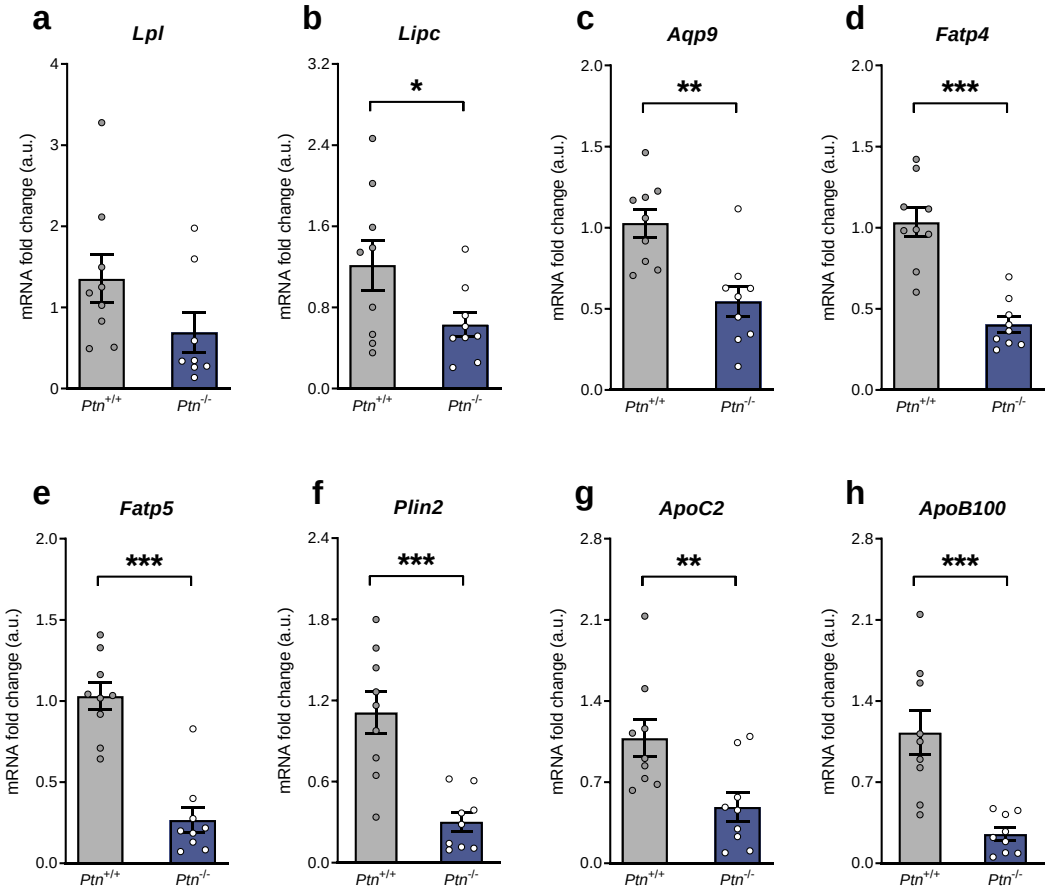

Figure 45. Pleiotrophin deletion alters transporters and enzymes of lipoprotein metabolism in mice on day 18 of pregnancy. *a) Lipoprotein lipase (Lpl) mRNA; b) Hepatic lipase (Lipc) mRNA; c) Aquaporin 9 (Aqp9) mRNA; d) Fatty acid transporter protein 4 (Fatp4) mRNA; e) Fatty acid transporter protein 5 (Fatp5) mRNA; f) Perilipin 2 (Plin2) mRNA; g) Apo C-II (ApoC2) mRNA; h) Apo B-100 (ApoB100) mRNA. Data are expressed as mean ± SEM (n=9 animals/group) *p<0.05, **p<0.01, ***p<0.001 for differences between $Ptn^{-/-}$ and $Ptn^{+/+}$ mice.*

The expression of the most abundant lipid droplet protein in the liver, *perilipin-2* (Figure 45f), the hepatic levels of *ApoC2* mRNA, a key component of VLDL and an activator of lipoprotein lipase (Figure 45g), and the expression of *ApoB100* mRNA, the apolipoprotein necessary for the assembly and secretion of VLDL (Figure 45h) were also decreased in the pregnant mice in which *Ptn* expression have been knocked-out.

3.7. *Ptn*$^{-/-}$ pregnant mice show an impaired expression of transcription factors

Pregnant *Ptn*$^{-/-}$ mice showed downregulation of mRNA expression of *Ppar-α* and *Ppar-γ1* (Figure 46a-b), whereas the expression of *Ppar-β/δ* and the cofactor *Pgc1α* presented no variation (Figures 46c-d). In addition, the expression of *Rxrα*, required for *Ppar-α* transcriptional activity on β-oxidation genes, and other important transcription factors

involved in the regulation of liver metabolism, such as *Srebp1*, *Fgf21*, and *Cebpα*, were also diminished in *Ptn*$^{-/-}$ when compared to control pregnant mice (Figure 46e-h).

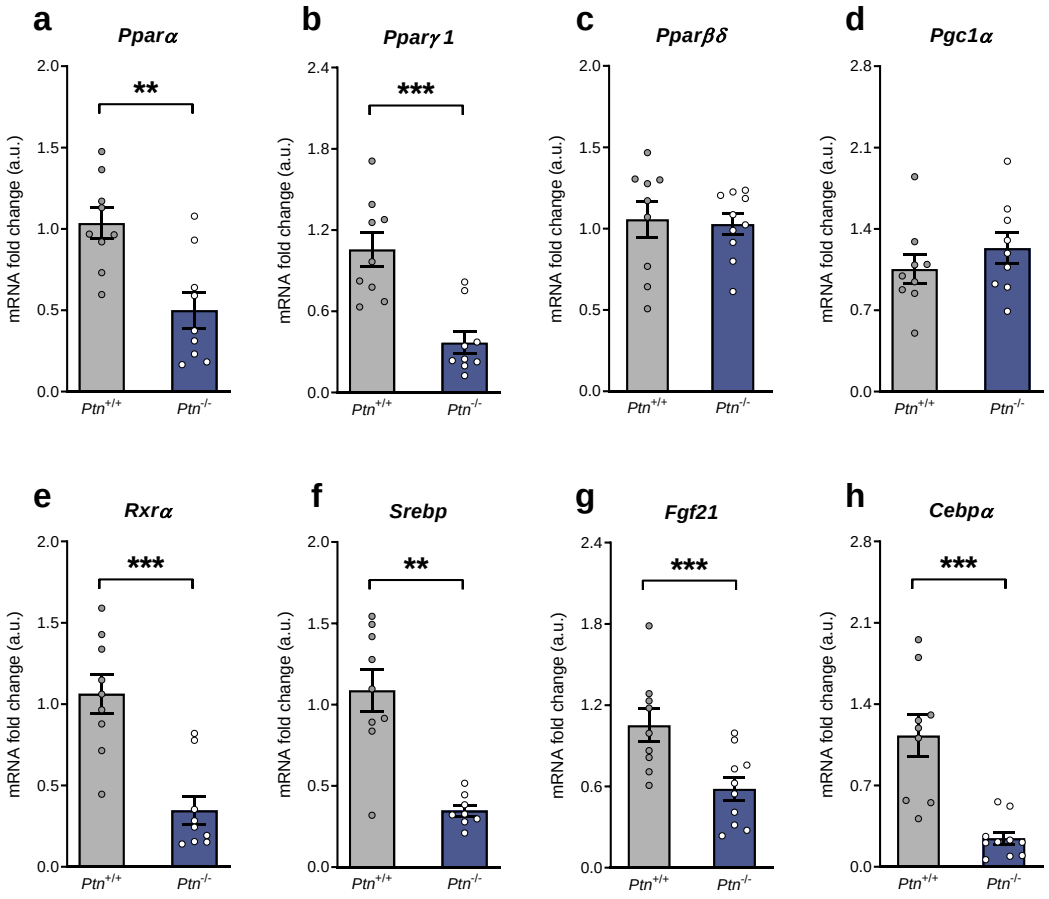

Figure 46. Deletion of pleiotrophin is associated with differential expression of genes involved in regulating lipid metabolism in the liver of 18 days pregnant mice. *a) Ppar-α mRNA; b) Ppar-γ1 mRNA; c) Ppar-βδ mRNA; d) Pgc1-α mRNA; e) Rxr-α mRNA; f) Srebp1 mRNA; g) Fgf21 mRNA; h) Cebpα mRNA. Data are expressed as mean ± SEM (n=3-9 animals/group) *p<0.05, **p<0.01, ***p<0.001 for differences between Ptn*$^{-/-}$ *and Ptn*$^{+/+}$ *mice.*

NUR77 (the mice isoform for NR4A1) is another transcription factor that has been implicated in the regulation of liver metabolism and is altered in *Ptn*-deficient mice. As shown, its gene expression was significantly increased in the knock-out mice compared to the control pregnant animals (Figure 47a), although its protein level was found to be significantly reduced in *Ptn*$^{-/-}$ mice compared to *Ptn*$^{+/+}$ animals (Figure 47b). As glycerol kinase has been discovered as a novel corepressor of NUR77 in the liver, we analysed the mRNA and protein of this enzyme and performed a correlation analysis of the expression levels of *Nur77* and *Gyk* mRNA. Notably, the mRNA and protein levels of glycerol kinase were significantly increased in *Ptn*$^{-/-}$ pregnant mice compared to the wild-type pregnant animals (Figure 47c-d). As shown in Figure 47e, *Gyk* mRNA has a significant positive

correlation with the mRNA of *Nur77* (r=0.7836 and r=0.6776 for $Ptn^{+/+}$ and $Ptn^{-/-}$, respectively; r=0.7443 for all animals; p<0.05 for all Pearson coefficients). Finally, we found that the abundance of glycerol kinase in the nuclei was significantly higher in $Ptn^{-/-}$ than in the $Ptn^{+/+}$ pregnant mice (Figure 47f), suggesting that translocation of the enzyme to the nuclei is favoured in the absence of PTN.

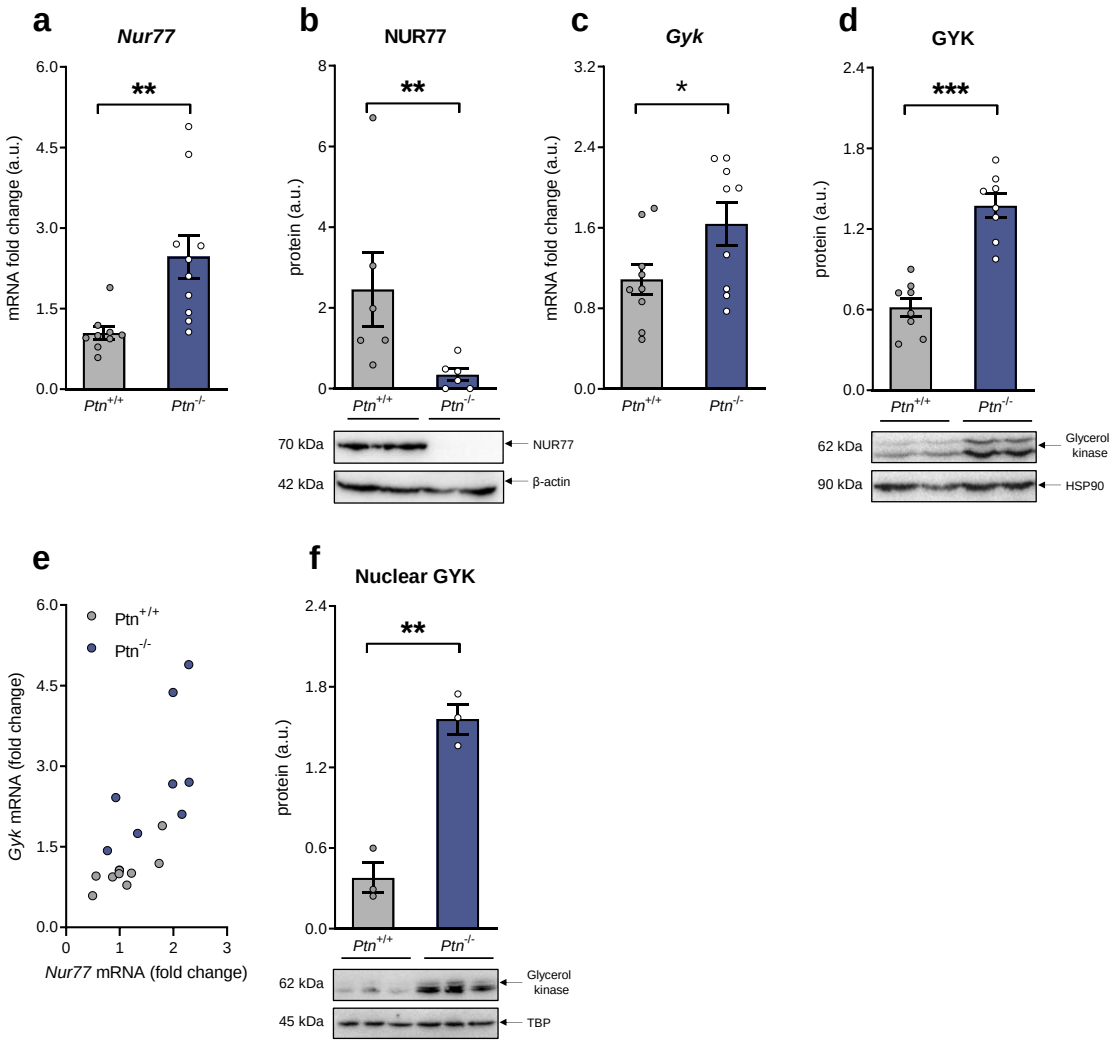

Figure 47. Deletion of pleiotrophin is associated with differential expression of genes involved in regulating glucose metabolism in the liver of 18 days pregnant mice. *a) Nur77 mRNA; b) NUR77 protein/β-actin; c) Glycerol kinase (Gyk) mRNA; d) Glycerol kinase protein/HSP90; e) Correlation analysis of glycerol kinase (Gyk) mRNA and Nur77 mRNA; f) Glycerol kinase nuclear protein/TBP protein. Data are expressed as mean ± SEM (n=3-9 animals/group) *p<0.05, **p<0.01, ***p<0.001 for differences between $Ptn^{-/-}$ and $Ptn^{+/+}$ mice.*

3.8. *Ptn*$^{-/-}$ pregnant mice show upregulation of midkine and reduced mRNA of *Hprt* and *Nampt*

Finally, we have also noticed that *Ptn* deficient pregnant mice show a 2-fold reduction in *Hprt* and *Nampt*, two enzymes responsible for synthesizing nucleotides and NAD, respectively (Figure 48).

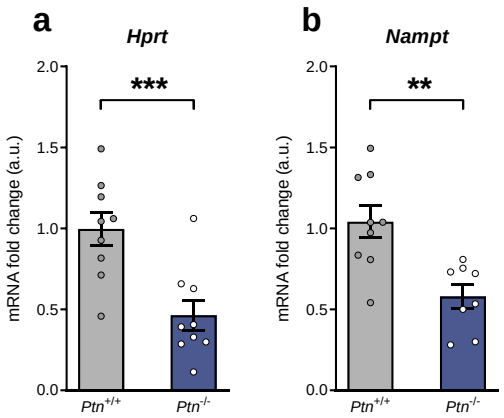

Figure 48. Deletion of pleiotrophin downregulates Hprt and Nampt in the liver of 18 days pregnant Ptn$^{-/-}$ mice. *a) Hypoxanthine guanine phosphoribosyl transferase (Hprt) mRNA; b) Nicotinamide phosphoribosyltransferase (Nampt) mRNA. Data are expressed as mean ± SEM (n=9 animals/group) *p<0.05, **p<0.01, ***p<0.001 for differences between Ptn$^{-/-}$ and Ptn$^{+/+}$ mice.*

4. DISCUSSION

In this study, we provide novel insights into the role of pleiotrophin as a key player in regulating maternal metabolism during pregnancy. Pleiotrophin has been shown to be involved in the development, especially at early stages of differentiation, it is expressed in the placenta, and its circulating levels are known to increase as pregnancy progresses (299). Although pleiotrophin has shown to have a role in the regulation of glucose homeostasis and energy metabolism in non-pregnant animals (71), little is known about the functions of this protein in maternal metabolism during pregnancy.

In our model, *Ptn*$^{-/-}$ animals experience a 3-fold increment in *Mk* expression. The midkine gene is expressed in pregnancy in the mid-gestational period, while *Ptn* reaches its maximum expression level around birth (42,60). These two cytokines that belong to the heparin-binding growth factor family had been demonstrated to have some overlapping functions (42). Thus, PTN may compensate for the lack of midkine and vice versa (60,93). Herradón et al. demonstrated that midkine regulates *Ptn* gene transcription and that knock-out mice for *Mk* present an increase in *Ptn* expression, indicating a compensatory and redundant function of this cytokine. On the other hand, when they evaluated midkine expression levels in *Ptn* knock-out mice, no differences were found (60). However, none of these findings evaluated the expression of these two cytokines in the liver or pregnancy before.

The maternal liver plays a key role in the regulation of whole-body metabolism during early pregnancy (300), including the accumulation of fat depots. Additionally, during late pregnancy, the augmented lipolytic activity of adipose tissue favours the release of free fatty acids and glycerol into the circulation, and these substrates are easily taken up and esterified in the liver. Liver triacylglycerides are rapidly released into the circulation, leading to increased VLDL levels and the development of maternal hyperlipemia (301).

In this study, we show that *Ptn* deletion compromise maternal increment of body weight during pregnancy and this reduced body weight cannot be fully explained just by a decrease in the conceptus weight, as the maternal body weight free of conceptus in *Ptn*$^{-/-}$ mice is also lower than in wild type animals. Moreover, at late pregnancy, *Ptn* deletion was associated with decreased liver weight and hepatic lipid content. Firstly, these data can be partially explained by the reduced expression of the enzymes involved in cholesterol synthesis and esterification. Secondly, *Ptn* deletion also reduced hepatic uptake of triacylglycerides from lipoproteins, as evidenced by the decreased expression of lipoprotein lipase and hepatic lipase and the lower expression of the main transporters involved in glycerol and fatty acids hepatic uptake (*Aqp9*, *Fatp4,* and *Fatp5*). Thirdly, deletion of *Ptn* is also associated with both a reduced expression of the key enzymes of lipogenesis, triacylglycerides synthesis and of perilipin 2, the main structural protein of lipid droplets, that is also involved in the regulation of their dynamic and triacylglycerides metabolism. As a result of these impairments, *Ptn* deficiency is associated with an altered lipid metabolism that averts the normal lipid accumulation that takes place in the liver during pregnancy. Consequently, although it has been established that at late pregnancy, circulating fatty acid and triacylglycerides levels are increased more than 250% (302,303), in *Ptn*$^{-/-}$ pregnant mice, the hepatic secretion of triacylglycerides as very-low-density lipoproteins (VLDL), and the circulating low-density lipoproteins (LDL) and VLDL/IDL fractions are significantly reduced. Accordingly, the mRNA of apolipoprotein B-100, which provides the structural framework required for the developing VLDL, and the mRNA of apolipoprotein C-II, a cofactor of lipoprotein lipase (304), are also decreased. In addition to these effects in the liver, we cannot discard other adaptations in extrahepatic tissues that may also contribute to the decrease in circulating lipids observed in the *Ptn*$^{-/-}$ pregnant mice. In this line of evidence, we have previously reported in this knock-out mouse model an augmented energy production from fatty acids instead of glucose in extrahepatic tissues or increased fatty acid oxidation by thermogenesis (71). Altogether, these results point out that, at late pregnancy, the deletion of *Ptn* is associated with a marked reduction in fatty acid, triacylglycerides, and cholesterol synthesis in the liver that may explain the diminished hepatic lipid accumulation (Figures 39, 43, 44) as well as the decrease in circulating NEFA and triacylglycerides levels observed in these animals.

We next explored whether *Ptn* deficiency was associated with the development of whole-body glucose intolerance and/or altered glucose metabolism. *Ptn*$^{-/-}$ pregnant mice have hypoinsulinemia and are glucose intolerant, suggesting that *Ptn* deletion could favour a diabetogenic state in the pregnant dams. The liver's decreased uptake and use of glucose in *Ptn*$^{-/-}$ pregnant mice might contribute to maternal hyperglycaemia, as the expression of the hepatic glucose transporter *Glut2* and the glycolytic enzymes were reduced in late *Ptn*$^{-/-}$ pregnant mice (Figure 40). Furthermore, the increased insulin:glucagon ratio in *Ptn*$^{-/-}$ pregnant mice in the absence of a significant increase in GIP may also contribute to the mobilization of stored nutrients, impairing fat accumulation and/or promoting the breakdown of adipose tissue depots (305).

It is known that most of the enzymes involved in glucose and lipid metabolism, including fatty acid transporters (306), are regulated by transcription factors as PPAR-α, PPAR-γ, RXR-α, FGF21, and SREBP (253,307,308). In fact, during the third trimester of pregnancy, the decrease in the nuclear hormone receptor liposensors, including RXRs, PPARs, or SREBP and the concomitant decrease in the expression of their target genes, has been proposed as one mechanism that leads to the alterations in lipid metabolism that characterise the third trimester of pregnancy (309). We found that deletion of *Ptn* further decreases the expression of these transcription factors, which may be involved in the altered lipid metabolism that we found in these animals.

Interestingly, the mRNA and protein of glycerol kinase were increased in the liver of these animals. Recently, it has been shown that glycerol kinase, apart from its kinase activity, transforming glycerol to glycerol 3-phosphate in an ATP-dependent reaction, has other functions (264,265) including an essential role in lipid metabolism by affecting transcription factors activity, as SREBP-1c or PPAR-α (310). Additionally, glycerol kinase is also a corepressor of NR4A1 (NUR77), a transcription factor that regulates hepatic glucose homeostasis. In fact, *Gyk* mRNA overexpression has been shown to suppress NR4A1 ability to regulate the expression of hepatic gluconeogenic genes, such as glucose 6 phosphatase and fructose 1,6-bisphosphatase, and to modulate hepatic glucose production in the unfed state and diabetes *in vitro* and *in vivo* (261,264). In this scenario, the increased amount of glycerol kinase in late pregnant *Ptn*$^{-/-}$ mice may suppress the transcriptional activity of NUR77 by attenuating its binding to gluconeogenic gene promoters, negatively regulating their transcription as has been found in other studies (264). Supporting this role of glycerol kinase, we found that deletion of *Ptn* is associated with an increased translocation of glycerol kinase into the nuclei of liver cells. Additionally, the proteasome degradation of NUR77 may be enhanced (Figure 47) as undetectable protein levels were found in the liver of *Ptn*$^{-/-}$ pregnant mice. In line with this hypothesis, it has been shown that SUMOylation and later

ubiquitination control NUR77 degradation and that for the SUMOylation of NUR77, the protein must be previously phosphorylated (311,312).

Additionally, glycerol-3-phosphate can also be employed in the pentose phosphate pathway to generate glucose-6-phosphate, which in the presence of glucose 6P dehydrogenase may be oxidized to obtain NADH and ribulose. In our *Ptn*$^{-/-}$ pregnant mice, the increased expression of glucose 6P dehydrogenase may lead to an increase in ribulose synthesis that could be employed for the *de novo* nucleotide synthesis to compensate for the decreased expression of the *Hprt* from the salvage pathway of nucleotides.

Moreover, the synthesis of NADH might also be compromised in *Ptn*$^{-/-}$ mice as the expression of *Nampt* (or *Visfatin*), the rate-limiting enzyme in NAD^+ synthesis, is also diminished. Moreover, *Nampt* has recently been demonstrated to regulate cellular processes, including lipid and glucose metabolism, inflammation, and insulin resistance (313) and the activity of NAD^+-dependent enzymes like sirtuins, PARPs, and NADases (314).

Given these results, it is tempting to speculate that deletion of *Ptn* may be associated in the liver with altered transcriptional activity modulated by glycerol kinase, impairing the pregnancy-related adaptations in both glucose and lipid metabolism, including glucose intolerance and a decreased capacity to store lipids (Figure 49).

The mouse is an important mammalian model to approach the study of human metabolism in pregnancy, particularly at a molecular level. Although the present study has some limitations, as we cannot discard the contributions of other organs, such as adipose tissue, to the observed changes in lipid metabolism in the liver, we suggest that this model will be valuable to elucidate the mechanisms underlying adaptations of liver metabolism during obese pregnancy, which is frequently associated to fatty liver. In fact, fatty liver is relatively common in human pregnancy because of the increasing prevalence of diabetes and/or obesity, and it is associated with adverse maternal and perinatal outcomes (315). Thus, future studies of pregnant *Ptn*$^{-/-}$ mice fed an obesogenic diet will provide additional information on the maternal factors that may protect pregnant mothers to develop fatty liver disease.

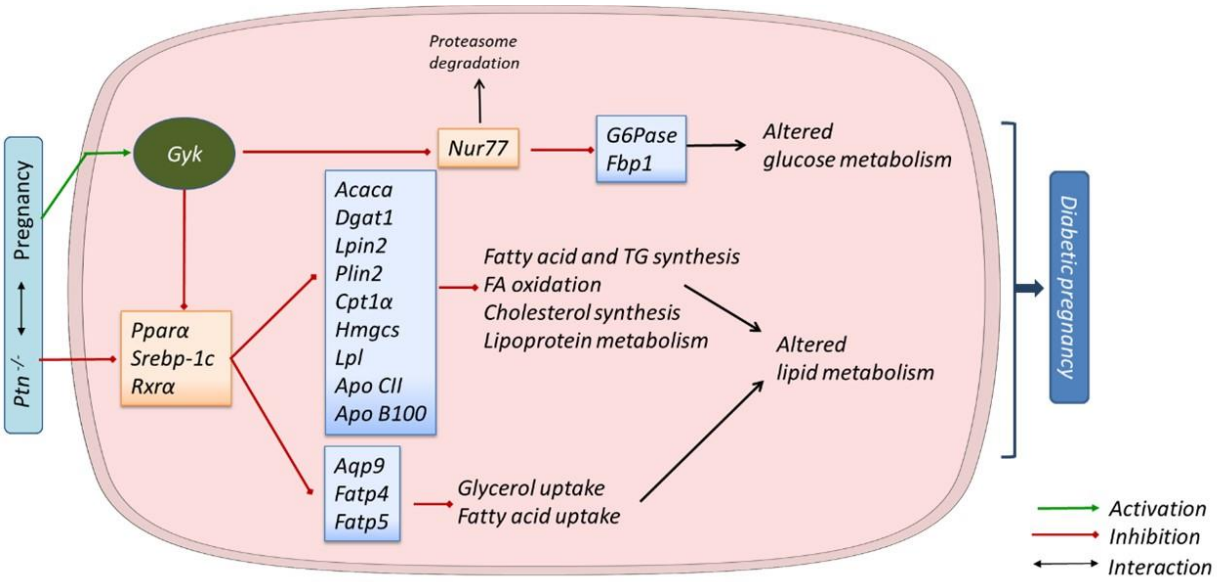

Figure 49. Schematic representation of the modifications in maternal hepatic metabolism during late pregnancy in Ptn$^{-/-}$ mice. *Image taken from Zapatería, B. et.al. (298).*

GENERAL DISCUSSION, STUDY LIMITATIONS AND FUTURE PERSPECTIVES

Insulin resistance is a common feature that is present in both physiological (ageing and pregnancy) or pathological (diabetes, NAFLD, obesity or metabolic syndrome) situations. The liver plays a major role in regulating the whole-body homeostasis and has close communication with other peripheral organs like the adipose tissue and pancreas. In previous studies of our group, we have described that the cytokine pleiotrophin is a regulator of insulin sensitivity, adipose tissue lipid turnover and expansibility, brown adipose tissue functionality and energy metabolism (71). In this thesis, we have examined whether pleiotrophin is involved in the changes in liver metabolism during ageing and late pregnancy, two physiological conditions associated with the development of insulin resistance, and thereby if this cytokine could be a potential target for developing therapies against diseases characterised by the disruption of hepatic homeostasis.

PTN is a heparin-binding growth factor that shares family with midkine (MK). Both cytokines have been suggested to have overlapping functions, and some studies have also proposed that midkine regulates gene expression of PTN. The increase in *Ptn* expression when *Mk* is deleted, and not vice versa, supports this hypothesis (60). However, we have shown that *Mk* expression is 2-3-fold upregulated in 3 months old *Ptn* deficient non-pregnant and pregnant mice, suggesting that the overlap in the functions is not total.

During early pregnancy, the mother accumulates fat depots as triacylglycerides that later on, during late pregnancy, are broken down as a consequence of the increased adipose tissue lipolytic activity and the products of lipolysis (free fatty acids and glycerol) are released to blood. Adipose tissue depots increase with age due to a chronic positive calorie balance, reduced physical activity, and a lower basal metabolic rate (316). In particular, during ageing, the organism also tends to accumulate fat in visceral tissues, and there is a reduction of catecholamine-induced lipolysis in visceral adipose tissue (317). In this thesis, we show that *Ptn* deletion is associated with a reduction in the increment of body weight and with impaired expandability of adipose tissue. In this context, *Ptn* deletion compromises both maternal increment of body weight during pregnancy and the age-related increment of body weight. Furthermore, we have also observed that the weight of periovarian and retroperitoneal adipose tissues in $Ptn^{-/-}$ mice were higher in young animals and lower in the old ones compared with their age-matched controls, suggesting a switch in fat distribution evolving from greater adiposity in young mice to a slimness in older animals.

In addition, our previous results revealed that in the periovarian adipose tissue, *Ptn* deficiency is associated with a decreased mRNA *of Ppar-γ* and its coactivator *Pgc-1α* (71). PPAR-*γ* is critical for adipocyte function and regulates genes involved in lipid and glucose homeostasis (318). In fact, deletion of *Ppar-γ2* reduces adipose tissue expandability, which is highly associated with the development of severe insulin resistance (319). Moreover,

young *Ptn*$^{-/-}$ animals also exhibit reduced expression of *Lpl* and *Cpt1α*, whereas *Ucp-2* and *Tnfα* expression were increased. Thus, these results may suggest that deletion of *Ptn* could be involved in the enhanced inflammation of periovarian tissue and contribute to the age-related impairment of both glucose and lipid metabolism, including the development of insulin resistance and decreased capacity of the white adipose tissue to store lipids (71).

Similarly, in this thesis we show that *Ptn* deletion not only affects body weight and adiposity but also renders mice with decreased liver weight in both animal models. Parallel to this, hepatic lipid content is reduced in pregnant and old mice lacking *Ptn*. Pleiotrophin deletion downregulates the expression of essential enzymes of lipogenesis, triacylglycerides and cholesterol synthesis, as well as the mRNA of the apolipoproteins required for VLDL assembly. These changes contribute to the reduced lipid accumulation in the liver observed in both models. Moreover, in the liver, pleiotrophin deficiency was associated with lower mRNA levels of hepatic lipase and glycerol and fatty acid transporters. Besides, *Ptn* deletion provokes a reduction in mRNA levels of the enzymes of β-oxidation and block the increment in the levels of ketone bodies associated with age, which could be explained by the downregulation of *Ppar-α* and *Srebp-1c*, the main regulators of the liver metabolism.

Accordingly, similar results have been obtained by our group in a diet induced-obesity model in which *Ptn*$^{+/+}$ and *Ptn*$^{-/-}$ mice were fed either with standard or with a high-fat diet (HFD) for 80 days. In this DIO model, we have observed a lower weight gain and lower liver weight in *Ptn*$^{-/-}$ mice. Besides, liver lipid accumulation was reduced in the *Ptn*$^{-/-}$ animals as the tissue content of TAGs, cholesteryl esters, and cholesterol were lower compared to their respective controls. Our results showed that *Ptn* deletion reduced the expression of the enzymes involved in hepatic lipid synthesis. Although glycerol and fatty acid esterification is favoured in *Ptn*$^{+/+}$ mice on a HFD, as evidenced by an increase in *Lpin2, Dgat1* and *Dgat2* expression, this effect is not observed in *Ptn*$^{-/-}$ mice. In fact, *Ptn* deletion was associated in the liver with decreased mRNA of the enzymes involved in both the triacylglyceride (*Gpat, Lpin2, Dgat1* and *Dgat2*) and fatty acid synthesis (*Acc* and *Fas*) (72).

Altogether these results suggest that *Ptn* deletion is associated with changes in the metabolism of lipids that prevents their hepatic accumulation, which is beneficial as ectopic deposition of fat is associated with several pathologies such as non-alcoholic fatty liver, steatosis, diabetes, and insulin resistance.

Next, we investigated whether *Ptn* deletion was associated with glucose intolerance and/or impaired glucose metabolism. *Ptn*$^{-/-}$ pregnant and *Ptn*$^{-/-}$ old mice are glucose intolerant, as reflected by the glucose tolerance tests. Moreover, old *Ptn*-deficient mice are hyperinsulinemic and insulin resistant, as evidenced by the HOMA-IR and QUICKI indexes.

Furthermore, similar results were found in the diet induced-obesity model, in which mice lacking *Ptn* fed with a standard diet exhibit hyperinsulinemia and insulin resistance similar to control mice fed with HFD (72). These results suggest that *Ptn* deletion could promote glucose intolerance in pregnancy and ageing. This impaired glucose tolerance was associated with a downregulation of the glycolytic enzymes and a decrease in liver glucose disposal both in late pregnant and 15-months-old *Ptn*$^{-/-}$ mice.

Several transcription factors such as PPAR-α, PPAR-*γ*, RXR-α, FGF21 and SREBP are involved in the regulation of the transcription of the key enzymes of liver metabolism. In our models, the expression of all these factors above mentioned is lower in both 15 months-old and late pregnant *Ptn*$^{-/-}$ mice, which could explain at least in part the reduced liver lipid synthesis observed both in late gestation and in late life.

One of the most relevant contributions of this thesis is the finding that the deletion of *Ptn* is associated with an increment in the expression of glycerol kinase, confirming the moonlighting role of this enzyme as a regulator of liver metabolism (298). In fact, recent research has shown that apart from its kinase activity, glycerol kinase has other functions (264,265). Glycerol kinase has been shown to regulate lipid metabolism through its capacity to modulate the activity of transcription factors like SREBP-1C and PPAR-α. In addition, glycerol kinase regulates hepatic glucose homeostasis by corepressing NUR77 (264,265). Different studies have shown that the overexpression of *Gyk* suppresses NUR77 ability to regulate the expression of some gluconeogenic genes as well as hepatic glucose production *in vitro* and *in vivo* (261,264,265). We showed that when *Ptn* is deleted, mRNA and protein expression of glycerol kinase is upregulated. These higher levels of glycerol kinase may inhibit NUR77 transcriptional activity by hindering its binding to the promoter region of its target genes. Accordingly, we found that even though the mRNA of *Gyk* and *Nur77* was increased in *Ptn*-deficient mice, the overexpression of GYK protein matches with the lowest of NUR77 in *Ptn*$^{-/-}$ mice. This effect is particularly noticeable in the gestation rather than in the ageing model, so we used these mice to investigate whether GYK can translocate into the nuclei. Supporting our hypothesis, we found an enhanced presence of glycerol kinase in the nuclei of hepatic cells from *Ptn*$^{-/-}$ mice.

We have also corroborated that PTN is involved in regulating the cellular balance between glycolysis and mitochondrial respiration, which contributes to the cellular oxidative stress and the response of the liver as evidenced by the OCR, the spare respiratory capacity and the uncoupling efficiency.

Additionally, we have shown that in the liver *Ptn* deletion and ageing are associated with enhanced infiltration of macrophages and secretion of pro-inflammatory cytokines as

suggested by the increased mRNA of *Cd68*, *F4/80*, *Cd-11b*, *Cd-11c*, *Il-1β*, and *Tnfα*, which can contribute to the observed effects.

Although this thesis has been directed to the evaluation of the role of pleiotrophin in liver metabolism, other peripheral organs can contribute to the observed changes in the plasma biochemical profile, in the glucose tolerance and in the energetic homeostasis (Figure 50). Supporting this hypothesis, current literature provides solid evidence that brown and beige adipocytes improve plasmatic parameters and influence hepatic energy metabolism (320). In fact, increased energy expenditure helps the liver handle lipid homeostasis, as illustrated by several studies that have shown that increased BAT activity prevents the development of NAFLD in rodents (320). Moreover, alterations in white (WAT) and brown (BAT) adipose tissues have been shown to aid the development of liver disorders (320). We have shown that pleiotrophin deficiency is associated with changes in energy homeostasis, as evidenced by previous studies in metabolic cages (71). In the fed state, $Ptn^{-/-}$ mice had a reduction in the RER values when compared to $Ptn^{+/+}$. According to this data, $Ptn^{-/-}$ mice consumed a combination of glucose and fatty acids and further increased this consumption during the fasting state, pointing to an augmented energy production from fatty acids. The main oxidative tissue in which fatty acids are used as energy substrates by β-oxidation is the skeletal muscle (220). These mice exhibited lesser physical activity than the controls, so we assumed that fatty acids were not consumed by the skeletal muscle and thereby redirected to other tissues for oxidation. Accordingly, the energy expenditure of $Ptn^{-/-}$ mice accounted for cold-induced thermogenesis was higher than in $Ptn^{+/+}$ animals. Moreover, UCP-1 protein expression, DIO2 expression and activity, and T_3 concentration were increased in $Ptn^{-/-}$ mice. Thus, *Ptn* deletion in BAT may account for the higher activation of the brown adipose tissue and the consequent rise in body temperature. The greater use of fatty acids as energy substrates despite glucose availability may contribute to the lower plasma concentrations of TAGs and fatty acids and the reduced adiposity of WAT depots. In view of these results, we have proposed that $Ptn^{-/-}$ lipodystrophic phenotype is associated with an active mobilisation of lipids from WAT that sustains the enhanced thermogenesis in BAT (71). Similar results were obtained in a later study from our group, with the administration of a HFD to $Ptn^{+/+}$ and $Ptn^{-/-}$ mice. In this research, we found that *Ptn* deletion leads to the browning of WAT as evidenced by an increase in the UCP1-expressing adipocytes in the perigonadal adipose tissue and by a marked increase in the expression of BAT markers such as *Ucp-1*, *Pgc-1α* and *Cidea* in white adipocytes. This browning may also contribute to the elevated thermogenesis and to the reduction in ectopic lipid deposition in $Ptn^{-/-}$ mice (72). In the gestation model, activation of brown adipose tissue or browning of WAT has not been assessed, but due to the similar phenotype of these animals, we hypothesise that it would behave in a similar manner.

On the other hand, it has to be borne in mind that PTN exerts effects on other organs and systems of the body. For example, in the central nervous system (CNS) its expression is higher than in peripheric organs. Upregulation of PTN has been found in a variety of brain disorders characterised by neuroinflammation like Parkinson's disease, Alzheimer's disease, tumours, ischemia and more recently in addictive disorders. Additionally, recent evidence from the group of Dr Herradón has highlighted that PTN plays an essential role in neuroinflammation through microglia and astrocytic activation, however, this process is highly dependent on the inflammatory stimulus. After treatment with LPS, overexpression of PTN enhances the production and release of pro-inflammatory cytokines (IL-6, MCP-1 and TNFα). The fact that no effect was detected in basal conditions prompted the authors to propose that PTN is a key factor in promoting the effects triggered by an inflammatory stimulus, but it is not capable of sparking the pro-inflammatory cascade on its own (91).

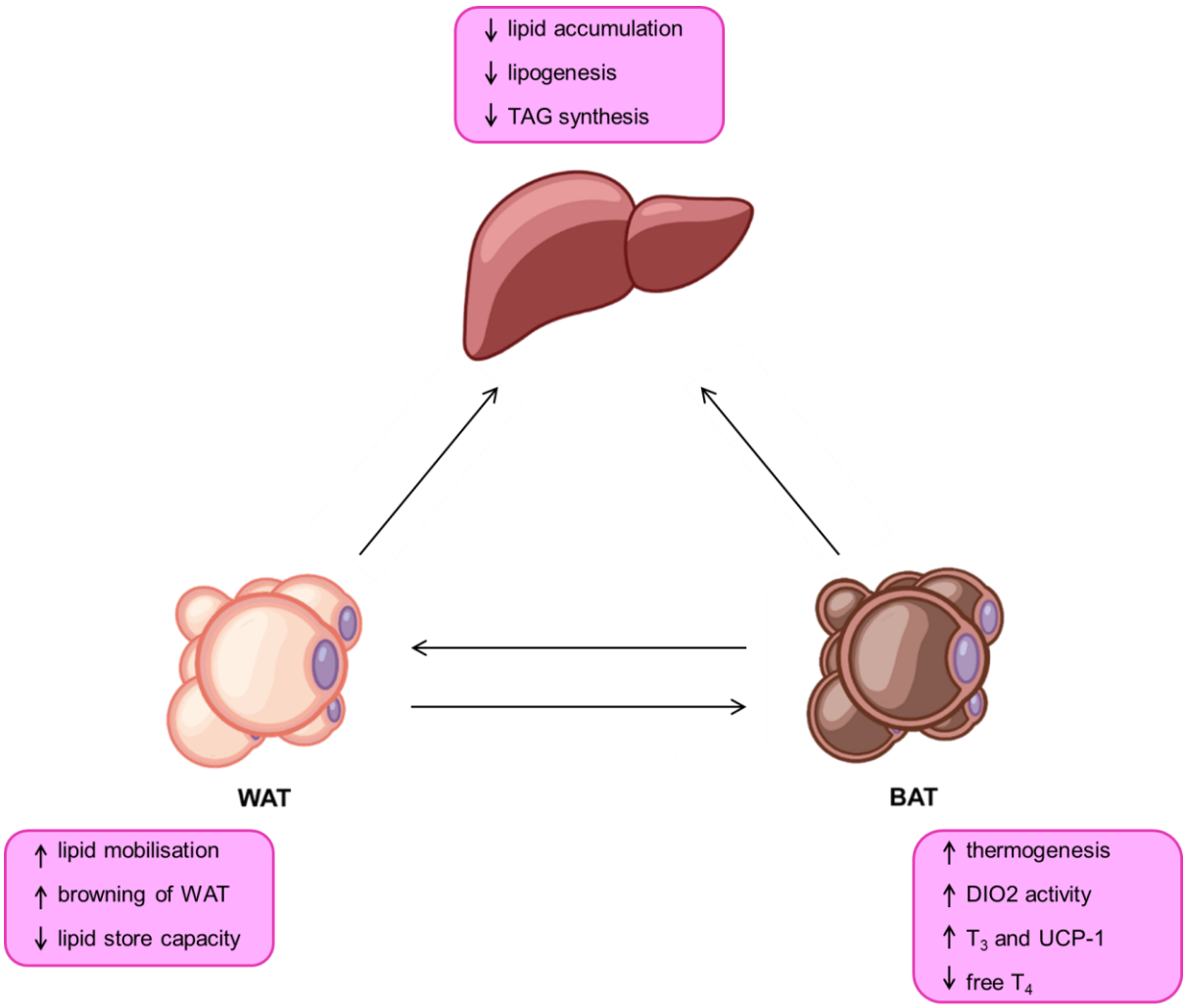

Figure 50. Effects of Ptn deletion in the liver, WAT and BAT, and the crosstalk between organs.

Although we provide a wealth of data on the novel and important role of pleiotrophin in the maintenance of whole-body homeostasis and, in particular, in the liver, further research is needed to completely elucidate PTN's functions. Currently, we have some preliminary data and continue working with hepatocytes in cell culture to evaluate the effect of exogenous PTN addition on the insulin signalling pathway. Besides, it would be of interest silencing *Ptn* in these hepatocytes to corroborate the effects obtained from the knock-out model. Moreover, another key point would be to evaluate if the changes associated with *Ptn* deletion during ageing also occur in male mice, as sexual hormones have an important role in regulating physiological changes, and sexual dimorphism is common in several aspects.

CONCLUSIONS / CONCLUSIONES

CONCLUSIONS

1. *Ptn* deletion is associated with a reduction in the hepatic accumulation of lipids due to a diminished expression of the enzymes involved in the fatty acids and TAG synthesis and β-oxidation pathways.
2. In the absence of *Ptn*, the aged liver has an increased infiltration of macrophages and increased production of pro-inflammatory cytokines.
3. Pleiotrophin plays an essential role in biogenesis and mitochondrial function both *in vivo* and *in vitro* and regulates the balance between glycolysis and mitochondrial respiration, as well as the response to oxidative stress.
4. Pleiotrophin deletion impairs the glucose and lipid metabolism during pregnancy, which, together with a defective PPARα and NUR77 activation, may account for the development of a diabetogenic state in the mother.
5. Glycerol kinase has a moonlighting role in pregnancy, modulating the expression and activity of several transcription factors, which impairs the pregnancy-related adaptations of glucose and lipid metabolism in the liver.
6. Pleiotrophin deletion reduces the ectopic accumulation of fat and enhances thermogenesis, which diminishes the risk of developing hepatic steatosis and non-alcoholic fatty liver disease (NAFLD).

CONCLUSIONES

1. La deleción de *Ptn* se asocia a una reducción en la acumulación hepática de lípidos debido a una diminución en la expresión de las enzimas que participan en las rutas de síntesis de ácidos grasos y TAG, y en la beta-oxidación.

2. En ausencia de *Ptn*, el hígado envejecido presenta una mayor infiltración de macrófagos y un incremento en la producción de citoquinas proinflamatorias.

3. La pleiotrofina desempeña un papel fundamental en la biogénesis y función mitocondrial *in vivo* e *in vitro*, regulando el balance entre la glucolisis y la respiración mitocondrial, así como la respuesta al estrés oxidativo.

4. La deleción de *Ptn* altera el metabolismo glucídico y lipídico durante la gestación, lo que junto con una activación defectuosa de PPARα y NUR77 puede explicar el desarrollo de un estado diabetogénico en la madre.

5. La enzima glicerol quinasa tiene un papel regulador durante el embarazo modulando la expresión y actividad de diversos factores de transcripción, lo cual altera las adaptaciones hepáticas del metabolismo de carbohidratos y lípidos asociadas a la gestación.

6. La deleción de pleiotrofina reduce la acumulación ectópica de grasa y aumenta la termogénesis, lo cual disminuye el riesgo de desarrollar esteatosis hepática y la enfermedad del hígado graso no alcohólico (NAFLD).

REFERENCES

(1) Racanelli V, Rehermann B. The liver as an immunological organ. Hepatology 2006 -;43(Supplement 1):S54.

(2) Baffy G. Kupffer cells in non-alcoholic fatty liver disease: the emerging view. J Hepatol 2009 -;51(1):212.

(3) Dixon LJ, Barnes M, Tang H, Pritchard MT, Nagy LE. Kupffer cells in the liver. Comprehensive Physiology 2013 -;3(2):785.

(4) Rui L. Energy metabolism in the liver. Comprehensive Physiology 2014 -;4(1):177.

(5) Matschinsky FM, Wilson DF. The Central Role of Glucokinase in Glucose Homeostasis: A Perspective 50 Years After Demonstrating the Presence of the Enzyme in Islets of Langerhans. Frontiers in physiology 2019 -;10:148.

(6) Chiang J. Liver Physiology: Metabolism and Detoxification. In: McManus LM, Mitchell RN, editors. Pathobiology of Human Disease San Diego: Academic Press; 2014. p. 1770-1782.

(7) Blanco A, Blanco G. Chapter 14 - Carbohydrate Metabolism. In: Blanco A, Blanco G, editors. Medical Biochemistry: Academic Press; 2017. p. 283-323.

(8) Kohlmeier M. Chapter 6 - Carbohydrates, Alcohols, and Organic Acids. In: Kohlmeier M, editor. Nutrient Metabolism (Second Edition) San Diego: Academic Press; 2015. p. 187-242.

(9) Litwack G. Chapter 8 - Glycolysis and Gluconeogenesis. In: Litwack G, editor. Human Biochemistry Boston: Academic Press; 2018. p. 183-198.

(10) Ge T, Yang J, Zhou S, Wang Y, Li Y, Tong X. The Role of the Pentose Phosphate Pathway in Diabetes and Cancer. Frontiers in endocrinology 2020 -;11:365.

(11) Zhang X, Yang S, Chen J, Su Z. Unraveling the Regulation of Hepatic Gluconeogenesis. Frontiers in endocrinology 2019 -;9:802.

(12) Pelley JW. 13 - Integration of Carbohydrate, Fat, and Amino Acid Metabolism. In: Pelley JW, editor. Elsevier's Integrated Review Biochemistry (Second Edition) Philadelphia: W.B. Saunders; 2012. p. 109-117.

(13) Hodson L, Gunn PJ. The regulation of hepatic fatty acid synthesis and partitioning: the effect of nutritional state (vol 15, pg 689, 2019). Nat Rev Endocrinol 2020 JUN;16(6):340-340.

(14) Takeuchi K, Reue K. Biochemistry, physiology, and genetics of GPAT, AGPAT, and lipin enzymes in triglyceride synthesis. American Journal of Physiology - Endocrinology and Metabolism 2009;296(6):E1195.

(15) Karasawa K, Tanigawa K, Harada A, Yamashita A. Transcriptional Regulation of Acyl-CoA:Glycerol- sn -3-Phosphate Acyltransferases. International journal of molecular sciences 2019 -;20(4).

(16) Coleman RA, Lee DP. Enzymes of triacylglycerol synthesis and their regulation. Prog Lipid Res 2004 March 2004;43(2):134-176.

(17) Coleman RA, Mashek DG. Mammalian triacylglycerol metabolism: synthesis, lipolysis, and signaling. Chem Rev 2011 -;111(10):6359.

(18) Reddy JK, Hashimoto T. PEROXISOMAL beta-OXIDATION AND PEROXISOME PROLIFERATOR-ACTIVATED RECEPTOR alpha: An Adaptive Metabolic System. Annu Rev Nutr 2001 -;21(1):193.

(19) Reddy JK, Sambasiva Rao M. Lipid Metabolism and Liver Inflammation. II. Fatty liver disease and fatty acid oxidation. American Journal of Physiology - Gastrointestinal and Liver Physiology 2006 -;290(5):G852.

(20) Calder PC. Fatty Acids: Metabolism. In: Caballero B, Finglas PM, Toldrá F, editors. Encyclopedia of Food and Health Oxford: Academic Press; 2016. p. 632-644.

(21) Hess RS. Chapter 64 - Diabetic Ketoacidosis. In: Silverstein DC, Hopper K, editors. Small Animal Critical Care Medicine (Second Edition) St. Louis: W.B. Saunders; 2015. p. 343-346.

(22) Iizuka K. Chapter 22 - The Role of Carbohydrate Response Element–Binding Protein in the Development of Liver Diseases. In: Watson RR, Preedy VR, editors. Dietary Interventions in Liver Disease: Academic Press; 2019. p. 263-274.

(23) Trapani L, Segatto M, Pallottini V. Regulation and deregulation of cholesterol homeostasis: The liver as a metabolic "power station". World journal of hepatology 2012 -;4(6):184.

(24) Malhotra P, Gill RK, Saksena S, Alrefai WA. Disturbances in Cholesterol Homeostasis and Non-alcoholic Fatty Liver Diseases. Frontiers in medicine 2020 -;7:467.

(25) Baynes JW, Dominiczak MH. Bioquímica médica. 5ª ed.: Elsevier; 2019.

(26) Stanley LA. Chapter 27 - Drug Metabolism. In: Badal S, Delgoda R, editors. Pharmacognosy Boston: Academic Press; 2017. p. 527-545.

(27) Krellman JW, Croll SD, Ruiz HH, Marciano VA, Mondrow B. Behavioral and neuroanatomical abnormalities in pleiotrophin knockout mice. PLoS ONE 2014 -;9(7).

(28) Tezuka K, Takeshita S, Hakeda Y, Kumegawa M, Kikuno R, Hashimoto-Gotoh T. Isolation of mouse and human cDNA clones encoding a protein expressed specifically in osteoblasts and brain tissues. Biochem Biophys Res Commun 1990 11/30;173(1):246-251.

(29) Li YS, Milner PG, Chauhan AK, Watson MA, Hoffman RM, Kodner CM, et al. Cloning and expression of a developmentally regulated protein that induces mitogenic and neurite outgrowth activity. Science 1990 12/21;250(4988):1690-1694.

(30) Kovesdi I, Fairhurst JL, Kretschmer PJ, Böhlen P. Heparin-binding neurotrophic factor (HBNF) and MK, members of a new family of homologous, developmentally regulated proteins. Biochem Biophys Res Commun 1990 10/30;172(2):850-854.

(31) Merenmies J, Rauvala H. Molecular cloning of the 18-kDa growth-associated protein of developing brain. J Biol Chem 1990 10/05;265(28):16721-16724.

(32) Zhu X, Bai Y, Yu W, Pan C, Jin E, Song D, et al. The Effects of Pleiotrophin in Proliferative Diabetic Retinopathy. PLoS ONE 2015 -;10(1):1.

(33) Bertram S, Roll L, Reinhard J, Groß K, Dazert S, Faissner A, et al. Pleiotrophin increases neurite length and number of spiral ganglion neurons in vitro. Exp Brain Res 2019 11;237(11):2983-2993.

(34) Wang X. Pleiotrophin: Activity and mechanism. Advances in Clinical Chemistry, Vol 98 2020 2020;98:51-89.

(35) Milner PG, Li YS, Hoffman RM, Kodner CM, Siegel NR, Deuel TF. A novel 17 kD heparin-binding growth factor (HBGF-8) in bovine uterus: purification and N-terminal amino acid sequence. Biochem Biophys Res Commun 1989 12/29;165(3):1096-1103.

(36) Rauvala H. An 18-kd heparin-binding protein of developing brain that is distinct from fibroblast growth factors. EMBO J 1989 10;8(10):2933-2941.

(37) Muramatsu T. Midkine (MK), the product of a retinoic acid responsive gene, and pleiotrophin constitute a new protein family regulating growth and differentiation. Int J Dev Biol 1993 03;37(1):183-188.

(38) Papadimitriou E, Pantazaka E, Castana P, Tsalios T, Polyzos A, Beis D. Pleiotrophin and its receptor protein tyrosine phosphatase beta/zeta as regulators of angiogenesis and cancer. Biochim Biophys Acta 2016 12;1866(2):252-265.

(39) Pantazaka E, Papadimitriou E. PTN (pleiotrophin). Atlas Genet Cytogenet Oncol Haematol 2012;16(11):821-837.

(40) Kilpelainen I, Kaksonen M, Avikainen H, Fath M, Linhardt RJ, Raulo E, et al. Heparin-binding growth-associated molecule contains two heparin-binding beta -sheet domains that are homologous to the thrombospondin type I repeat. J Biol Chem 2000 05/01;275(18):13564-70.

(41) Deuel TF, Zhang N, Yeh H, Silos-Santiago I, Wang Z. Pleiotrophin: a cytokine with diverse functions and a novel signaling pathway. Arch Biochem Biophys 2002 01/15;397(2):162-171.

(42) Xu C, Zhu S, Wu M, Han W, Yu Y. Functional receptors and intracellular signal pathways of midkine (MK) and pleiotrophin (PTN). Biol Pharm Bull 2014.

(43) Maeda N, Nishiwaki T, Shintani T, Hamanaka H, Noda M. 6B4 proteoglycan/phosphacan, an extracellular variant of receptor-like protein-tyrosine phosphatase zeta/RPTPbeta, binds pleiotrophin/heparin-binding growth-associated molecule (HB-GAM). J Biol Chem 1996 08/30;271(35):21446-21452.

(44) Muramatsu T. Midkine and pleiotrophin: two related proteins involved in development, survival, inflammation and tumorigenesis. J Biochem 2002 09;132(3):359-371.

(45) Multhaupt HAB, Yoneda A, Whiteford JR, Oh E, Lee W, Couchman JR. Syndecan signaling: when, where and why? J Physiol Pharmacol 2009 10;60 Suppl 4:31-38.

(46) Kuo AH, Stoica GE, Riegel AT, Wellstein A. Recruitment of insulin receptor substrate-1 and activation of NF-κB essential for midkine growth signaling through anaplastic lymphoma kinase. Oncogene 2007 02/08;26(6):859-869.

(47) Huang H. Anaplastic Lymphoma Kinase (ALK) Receptor Tyrosine Kinase: A Catalytic Receptor with Many Faces. International journal of molecular sciences 2018 -;19(11).

(48) Stoica GE, Kuo A, Aigner A, Sunitha I, Souttou B, Malerczyk C, et al. Identification of anaplastic lymphoma kinase as a receptor for the growth factor pleiotrophin. J Biol Chem 2001 05/18;276(20):16772-16779.

(49) Moog-Lutz C, Degoutin J, Gouzi JY, Frobert Y, Brunet-de Carvalho N, Bureau J, et al. Activation and inhibition of anaplastic lymphoma kinase receptor tyrosine kinase by monoclonal antibodies and absence of agonist activity of pleiotrophin. J Biol Chem 2005 07/15;280(28):26039-26048.

(50) Mourali J, Bénard A, Lourenço FC, Monnet C, Greenland C, Moog-Lutz C, et al. Anaplastic lymphoma kinase is a dependence receptor whose proapoptotic functions are activated by caspase cleavage. Mol Cell Biol 2006 08;26(16):6209-6222.

(51) Mathivet T, Mazot P, Vigny M. In contrast to agonist monoclonal antibodies, both C-terminal truncated form and full length form of Pleiotrophin failed to activate vertebrate ALK (anaplastic lymphoma kinase)? Cell Signal 2007 12;19(12):2434-2443.

(52) Perez-Pinera P, Zhang W, Chang Y, Vega JA, Deuel TF. Anaplastic Lymphoma Kinase Is Activated Through the Pleiotrophin/Receptor Protein-tyrosine Phosphatase β/ζ Signaling Pathway. J Biol Chem 2007 09/28;282(39):28683-28690.

(53) Stoica GE, Kuo A, Powers C, Bowden ET, Sale EB, Riegel AT, et al. Midkine binds to anaplastic lymphoma kinase (ALK) and acts as a growth factor for different cell types. J Biol Chem 2002 09/27;277(39):35990-35998.

(54) Premont R, Michelotti GA, Tucker A, Swiderska-Syn M, Machado MV, Choi SS, et al. Pleiotrophin regulates the ductular reaction by controlling the migration of cells in liver progenitor niches. Gut 2016 -;65(4):683.

(55) Polykratis A, Katsoris P, Courty J, Papadimitriou E. Characterization of heparin affin regulatory peptide signaling in human endothelial cells. J Biol Chem 2005 06/10;280(23):22454-22461.

(56) Herradón G, Pérez-García C. Targeting midkine and pleiotrophin signalling pathways in addiction and neurodegenerative disorders: recent progress and perspectives. Br J Pharmacol 2014 02;171(4):837-848.

(57) Perez-Pinera P, Chang Y, Deuel TF. Pleiotrophin, a multifunctional tumor promoter through induction of tumor angiogenesis, remodeling of the tumor microenvironment, and activation of stromal fibroblasts. Cell Cycle 2007 12/01;6(23):2877-2883.

(58) Kinnunen T, Kaksonen M, Saarinen J, Kalkkinen N, Peng HB, Rauvala H. Cortactin-Src kinase signaling pathway is involved in N-syndecan-dependent neurite outgrowth. J Biol Chem 1998 04/24;273(17):10702-10708.

(59) Bjorge JD, Jakymiw A, Fujita DJ. Selected glimpses into the activation and function of Src kinase. Oncogene 2000 11/20;19(49):5620-5635.

(60) Herradon G. Midkine regulates pleiotrophin organ-specific gene expression: Evidence for transcriptional regulation and functional redundancy within the pleiotrophin/midkine developmental gene family. Biochemical & Biophysical Research Communications 2005;333(3):714-722.

(61) Neumann JR, Dash-Wagh S, Jack A, Räk A, Jüngling K, Hamad MIK, et al. The primate-specific peptide Y-P30 regulates morphological maturation of neocortical dendritic spines. PLoS One 2019 02/13;14(2):e0211151.

(62) Neumann JR, Dash-Wagh S, Jüngling K, Tsai T, Meschkat M, Räk A, et al. Y-P30 promotes axonal growth by stabilizing growth cones. Brain Struct Funct 2015 07;220(4):1935-1950.

(63) Tang C, Wang M, Wang P, Wang L, Wu Q, Guo W. Neural Stem Cells Behave as a Functional Niche for the Maturation of Newborn Neurons through the Secretion of PTN. Neuron 2019 01/02;101(1):32.

(64) Cui R, Lwigale P. Expression of the heparin-binding growth factors Midkine and pleiotrophin during ocular development. Gene Expr Patterns 2019 06;32:28-37.

(65) Mitsiadis TA, Salmivirta M, Muramatsu T, Muramatsu H, Rauvala H, Lehtonen E, et al. Expression of the heparin-binding cytokines, midkine (MK) and HB-GAM (pleiotrophin) is associated with epithelial-mesenchymal interactions during fetal development and organogenesis. Development 1995 01/01;121(1):37-51.

(66) Kadomatsu K, Muramatsu T. Midkine and pleiotrophin in neural development and cancer. Cancer Lett 2004 02/20;204(2):127-143.

(67) Tanga N, Kuboyama K, Kishimoto A, Kiyonari H, Shiraishi A, Suzuki R, et al. The PTN-PTPRZ signal activates the AFAP1L2-dependent PI3K-AKT pathway for oligodendrocyte differentiation: Targeted inactivation of PTPRZ activity in mice. Glia 2019 05;67(5):967-984.

(68) Kuboyama K, Fujikawa A, Suzuki R, Tanga N, Noda M. Role of Chondroitin Sulfate (CS) Modification in the Regulation of Protein-tyrosine Phosphatase Receptor Type Z (PTPRZ) Activity: PLEIOTROPHIN-PTPRZ-A SIGNALING IS INVOLVED IN OLIGODENDROCYTE DIFFERENTIATION. J Biol Chem 2016 08/26;291(35):18117-18128.

(69) Yang S, Xue D, Wu B, Sun H, Li X, Dong F, et al. Pleiotrophin is involved in the amniotic epithelial cell-induced differentiation of human umbilical cord blood-derived mesenchymal stem cells into dopaminergic neuron-like cells. Neurosci Lett 2013 02/28;539:86-91.

(70) Gu D, Yu B, Zhao C, Ye W, Lv Q, Hua Z, et al. The effect of pleiotrophin signaling on adipogenesis. FEBS Lett 2007 -;581(3):382.

(71) Sevillano J, Sánchez-Alonso MG, Zapatería B, Calderón M, Alcalá M, Limones M, et al. Pleiotrophin deletion alters glucose homeostasis, energy metabolism and brown fat thermogenic function in mice. Diabetologia 2019 -;62(1):123.

(72) Zuccaro A, Zapatería B, Sánchez-Alonso MG, Haro M, Limones M, Terrados G, et al. Pleiotrophin Deficiency Induces Browning of Periovarian Adipose Tissue and Protects against High-Fat Diet-Induced Hepatic Steatosis. International journal of molecular sciences 2021 -;22(17).

(73) Ledoux D, Caruelle D, Sabourin JC, Liu J, Crepin M, Barritault D, et al. Cellular distribution of the angiogenic factor heparin affin regulatory peptide (HARP) mRNA and protein in the human mammary gland. J Histochem Cytochem 1997 09;45(9):1239-1245.

(74) Rosenfield SM, Bowden ET, Cohen-Missner S, Gibby KA, Ory V, Henke RT, et al. Pleiotrophin (PTN) expression and function and in the mouse mammary gland and mammary epithelial cells. PLoS One 2012;7(10):e47876.

(75) Hatziapostolou M, Polytarchou C, Katsoris P, Courty J, Papadimitriou E. Heparin affin regulatory peptide/pleiotrophin mediates fibroblast growth factor 2 stimulatory effects on human prostate cancer cells. J Biol Chem 2006 10/27;281(43):32217-32226.

(76) Chen H, Campbell RA, Chang Y, Li M, Wang CS, Li J, et al. Pleiotrophin produced by multiple myeloma induces transdifferentiation of monocytes into vascular endothelial cells: a novel mechanism of tumor-induced vasculogenesis. Blood 2009 02/26;113(9):1992-2002.

(77) Choudhuri R, Zhang HT, Donnini S, Ziche M, Bicknell R. An angiogenic role for the neurokines midkine and pleiotrophin in tumorigenesis. Cancer Res 1997 05/01;57(9):1814-1819.

(78) Yao J, Zhang L, Huang X, Li W, Gao S. Pleiotrophin and N-syndecan promote perineural invasion and tumor progression in an orthotopic mouse model of pancreatic cancer. World J Gastroenterol 2017 06/07;23(21):3907-3914.

(79) Diamantopoulou Z, Kitsou P, Menashi S, Courty J, Katsoris P. Loss of receptor protein tyrosine phosphatase β/ζ (RPTPβ/ζ) promotes prostate cancer metastasis. J Biol Chem 2012 11/23;287(48):40339-40349.

(80) Lu KV, Jong KA, Kim GY, Singh J, Dia EQ, Yoshimoto K, et al. Differential Induction of Glioblastoma Migration and Growth by Two Forms of Pleiotrophin. J Biol Chem 2005 07/22;280(29):26953-26964.

(81) Himburg HA, Muramoto GG, Daher P, Meadows SK, Russell JL, Doan P, et al. Pleiotrophin regulates the expansion and regeneration of hematopoietic stem cells. Nat Med 2010 04;16(4):475-482.

(82) Himburg HA, Harris JR, Ito T, Daher P, Russell JL, Quarmyne M, et al. Pleiotrophin regulates the retention and self-renewal of hematopoietic stem cells in the bone marrow vascular niche. Cell Rep 2012 10/25;2(4):964-975.

(83) Himburg HA, Yan X, Doan PL, Quarmyne M, Micewicz E, McBride W, et al. Pleiotrophin mediates hematopoietic regeneration via activation of RAS. J Clin Invest 2014 11;124(11):4753-4758.

(84) Yeh H, He YY, Xu J, Hsu CY, Deuel TF. Upregulation of pleiotrophin gene expression in developing microvasculature, macrophages, and astrocytes after acute ischemic brain injury. J Neurosci 1998 05;18(10):3699-3707.

(85) Blondet B, Carpentier G, Lafdil F, Courty J. Pleiotrophin cellular localization in nerve regeneration after peripheral nerve injury. J Histochem Cytochem 2005 08;53(8):971-977.

(86) Lamprou M, Kaspiris A, Panagiotopoulos E, Giannoudis PV, Papadimitriou E. The role of pleiotrophin in bone repair. Injury 2014 12;45(12):1816-1823.

(87) Ochiai K, Muramatsu H, Yamamoto S, Ando H, Muramatsu T. The role of midkine and pleiotrophin in liver regeneration. Liver Int 2004 10;24(5):484-491.

(88) Pufe T, Bartscher M, Petersen W, Tillmann B, Mentlein R. Expression of pleiotrophin, an embryonic growth and differentiation factor, in rheumatoid arthritis. Arthritis Rheum 2003 03;48(3):660-667.

(89) Shen D, Podolnikova NP, Yakubenko VP, Ardell CL, Balabiyev A, Ugarova TP, et al. Pleiotrophin, a multifunctional cytokine and growth factor, induces leukocyte responses through the integrin Mac-1. J Biol Chem 2017 11/17;292(46):18848-18861.

(90) Yokoi H, Kasahara M, Mori K, Ogawa Y, Kuwabara T, Imamaki H, et al. Pleiotrophin triggers inflammation and increased peritoneal permeability leading to peritoneal fibrosis. Kidney Int 2012 01/15;81(2):160-169.

(91) Fernández-Calle R, Vicente-Rodríguez M, Gramage E, Pita J, Pérez-García C, Ferrer-Alcón M, et al. Pleiotrophin regulates microglia-mediated neuroinflammation. J NEUROINFLAMMATION 2017 03/04;14:1-10.

(92) Fernández-Calle R, Vicente-Rodríguez M, Gramage E, de la Torre-Ortiz C, Pérez-García C, Ramos MP, et al. Endogenous pleiotrophin and midkine regulate LPS-induced glial responses. Neurosci Lett 2018 01/01;662:213-218.

(93) Asahina K, Sato H, Yamasaki C, Kataoka M, Shiokawa M, Katayama S, et al. Pleiotrophin/heparin-binding growth-associated molecule as a mitogen of rat hepatocytes and its role in regeneration and development of liver. Am J Pathol.2002 Jun;160(6):2191-205.doi: 10.1016/S0002-9440(10)61167-4. 2002.

(94) Antoine M, Tag CG, Wirz W, Borkham-Kamphorst E, Sawitza I, Gressner AM, et al. Upregulation of pleiotrophin expression in rat hepatic stellate cells by PDGF and hypoxia: implications for its role in experimental biliary liver fibrogenesis. Biochem Biophys Res Commun 2005 12/02;337(4):1153-1164.

(95) Laaroubi K, Vacherot F, Delbé J, Caruelle D, Barritault D, Courty J. Biochemical and mitogenic properties of the heparin-binding growth factor HARP. Prog Growth Factor Res 1995;6(1):25-34.

(96) Milhiet PE, Vacherot F, Caruelle JP, Barritault D, Caruelle D, Courty J. Upregulation of the angiogenic factor heparin affin regulatory peptide by progesterone in rat uterus. J Endocrinol 1998 09;158(3):389-399.

(97) Orr B, Vanpoucke G, Grace OC, Smith L, Anderson RA, Riddick ACP, et al. Expression of pleiotrophin in the prostate is androgen regulated and it functions as an autocrine regulator of mesenchyme and cancer associated fibroblasts and as a paracrine regulator of epithelia. Prostate 2011 02/15;71(3):305-317.

(98) Vacherot F, Laaroubi K, Caruelle D, Delbe J, Barritault D, Caruelle JP, et al. Upregulation of heparin-affin regulatory peptide by androgen. In Vitro Cell Dev Biol Anim 1995 10;31(9):647-648.

(99) Zhang Q, Guo B, Hui Q, Chang P, Tao K. miR-137 Inhibits Proliferation and Metastasis of Hypertrophic Scar Fibroblasts via Targeting Pleiotrophin. Cell Physiol Biochem 2018;49(3):985-995.

(100) Yi C, Xie W, Li F, Lv Q, He J, Wu J, et al. MiR-143 enhances adipogenic differentiation of 3T3-L1 cells through targeting the coding region of mouse pleiotrophin. FEBS Lett 2011 10/20;585(20):3303-3309.

(101) Zhang L, Liu X, Liu J, Zhou Z, Song Y, Cao B, et al. miR-182 aids in receptive endometrium development in dairy goats by down-regulating PTN expression. PLoS One 2017 07/05;12(7):e0179783.

(102) Bai P, Xia N, Sun H, Kong Y. Pleiotrophin, a target of miR-384, promotes proliferation, metastasis and lipogenesis in HBV-related hepatocellular carcinoma. J Cell Mol Med 2017 11;21(11):3023-3043.

(103) Amet LEA, Lauri SE, Hienola A, Croll SD, Lu Y, Levorse JM, et al. Enhanced Hippocampal Long-Term Potentiation in Mice Lacking Heparin-Binding Growth-Associated Molecule. Molecular and Cellular Neuroscience 2001 June 2001;17(6):1014-1024.

(104) Ruiz J, Antequera T, Andres AI, Petron MJ, Muriel E. Improvement of a solid phase extraction method for analysis of lipid fractions in muscle foods. Anal Chim Acta 2004 23 August 2004;520(1):201-205.

(105) United Nations, Department of Economic and Social Affairs, Population Division (2020). World Population Ageing 2019 (ST/ESA/SER.A/444). 2020.

(106) Houtkooper RH, Argmann C, Houten SM, Cantó C, Jeninga EH, Andreux PA, et al. The metabolic footprint of aging in mice. Scientific reports 2011 -;1:134.

(107) Carrascosa JM, Andrés A, Ros M, Bogónez E, Arribas C, Fernández-Agulló T, et al. Development of insulin resistance during aging: involvement of central processes and role of adipokines. Curr Protein Peptide Sci 2011 -;12(4):305.

(108) López-Otín C, Blasco MA, Partridge L, Serrano M, Kroemer G. The hallmarks of aging. Cell 2013 06/06;153(6):1194-1217.

(109) Aunan JR, Watson MM, Hagland HR, Søreide K. Molecular and biological hallmarks of ageing. Br J Surg 2016 -;103(2):e29.

(110) Hunt NJ, Kang SWS, Lockwood GP, Le Couteur DG, Cogger VC. Hallmarks of Aging in the Liver. Computational and structural biotechnology journal 2019 -;17:1151.

(111) Kuk JL, Saunders TJ, Davidson LE, Ross R. Age-related changes in total and regional fat distribution. Ageing research reviews 2009 -;8(4):339.

(112) Gan L, Chitturi S, Farrell GC. Mechanisms and implications of age-related changes in the liver: nonalcoholic fatty liver disease in the elderly. Curr Gerontol Geriatr Res 2011;2011:831536.

(113) Cree MG, Newcomer BR, Katsanos CS, Sheffield-Moore M, Chinkes D, Aarsland A, et al. Intramuscular and liver triglycerides are increased in the elderly. J Clin Endocrinol Metab 2004 -;89(8):3864.

(114) Stanforth PR, Jackson AS, Green JS, Gagnon J, Rankinen T, Després JP, et al. Generalized abdominal visceral fat prediction models for black and white adults aged 17-65 y: the HERITAGE Family Study. International journal of obesity and related metabolic disorders : journal of the International Association for the Study of Obesity 2004 -;28(7):925.

(115) Scarpace PJ, Tümer N. Peripheral and hypothalamic leptin resistance with age-related obesity. Physiol Behav 2001 -;74(4-5):721.

(116) Fernández-Galaz C, Fernández-Agulló T, Pérez C, Peralta S, Arribas C, Andrés A, et al. Long-term food restriction prevents ageing-associated central leptin resistance in wistar rats. Diabetologia 2002 -;45(7):997.

(117) Arai Y, Kamide K, Hirose N. Adipokines and Aging: Findings From Centenarians and the Very Old. Frontiers in Endocrinology 2019 03/01;10.

(118) Bik W, Baranowska-Bik A, Wolinska-Witort E, Martynska L, Chmielowska M, Szybinska A, et al. The relationship between adiponectin levels and metabolic status in centenarian, early elderly, young and obese women. Neuro endocrinology letters 2006 -;27(4):493.

(119) Gulcelik NE, Halil M, Ariogul S, Usman A. Adipocytokines and aging: adiponectin and leptin. Minerva Endocrinol 2013 -;38(2):203.

(120) Brook MS, Wilkinson DJ, Phillips BE, Perez-Schindler J, Philp A, Smith K, et al. Skeletal muscle homeostasis and plasticity in youth and ageing: impact of nutrition and exercise. Acta Physiologica 2016 -;216(1):15.

(121) Boengler K, Kosiol M, Mayr M, Schulz R, Rohrbach S. Mitochondria and ageing: role in heart, skeletal muscle and adipose tissue. Journal of Cachexia, Sarcopenia and Muscle 2017 -;8(3):349.

(122) Feldman HA, Longcope C, Derby CA, Johannes CB, Araujo AB, Coviello AD, et al. Age trends in the level of serum testosterone and other hormones in middle-aged men: longitudinal results from the Massachusetts male aging study. J Clin Endocrinol Metab 2002 -;87(2):589.

(123) Visser M, Pahor M, Taaffe DR, Goodpaster BH, Simonsick EM, Newman AB, et al. Relationship of Interleukin-6 and Tumor Necrosis Factor-{alpha} With Muscle Mass and Muscle Strength in Elderly Men and Women: The Health ABC Study. Journals of Gerontology Series A: Biological Sciences and Medical Sciences 2002 -;57(5):M326.

(124) Schaap LA, Pluijm SMF, Deeg DJH, Harris TB, Kritchevsky SB, Newman AB, et al. Higher Inflammatory Marker Levels in Older Persons: Associations With 5-Year Change in Muscle Mass and Muscle Strength. Journals of Gerontology Series A: Biological Sciences and Medical Sciences 2009 -;64(11):1183.

(125) McNeil CJ, Doherty TJ, Stashuk DW, Rice CL. Motor unit number estimates in the tibialis anterior muscle of young, old, and very old men. Muscle Nerve 2005 -;31(4):461.

(126) Goodpaster BH, Carlson CL, Visser M, Kelley DE, Scherzinger A, Harris TB, et al. Attenuation of skeletal muscle and strength in the elderly: The Health ABC Study. J Appl Physiol 2001 -;90(6):2157.

(127) Alway SE, Myers MJ, Mohamed JS. Regulation of satellite cell function in sarcopenia. Frontiers in Aging Neuroscience 2014 -;6.

(128) Fulle S, Protasi F, Di Tano G, Pietrangelo T, Beltramin A, Boncompagni S, et al. The contribution of reactive oxygen species to sarcopenia and muscle ageing. Exp Gerontol 2004 -;39(1):17.

(129) Marzetti E, Calvani R, Cesari M, Buford TW, Lorenzi M, Behnke BJ, et al. Mitochondrial dysfunction and sarcopenia of aging: From signaling pathways to clinical trials. Int J Biochem Cell Biol 2013 -;45(10):2288.

(130) Distefano G, Goodpaster BH. Effects of Exercise and Aging on Skeletal Muscle. Cold Spring Harbor perspectives in medicine 2018 -;8(3).

(131) Joanisse S, Nederveen JP, Baker JM, Snijders T, Iacono C, Parise G. Exercise conditioning in old mice improves skeletal muscle regeneration. FASEB journal : official publication of the Federation of American Societies for Experimental Biology 2016 -;30(9):3256.

(132) Shavlakadze T, McGeachie J, Grounds MD. Delayed but excellent myogenic stem cell response of regenerating geriatric skeletal muscles in mice. Biogerontology 2010 -;11(3):363.

(133) Brack AS, Conboy MJ, Roy S, Lee M, Kuo CJ, Keller C, et al. Increased Wnt Signaling During Aging Alters Muscle Stem Cell Fate and Increases Fibrosis. Science 2007 -;317(5839):807.

(134) Elobeid A, Libard S, Leino M, Popova SN, Alafuzoff I. Altered Proteins in the Aging Brain. J Neuropathol Exp Neurol 2016 -;75(4):316.

(135) Wyss-Coray T. Ageing, neurodegeneration and brain rejuvenation. Nature 2016 -;539(7628):180.

(136) Mrak RE, Griffin ST, Graham DI. Aging-associated changes in human brain. J Neuropathol Exp Neurol 1997 -;56(12):1269.

(137) Ure JA. TDP-43 y su incidencia en demencias degenerativas. Neurología Argentina 2021 -;13(1):37.

(138) van den Beld, Annewieke W, Kaufman J, Zillikens MC, Lamberts SWJ, Egan JM, van der Lely, Aart J. The physiology of endocrine systems with ageing. The Lancet Diabetes & Endocrinology 2018 -;6(8):647.

(139) Chahal H, Drake W. The endocrine system and ageing. J Pathol 2007 -;211(2):173.

(140) Vitale G, Pellegrino G, Vollery M, Hofland LJ. ROLE of IGF-1 System in the Modulation of Longevity: Controversies and New Insights From a Centenarians' Perspective. Frontiers in endocrinology 2019 -;10:27.

(141) Chapman IM. Endocrinology of anorexia of ageing. Best practice & research.Clinical endocrinology & metabolism 2004 -;18(3):437.

(142) Janssens JP, Pache JC, Nicod LP. Physiological changes in respiratory function associated with ageing. The European respiratory journal 1999 -;13(1):197.

(143) Curtis E, Litwic A, Cooper C, Dennison E. Determinants of Muscle and Bone Aging. J Cell Physiol 2015 -;230(11):2618.

(144) Goltzman D. The Aging Skeleton. Adv Exp Med Biol 2019 -;1164:153.

(145) Rahmati M, Nalesso G, Mobasheri A, Mozafari M. Aging and osteoarthritis: Central role of the extracellular matrix. Ageing research reviews 2017 -;40:20.

(146) Sheedfar F, Di Biase S, Koonen D, Vinciguerra M. Liver diseases and aging: friends or foes? Aging Cell 2013 12;12(6):950-954.

(147) Wynne HA, Cope LH, Mutch E, Rawlins MD, Woodhouse KW, James OF. The effect of age upon liver volume and apparent liver blood flow in healthy man. Hepatology 1989 -;9(2):297.

(148) Kim IH, Kisseleva T, Brenner DA. Aging and liver disease. Curr Opin Gastroenterol 2015 -;31(3):184.

(149) Schmucker DL. Aging and the liver: an update. The journals of gerontology.Series A, Biological sciences and medical sciences 1998 -;53(5):B315.

(150) Duncan AW. Aneuploidy, polyploidy and ploidy reversal in the liver. Semin Cell Dev Biol 2013 -;24(4):347.

(151) Lebel M, C. de Souza-Pinto N, A. Bohr V. Metabolism, Genomics, and DNA Repair in the Mouse Aging Liver. Current Gerontology and Geriatrics Research 2011 -;2011(1).

(152) Bacalini MG, Franceschi C, Gentilini D, Ravaioli F, Zhou X, Remondini D, et al. Molecular Aging of Human Liver: An Epigenetic/Transcriptomic Signature. The journals of gerontology.Series A, Biological sciences and medical sciences 2019 -;74(1):1.

(153) Irvine KM, Skoien R, Bokil NJ, Melino M, Thomas GP, Loo D, et al. Senescent human hepatocytes express a unique secretory phenotype and promote macrophage migration. World journal of gastroenterology 2014 -;20(47):17851.

(154) Campisi J. Aging, Cellular Senescence, and Cancer. Annu Rev Physiol 2013 -;75(1):685.

(155) Ogrodnik M, Miwa S, Tchkonia T, Tiniakos D, Wilson CL, Lahat A, et al. Cellular senescence drives age-dependent hepatic steatosis. Nature communications 2017 -;8:15691.

(156) Navarro A, Boveris A. Rat brain and liver mitochondria develop oxidative stress and lose enzymatic activities on aging. American Journal of Physiology - Regulatory, Integrative and Comparative Physiology 2004 -;287(5):R1244.

(157) Cellerino A, Ori A. What have we learned on aging from omics studies? Semin Cell Dev Biol 2017 -;70:177.

(158) Schneider JL, Cuervo AM. Liver autophagy: much more than just taking out the trash. Nature Reviews Gastroenterology & Hepatology 2014;11(3):187.

(159) Takamura A, Komatsu M, Hara T, Sakamoto A, Kishi C, Waguri S, et al. Autophagy-deficient mice develop multiple liver tumors. Genes Dev 2011 -;25(8):795.

(160) Yin XM, Ding WX, Gao W. Autophagy in the liver. Hepatology 2008 -;47(5):1773.

(161) Madrigal-Matute J, Cuervo AM. Regulation of Liver Metabolism by Autophagy. Gastroenterology 2016 -;150(2):328.

(162) Allaire M, Gilgenkrantz H. The aged liver: Beyond cellular senescence. Clinics and research in hepatology and gastroenterology 2020 -;44(1):6.

(163) Schneider JL, Villarroya J, Diaz-Carretero A, Patel B, Urbanska AM, Thi MM, et al. Loss of hepatic chaperone-mediated autophagy accelerates proteostasis failure in aging. Aging cell 2015 -;14(2):249.

(164) Sawada N, Ishikawa T. Reduction of Potential for Replicative but not Unscheduled DNA Synthesis in Hepatocytes Isolated from Aged as Compared to Young Rats. Cancer Res 1988 American Association for Cancer Research;48(6):1618-1622.

(165) Sawada N. Hepatocytes from old rats retain responsiveness of c-myc expression to EGF in primary culture but do not enter S phase. Exp Cell Res 1989 -;181(2):584.

(166) Timchenko NA. Aging and liver regeneration. Trends in endocrinology and metabolism: TEM 2009 -;20(4):171.

(167) Cheng Y, Wang X, Wang B, Zhou H, Dang S, Shi Y, et al. Aging-associated oxidative stress inhibits liver progenitor cell activation in mice. Aging 2017 -;9(5):1359.

(168) Ikeyama S, Wang X, Li J, Podlutsky A, Martindale JL, Kokkonen G, et al. Expression of the Pro-apoptotic Genegadd153/chopIs Elevated in Liver with Aging and Sensitizes Cells to Oxidant Injury*. J Biol Chem 2003 -;278(19):16726.

(169) McLean AJ, Cogger VC, Chong GC, Warren A, Markus AM, Dahlstrom JE, et al. Age-related pseudocapillarization of the human liver. J Pathol 2003 -;200(1):112.

(170) Cogger VC, Warren A, Fraser R, Ngu M, McLean AJ, Le Couteur DG. Hepatic sinusoidal pseudocapillarization with aging in the non-human primate. Exp Gerontol 2003 -;38(10):1101.

(171) Simon-Santamaria J, Malovic I, Warren A, Oteiza A, Le Couteur D, Smedsrød B, et al. Age-related changes in scavenger receptor-mediated endocytosis in rat liver sinusoidal endothelial cells. Journals of Gerontology Series A: Biological Sciences & Medical Sciences 2010 -;65A(9):951.

(172) Maeso-Díaz R, Ortega-Ribera M, Fernández-Iglesias A, Hide D, Muñoz L, Hessheimer AJ, et al. Effects of aging on liver microcirculatory function and sinusoidal phenotype. Aging cell 2018 -;17(6):e12829.

(173) Fontana L, Zhao E, Amir M, Dong H, Czaja MJ, Tanaka K. Aging promotes the development of diet-induced murine steatohepatitis but not steatosis. Hepatology 2013 -;57(3):995.

(174) Franceschi C, Bonafé M, Valensin S, Olivieri F, De Luca M, Ottaviani E, et al. Inflamm-aging: An Evolutionary Perspective on Immunosenescence. Ann N Y Acad Sci 2000 -;908(1):244.

(175) Ju C, Reilly TP, Bourdi M, Radonovich MF, Brady JN, George JW, et al. Protective role of Kupffer cells in acetaminophen-induced hepatic injury in mice. Chem Res Toxicol 2002 -;15(12):1504.

(176) Nagy LE. Recent Insights into the Role of the Innate Immune System in the Development of Alcoholic Liver Disease. Exp Biol Med 2003 -;228(8):882.

(177) Chiang DJ, Pritchard MT, Nagy LE. Obesity, diabetes mellitus, and liver fibrosis. American journal of physiology.Gastrointestinal and liver physiology 2011 -;300(5):G697.

(178) Ramachandran P, Iredale JP. Macrophages: central regulators of hepatic fibrogenesis and fibrosis resolution. J Hepatol 2012 -;56(6):1417.

(179) Stahl EC, Haschak MJ, Popovic B, Brown BN. Macrophages in the Aging Liver and Age-Related Liver Disease. Frontiers in immunology 2018 -;9:2795.

(180) Hilmer SN, Cogger VC, Le Couteur DG. Basal Activity of Kupffer Cells Increases With Old Age. Journals of Gerontology Series A: Biological Sciences & Medical Sciences 2007 -;62(9):973.

(181) Marcos R, Lopes C, Malhão F, Correia-Gomes C, Fonseca S, Lima M, et al. Stereological assessment of sexual dimorphism in the rat liver reveals differences in hepatocytes and Kupffer cells but not hepatic stellate cells. J Anat 2016 -;228(6):996.

(182) Frith J, Day CP, Henderson E, Burt AD, Newton JL. Non-alcoholic fatty liver disease in older people. Gerontology 2009 -;55(6):607.

(183) Lalia AZ, Dasari S, Johnson ML, Robinson MM, Konopka AR, Distelmaier K, et al. Predictors of Whole-Body Insulin Sensitivity Across Ages and Adiposity in Adult Humans. Journal of Clinical Endocrinology & Metabolism 2016 -;101(2):626.

(184) Chia CW, Egan JM, Ferrucci L. Age-Related Changes in Glucose Metabolism, Hyperglycemia, and Cardiovascular Risk. Circ Res 2018 -;123(7):886.

(185) Gaspar RC, Muñoz VR, Nakandakari SCBR, Vieira RFL, da Conceição LR, de Oliveira F, et al. Aging is associated with increased TRB3, ER stress, and hepatic glucose production in the liver of rats. Exp Gerontol 2020 -;139:111021.

(186) de Moura LP, Souza Pauli LS, Cintra DE, de Souza CT, da Silva ASR, Marinho R, et al. Acute exercise decreases PTP-1B protein level and improves insulin signaling in the liver of old rats. Immunity & ageing : I & A 2013 -;10(1):8.

(187) Kumashiro N, Beddow SA, Vatner DF, Majumdar SK, Cantley JL, Guebre-Egziabher F, et al. Targeting pyruvate carboxylase reduces gluconeogenesis and adiposity and improves insulin resistance. Diabetes 2013 -;62(7):2183.

(188) Marinho R, Mekary RA, Muñoz VR, Gomes RJ, Pauli JR, de Moura LP. Regulation of hepatic TRB3/Akt interaction induced by physical exercise and its effect on the hepatic glucose production in an insulin resistance state. Diabetology & metabolic syndrome 2015 -;7:67.

(189) Muñoz VR, Gaspar RC, Crisol BM, Formigari GP, Sant'Ana MR, Botezelli JD, et al. Physical exercise reduces pyruvate carboxylase (PCB) and contributes to hyperglycemia reduction in obese mice. The journal of physiological sciences : JPS 2018 -;68(4):493.

(190) Pereira RM, Rodrigues KCDC, Anaruma CP, Sant'Ana MR, de Campos TDP, Gaspar RS, et al. Short-term strength training reduces gluconeogenesis and NAFLD in obese mice. J Endocrinol 2019 -;241(1):59.

(191) Jackson RA, Hawa MI, Roshania RD, Sim BM, DiSilvio L, Jaspan JB. Influence of aging on hepatic and peripheral glucose metabolism in humans. Diabetes 1988 -;37(1):119.

(192) Chen M, Bergman RN, Pacini G, Porte D Jr. Pathogenesis of age-related glucose intolerance in man: insulin resistance and decreased beta-cell function. J Clin Endocrinol Metab 1985 -;60(1):13.

(193) Fink RI, Wallace P, Olefsky JM. Effects of aging on glucose-mediated glucose disposal and glucose transport. J Clin Invest 1986 -;77(6):2034.

(194) Russell SJ, Kahn CR. Endocrine regulation of ageing. Nature reviews.Molecular cell biology 2007 -;8(9):681.

(195) Harrison DE, Strong R, Sharp ZD, Nelson JF, Astle CM, Flurkey K, et al. Rapamycin fed late in life extends lifespan in genetically heterogeneous mice. Nature 2009 -;460(7253):392.

(196) Johnson AA, Stolzing A. The role of lipid metabolism in aging, lifespan regulation, and age-related disease. Aging cell 2019 -;18(6):e13048.

(197) Bertolotti M, Lonardo A, Mussi C, Baldelli E, Pellegrini E, Ballestri S, et al. Nonalcoholic fatty liver disease and aging: epidemiology to management. World journal of gastroenterology 2014 -;20(39):14185.

(198) Woudstra TD, Drozdowski LA, Wild GE, Clandinin MT, Agellon LB, Thomson ABR. The age-related decline in intestinal lipid uptake is associated with a reduced abundance of fatty acid-binding protein. Lipids 2004 -;39(7):603.

(199) Wang G, Bonkovsky HL, de Lemos A, Burczynski FJ. Recent insights into the biological functions of liver fatty acid binding protein 1. J Lipid Res 2015 -;56(12):2238.

(200) Shi J, Zhang Y, Gu W, Cui B, Xu M, Yan Q, et al. Serum liver fatty acid binding protein levels correlate positively with obesity and insulin resistance in Chinese young adults. PloS one 2012 -;7(11):e48777.

(201) Kawano Y, Cohen DE. Mechanisms of hepatic triglyceride accumulation in non-alcoholic fatty liver disease. J Gastroenterol 2013 -;48(4):434.

(202) Yellaturu CR, Deng X, Cagen LM, Wilcox HG, Mansbach CM 2nd, Siddiqi SA, et al. Insulin enhances post-translational processing of nascent SREBP-1c by promoting its phosphorylation and association with COPII vesicles. The Journal of biological chemistry 2009 -;284(12):7518.

(203) Savage DB, Choi CS, Samuel VT, Liu ZX, Zhang D, Wang A, et al. Reversal of diet-induced hepatic steatosis and hepatic insulin resistance by antisense oligonucleotide inhibitors of acetyl-CoA carboxylases 1 and 2. J Clin Invest 2006 -;116(3):817.

(204) Kineman RD, Majumdar N, Subbaiah PV, Cordoba-Chacon J. Hepatic PPARγ Is Not Essential for the Rapid Development of Steatosis After Loss of Hepatic GH Signaling, in Adult Male Mice. Endocrinology 2016 -;157(5):1728.

(205) Gong Z, Tas E, Yakar S, Muzumdar R. Hepatic lipid metabolism and non-alcoholic fatty liver disease in aging. Mol Cell Endocrinol 2017 -;455(1):115.

(206) Levadoux E, Morio B, Montaurier C, Puissant V, Boirie Y, Fellmann N, et al. Reduced whole-body fat oxidation in women and in the elderly. Int J Obes Relat Metab Disord 2001 01;25(1):39-44.

(207) Shimada M, Cheng J, Sanyal A. Fatty Liver, NASH, and Alcoholic Liver Disease. In: McManus LM, Mitchell RN, editors. Pathobiology of Human Disease San Diego: Academic Press; 2014. p. 1817-1824.

(208) Brenachot X, Ramadori G, Ioris R, Veyrat-Durebex C, Altirriba J, Aras E, et al. Hepatic protein tyrosine phosphatase receptor gamma links obesity-induced inflammation to insulin resistance. Nature Communications 2017 -;8(1):1.

(209) Weng T, Gao L, Bhaskaran M, Guo Y, Gou D, Narayanaperumal J, et al. Pleiotrophin regulates lung epithelial cell proliferation and differentiation during fetal lung development via beta-catenin and Dlk1. The Journal of biological chemistry 2009 -;284(41):28021.

(210) Wang Y, Viscarra J, Kim SJ, Sul HS. Transcriptional regulation of hepatic lipogenesis. Nature reviews.Molecular cell biology 2015;16(11):678.

(211) Canbay A, Bechmann L, Gerken G. Lipid metabolism in the liver. Z Gastroenterol 2007 -;45(1):35.

(212) Nguyen P, Leray V, Serisier S, Le Bloc'H J, Siliart B, Dumon H, et al. Liver lipid metabolism. J Anim Physiol Anim Nutr 2008 -;92(3):272.

(213) Mashek DG. Hepatic fatty acid trafficking: multiple forks in the road. Advances in nutrition (Bethesda, Md.) 2013;4(6):697.

(214) Kuhla A, Blei T, Jaster R, Vollmar B. Aging is associated with a shift of Fatty metabolism toward lipogenesis. J Gerontol A Biol Sci Med Sci 2011 11;66A(11):1192-1200.

(215) Monetti M, Levin MC, Watt MJ, Sajan MP, Marmor S, Hubbard BK, et al. Dissociation of Hepatic Steatosis and Insulin Resistance in Mice Overexpressing DGAT in the Liver. Cell Metabolism 2007 -;6(1):69.

(216) Nguyen D, Samson SL, Reddy VT, Gonzalez EV, Sekhar RV. Impaired mitochondrial fatty acid oxidation and insulin resistance in aging: novel protective role of glutathione. Aging Cell 2013 06;12(3):415-425.

(217) Solomon TPJ, Marchetti CM, Krishnan RK, Gonzalez F, Kirwan JP. Effects of aging on basal fat oxidation in obese humans. Metabolism 2008 08;57(8):1141-1147.

(218) Toth MJ, Arciero PJ, Gardner AW, Calles-Escandon J, Poehlman ET. Rates of free fatty acid appearance and fat oxidation in healthy younger and older men. J Appl Physiol (1985) 1996 02;80(2):506-511.

(219) Nishikawa S, Doi K, Nakayama H, Uetsuka K. The Effect of Fasting on Hepatic Lipid Accumulation and Transcriptional Regulation of Lipid Metabolism Differs between C57BL/6J and BALB/cA Mice Fed a High-fat Diet. Toxicol Pathol 2008 -;36(6):850.

(220) Speakman JR. Measuring energy metabolism in the mouse - theoretical, practical, and analytical considerations. Frontiers in physiology 2013 -;4:34.

(221) Lee Y, Hirose H, Ohneda M, Johnson JH, McGarry JD, Unger RH. Beta-cell lipotoxicity in the pathogenesis of non-insulin-dependent diabetes mellitus of obese rats: impairment in adipocyte-beta-cell relationships. Proc Natl Acad Sci U S A 1994 -;91(23):10878.

(222) Prato S, Enzi G, Vigili de Kreutzenberg S, Lisato G, Riccio A, Maifreni L, et al. Insulin regulation of glucose and lipid metabolism in massive obesity. Diabetologia 1990 -;33(4):228.

(223) Hipkiss AR. Does Chronic Glycolysis Accelerate Aging Could This Explain How Dietary Restriction Works. Ann N Y Acad Sci 2006;1067(1):361.

(224) Ingram DK, Roth GS. Glycolytic inhibition as a strategy for developing calorie restriction mimetics. Exp Gerontol 2011 February–March 2011;46(2):148-154.

(225) Hipkiss AR. Aging, Alzheimer's Disease and Dysfunctional Glycolysis; Similar Effects of Too Much and Too Little. Aging and disease 2019 -;10(6):1328.

(226) Magnusson I, Rothman DL, Katz LD, Shulman RG, Shulman GI. Increased rate of gluconeogenesis in type II diabetes mellitus. A 13C nuclear magnetic resonance study. J Clin Invest 1992 -;90(4):1323.

(227) Satrústegui J, Cuezva JM, Machado A. Increased basal gluconeogenesis in the aged rat. FEBS Lett 1986 -;197(1-2):159.

(228) Bakala H, Ladouce R, Baraibar MA, Friguet B. Differential expression and glycative damage affect specific mitochondrial proteins with aging in rat liver. Biochimica et Biophysica Acta (BBA) - Molecular Basis of Disease 2013 December 2013;1832(12):2057-2067.

(229) Roichman A, Elhanati S, Aon MA, Abramovich I, Di Francesco A, Shahar Y, et al. Restoration of energy homeostasis by SIRT6 extends healthy lifespan. Nature Communications 2021 -;12(1).

(230) Yang Y, Tarabra E, Yang GS, Vaitheesvaran B, Palacios G, Kurland IJ, et al. Alteration of de novo glucose production contributes to fasting hypoglycaemia in Fyn deficient mice. PloS one 2013 -;8(11):e81866.

(231) Hughey C, Wasserman D, Lee-Young R, Lantier L. Approach to assessing determinants of glucose homeostasis in the conscious mouse. Mammalian Genome 2014 -;25:522.

(232) Cereghetti GM, Scorrano L. The many shapes of mitochondrial death. Oncogene 2006 -;25(34):4717.

(233) Son JM, Sarsour EH, Kakkerla Balaraju A, Fussell J, Kalen AL, Wagner BA, et al. Mitofusin 1 and optic atrophy 1 shift metabolism to mitochondrial respiration during aging. Aging Cell 2017 -;16(5):1136.

(234) Lee S, Jeong S, Lim W, Kim S, Park Y, Sun X, et al. Mitochondrial Fission and Fusion Mediators, hFis1 and OPA1, Modulate Cellular Senescence*. J Biol Chem 2007 -;282(31):22977.

(235) Park YY, Lee S, Karbowski M, Neutzner A, Youle RJ, Cho H. Loss of MARCH5 mitochondrial E3 ubiquitin ligase induces cellular senescence through dynamin-related protein 1 and mitofusin 1. J Cell Sci 2010 -;123(Pt 4):619.

(236) Ljubicic V, Menzies KJ, Hood DA. Mitochondrial dysfunction is associated with a pro-apoptotic cellular environment in senescent cardiac muscle. Mech Ageing Dev 2010 -;131(2):79.

(237) Lasry A, Ben-Neriah Y. Senescence-associated inflammatory responses: aging and cancer perspectives. Trends Immunol 2015 -;36(4):217.

(238) Kim DH, Lee B, Lee J, Kim ME, Lee JS, Chung JH, et al. FoxO6-mediated IL-1β induces hepatic insulin resistance and age-related inflammation via the TF/PAR2 pathway in aging and diabetic mice. Redox biology 2019 -;24:101184.

(239) Loréal O, Clément B, Schuppan D, Rescan PY, Rissel M, Guillouzo A. Distribution and cellular origin of collagen VI during development and in cirrhosis. Gastroenterology 1992 -;102(3):980.

(240) Liu Y, Zhang J, Chen Y, Sohel H, Ke X, Chen J, et al. The correlation and role analysis of COL4A1 and COL4A2 in hepatocarcinogenesis. Aging 2020 -;12(1):204.

(241) Gagliano N, Arosio B, Grizzi F, Masson S, Tagliabue J, Dioguardi N, et al. Reduced collagenolytic activity of matrix metalloproteinases and development of liver fibrosis in the aging rat. Mech Ageing Dev 2002 -;123(4):413.

(242) Delire B, Lebrun V, Selvais C, Henriet P, Bertrand A, Horsmans Y, et al. Aging enhances liver fibrotic response in mice through hampering extracellular matrix remodeling. Aging 2016 -;9(1):98.

(243) Podolsky MJ, Yang CD, Valenzuela CL, Datta R, Huang SK, Nishimura SL, et al. Age-dependent regulation of cell-mediated collagen turnover. JCI insight 2020 -;5(10).

(244) Weng T, Liu L. The role of pleiotrophin and β-catenin in fetal lung development. Respiratory Research 2010 -;11(1):1.

(245) Cabrae R, Dubuquoy C, Caüzac M, Morzyglod L, Guilmeau S, Noblet B, et al. Insulin activates hepatic Wnt/β-catenin signaling through stearoyl-CoA desaturase 1 and Porcupine. Scientific Reports 2020 -;10(1).

(246) Meng K, Rodriguez-Peña A, Dimitrov T, Chen W, Yamin M, Noda M, et al. Pleiotrophin signals increased tyrosine phosphorylation of beta beta-catenin through inactivation of the intrinsic catalytic activity of the receptor-type protein tyrosine phosphatase beta/zeta. Proc Natl Acad Sci U S A 2000 -;97(6):2603.

(247) Bolik J, Tirnitz-Parker J, Schmidt-Arras D. ADAM and ADAMTS Proteases in Hepatic Disorders. Journal of Renal and Hepatic Disorders 2019;3(1):23-32.

(248) Bourd-Boittin K, Bonnier D, Leyme A, Mari B, Tuffery P, Samson M, et al. Protease profiling of liver fibrosis reveals the ADAM metallopeptidase with thrombospondin type 1 motif, 1 as a central activator of transforming growth factor beta. Hepatology 2011 -;54(6):2173.

(249) MacArthur JM, Bishop JR, Stanford KI, Wang L, Bensadoun A, Witztum JL, et al. Liver heparan sulfate proteoglycans mediate clearance of triglyceride-rich lipoproteins independently of LDL receptor family members. J Clin Invest 2007 -;117(1):153.

(250) Schüring A, Lutz F, Tüttelmann F, Gromoll J, Kiesel L, Götte M. Role of syndecan-3 polymorphisms in obesity and female hyperandrogenism. Journal of Molecular Medicine 2009 -;87(12):1241.

(251) Strader AD, Reizes O, Woods SC, Benoit SC, Seeley RJ. Mice lacking the syndecan-3 gene are resistant to diet-induced obesity. J Clin Invest 2004 -;114(9):1354.

(252) Weiner OH, Zoremba M, Gressner AM. Gene expression of syndecans and betaglycan in isolated rat liver cells. Cell Tissue Res 1996 -;285(1):11.

(253) Rakhshandehroo M. Peroxisome Proliferator-Activated Receptor Alpha Target Genes. PPAR Research 2010:1-21.

(254) Louet JF, Chatelain F, Decaux JF, Park EA, Kohl C, Pineau T, et al. Long-chain fatty acids regulate liver carnitine palmitoyltransferase I gene (L-CPT I) expression through a peroxisome-proliferator-activated receptor alpha (PPARalpha)-independent pathway. Biochem J 2001 02/15;354:189-197.

(255) Vilà L, Roglans N, Alegret M, Camins A, Pallàs M, Sánchez RM, et al. Hypertriglyceridemia and hepatic steatosis in senescence-accelerated mouse associate to changes in lipid-related gene expression. J Gerontol A Biol Sci Med Sci 2007 11;62(11):1219-1227.

(256) Hashimoto T, Fujita T, Usuda N, Cook W, Qi C, Peters JM, et al. Peroxisomal and mitochondrial fatty acid beta-oxidation in mice nullizygous for both peroxisome proliferator-activated receptor alpha and peroxisomal fatty acyl-CoA oxidase. Genotype correlation with fatty liver phenotype. The Journal of biological chemistry 1999 -;274(27):19228.

(257) Lee YK, Park JE, Lee M, Hardwick JP. Hepatic lipid homeostasis by peroxisome proliferator-activated receptor gamma 2. Liver Res 2018 12;2(4):209-215.

(258) Lee C, Olson P, Hevener A, Mehl I, Chong L, Olefsky JM, et al. PPARdelta regulates glucose metabolism and insulin sensitivity. Proc Natl Acad Sci U S A 2006 02/28;103(9):3444-3449.

(259) Shan W, Nicol CJ, Ito S, Bility MT, Kennett MJ, Ward JM, et al. Peroxisome proliferator-activated receptor-beta/delta protects against chemically induced liver toxicity in mice. Hepatology 2008 01;47(1):225-235.

(260) Kim S, Kim H, Kim T, Im S, Park S, Lee I, et al. SREBP-1c mediates the insulin-dependent hepatic glucokinase expression. J Biol Chem 2004 -;279(29):30823.

(261) Pei L. NR4A orphan nuclear receptors are transcriptional regulators of hepatic glucose metabolism. Nature Medicine 2006;12(9):1048-1056.

(262) Chao LC, Zhang Z, Pei L, Saito T, Tontonoz P, Pilch PF. Nur77 coordinately regulates expression of genes linked to glucose metabolism in skeletal muscle. Mol Endocrinol 2007 -;21(9):2152.

(263) Kanzleiter T, Preston E, Wilks D, Ho B, Benrick A, Reznick J, et al. Overexpression of the orphan receptor Nur77 alters glucose metabolism in rat muscle cells and rat muscle in vivo. Diabetologia 2010 -;53(6):1174.

(264) Lili Miao. Glycerol kinase interacts with nuclear receptor NR4A1 and regulates glucose metabolism in the liver. FASEB Journal 2019;33(6):6736-6748.

(265) Sriram G, Parr LS, Rahib L, Liao JC, Dipple KM. Moonlighting function of glycerol kinase causes systems-level changes in rat hepatoma cells. Metab Eng 2010 -;12(4):332.

(266) Zeng Z, Liu F, Li S. Metabolic Adaptations in Pregnancy: A Review. Ann Nutr Metab 2017 -;70(1):59.

(267) Villar J, Kestler E, Castillo P, Menendez R, Cogswell M, Repke JT. Effect of fat and fat-free mass deposition during pregnancy on birth weight. Obstet Gynecol 1992 -;167(5):1344.

(268) López-Luna P, Muñoz T, Herrera E. Body fat in pregnant rats at mid- and late-gestation. Life Sci 1986 -;39(15):1389.

(269) López-Luna P, Maier I, Herrera E. Carcass and tissue fat content in the pregnant rat. Neonatology 1991 -;60(1):29.

(270) Herrera E. Lipid metabolism in pregnancy and its consequences in the fetus and newborn. Endocrine 2002 -;19(1):43.

(271) Herrera E. Metabolic adaptations in pregnancy and their implications for the availability of substrates to the fetus. Eur J Clin Nutr 2000 -;54(S1):47.

(272) Herrera E, Ortega-Senovilla H. Lipid metabolism during pregnancy and its implications for fetal growth. Curr Pharm Biotechnol 2014 -;15(1):24.

(273) Sivan E, Homko CJ, Chen X, Reece EA, Boden G, Sivan E, et al. Effect of insulin on fat metabolism during and after normal pregnancy. Diabetes 1999 -;48(4):834.

(274) Stanley K, Fraser R, Bruce C. Physiological changes in insulin resistance in human pregnancy: longitudinal study with the hyperinsulinaemic euglycaemic clamp technique. British Journal of Obstetrics & Gynaecology 1998 -;105(7):756.

(275) Muñoz C, López-Luna P, Herrera E. Glucose and insulin tolerance tests in the rat on different days of gestation. Biol Neonate 1995 -;68(4):282.

(276) Herrera E, Muñoz C, López-Luna P, Ramos P. Carbohydrate-lipid interactions during gestation and their control by insulin. Brazilian journal of medical and biological research = Revista brasileira de pesquisas medicas e biologicas 1994 -;27(11):2499.

(277) Alvarez JJ, Montelongo A, Iglesias A, Lasunción MA, Herrera E. Longitudinal study on lipoprotein profile, high density lipoprotein subclass, and postheparin lipases during gestation in women. J Lipid Res 1996 February 1996;37(2):299-308.

(278) Carrara MA, Batista MR, Saruhashi TR, Felisberto-Junior AM, Guilhermetti M, Bazotte RB. Coexistence of insulin resistance and increased glucose tolerance in pregnant rats: A physiological mechanism for glucose maintenance. Life Sci 2012 -;90(21-22):831.

(279) Herrera E, Desoye G. Maternal and fetal lipid metabolism under normal and gestational diabetic conditions. Hormone molecular biology and clinical investigation 2016 -;26(2):109.

(280) Hadden DR, McLaughlin C. Normal and abnormal maternal metabolism during pregnancy. Seminars in Fetal & Neonatal Medicine 2009 -;14(2):66.

(281) Butte NF. Carbohydrate and lipid metabolism in pregnancy: normal compared with gestational diabetes mellitus. Am J Clin Nutr 2000 -;71(5):1256S.

(282) LAIN KY, CATALANO PM. Metabolic Changes in Pregnancy. Clin Obstet Gynecol 2007 -;50(4):938.

(283) Parrettini S, Caroli A, Torlone E. Nutrition and Metabolic Adaptations in Physiological and Complicated Pregnancy: Focus on Obesity and Gestational Diabetes. Frontiers in endocrinology 2020 -;11:611929.

(284) Powe C, Huston Presley L, Locascio J, Catalano P. Augmented insulin secretory response in early pregnancy. Diabetologia 2019 -;62(8):1445.

(285) Zhang L, Song X, Zhou L, Liang G, Xu H, Wang F, et al. Accumulation of intestinal tissue 3-deoxyglucosone attenuated GLP-1 secretion and its insulinotropic effect in rats. Diabetology & metabolic syndrome 2016 -;8:78.

(286) Catalano PM, Hoegh M, Minium J, Huston-Presley L, Bernard S, Kalhan S, et al. Adiponectin in human pregnancy: implications for regulation of glucose and lipid metabolism. Diabetologia 2006 -;49(7):1677.

(287) Sitruk-Ware R. Progestins and cardiovascular risk markers. Steroids 2000 -;65(10-11):651.

(288) Wu Z, Bidlingmaier M, Friess SC, Kirk SE, Buchinger P, Schiessl B, et al. A new nonisotopic, highly sensitive assay for the measurement of human placental growth hormone: development and clinical implications. J Clin Endocrinol Metab 2003 -;88(2):804.

(289) Barbour LA, McCurdy CE, Hernandez TL, Kirwan JP, Catalano PM, Friedman JE. Cellular mechanisms for insulin resistance in normal pregnancy and gestational diabetes. Diabetes Care 2007 -;30 Suppl 2:S112.

(290) Boyle CN, Le Foll C. Amylin and Leptin interaction: Role During Pregnancy, Lactation and Neonatal Development. Neuroscience 2020 -;447(1):136.

(291) Pérez-Pérez A, Toro A, Vilariño-García T, Maymó J, Guadix P, Dueñas JL, et al. Leptin action in normal and pathological pregnancies. J Cell Mol Med 2018 -;22(2):716.

(292) Adu-Gyamfi EA, Fondjo LA, Owiredu WKBA, Czika A, Nelson W, Lamptey J, et al. The role of adiponectin in placentation and preeclampsia. Cell Biochem Funct 2020 -;38(1):106.

(293) Buchanan TA, Xiang A, Kjos SL, Watanabe R. What is gestational diabetes? Diabetes Care 2007 -;30 Suppl 2:S105.

(294) Gestational diabetes mellitus. Diabetes Care 2004 -;27 Suppl 1:S88.

(295) Ryan E. Diagnosing gestational diabetes. Diabetologia 2011 -;54(3):480.

(296) Coustan DR. Gestational Diabetes Mellitus. Clin Chem 2013 -;59(9):1310.

(297) Mónica Díez-Hochleitner Ruiz. Exposoma de la placenta: efecto de la adiposidad materna en el metabolismo de la placentaUniversidad San Pablo CEU; 2016.

(298) Zapatería B, Sevillano J, Sánchez-Alonso MG, Limones M, Pizarro-Delgado J, Zuccaro A, et al. Deletion of pleiotrophin impairs glucose tolerance and liver metabolism in pregnant mice: Moonlighting role of glycerol kinase. FASEB J 2021;35(10):e21911.

(299) Ball M, Carmody M, Wynne F, Dockery P, Aigner A, Cameron I, et al. Expression of pleiotrophin and its receptors in human placenta suggests roles in trophoblast life cycle and angiogenesis. Placenta.2009 Jul;30(7):649-53.doi: 10.1016/j.placenta.2009.05.001.Epub 2009 May 28. 2009 2009 Jul.

(300) Torres N. Protein restriction during pregnancy affects maternal liver lipid metabolism and fetal brain lipid composition in the rat. American Journal of Physiology: Endocrinology & Metabolism 2010;298:E270-8.

(301) Herrera E, Lasunción M, Gomez-Coronado D, Aranda P, López-Luna P, Maier I. Role of lipoprotein lipase activity on lipoprotein metabolism and the fate of circulating triglycerides in pregnancy. Am J Obstet Gynecol.1988 Jun;158(6 Pt 2):1575-83.doi: 10.1016/0002-9378(88)90193-7. 1988 1988 Jun.

(302) Darmady JM, Postle AD. Lipid metabolism in pregnancy. Br J Obstet Gynaecol.1982 Mar;89(3):211-5.doi: 10.1111/j.1471-0528.1982.tb03616.x. 1982.

(303) Haggarty P. Fatty Acid Supply to the Human Fetus. Annual Review of Nutrition 2010;30(1):237-265.

(304) Wolska A. Apolipoprotein C-II: New findings related to genetics, biochemistry, and role in triglyceride metabolism. Atherosclerosis (00219150) 2017;267:49-61.

(305) Kalra S, Gupta Y. The Insulin:Glucagon Ratio and the Choice of Glucose-Lowering Drugs. Diabetes Ther.2016 Mar;7(1):1-9.doi: 10.1007/s13300-016-0160-4.Epub 2016 Mar 10. 2016 2016 Mar.

(306) Ambühl P, Amemiya M, Preisig P, Moe O, Alpern R. Chronic hyperosmolality increases NHE3 activity in OKP cells. J Clin Invest.1998 Jan 1;101(1):170-7.doi: 10.1172/JCI62. 1998 1998 Jan 1.

(307) Horton JD. Combined analysis of oligonucleotide microarray data from transgenic and knockout mice identifies direct SREBP target genes. Proceedings of the National Academy of Sciences of the United States of America 2003;100(21):12027-12033.

(308) Wang Y. PPARs as Metabolic Regulators in the Liver: Lessons from Liver-Specific PPAR-Null Mice. International Journal of Molecular Sciences 2020;21(6):2061-2062.

(309) Feingold KR, Sweeney TR, Moser AH, Shigenaga JK, Grunfeld C. Decreased nuclear hormone receptor expression in the livers of mice in late pregnancy. American Journal of Physiology - Endocrinology and Metabolism 2006 -;290(6):E1313.

(310) MacLennan N, Rahib L, Shin C, Fang Z, Horvath S, Dean J, et al. Targeted disruption of glycerol kinase gene in mice: expression analysis in liver shows alterations in network partners related to glycerol kinase activity. Hum Mol Genet.2006 Feb 1;15(3):405-15.doi: 10.1093/hmg/ddi457.Epub 2005 Dec 20. 2006.

(311) Zárraga-Granados G, Muciño-Hernández G, Villamizar-Gálvez W, Peñas-Rincón A, Castro-Obregón S, Sánchez-Carbente MR, et al. The nuclear receptor NR4A1 is regulated by SUMO modification to induce autophagic cell death. PLoS ONE 2020 -;15(3).

(312) Zhang L, Xie F, Zhou F, Zhang J, Ten Dijke P. SUMO-triggered ubiquitination of NR4A1 controls macrophage cell death. Cell Death Differ 2017 -;24(9):1530.

(313) Xiong X, Yu J, Fan R, Zhang C, Xu L, Sun X, et al. NAMPT overexpression alleviates alcohol-induced hepatic steatosis in mice. PloS one 2019 -;14(2):e0212523.

(314) Audrito V, Messana V, Deaglio S. NAMPT and NAPRT: Two Metabolic Enzymes With Key Roles in Inflammation. Front Oncol 2020;10:358.

(315) Sarkar M, Grab J, Dodge JL, Gunderson EP, Rubin J, Irani RA, et al. Non-alcoholic fatty liver disease in pregnancy is associated with adverse maternal and perinatal outcomes. J Hepatol 2020 -;73(3):516.

(316) Siervo M, Lara J, Celis-Morales C, Vacca M, Oggioni C, Battezzati A, et al. Age-related changes in basal substrate oxidation and visceral adiposity and their association with metabolic syndrome. Eur J Nutr 2016 -;55(4):1755.

(317) Camell CD, Sander J, Spadaro O, Lee A, Nguyen KY, Wing A, et al. Inflammasome-driven catecholamine catabolism in macrophages blunts lipolysis during ageing. Nature 2017 -;550(7674):119.

(318) Janani C, Ranjitha Kumari BD. PPAR gamma gene – A review. Diabetes & Metabolic Syndrome: Clinical Research & Reviews 2015 -;9(1):46.

(319) Medina-Gomez G, Gray SL, Yetukuri L, Shimomura K, Virtue S, Campbell M, et al. PPAR gamma 2 prevents lipotoxicity by controlling adipose tissue expandability and peripheral lipid metabolism. PLoS genetics 2007 -;3(4):e64.

(320) Scheja L, Heeren J. Metabolic interplay between white, beige, brown adipocytes and the liver. J Hepatol 2016 -;64(5):1176.

(321) Fernández-Calle R, Galán-Llario M, Gramage E, Zapatería B, Vicente-Rodríguez M, Zapico JM, et al. Role of RPTPβ/ζ in neuroinflammation and microglia-neuron communication. Scientific Reports 2020 -;10(1).

APPENDIXES

APPENDIX 1

Primer sets used for qPCR analysis of the gene expression in the liver of mice from the different experimental models.

Gene ID	Primer forward	Primer reverse
Acadl	5′ -CTTGGGAAGAGCAAGCGTACT- 3′	5′ -CTGTTCTTTTGTGCCGTAATTCG- 3′
Acadvl	5′ -GGAGGACGACACTTTGCAGG- 3′	5′ -AGCGAGCATACTGGGTATTAGA- 3′
Acat2	5′ -CACGAAATGGGGACAACTG- 3′	5′ -AACCTGCCGTCAAGACA- 3′
Acc	5′ -GTCCCCAGGGATGAACCAATA- 3′	5′ -GCCATGCTCAACCAAAGTAGC- 3′
Acly	5′ -AAGCCTTTGACAGCGGCATCATT- 3′	5′ -TTGAGGATCTGCACTCGCATGTCT- 3′
Acox1	5′ -TCGAAGCCAGCGTTACGAG- 3′	5′ -ATCTCCGTCTGGGCGTAGG- 3′
Adamts1	5′ -TTTTGCTACTCCTGTTCATGG- 3′	5′ -CGTTTGCCTTCACAGTACTTC- 3′
Akgdh	5′ -AACAAGAAGACCCACCTGACAGA- 3′	5′ -CGGATCAACTCCAGGAGCAT- 3′
ApoB100	5′ -AAGCACCTCCGAAAGTACGTG- 3′	5′ -CTCCAGCTCTACCTTACAGTTGA- 3′
ApoC2	5′ -GCATGGATGAGAAACTCAGGG- 3′	5′ -AAAATGCCTGCGTAAGTGCTC- 3′
Aqp9	5′ -CTATGACGGACTCATGGCCTTT- 3′	5′ -ATGAACGCCGTTCCATTTTCT- 3′
Arg	5′ -CTCCAAGCCAAAGTCCTTAGAG- 3′	5′ -AGGAGCTGTCATTAGGGACATC- 3′
Bip	5′ -ACTTGGGGACCACCTATTCCT- 3′	5′ -ATCGCCAATCAGACGCTCC- 3′
Cd-11b	5′ -CAGTGCTGGGAGACGTGAAT- 3′	5′ -CACTCAGAGACTGCCCGAAG- 3′
Cd-11c	5′ -TGAGAATCAGCTGAAGGAGAAGA- 3′	5′ -GGGGTACAAGAAGGCACCTC- 3′
Cd68	5′ -TGGCGGTGGAATACAATGTG- 3′	5′ -GATGAATTCTGCGCCATGAA- 3′
Cebpα	5′ -GGAACTTGAAGCACAATCGATC- 3′	5′ -TGGTTTAGCATAGACGTGCACA- 3′
Chop	5′ -CCCTGCCTTTCACCTTGG- 3′	5′ -CCGCTCGTTCTCCTGCTC- 3′
Col4a1	5′ -TCTGGCTGTGGAAAATGTGA- 3′	5′ -GTTCTCCAGCATCACCCTTT- 3′
Col6a2	5′ -CATTGGCTAACATGACGCAG- 3′	5′ -GAGTTAGCGATGTCCCTCAG- 3′
Cox-2	5′ -ACGGAGAGAGTTCATCCCTGA- 3′	5′ -ACCCAGGTCCTCGCTTATGA- 3′
Cps1	5′ -CATGGAACATCCAGCCGAATTGG- 3′	5′ -GATGGCACATCCTCAGAGCCTT- 3′
Cpt1α	5′ -ACCCTGAGGCATCTATTGACAG- 3′	5′ -ATGACATACTCCCACAGATGGC- 3′
Cs	5′ -GGACAATTTTCCAACCAATCTGC- 3′	5′ -TCGGTTCATTCCCTCTGCATA- 3′
Ctnnb	5′ -CTTGGATTCTGGAATCCATTC- 3′	5′ -ATACTGCCCGTCAATATCAG- 3′
Dgat1	5′ -GCCCCATGCGTGATTATTGC- 3′	5′ -CACTGGAGTGATAGACTCAACCA- 3′
Dgat2	5′ -AACCGAGACACCATAGACTACTT- 3′	5′ -CTTCAGGGTGACTGCGTTCTT- 3′
Edem	5′ -AAGCCCTCTGGAACTTGCG- 3′	5′ -AACCCAATGGCCTGTCTGG- 3′
F4/80	5′ -CAGATACAGCAATGCCAAGCA- 3′	5′ -GATTGTGAAGGTAGCATTCACAAGTG- 3′
Fasn	5′ -AGAGATCCCGAGACGCTTCT- 3′	5′ -GCCTGGTAGGCATTCTGTAGT- 3′
Fatp4	5′ -CCAGTAGTGTGGCCAACTTCCT- 3′	5′ -CCACAGACCCACAAACTCATTG- 3′
Fatp5	5′ -GAATCGGGAGGCAGAGAACT- 3′	5′ -AGCGGGTCATACAAGTGAGC- 3′
Fbp1	5′ -CAGGGACGTGAAGATGAAGAAGAA- 3′	5′ -TTGTTGGCGGGGTATAAAAAGA- 3′
Fgf21	5′ -GGAGCTCTCTATGGATCGCCT- 3′	5′ -TGTAACCGTCCTCCAGCAGC- 3′
G6pc	5′ -CGACTCGCTATCTCCAAGTGA- 3′	5′ -GTTGAACCAGTCTCCGACCA- 3′
G6pd	5′ -CTGGAACCGCATCATAGTGGAG- 3′	5′ -CCTGATGATCCCAAATTCATCAAAATAG- 3′
Gck	5′ -TAAAGATGTTGCCCACCTACG- 3′	5′ -GGAATACATCTGGTGTTTCGTCT- 3′
Glud1	5′ -TCCGTTACAGCACTGACGTGAG- 3′	5′ -ACGCCTGCTTTAGCACCTCCAA- 3′
Glut2	5′ -TCCCTTGGTTCATGGTTGCT- 3′	5′ -GGAAGTCCGCAATGTACTGGA- 3′
Gpat	5′ -ACGCACACAAGGCACAGAG- 3′	5′ -TGCTGCTCAGTACATTCTCAGTA- 3′
Gsk-3b	5′ -GAGCCACTGATTACACGTCCAG- 3′	5′ -CCAACTGATCCACACCACTGTC- 3′

Gyk	5′ -GTCAGCAACCAGAGGGAAACC- 3′	5′ -CCACGGCATTATAGAGAGGCT- 3′
Hadha	5′ -AGCAACACGAATATCACAGGAAG- 3′	5′ -AGGCACACCCACCATTTTGG- 3′
Hk-III	5′ -CTGAGTCAAGGCTGTATCCTCC- 3′	5′ -TGCACCAGTTCAGCATCTGAGG- 3′
Hmgcr	5′ -TGACCTTTCTAGAGCGAGTGC- 3′	5′ -GTGCCAACTCCAATCACAAG- 3′
Hmgcs	5′ -CGGATCGTGAAGACATCAACTC- 3′	5′ -CGCCCAATGCAATCATAGGAA- 3′
Hprt	5′ -TGCTCGAGATGTCATGAAGG- 3′	5′ -TATGTCCCCCGTTGACTGAT- 3′
Idh3g	5′ -GGTGCTGCAAAGGCAATGC- 3′	5′ -TATGCCGCCCACCATACTTAG- 3′
Il-1β	5′ -GCTGAAAGCTCTCCACCTCA- 3′	5′ -AGGCCACAGGTATTTTGTCG- 3′
Il-6	5′ - TAGTCCTTCCTACCCCAATTTCC- 3′	5′ -TTGGTCCTTAGCCACTCCTTC- 3′
iNos	5′ -GGATGAGCTCATCTTTGCCACC- 3′	5′ -GCATCTGGTAGCCAGCGTACC- 3′
Ldh	5′ -TGTCTCCAGCAAAGACTACTGT- 3′	5′ -GACTGTACTTGACAATGTTGGGA- 3′
Ldlr	5′ -CTCCTGCATTCACGGTAGCC- 3′	5′ -CCCACTGTGACACTTGAACTTG- 3′
Lipc	5′ -TTCTCGGAGCAAAGTTCACCTAAT- 3′	5′ -GTGATTCTTCCAATCTTGTTCTTC- 3′
Lpin2	5′ -AGTTGACCCCATCACCGTAG- 3′	5′ -CCCAAAGCATCAGACTTGGT- 3′
Lpl	5′ -TGGAGAAGCCATCCGTGTG- 3′	5′ -TCATGCGAGCACTTCACCAG- 3′
Mdh1	5′ -TCAGTTAAGGTCATTGTTGTG- 3′	5′ -AAGAGCAATTTGAGATTTTGC- 3′
Mdh2	5′ -AGAGCTAAAGGGTTTGGATC- 3′	5′ -TTGGGGAAAGTCAACCTT- 3′
Mfn1	5′ -GTGAGCTTCACCAGTGCAAA- 3′	5′ -CACAGTCGAGCAAAAGTAGTGG- 3′
Mfn2	5′ -CATTCTTGTGGTCGGAGGAG- 3′	5′ -AAGGAGAGGGCGATGAGTCT- 3′
Mk	5′ -TGATGGGAGCACTGGCAC- 3′	5′ -CATTGTACCGCGCCTTCTT- 3′
Nur77	5′ -TTGAGTTCGGCAAGCCTACC- 3′	5′ -GTGTACCCGTCCATGAAGGTG- 3′
Opa1	5′ -TTCTGAGGCCCTTCTCTTGT- 3′	5′ -TGATCTGTTGCTCGAAATGC- 3′
Pc	5′ -GGCGCATGAGTTCTCCAACA- 3′	5′ -GTAGGCCCGGGTGTAATTCTC- 3′
Pdha1	5′ -GAAATGTGACCTTCATCGGCT- 3′	5′ -TGATCCGCCTTTAGCTCCATC- 3′
Pdi	5′ -ACCTGCTGGTGGAGTTCTATG- 3′	5′ -CGGCAGCTTTGGCATACT- 3′
Pepck	5′ -AAGCATTCAACGCCAGGTTC- 3′	5′ -GGGCGAGTCTGTCAGTTCAAT- 3′
Pfk1	5′ -GAACTACGCACACTTGACCAT- 3′	5′ -CTCCAAAACAAAGGTCCTCTGG- 3′
Pgc1α	5′ -CCCTTCTTTGCCATTGAATC- 3′	5′ -AATGTTAGGAAAGTTTAGCATCTGG- 3′
Pk	5′ -CTGGATGGGGCTGACTGTAT- 3′	5′ -GGCGTAGCTCCTCAAACAAC- 3′
Plin2	5′ -GACAGGATGGAGGAAAGACTGC- 3′	5′ -GGTAGTCGTCACCACATCCTTC- 3′
Pparα	5′ -CACGCATGTGAAGGCTGTAA- 3′	5′ -CAGCTCCGATCACACTTGTC- 3′
Pparβδ	5′ -ACCCTTTGTCATCCACGA- 3′	5′ -GGATGTTCTTGGCGAACT- 3′
Pparγ1	5′ -TTTAAAAACAAGACTACCCTTTACTGAAATT- 3′	5′ -AGAGGTCCACAGAGCTGATTCC- 3′
Ptn	5′ -TTGGGGAGAATGTGACCTCAATAC- 3′	5′ -GGCTTGGAGATGGTGACAGTTTTC- 3′
Rpl13	5′ -GGTGCCCTACAGTTAGATACCAC- 3′	5′ -TTTGTTTCGCCTCCTTGGGTC- 3′
Rptpg	5′ -AGCATATCAGGACACAGCGGAAC- 3′	5′ -TCCCGAGAATGGCTTCCAAC- 3′
Rxrα	5′ -ACATCTGCGCTATCTGTGGG- 3′	5′ -TGTCGATCAGGCAGTCCTTG- 3′
Scd1	5′ -TTCTTGCGATACACTCTGGTGC- 3′	5′ -CGGGATTGAATGTTCTTGTCGT- 3′
Sdc3	5′ -TGATGATGAACTAGACGACC- 3′	5′ -AGAAAGGAGTTCCTCAAATGG- 3′
Soat	5′ -AGACTTGGTGCAATGGACTCGAC- 3′	5′ -CATAGGGCCCGATCCAACAG- 3′
Srebp-1c	5′ -AGGCCATCGACTACATCCG -3′	5′ -TCCATAGACACATCTGTGCCTC -3′
Tkt	5′ -TGGCATACACAGGCAAATACTT -3′	5′ -TCCAGCTTGTAAATTCCAGCAA -3′
Tlr4	5′ -CCCTCAGCACTCTTGATTGC -3′	5′ -TGCTTCTGTTCCTTGACCCA -3′
Tnfα	5′ -AGGCACTCCCCCAAAAGATG -3′	5′ -TGAGGGTCTGGGCCATAGAA -3′
Wnt-4	5′ -CGAGGAGTGCCAATACCAGT	5′ -GTCACAGCCACACTTCTCCA
Wnt-5b	5′ -TCTCCGCCTCACAAAAGTCT	5′ -CACAGACACTCTCAAGCCCA

APPENDIX 2

Antibodies used for the analysis of protein expression in the liver of mice from the different experimental models.

Primary antibodies		
Target	**Concentration**	**Reference**
Glycerol kinase	1:2000	A6377, ABclonal
NUR77	1:1000	A13316, ABclonal
Acetyl CoA carboxylase	1:500	05-1098, Merck
Phospho-acetyl CoA carboxylase (Ser79)	1:500	07-303, Merck
HSP90	1:500	05-594, Merck
β-actin	1:5000	A5316, Merck
TBP	1:1000	T1827, Merck
Secondary antibodies		
Target	**Concentration**	**Reference**
Rabbit immunoglobulin HRP-linked	1:10000	A0545, Merck
Mouse immunoglobulin HRP-linked	1:10000	A9044, Merck

APPENDIX 3. PUBLICATIONS

Sevillano, J., Sánchez-Alonso, M.G., **Zapatería, B**. et al. Pleiotrophin deletion alters glucose homeostasis, energy metabolism and brown fat thermogenic function in mice. Diabetologia 62, 123–135 (2019). https://doi.org/10.1007/s00125-018-4746-4

Fernández-Calle, R., Galán-Llario, M., Gramage, E., **Zapatería, B.** et al. Role of RPTPβ/ζ in neuroinflammation and microglia-neuron communication. Sci Rep 10, 20259 (2020). https://doi.org/10.1038/s41598-020-76415-5

Zuccaro, A.; **Zapatería, B.**; Sánchez-Alonso, M.G.; Haro, M.; Limones, M.; Terrados, G.; Izquierdo, A.; Corrales, P.; Medina-Gómez, G.; Herradón, G.; et al. Pleiotrophin Deficiency Induces Browning of Periovarian Adipose Tissue and Protects against High-Fat Diet-Induced Hepatic Steatosis. Int. J. Mol. Sci. 2021, 22, 9261. https://doi.org/10.3390/ijms22179261

Zapatería B, Sevillano J, Sánchez-Alonso MG, et al. Deletion of pleiotrophin impairs glucose tolerance and liver metabolism in pregnant mice: Moonlighting role of glycerol kinase. *FASEB J*. 2021;35:e21911. https://doi.org/10.1096/fj.20210 1181R

APPENDIX 4. WORK SUBMITTED TO NATIONAL OR INTERNATIONAL CONFERENCES

1. **Title of the work:** Pleiotrophin: a novel modulator of the metabolic activity of the liver.

   Name of the conference: Mechanisms of insulin resistance (MOIR) symposium

   Organising entity: Mecanismos Moleculares y Comunicación Intertisular en la Resistencia a la Insulina. **Date:** 2021

2. **Title of the work:** *Ptn* deficiency prevents age-related NAFLD

   Name of the conference: Metabolism of Ageing (online)

   Organising entity: Biochemical Society and British Society for Research on Ageing. **Date:** 2021

3. **Title of the work:** Deletion of pleiotrophin is associated with impaired glucose tolerance and liver metabolism in the pregnant mice: moonlighting role of gycerol kinase.

   Name of the conference: DPSG Anual Meeting (virtual)

   Organising entity: DPSG **Date:** 2021

4. **Title of the work:** Role of pleiotrophin in the glucose tolerance and in the hepatic metabolism in the pregnant mice.

   Name of the conference: DPSG Annual Meeting (virtual)

   Organising entity: DPSG **Date:** 2020

5. **Title of the work:** Is pleiotrophin a regulating factor of liver metabolism?

   Name of the conference: 42nd Congress of the Spanish Society of Biochemistry and Molecular Biology (SEBBM) 2019

   Organising entity: Spanish Society of Biochemistry and Molecular Biology (SEBBM) **Date:** 2019

6. **Title of the work:** Role of pleiotrophin in hepatic metabolism: characterisation in an aging model.

   Name of the conference: XIII Annual Congress of Biotechnology

   Organising entity: Federación Española de Biotecnólogos **Date:** 2019

7. **Title of the work:** La pleiotrofina como potencial diana terapéutica en enfermedades relacionadas con el metabolismo lipídico hepático.

   Name of the conference: Farmadrid 28

   Organising entity: Instituto Fundación Teófilo Hernando y Hospital Universitario de La Princesa **Date:** 2019

8. **Title of the work:** La expresión cerebral de pleiotrofina modula la neuroinflamación y la inflamación hepática producidas por LPS.

   Name of the conference: Farmadrid 28

   Organising entity: Instituto Fundación Teófilo Hernando y Hospital Universitario de La Princesa **Date:** 2019

9. **Title of the work:** Role of pleiotrophin in hepatic metabolism: characterisation in an aging model.

   Name of the conference: 6th Symposium on Biomedical Research. Advances and Perspectives in Molecular Endocrinology.

   Organising entity: Universidad Autónoma de Madrid **Date:** 2019

10. **Title of the work:** Role of pleiotrophin in lipid metabolism.

    Name of the conference: Mechanisms of insulin resistance (MOIR) symposium

    Organising entity: Mecanismos Moleculares y Comunicación Intertisular en la Resistencia a la Insulina. **Date:** 2018

11. **Title of the work:** Role of pleiotrophin in lipid metabolism in a model of diet induced obesity.

    Name of the conference: IV World Congress of Public Health Nutrition - XII Congreso Nacional de la Sociedad Española de Nutrición Comunitaria (SENC) – NUTRIMAD 2018

    Organising entity: Sociedad Española de Nutrición Comunitaria **Date:** 2018

12. **Title of the work:** Role of pleiotrophin in lipid metabolism in a model of diet induced obesity.

    Name of the conference: 41st Congress of the Spanish Society of Biochemistry and Molecular Biology (SEBBM) 2018

    Organising entity: Spanish Society of Biochemistry and Molecular Biology (SEBBM) **Date:** 2018

13. **Title of the work:** Role of pleiotrophin in lipid metabolism. Effect of aging.

    Name of the conference: 41st Congress of the Spanish Society of Biochemistry and Molecular Biology (SEBBM) 2018

    Organising entity: Spanish Society of Biochemistry and Molecular Biology (SEBBM) **Date:** 2018